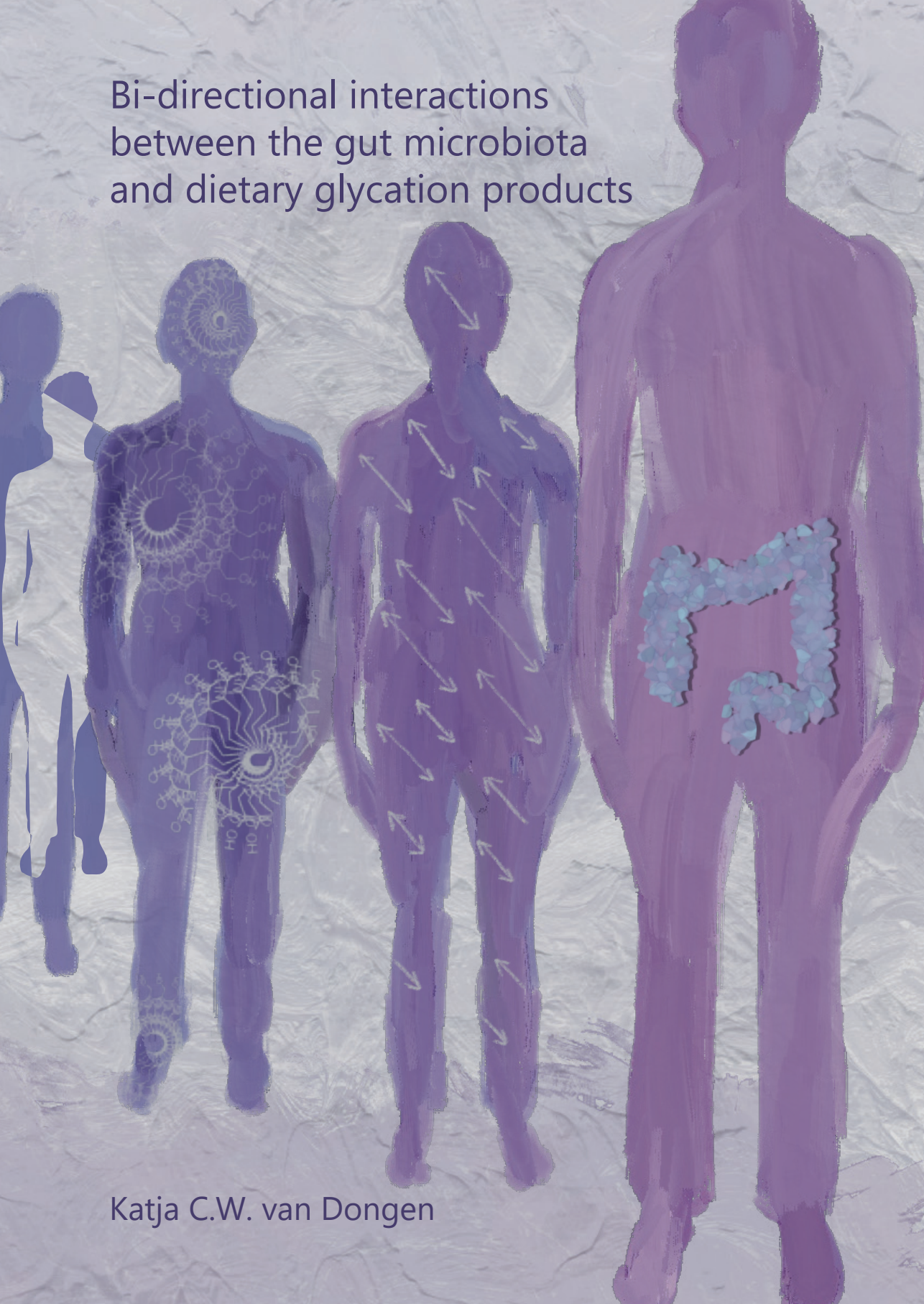# Bi-directional interactions between the gut microbiota and dietary glycation products

Katja C.W. van Dongen

Propositions

1. Risk assessment of dietary glycation products should take endogenous levels into account.
   (this thesis)

2. Exposure to dietary glycation products modifies gut microbial activity to better degrade these process contaminants.
   (this thesis)

3. The systems evaluating research performance in academia hamper scientific progress.

4. Use of volunteers introduces an inclusion bias in human intervention studies.

5. Developments to enable safe utilization of human feces for agricultural purposes get insufficient priority.

6. The increased interest for research on personalized nutrition reflects societal individualization.

7. Privatization of primary- and secondary education in the Netherlands is an undesirable consequence of problems in public education.

Propositions belonging to the thesis, entitled

'Bi-directional interactions between the gut microbiota and dietary glycation products'.

Katja C.W. van Dongen
Wageningen, June 10th 2022

Bi-directional interactions between the gut microbiota and dietary glycation products

Katja C.W. van Dongen

Thesis committee

Promotor
Prof. Dr I.M.C.M. Rietjens
Professor of Toxicology
Wageningen University & Research

Co-promotors
Dr K. Beekmann
Scientist, Toxicology
Wageningen University & Research

Dr C. Belzer
Associate professor at the Laboratory of Microbiology
Wageningen University & Research

Other members
Prof. Dr E. Feskens, Wageningen University & Research
Prof. Dr D. Marko, University of Vienna, Austria
Dr J. Penders, Maastricht University
Dr S.P.J. van Leeuwen, Wageningen University & Research

Bi-directional interactions between the gut microbiota and dietary glycation products

Katja C.W. van Dongen

Table of contents

General introduction

1.1 Background information

Dietary habits change throughout time[1], which can be driven by multiple factors such as technical innovations[2] and/or environmental and health concerns[3]. These changes in dietary habits can also result in other and possibly new emerging risks relevant for food safety. For example, since the industrial revolution the numbers of (highly) processed food products that are part of the habitual Western diet increased[2]. The processing of food products has several advantages including easier access to food products, increased shelf lives and reduced microbial hazards[4]. However, besides the aforementioned advantages, during these food processing operations and also during home food preparation (e.g., roasting, frying) food process contaminants can be formed. Examples of these include acrylamide[5], furans[6] and glycation products. Glycation products have been found in a variety of food products (e.g. baked products, fried potatoes, infant formula), are formed upon heating, and comprise a wide diversity of individual compounds[7–9]. These include early stage Maillard reaction products, such as the Amadori product fructoselysine, which are again precursors for more advanced products including the advanced glycation end products (AGEs), such as carboxymethyllysine[10]. Especially in the Western diet the dietary intake of AGEs and their precursors is high[11]. AGEs have been associated with adverse health effects[12], which will be further introduced in the following section (**1.2**). AGEs and their precursors are interesting and relevant compounds to investigate for several reasons. First of all, upon dietary exposure to AGEs and their precursors, they can reach the gut microbiota. This may lead to interactions with the gut microbiota, which could affect the toxicokinetics of the dietary constituent or have toxicodynamic consequences. Toxicokinetics refers to the absorption, distribution, metabolism and excretion (ADME) characteristics of a compound, while toxicodynamics refers to the effect of the respective compound on host health which can be exerted directly or possibly mediated via the gut microbiota (**Figure 1.1**). The role of the gut microbiota in host health and disease has been increasingly studied over the past years and will be further introduced later in this chapter (Section **1.3**). In addition, AGEs and their precursors are an interesting group of compounds to study as besides being present in food, they can also be formed inside the body (endogenous formation). AGEs have been associated with multiple health effects. However, whether these are causal relations, what the underlying mechanisms are and to what extent these health effects can be attributed to endogenous or exogenous glycation products remains unclear.

The work presented in this thesis provides information regarding the relevance of the differences in toxicokinetics and toxicodynamics of exogenous as compared to endogenous glycation products (AGEs and their precursors) when evaluating the toxicological characteristics of dietary glycation products (**Chapter 2**) and focuses on the interactions between exogenous dietary AGEs and their precursors and the gut microbiota (**Chapters 3 – 6**), all studied from a toxicological perspective. Also in the field of toxicology increased interest has been shown in the role of the gut microbiota and its relevance for new toxicity testing strategies, which requires an interdisciplinary approach[13]. More information on the gut microbiota will be provided in Section **1.3**.

The current chapter of this thesis provides an introduction into glycation products (Section **1.2**), the gut microbiota (Section **1.3**) and how toxicological and microbial research can be combined (Section **1.4**). Eventually, the aim and outline of this thesis will be presented (Section **1.5**).
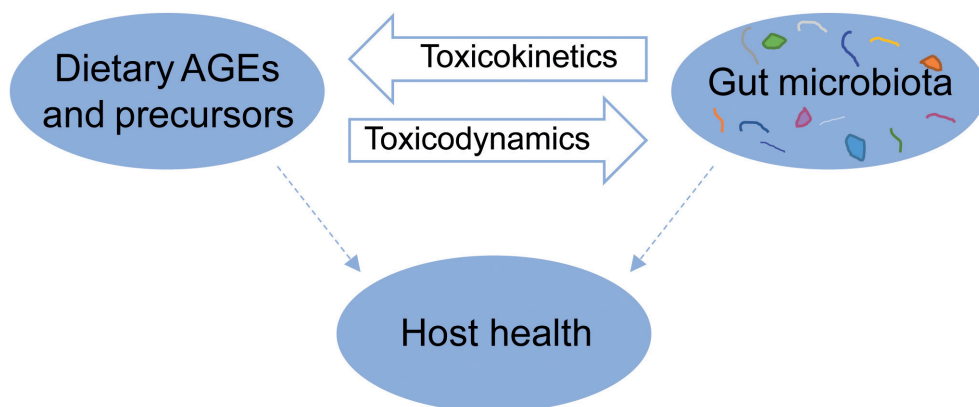
Figure 1.1 Dietary advanced glycation end products (AGEs) and their precursors can interact with the (human) gut microbiota bi-directionally. The gut microbiota can metabolize at least some of the dietary AGEs and precursors and thus have consequences for their toxicokinetic characteristics. In addition, exposure of dietary AGEs and precursors seem to result in effects on the gut microbiota itself and thus represent a toxicodynamic effect. Besides possible effects of dietary AGEs and their precursors on host health as mediated via the gut microbiota, dietary exposure to AGEs and precursors can also directly affect host health.

1.2 Glycation products

Glycation products can be formed upon heating and include compounds that are derived from the Maillard reaction. These comprise Amadori products (e.g. fructoselysine) which are early stage products formed via non-enzymatic reactions by binding of the carbonyl group of a reducing sugar to the amino group of an amino acid which can again turn into AGEs (e.g. carboxymethyllysine)[9,14] (**Figure 1.2**). In addition, reactive α-dicarbonyls, also often referred to as α-oxoaldehydes or just dicarbonyls as in this thesis, can react with the amine group of an amino acid which also leads to AGE formation (e.g. methylglyoxal, glyoxal, 3-deoxyglucosone)[9]. Whether the respective amino acid is in its free, peptide- or protein-bound form determines the formation of a free, peptide- or protein-bound AGE or precursor[15]. When multiple amino acid residues are involved in AGE formation, cross-linking AGEs can be formed which can result in cross-linking of proteins[9]. The involvement of different combinations of substances (i.e. different amino acids, reducing sugars, reactive dicarbonyls) in the formation of (precursors of) AGEs leads to an overall heterogenous group of compounds, of which only 5-10 derivatives have been actually detected and quantified in food[10]. These include AGEs such as carboxymethyllysine, carboxyethyllysine, MG-H1 and the precursor fructoselysine[7,8]. Whether the respective glycation product is a low molecular mass (LMM) (e.g. free) or high molecular mass (HMM) compound (e.g. protein-bound, cross-linked), is of relevance as the molecular mass can affect the toxicokinetic and toxicodynamic properties[15].

Human internal exposure to AGEs can result from exogenous dietary AGEs and their precursors, but also from endogenous formation of AGEs. This will be further introduced in the following paragraph.

1.2.1 Exogenous and endogenous AGEs and their precursors

As mentioned above, exogenous AGEs and their precursors can be present in the diet and are formed upon heating. Endogenous AGEs are in general formed via the same mechanisms as exogenous AGEs but at slower rates due to lower physiological temperatures. Many associations of AGEs with adverse health effects in humans and animals have been reported[12], such as cardiovascular diseases[16], diabetes[17] and effects on the gastrointestinal tract[18] including effects on the gut microbiota composition[19,20]. Exposure to dietary AGEs has also been associated with adverse biological effects[12,21,22] while also associations between endogenous AGE levels and adverse biological effects have been reported[23–25]. In addition, some dietary exogenous glycation products, such as for example carboxymethyllysine, MG-H1 and fructoselysine have been found to accumulate in plasma, organs (e.g. kidney, liver) and tissues[26–30]. However, the aforementioned associations between exogenous dietary AGEs and precursors, endogenous AGEs and adverse health effects are not observed consistently[12]. Differences in tested materials in human and animal studies (e.g. providing a heated diet high in AGEs versus administration of individual AGEs) could lead to differences in ADME characteristics and biological effects, as these differ between individual AGEs and precursors since they depend for example on whether the compounds are present in their LMM or HMM form[15]. The differences in toxicokinetics and toxicodynamics of different AGEs and precursors are reviewed and described in more detail in **Chapter 2**, in which characteristics of LMM and HMM glycation products and also of their dicarbonyl precursors are evaluated considering their exogenous or endogenous nature. The toxicodynamic effects of AGEs may relate to three mode of actions which are: binding to the receptor for AGEs (RAGE), dicarbonyl stress resulting in endogenous AGE formation, cross linking and protein damage, and interactions with the gut microbiota. This is also discussed in more detail in **Chapter 2** and related to the LMM or HMM forms of endogenous and exogenous AGEs and precursors.

Considering the differences in toxicokinetics and toxicodynamics of different AGEs and their precursors, there is a need for data relevant for individual glycation products. In this thesis especially the AGE carboxymethyllysine and its precursor fructoselysine are studied which are further introduced in the following paragraphs.

1.2.2 Fructoselysine

Fructoselysine is formed via a reaction between the reducing sugar glucose and the amino acid lysine, which is formed via a reversible Schiff base that rearranges into the Amadori product fructoselysine[14] (**Figure 1.2**). From fructoselysine, carboxymethyllysine (see Section **1.2.3**) can be formed via the Hodge pathway (a series of dehydration, fragmentation, oxidation and cyclization reactions)[14]. The daily intake of both free and protein-bound fructoselysine in the Western diet is reported to be 500-1,000 mg, corresponding to 7.1-14.3 mg/kg bw/day for a 70 kg adult[11]. When ingested, dietary fructoselysine seems to be bioavailable to some extent, as in rats 60% of the orally administered LMM fructoselysine could be recovered in urine[31,32]. HMM dietary fructoselysine exposure of rats resulted in a dose-dependent increase of fructoselysine in plasma, liver and kidney, of which the form (i.e. LMM or HMM fructoselysine) was not further characterized[30]. Humans who consumed a test meal high in fructoselysine (actual form not specified) excreted only ±3% of the ingested dose in urine and ±1% in feces within the 72 hours following intake[33]. The fate

of the remaining >95% was not elucidated. *In vitro* intestinal absorption experiments with Caco-2 monolayers showed that free fructoselysine is transported, albeit poorly, via simple diffusion[34] and dipeptide bound fructoselysine can be partially absorbed via the peptide transporter PEPT1[35]. HMM fructoselysine seems to be absorbed inefficiently and needs to be degraded to LMM forms prior to absorption by enzymes derived from the host and or/ microbiota in the intestinal tract[12,31,36]. In infants, excretion of fructoselysine upon exposure through administration of heat-treated milk protein was reported to be in urine up to 16% of the dose and in feces up to 55% of the dose[37]. Fecal excretion of fructoselysine seems to be higher in formula-fed (FF) infants compared to adults (fecal fructoselysine excretion being 55% of the dose for infants compared to 1% of the dose for adults)[33,37].

The incomplete recovery of orally administered fructoselysine implies that fructoselysine is metabolized in the body, and considering the low intestinal absorption this is likely to occur in the intestinal tract[19,33]. Gut microbiota present in fecal samples have been reported to be able to degrade fructoselysine as shown by *in vitro* small batch fermentations with human fecal samples[11]. In addition, specific microbes have been reported to be able to degrade fructoselysine (i.e. *Escherichia coli*[38], *Bacillus subtilis*[39], and *Intestinimonas butyriciproducens* AF211[40]). The latter studies revealed genes involved in the bacterial degradation of fructoselysine into fructoselysine-6-phosphate (i.e. frlD and yhfQ), which can subsequently be further metabolized by bacteria and eventually result in production of bacterial metabolites such as the short chain fatty acid (SCFA) butyrate as in the case for *I. butyriciproducens*[40].

Considering toxicodynamic effects, fructoselysine itself has not been shown able to interact with RAGE[41]. However, fragmentation of fructoselysine can lead to formation of the reactive dicarbonyls glyoxal and 3-deoxyglucosone[14,42,43], which can consequently lead to so-called dicarbonyl stress and to newly formed (HMM) AGEs (**Figure 1.2**). In addition, as previously mentioned, fructoselysine is of relevance as it is a direct precursor for the AGE carboxymethyllysine which is further introduced in the following paragraph.

1.2.3 Carboxymethyllysine
Besides formation via rearrangement of fructoselysine, the AGE carboxymethyllysine can be formed via reactions between lysine and the dicarbonyls glyoxal or 3-deoxyglucosone[9,44] (**Figure 1.2**). The daily intake of dietary carboxymethyllysine is reported to be 2.1 mg/day in a Western diet, corresponding to a daily intake of 0.3 mg/kg bw for a 70 kg adult[11]. Systemic uptake of dietary carboxymethyllysine seems to occur at least to some extent. In rats, orally administered HMM carboxymethyllysine was excreted in urine (26-29% of the dose) as well as in feces (15-22% of the dose)[30], likely being absorbed following intestinal degradation of the HMM form to the LMM form. Another study in rats reported comparable recoveries of carboxymethyllysine in urine upon oral exposure to HMM or LMM carboxymethyllysine[45]. However in humans no increases in urinary carboxymethyllysine were found upon providing a diet rich in carboxymethyllysine, of which the actual form, LMM or HMM, was not specified[46]. *In vitro* studies with Caco-2 monolayers showed that LMM carboxymethyllysine can be absorbed, albeit slow[34].

Considering the incomplete recovery of orally administered carboxymethyllysine and the possible degradation of HMM carboxymethyllysine into LMM carboxymethyllysine upon interaction with digestive enzymes[36], at least part of dietary administered carboxymethyllysine seems to be metabolized, possibly by the gut microbiota as carboxymethyllysine seems to reach the colon. Indeed, gut microbiota present in fecal samples have been reported to partly degrade carboxymethyllysine[11], and different individual bacterial strains have been reported to degrade carboxymethyllysine as well (i.e. *Escherichia coli*[47], *Cloacibacillus eryverenis*[48]).
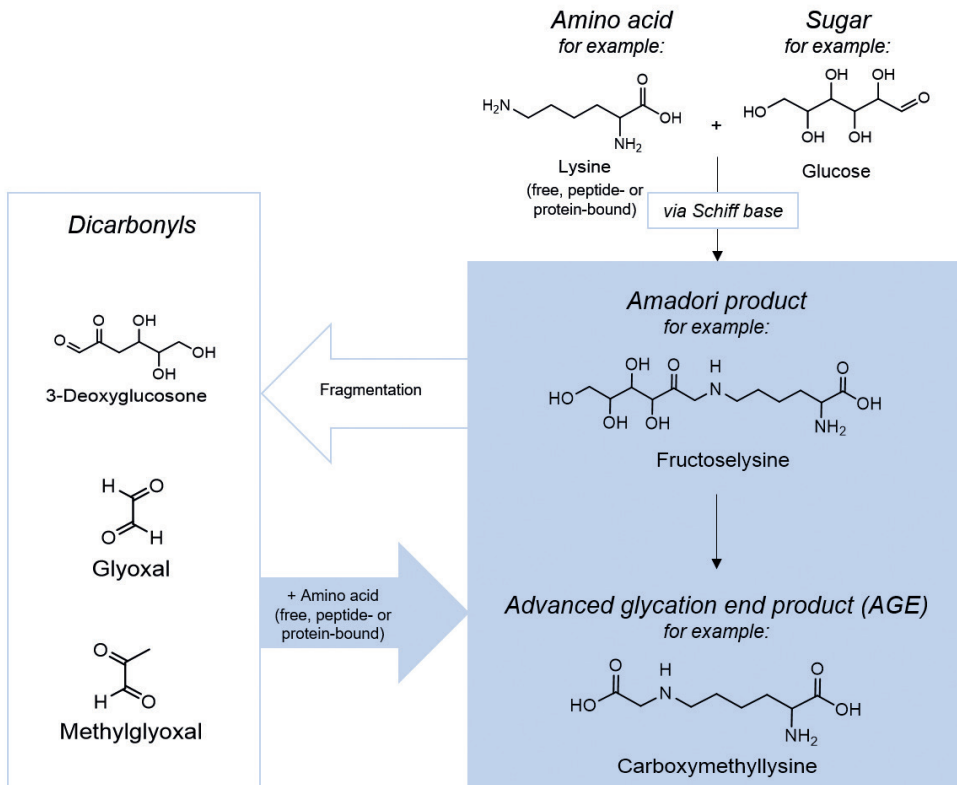
Figure 1.2 The Amadori product fructoselysine can be formed via reaction of lysine and glucose, and possible rearrangement reactions can result in formation of the advanced glycation end product (AGE) carboxymethyllysine. Reactive dicarbonyls (e.g. 3-deoxyglucosone, glyoxal and methylglyoxal) are also involved in AGE formation, for example a reaction between 3-deoxyglucosone or glyoxal with lysine can result in formation of carboxymethyllysine. Dicarbonyls can be formed via multiple pathways and also by fragmentation of early Maillard reaction products such as the Amadori product fructoselysine.

Considering toxicodynamic effects, carboxymethyllysine seems able to interact with RAGE but only in its HMM form and not in its free form[41,49]. Interactions with RAGE can lead to adverse effects, such as a pro-inflammatory response[50]. Relevant for both fructoselysine and carboxymethyllysine is that their exposure to the gut microbiota can lead to an additional

toxicodynamic effect. Multiple studies reported alterations in gut microbiota composition upon a heated diet rich in AGEs[19,20,51] and upon oral exposure to carboxymethyllysine alone as well[52]. Alterations of gut microbiota have been linked to disease[53] and thus it seems relevant to consider this effect when evaluating possible adverse effects of dietary AGEs. Besides this possible role for the gut microbiota in toxicodynamic effects of AGEs, the gut microbiota can also affect toxicokinetic properties (i.e. being involved in metabolism) as introduced above. The bi-directional interactions between dietary derived glycation products and the gut microbiota will be studied in this thesis, and thus the gut microbiota will be further introduced in the following section.

1.3 Gut microbiota

The human microbiome consists of trillion microorganisms which are dominated by bacteria but also include fungi, archaea, protozoa and viruses[54]. These microorganisms are located on and in the host organism being present for example on the skin, in saliva and with the highest amounts in the gastrointestinal tract[54]. The lower part of the gastrointestinal tract (e.g. the colon) harbors the highest microbial densities compared to upper parts of the gastrointestinal tract (e.g. the small intestine)[55]. The gut microbiota consists of a high diversity of different bacteria which encode a broad diversity of enzymes[56], and the gut microbiota play an important role in host health and disease[57]. For example the gut microbiota can synthesize essential vitamins and nutrients, is involved in digestion and plays a central role in bacterial colonization resistance and the immune system[56]. The gut microbiota can transform dietary ingested compounds (e.g. xenobiotics and nutrients) while on the other hand exposure to these ingested chemicals can also possibly affect the gut microbiota itself[58]. The latter can possibly induce a perturbation of the gut microbiota leading to an alternative, possibly unhealthy state[57] which is often referred to as dysbiosis[59].

The gut microbiota develops over age, depends on environmental factors and the host genotype[60–62]. Consequently, interindividual as well as interspecies differences considering the gut microbiota exist[63]. In the following sections the human and infant gut microbiota are further introduced followed by a section on possible methods to study interactions between dietary derived compounds and the gut microbiota.

1.3.1 Human gut microbiota
In humans, the colon harbors the highest density of bacterial cells in the gastrointestinal tract[55] of which the majority belongs to the bacterial phyla Firmicutes and Bacteroidetes[64]. The human genome is exceeded by the gut microbial genome by two orders of magnitude[54,65] and the subsequent diversity of biochemical and metabolic activities of the gut microbiota complement those of the host[65]. The human gut microbiota has been reported to be related to multiple diseased states including (chronic) gastrointestinal disorders, type 2 diabetes and obesity[66–68]. The human gut microbiota composition varies amongst individuals while, in spite of this variation, generic metabolic pathways were reported to remain relatively stable amongst a healthy human population[67]. The diet has been proposed to play a major role in shaping the gut microbial composition and function[62]. In addition to differences in gut microbiota between individuals, differences within one individual exist as well (i.e.

temporal variability)[69]. These intraindividual differences reflect the dynamic characteristics of the gut microbiota, as the gut microbiota is not a static ecosystem but changes over time[69]. These changes occur during ageing (e.g. the infant gut microbiota is distinct from the adult human gut microbiota, see Section **1.3.2**) but for example also upon changes in dietary habits[69]. In addition, as mentioned above, exposure to exogenous compounds (e.g. dietary or pharmaceutical-derived chemicals) can induce dysbiosis[59]. An obvious example of this is the administration of antibiotics which affect the gut microbiota composition[70], but also foodborne chemicals such as mycotoxins have been reported to affect the gut microbiota[71]. In addition, the metabolic capacity of the gut microbiota has been reported to be comparable in activity to that of the liver[65] and can be involved in biotransformation of dietary, industrial-derived and pharmaceutical-derived exogenous compounds as has been reported for e.g. polyphenolic compounds, melamine and certain anti-inflammatory drugs[56]. Together this comprises the possible bi-directional interactions between the gut microbiota and exogenous (dietary) derived constituents (i.e. toxicodynamics and toxicokinetics), and makes the gut microbiota a relevant "organ" to study from a toxicological perspective[13]. Models to study the role of the gut microbiota are further introduced in Section **1.3.3**.

1.3.2 Infant gut microbiota

The gut microbiota is shaped throughout life, with infancy being reported as a crucial time frame in human life for gut microbiota development[72]. The gut microbiota development in early life is of importance for infant health but can also have consequences later in life[73,74]. Multiple factors drive the infant gut microbiota development such as the mode of delivery, antibiotic use, host factors and the feeding mode[75]. Differences in the infant gut microbiota upon breast-feeding or formula-feeding have been reported and can be both of compositional and functional nature[76–79]. Reported differences between the gut microbiota of breast-fed (BF) and formula-fed (FF) infants include differences in the presence of specific *Bifidobacterium spp.*[72] and reported differences in the fecal metabolome[77,78]. Exclusive breastfeeding is recommended by the World Health Organization during the first six months of life[80] and offers complete nutrition for the infant[81]. The composition of breast milk is used as a reference for infant formula development, such as the presence of human milk oligosaccharides (HMOs) in breast milk[82] which are considered as key bioactive components[83] and known to influence the composition of the infant gut microbiota[84]. Advances have been made in infant formula development, such as including products which aim to mimic some of the benefits of HMOs (e.g. fructo-oligosaccharides, FOS, and galacto-oligosaccharides, GOS)[83,85]. However, despite several developments, the differences between the complex human milk composition and infant formula have not yet been overcome, and also include differences induced by food processing. Extensive heating is applied during the production process of infant formula to ensure microbial safety, which also introduces the formation of processing contaminants such as glycation products[86], including fructoselysine. Compared to human breast milk, fructoselysine is present in ~239-fold higher levels in infant formula[87] and this results in differences in dietary exposure to fructoselysine of BF and FF infants. Whether this difference in dietary fructoselysine exposure as part of the different types of nutrition (i.e. breast milk and infant formula) can be related to differences in the infant gut microbiota is further investigated in **Chapter 5**.

1.3.3 Models to study the gut microbiota

Different aspects of the gut microbiota can be studied. As mentioned above, both the role of the gut microbiota in metabolism can be studied (toxicokinetics) as well as the effect on the gut microbiota itself (toxicodynamics). Depending on the research question, a suitable model can be selected. Both *in vitro* as well as *in vivo* models exist, which all have advantages and disadvantages.

In this thesis, an *in vitro* model is applied to study toxicokinetics. The model consists of anaerobic incubations of fecal samples with the substrate of interest (**Chapters 3, 4, 5**). Fecal samples have been widely applied to study the gut microbiota and present major advantages over the use of samples directly taken from the gut (e.g. by naso- and oro-intestinal catheters[88]), as the collection of fecal samples is easier, cheaper and implies less discomfort for the donating volunteer. These advantages also make it relatively easy to collect samples from multiple individuals, enabling the study of inter- as well as intraindividual differences. It is of interest to note that although fecal samples are not sampled directly from the colon several studies reported that the microbiota in fecal samples are comparable to those in the colon[89–91], supporting the use of the anaerobic fecal incubations as a model for metabolism by the human gut microbiota. In **Chapter 6** an *in vivo* mice model was used to study toxicodynamics, since the *in vitro* model applied in the other chapters does not include a host compartment. The latter is needed when the role of the gut microbiota in host health, for example upon dietary exposure, is of interest, as an *in vivo* model can cover the interplay between the gut microbiota and the host[92] and can thus be of relevance to study toxicodynamic effects. A mice model was used since these have been widely applied before to study specific or generic interactions between the gut microbiota, the host and e.g. diets or pharmaceuticals[92].

The bacterial composition of the fecal samples studied in this project has been analyzed by 16S rRNA amplicon sequencing. With this widely used method, primers target a variable region of a gene of interest which is amplified and subsequently sequenced, in order to assess the bacterial taxonomy of the sample of interest[93]. This is a relatively fast and affordable method to obtain information on the bacterial composition. However, the taxonomic resolution is often limited to genus level and thus does not provide all information as bacteria can differ up to species and strain level[93]. With metagenomic sequencing all microbial genomes within the sample of interest are sequenced which can provide information on a higher taxonomic resolution compared to 16S rRNA amplicon sequencing[94]. However, metagenomic sequencing is more cost- and time intensive compared to 16S rRNA amplicon sequencing[93].

Another option to gain information on the actual functional output is to measure the metabolome in fecal samples or upon *in vitro* experiments. This metabolomics approach provides a functional readout of the gut microbiota[91], often obtained by the application of mass-spectrometry techniques[95]. With this approach a wide range of small molecules resulting from biochemical pathways can be measured[96]. The metabolome can provide insights in effects induced by an exogenous exposure on the gut mcirobiota[95,97] and might thus be suitable to study toxicodynamics. Mass-spectrometry techniques can also be applied to quantify a specific, targeted chemical of interest, as done in this thesis. This can be used to quantify the toxicokinetic effects of the gut microbiota on the substrate of interest. Inter-

and intraindividual differences in substrate depletion and metabolism attributed to the gut microbiota can be quantified, and *in vitro* obtained data can be further extrapolated to the *in vivo* situation, as will be introduced in the following section (**1.4**).

1.4 Integrating microbiological research in toxicological test strategies

Current developments in toxicological test strategies aim to improve prediction of adverse events, to reduce the use of *in vivo* animal tests, and to develop human relevant methods for risk assessment. In line with this, the term new approach methodologies (NAMs) has been introduced which refers to methodologies that combine the use of *in vitro* assays and *in silico* methods, to facilitate extrapolation of *in vitro* obtained results to the *in vivo* situation by QIVIVE (quantitative *in vitro* to *in vivo* extrapolation), the latter for example by using physiological based kinetic (PBK) models[98,99]. PBK models describe the ADME characteristics of a chemical by using mathematical equations and by including different compartments of the human body. These ADME characteristics (describing toxicokinetics) are relevant for the eventual toxicological outcome of the chemical of interest. Metabolism can for example be described by obtaining *in vitro* Michaelis-Menten kinetic parameters (i.e. V_{max}, K_m and kcat)[99] which can be used as input parameters in a PBK model[100]. Considering the metabolic capacity of the gut microbiota as introduced in Section **1.3**, it would be relevant to also be able to describe the role of the gut microbiota for toxicokinetics, when this is applicable for the chemical of interest. Previous studies have indeed successfully included a compartment of the gut microbiota in a PBK model[100,101]. The *in vitro* anaerobic fecal incubations used in this thesis were optimized to be able to describe and quantify gut microbial metabolic activities, in order to enable adequate kinetic quantification of interindividual as well as intraindividual differences. With this approach focusing on the quantification of gut microbial kinetics, the role of the gut microbiota can be integrated in toxicity test strategies. Moving from composition to function in gut microbial research[91] will be a prerequisite for toxicological test strategies.

1.5 Aim and outline of the thesis

The aim of this thesis was to characterise effects of selected foodborne glycation products on the gut microbiota and vice versa, and of interindividual and intraindividual differences in gut microbial reactions using the Amadori product fructoselysine and the AGE carboxymethyllysine as the model compounds. This will contribute to the better understanding of this bi-directional interaction between the gut microbiota and AGEs and their precursors known to be present in food.

In this chapter, **Chapter 1**, background information and the aims and outline of the thesis are presented.

To better understand the potential toxicity of foodborne glycation products, toxicokinetics and toxicodynamics of both exogenous and endogenous AGEs and their precursors are compared and reviewed in **Chapter 2** taking into account the differences in these characteristics for HMM and LMM compounds.

In **Chapter 3** the gut microbial metabolism of the LMM AGE precursor fructoselysine was quantified. A human-based *in vitro* model consisting of anaerobic fecal incubations was applied to quantify interindividual differences in the kinetics of gut microbial fructoselysine degradation and SCFA formation. 16S rRNA amplicon sequencing of the applied human fecal samples was performed to obtain insight in microbial taxa of possible relevance.

In **Chapter 4** a similar *in vitro* approach was applied to study interindividual differences but also intraindividual differences in the gut microbial degradation activities of both the LMM AGE carboxymethyllysine and its LMM precursor fructoselysine. Intraindividual differences were quantified to include the dynamic aspects of the gut microbiota. The gut microbial degradation activities of fructoselysine and carboxymethyllysine were compared, and microbial taxa of possible relevance in these reactions were analyzed by 16S rRNA amplicon sequencing.

In **Chapter 5**, functional differences in the gut microbial fructoselysine degradation activities of BF and FF infants were evaluated, in view of their different diets and resulting fructoselysine exposures. This study aimed to provide combined insight in the bi-directional interaction between the gut microbiota and dietary fructoselysine exposure.

In **Chapter 6** *in vivo* toxicodynamic effects of a heated diet high in AGEs on the gut microbiota of mice were assessed, in addition to the effects of the AGE exposure on the AGE levels in plasma, kidney and liver, and the question of whether the observed effects were reversible.

Finally in **Chapter 7,** the results of the previous chapters are discussed in some more detail and placed in a wider perspective. The effects of dietary AGEs and their precursors on human health are discussed, as well as the applicability domain of the applied *in vitro* model and how to move from association to causation. In addition, dietary and gut microbiological research is discussed from a toxicological perspective and future research perspectives for dietary glycation products related to human health are provided.
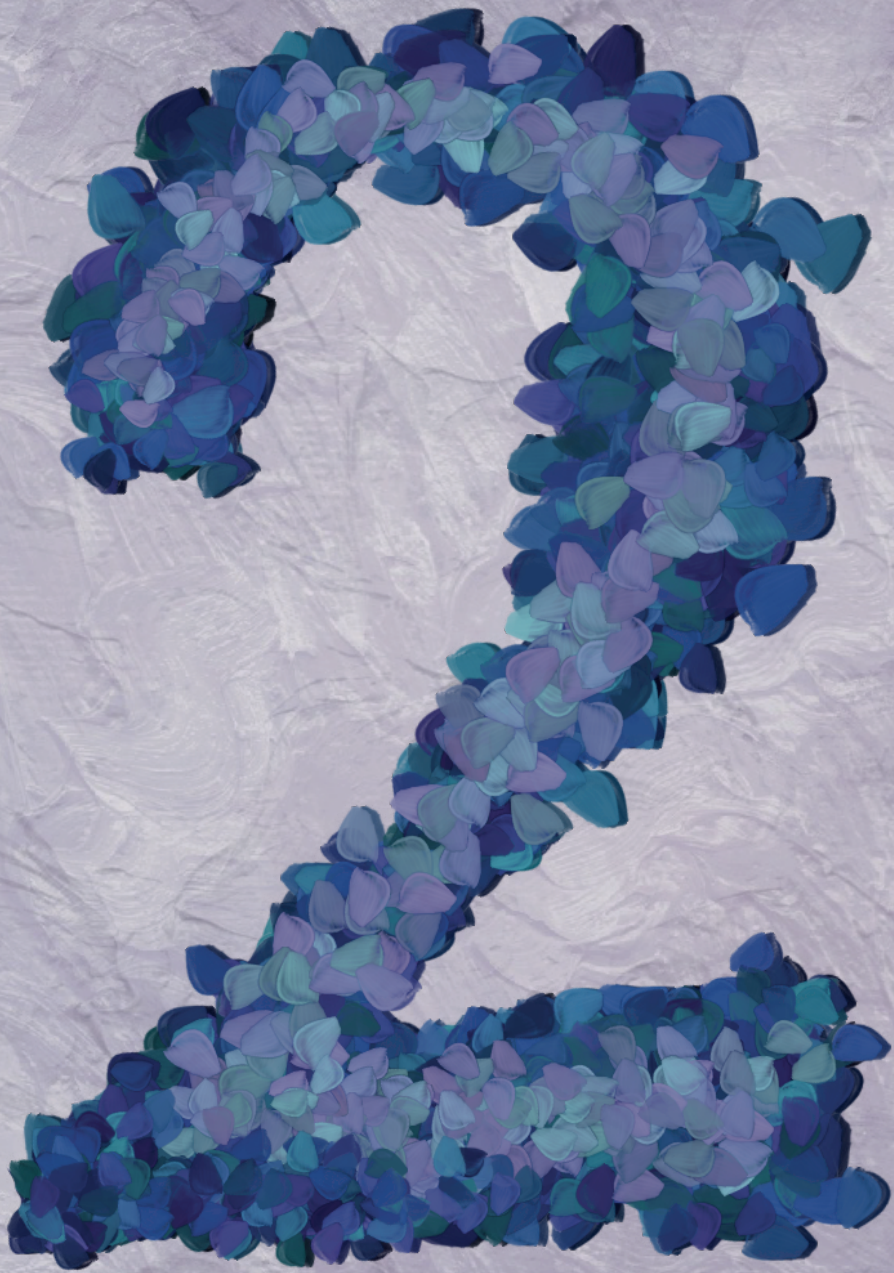
Differences in kinetics and dynamics of endogenous versus exogenous advanced glycation end products (AGEs) and their precursors

Katja C.W. van Dongen, Leonie Kappetein, Ignacio Miro Estruch, Clara Belzer, Karsten Beekmann, Ivonne M.C.M. Rietjens

Abstract

Advanced glycation end products (AGEs) and their precursors are a heterogenous group of compounds being associated with adverse health effects. AGEs can be formed endogenously and in exogenous sources including food. This review investigates the roles of endogenously versus exogenously formed AGEs in the potential induction of adverse health effects, focusing on differences in toxicokinetics and toxicodynamics of low molecular mass (LMM), high molecular mass (HMM) AGEs and their (dicarbonyl) precursors. Based on the available data, exogenous LMM AGEs seem to be bioavailable and together with their precursors they may contribute to dicarbonyl stress and protein cross linking resulting in formation of endogenous AGEs. Bioavailability of exogenous HMM AGEs and precursors appears limited, while these can bind to the AGE receptor (RAGE), initiating adverse health effects. Together, this suggests that adverse health effects via RAGE-binding in relevant tissues will more likely result from endogenously formed AGEs. Effects on gut microbiota composition and functionality induced by AGEs and their precursors is proposed as a third mode of action. Overall, there is a need for studies which better discriminate between free and peptide or protein-bound AGEs and their precursors in order to enable further elucidation of the contributions of these different types of glycation products to the ultimate biological effects.

2.1 Introduction

Glycation products are a heterogenous group of compounds which include advanced glycation end products (AGEs) and their precursors such as Amadori products and reactive dicarbonyls. AGEs have been associated with adverse health effects (i.e. chronic diseases, atherosclerosis, inflammation) in both human and animal studies[23–25]. AGEs can be formed endogenously (i.e. in the host) but are also abundantly present in exogenous sources such as food products and tobacco smoke[12]. Especially in the Western diet AGEs and their precursors are abundant[102,103]. The question remains however to what extent exogenous glycation products contribute to the endogenous AGE pool and to the associated potential adverse health effects. This review aims to provide a state-of-the-art overview of the toxicokinetics and toxicodynamics of endogenously formed and exogenous dietary AGEs and their precursors in order to evaluate their potential contributions to the adverse effects on human health, herein distinguishing between free, low molecular mass (LMM), and protein-bound, high molecular mass (HMM) glycation products and their dicarbonyl precursors.

First, an overview of the types of glycation products considered in this review will be presented. The second section of this review will give an overview of the toxicokinetics of exogenous and endogenously formed AGEs and their precursors. The third section of the review provides an overview of the toxicodynamics and modes of action in the host. Finally, the findings will be discussed and recommendations for future research will be provided.

2.2 Endogenous and exogenous glycation products

Exposure to glycation products results from endogenous formation or from intake of glycation products formed exogenously and present in for example food or cigarette smoke. Due to the involvement of various precursors (e.g. dicarbonyls), multiple amino acid residues, and the formation of free and peptide- or protein-bound AGEs and precursors, the glycation products formed are a heterogenous group of compounds, consisting of cross-linked and non-crosslinked, HMM and LMM AGEs and precursors. HMM glycation products refer to products formed by reaction with a protein-bound amino acid residue while LMM glycation products refer to products formed by reaction with a free amino acid residue.

2.2.1 Exogenous formation of AGEs and their precursors

Exogenous AGEs and their precursors present in food products (i.e. bread, milk (powder), processed food products) can be formed at high rates during heating applied to improve the quality and taste of the product, its shelf life, for safety reasons, or to produce the desired food product[12]. During this process, AGEs and their precursors are formed via multiple pathways of the non-enzymatic Maillard reaction[9,104–107]. First of all, the carbonyl group of a reducing sugar can bind to the amino group of a free, protein-bound or peptide-bound amino acid, forming a (reversible) Schiff base that spontaneously forms so-called Amadori products. These Amadori products are relevant precursors for AGEs as they can rearrange into AGEs via the Hodge pathway, which is a series of reactions including dehydration, fragmentation, oxidation and cyclization[106,108]. In addition to formation of AGEs via the Hodge pathway, the Schiff base or the covalently-bound Amadori product precursors can also be decomposed

via the Namiki pathway into reactive dicarbonyls, also referred to as α-oxoaldehydes (i.e. methylglyoxal, glyoxal, 3-deoxyglucosone)[106,108,109]. These reactive dicarbonyls can react with an unbound or bound amino acid and in this way form AGEs. Among the most abundant and most frequently studied Amadori products and AGEs in food are fructoselysine (FL), which is formed from glucose and lysine[8], and Nε-(carboxymethyl)lysine (CML)[110] which is formed by rearrangement from FL or via a reaction between lysine and the dicarbonyls glyoxal or 3-deoxyglucosone, respectively. Other AGEs include compounds like pyrraline, hydroxymethylfurfural (HMF), Nε-(carboxyethyl)-lysine (CEL) and Nδ-(5-hydro-5-methyl-4-imidazolon-2-yl)-ornithine (MG-H1) (**Figure 2.1**).

Reactive dicarbonyls are involved in the formation of multiple AGEs. The dicarbonyl glyoxal can form CML by reacting with lysine side chains[44]. By reacting with a cysteine group, the irreversible end-product S-carboxymethylcysteine can be formed[111]. If glyoxal reacts with arginine, more complex reactions occur leading to multiple glyoxal-arginine derived AGEs (i.e. carboxymethylarginine, the intermediates G-DH1 (N-(3,4-dihydroxy-1-imidazolidin-2-yl)ornithine) and G-DH2 ((5-(4,5-dihydroxy-2-imino-1-imidazolidinyl)norvaline)) and the subsequent imidazolone-derivatives G-H1, G-H2, G-H3)[9] (**Figure 2.1**). The dicarbonyl methylglyoxal is also involved in formation of multiple AGEs. Reaction with lysine residues can lead to CEL formation[112], while reactions with arginine residues can give rise to multiple products depending on the number of nitrogen atoms involved in cyclization and the pH. As such, MG-H1, MG-H2 (2-amino-5-(2-amino-5-hydro-5-methyl-4-imidazolon-1-yl)pentanoic acid) or MG-H3 (2-amino-5-(2-amino-4-hydro-4-methyl-5-imidazolon-1-yl)pentanoic acid) can be formed[113] (**Figure 2.1**). The dicarbonyl 3-deoxyglucosone can form the AGEs CML and pyrraline by reacting with lysine residues[114–117]. When 3-deoxyglucosone reacts with arginine residues, multiple products can be formed including 3DG-H1 (N-(5-hydro-5-(2,3,4,-trihydroxybutyl)-4-imidazolon-2-yl)orthinine), 3DG-H2 (5-(2-amino-5-hydro-5-(1,2,3-trihydroxybutyl)-4-imidazolon-1-yl)norvaline) and 3DG-H3 (5-(2-amino-4-hydro-4-(2,3,4-trihydroxybutyl)-5-imidazolon-1-yl)norvaline)[118] (**Figure 2.1**).

When dicarbonyls such as glyoxal, methylglyoxal and 3-deoxyglucosone react with two amino acid residues (both lysine or arginine) this leads to imidazole cross-linked AGEs such as GODIC (N6-(2-{[(4S)-4-ammonio-5-oxido-5-oxopentyl]amino}-3,5-dihydro-4H-imidazol-4-ylidene)-L-lysine) and GOLD (6-{1-[(5S)-5-ammonio-6-oxido-6-oxohexyl]imidazolium-3-yl}-L-norleucine) resulting from reactions with glyoxal, MODIC (2-ammonio-6-({2–[4-ammonio-5-oxido-5-oxopently)amino]-4-methyl-4,5-dihydro-1H-imidazol-5-ylidene}amino)hexanoate) and MOLD (6-{1-[(5S)-5-ammonio-6-oxido-6-oxohexyl]-4-methyl- imidazolium-3-yl}-L-norleucine) with involvement of methylglyoxal and DODIC (N 6 -{2-{[(4S)-4-ammonio-5-oxido-5-oxopentyl]amino}-5 -[(2S,3R)-2,3,4-trihydroxybutyl]-3,5-dihydro-4H-imida-zol-4-ylidene}-L-lysinate) and DOLD (1,3-di(Nε-lysino)-4-(2,3,4-trihydroxybutyl)-imidazolium) involving 3-deoxyglucosone[9] (**Figure 2.1**). When adduct formation or crosslinking occurs in proteins, HMM AGEs are formed.

In addition to the above mentioned major pathways of AGE formation, dicarbonyls and thus eventually AGEs can also be formed via lipid peroxidation of polyunsaturated fatty acids (PUFAs)[9] or via autoxidation of monosaccharides (i.e. Wolff pathway)[25,119].

2.2.2 Endogenous formation of AGEs and their precursors

In endogenous formation of AGEs and their precursors, the same pathways as described above that proceed via non-enzymatic reactions are involved, although they occur at lower rates compared to exogenous formation due to the lower physiological temperatures. In addition, specific endogenous AGE formation pathways include glycolysis and the so-called polyol pathway.

General metabolism of glucose or fructose via glycolysis can lead to formation of reactive metabolites including glyceraldehyde and methylglyoxal. Glyceraldehyde 3-phosphate and dihydroxyacetone phosphate, formed via glycolysis, can spontaneously and non-enzymatically degrade to methylglyoxal[120,121]. The formed methylglyoxal can react with (un) bound amino groups resulting in AGE formation. The AGE pentosidine can be formed by rearrangement of pentose-derived Amadori product precursors, but can also be formed in a reaction between lysine or arginine residues with e.g. ascorbate, 3-deoxyglucosone or glyceraldehyde[9]. The polyol pathway is active under hyperglycemic conditions and involves sorbitol formation from glucose. Sorbitol can be oxidized to fructose via sorbitol dehydrogenase[25,116]. Over-activation of this pathway leads to an increase in dicarbonyl formation via accumulation of upstream metabolites such as fructose[25].

Besides the above-mentioned endogenous glycation product formation pathways, endogenous lipid peroxidation, resulting from reactive oxygen species (ROS)-induced lipid peroxidation of PUFAs in biological membranes, can also lead to increased dicarbonyl and subsequent AGE formation[9]. AGEs formed via reactive dicarbonyls produced by lipid peroxidation are also referred to as ALEs (advanced lipoxidation end products), which in some cases can lead to the same reaction products because lipid peroxidation may result in the same reactive dicarbonyls[9]. In this review, we focus on the AGEs while ALEs which are formed exclusively and only following lipid peroxidation are not explicitly included.

Specific for endogenous Amadori product precursor and AGE formation is the formation of glycated albumin and hemoglobin (HbA1C), the latter having a widespread use as a biomarker to monitor glycemic control[122]. The Amadori product glucosyllysine can form a cross-linking adduct with arginine side chains, forming glucosepane[9], which is the most abundant cross-linking AGE found in extracellular matrix related to ageing and diabetic complications[123,124]. Another example is the AGE pyrraline which can form cross-links with cysteinyl thiol groups or other pyrraline adducts under oxidative conditions.

2.3 Toxicokinetics

Several studies have reported on toxicokinetics of AGEs and their precursors using either *in vitro,* animal or human based models. One important aspect to consider when evaluating literature studies is which analytical methods were used for quantifying and characterizing the studied glycation products[10]. General methods such as immuno-based methods or methods based on fluorescence which are unable to differentiate between the different glycation products have been frequently used, while more recently the application of liquid chromatography tandem mass spectrometry (LC-MS/MS) methods provides possibilities to

quantify and characterize individual AGEs and their precursors. In this section, we provide an overview of toxicokinetic characteristics of AGEs and their precursors published in literature based on the more specific and therefore preferred LC-MS/MS based methods, unless data using these methods were unavailable.
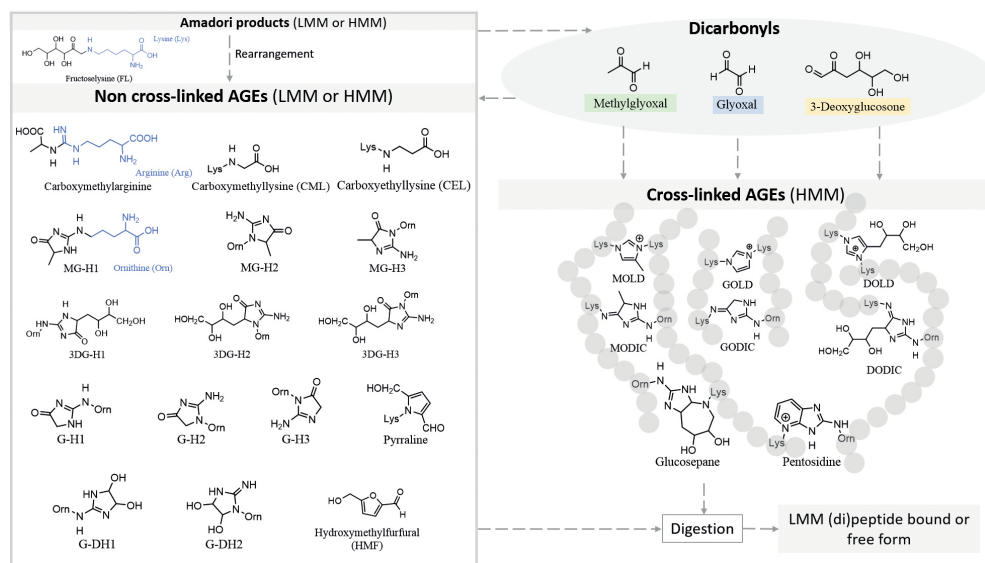

Figure 2.1. Structural formulas of AGEs and their precursors mentioned in-text including both non-crosslinked and cross-linked AGEs, Amadori product precursors and dicarbonyl precursors. Part of the structures visualized in blue show the structure of abbreviated side-chains. Abbreviations: AGE = advanced glycation end product; LMM = low molecular mass; HMM = high molecular mass. Structural formulas were compiled with ChemDraw 18.

2.3.1 Absorption

Studies reporting urinary excretion, plasma or tissue levels of AGEs upon their oral administration provide support for the absorption and systemic bioavailability of exogenous AGEs and their precursors[26,27,125–128]. However, these studies often do not quantify the actual levels of LMM glycation products and protein-bound glycation products consumed by the study subjects. Some studies however do characterize whether the AGEs or precursors dosed are given in their LMM or HMM. These studies reveal that dietary LMM glycation products like free FL are readily absorbed and bioavailable. In rats for example up to 60% of orally administered LMM labelled FL was recovered in urine[31]. In contrast, urinary FL excretion upon oral intake of LMM FL appeared to be substantially lower reported to amount to generally less than 10% of the dose in both rats and adult human, tested 3 up to 10 days upon exposure[30,129,130].

In young children, the excretion of FL upon administration of heat-treated milk protein was reported to be somewhat higher amounting to levels up to 16% of the dose in urine and up to 55% in feces[37], but in this study the % of LMM versus HMM FL and/or the potential presence

of dicarbonyl precursors in the administered heat treated milk sample remained undefined. The difference in absorption and bioavailability upon oral intake between LMM and HMM forms of the same AGE or precursor can be ascribed to the fact that HMM AGEs themselves cannot be absorbed efficiently but need to be degraded to LMM forms first by host and/or microbiota derived enzymes from the intestinal tract before being absorbed[12,31,131,132]. In line with the results for FL and these considerations, also free or dipeptide-bound CML was shown to be readily absorbed *in vitro* and in rats, while HMM CML may be absorbed less efficiently in mice due to insufficient release by the digestive enzymes and/or microbiota derived enzymes[12,131–133], with up to 30% of ingested casein-linked CML excreted in urine of rats[30].

In another study, 2 week oral exposure of mice to a diet containing 9.4-fold higher levels of total CML (exact form not defined) compared to the control diet, exposure to the diet high in CML did not result in an increase in LMM or HMM CML in the systemic circulation, whilst administration of a single oral dose of free LMM CML to rats resulted in an increase of free LMM CML in plasma reaching a C_{max} at 1 hour[134]. Another study on the uptake of CML in rats reported comparable recoveries for total CML in urine upon dosing HMM or LMM CML, suggesting that CML in both forms may be absorbed to a similar extent[45].

The limited systemic availability of HMM CML is also supported by the observation that dosing a diet rich in Maillard reaction products to adolescents did not result in an increase in urinary CML levels while fecal CML levels were 2.86 fold higher[135]. For other AGEs this may be different although studies using diets with Maillard reaction products cannot be fully conclusive when they do not discriminate between the levels of LMM or HMM AGEs and/or the presence of precursors actually consumed by the volunteers. In the case of exposure to HMM dietary AGEs and precursors via consumption of a diet rich in Maillard reaction products, proteolytic breakdown and/or metabolic degradation of the HMM protein-bound AGEs in the intestinal tract may be required to facilitate absorption and subsequent urinary excretion[32]. The fact however that consumption of a diet free of Maillard reaction products lowers the urinary excretion of free LMM pyrraline and FL by values up to 90% and that of free LMM pentosidine by 40%[32] supports that LMM AGEs or LMM AGE precursors originating form dietary exposure are bioavailable and may provide a substantial contribution to endogenous LMM AGEs and their precursors. In a study dosing eight diabetic patients with an AGE rich diet generated by heating chicken egg white with fructose at 90°C, a substantial increase in crosslinking AGE reactivity in serum and urine was detected a few hours post dosing[27] also supporting that at least part of the exposed AGEs and/or their precursors may be bioavailable. Given this result it is of interest to note that a study in which 500 micromole of methylglyoxal were ingested by human volunteers did not result in an increase of excreted methylglyoxal in 24 hours collected urine, while incubations of methylglyoxal in an *in vitro* simulated gastric and intestinal digestion model without gut bacteria revealed that only 20% of the initial methylglyoxal could be recovered after 8 hours[136]. Based on these results the authors concluded that dietary methylglyoxal is rapidly degraded during the digestion process in the intestine, and therefore of no influence on the systemic levels of methylglyoxal. A comparable study with 3-deoxuglucosone however led to an increase in urinary excretion of this AGE precursor, supporting that the compound is bioavailable[137].

It should be noted however, that in other *in vitro* studies with simulated gastrointestinal digestions mimicking the upper part of the gastrointestinal tract including oral, gastric and small intestinal phases reported dicarbonyl compounds and also dietary HMM AGEs to be almost unaltered[138,139]. Additional small batch fermentations with individual fecal slurries, however, resulted in decreasing concentrations of 3-deoxyglucosone, methylglyoxal and glyoxal[138].

In vitro studies using Caco-2 cell layers provided evidence that some free AGEs including CML are most likely transported across the intestinal barrier via passive diffusion[34], whereas for dipeptide bound AGEs active apical transporters, like the human intestinal peptide transporter (hPEPT1), may play a role, after which intracellular hydrolysis results in release of the free AGEs transferred via passive diffusion to the systemic circulation[35,140,141].

Taken together, it appears that only LMM AGEs and LMM AGE precursors may end up in the systemic circulation and contribute to the endogenous exposure[12]. Zhao et al. (2019) speculated that free AGEs might be less bioavailable than peptide-bound AGEs as uptake of free AGEs via diffusion can be slow and might be rate limiting while peptide-bound AGEs can enter the systemic circulation via multiple routes (e.g. paracellular, via hPEPT1)[142]. HMM protein-bound AGEs themselves are not absorbed efficiently but first require degradation to LMM forms, while bioavailability of LMM AGE precursors can contribute to the formation of endogenous LMM and HMM AGEs.

2.3.2 Distribution
Once absorbed, the LMM AGEs and precursors are detectable in plasma and distributed to various tissues including liver and especially the kidneys where they appear to accumulate. For example upon dosing of casein-bound FL to rats, the levels of protein-bound FL in whole kidneys were increased over 17- and 33-fold above control values (at low dose of 71.4 mg/day and high dose of 474 mg/day, respectively) while those in whole liver increased by only 1.1 and 1.4-fold[30]. Upon dosing casein-CML in a low and high dose (40 mg/day and 127.3 mg/day, respectively), concentrations of CML in whole kidney increased 269 and 741-fold and in liver tissue 1.0 and 1.2-fold for low and high dose, respectively[30] pointing at differences between these two model compounds and their major accumulation in the kidney compared to the liver. A high percentage of the FL, amounting to up to 27% of high dose casein FL administered to the rats, appeared to accumulate in the kidneys, while for the casein-CML administered rats this value amounted to only 1.4%. Levels of FL in kidney and liver after the control diet were higher compared to CML levels in the tissues after the control diet, indicating endogenous FL formation as FL content in the control diet was below the limit of detection (0.3 pmol)[30]. It is important to note that prior to absorption casein-bound FL and CML were likely degraded to LMM forms in the intestine.

For FL this relatively high level of distribution to the kidney as compared to the liver has been ascribed to the possible involvement of active transporters into the kidney[129], while uptake in the liver may proceed be limited to passive diffusion[143]. Later studies concluded that macrophage scavenger receptors expressed by liver endothelial cells are involved in uptake and subsequent lysosomal degradation of AGEs in the liver via endocytosis as studied

using uncharacterized AGE-BSA (bovine serum albumin) [144]. However the contribution of this system is debated to be also dependent on the sites and degree of the glycated proteins[145] and occurs slowly and is impaired by AGE-BSA exposure itself[146].

In a study with mice, long-term exposure for 30 days to $^{13}C_2$-labelled BSA-bound CML administered through the diet (at a dose of 40 mg/kg bw/day) compared to a low exposure in the control group (0.3 mg/kg bw/day) resulted in high accumulation of $^{13}C_2$-labelled CML in kidney, ileum, colon and lungs, and increased accumulation, although with up to 39-fold lower levels, in brain, testis, heart, muscle and liver tissue[29]. However, no distinction was made within this study between protein-bound and free levels of CML accumulating in the tissues as this was not part of the analysis. $^{12}C_2$-CML levels measured in kidney, ileum, colon and lungs – potentially both from exogenous and endogenous origin – were 5 to 9-fold lower compared to the $^{13}C_2$-levels exclusively from dietary origin[29]. These results show that dietary, protein-bound HMM CML significantly increased CML levels in multiple tissues, with high accumulation in the kidney, ileum, colon and lungs. In general, relevant to consider for distribution of AGEs to certain tissues is an AGE-exposure induced increase in the permeability of endothelial cells[147].

Upon oral administration of free CML (at a dose of 60 mg/kg bw/day) to rats fed a high fat diet for 12 weeks an increase in protein-bound CML levels was reported in the kidney (2.07-fold), heart (1.27-fold), lung (1.19 fold), pancreas (1.70-fold), and muscle (1.48-fold), whereas no statistical increase was found in the liver and spleen[133]. In a similar study from the same authors, oral administration of free CML (60 mg/kg bw/day for 12 weeks) combined with a regular diet and not a high fat diet as in their other study, a significant increase in protein-bound CML compared to the control was found in kidney (2.06-fold), liver (1.55-fold), heart (1.86-fold) and the lungs (1.41-fold) but not in the spleen, pancreas and serum[148]. It has to be noted that the dose of free CML administered in these studies is far above the normal estimated total (both free and protein-bound) dietary CML intake of 0.034–0.252 mg/kg bw/day for adults[21]. Given these generally less than 2-fold increases in the tissue levels of protein-bound CML upon long term intake of a dose level of free CML that exceeds normal dietary intake 2 to 3 orders of magnitude, this result implies that increases in tissue levels of protein-bound CML upon normal dietary intake of free CML may be negligible.

Other studies reported that higher AGE content of the diet resulted in an increased AGE level in serum[23]. In another study in 20 overweight but healthy individuals a two-week low AGE diet resulted in a decrease in the AGEs MG-H1, CML and CEL in their free form in urine but not in protein-bound levels in serum as measured by LC-MS/MS[149]. In a study with 261 adults, no correlation was found between dietary intake as assessed by a dietary recall and serum and urinary CML, quantified using immunobased methods[150]. The CODAM study included 450 individuals and found a positive correlation between dietary intake of protein-bound CML, CEL and MG-H1 and their free levels in both plasma and urine, but -again- not with their protein-bound form[26]. This indicates that – at least in humans – upon dosing protein-bound HMM AGEs degradation to LMM peptide-bound or free forms is a prerequisite for systemic availability.

A recent study in mice did distinguish between protein-bound and free CML, CEL and MG-H1 in both the diet and in tissues and plasma. A heated diet was orally administered for 10 weeks and compared to a standard diet. The heated diet contained increased levels of both free AGEs and protein-bound AGEs, with the latter covering the largest proportion. After 10 weeks of dietary intervention both free and protein-bound CML and CEL were increased in plasma in the mice receiving the heated diet, while MG-H1 was only increased in its free form. In liver only free CML and free MG-H1 were increased, while in kidney CML, CEL and MG-H1 were increased in their free form and only CML was increased in its protein-bound form[151]. This corroborates that free AGEs might be the preferred form in which protein-bound AGEs become bioavailable. In addition, the results for the three AGEs characterized in the study (i.e. CML, CEL and MG-H1) differed in their responsive patterns in both plasma and tissues, pointing at AGE specific kinetics and the importance of characterizing and measuring individual AGEs in both protein-bound and free forms.

In a study on the improvement of insulin resistance in human type 2 diabetic patients by restriction of glycation products in the diet it was reported that compared with nondiabetic healthy control individuals, the type 2 diabetic patients showed significantly higher fasting blood glucose, and higher serum levels of CML and methylglyoxal before the intervention. In these diabetic subjects a 50% dietary AGE restriction resulted in lower levels of serum CML and methylglyoxal and also of intracellular methylglyoxal compared to the levels before the intervention. Healthy subjects on the AGE restricted diet also showed reduced serum CML and methylglyoxal levels but intracellular levels of CML and methylglyoxal were unaffected. Thus, for both diabetic and healthy subjects there appeared to be a significant association between dietary AGEs and AGE level in serum[152]. A difference in serum CML and methylglyoxal levels upon intake of a diet high or low in total CML and methylglyoxal was also reported in non-obese diabetic (NOD) mice, supporting a correlation between ingested AGEs and AGEs in the systemic circulation[153], although it remains to be established whether the endogenous and exogenous levels refer to the same form of the AGEs. In similar studies in diabetic or apolipoprotein E-deficient (apoE$^{-/-}$) mice a difference in serum and in one of the studies also urinary levels of CML and methylglyoxal-derived AGEs was reported following several weeks of low versus high AGE diet[153–157]. In all these studies the AGEs were detected by immunological techniques so a differentiation between free or protein-bound AGEs and thus between LMM and HMM AGEs could not be made, which could have been achieved by appropriate sample preparation combined with LC-MS/MS[10].

2.3.3 Metabolism

Given the different nature of free LMM and protein-bound HMM AGEs their metabolism also proceeds in a different way. Upon oral intake, protein-bound exogenous HMM AGEs may be absorbed after enzymatic digestion into LMM AGEs, resulting in systemic exposure to the LMM AGEs, with the heating-induced AGE-mediated change in protein structure potentially to some extent hampering degradation by the digestive enzymes in the gastrointestinal tract (e.g. gut proteases)[12]. Upon oral intake also the LMM AGEs and the LMM AGE precursors may be degraded by the intestinal microbiota, thereby reducing their bioavailability. It was reported for example that 3-10% of orally administered bound Amadori rearrangement

products are excreted in urine while only 1-3 % appear in feces, indicating that a substantial part (about 80%) can be degraded by the gut microbiota[142,158]. Thus, the majority of orally ingested AGEs may serve as gut bacterial nutrients.

Sofar, some bacterial taxa (i.e. *Bacillus subtilis, Escherichia coli* and *Intestinimonas butyriciproducens* AF211) were shown to (partially) degrade FL with an identified key enzyme being a kinase (encoded by frlD/yhfQ)[39,40,159]. FL can for example be converted into fructoselysine 6-phosphate followed by conversion to lysine and glucose-6-phosphate by *E. coli*[159] and result in further production of the short chain fatty acid butyrate by *I. butyriciproducens* AF211[40]. An intracellular enzyme fructosamine 3-kinase found in mammalian but not in bacterial cells can phosphorylate FL into fructosamine 3-phosphate which turns into lysine and the reactive dicarbonyl and AGE-precursor 3-deoxyglucosone[119,160].

Using anaerobic fecal incubations with different free LMM AGEs and their precursors including FL, CML, pyrraline, and maltosine, it was demonstrated that the level of conversion varies with the glycation product studied, while also showing substantial interindividual variability[11,161]. While conversion of FL was complete within a few hours, maltosine was hardly degraded, while the conversion of CML and pyrraline amounted to about 60 and 20% upon 24 hours incubation with fecal slurries[11].

Once in the systemic circulation, AGEs can be partly taken up by liver cells and catabolized[162,163], depending on their structure and size. In addition, conversion by the glutathione dependent glyoxalase system may provide a pathway for detoxification of especially the dicarbonyl AGE precursors such as methylglyoxal and glyoxal. It has been reported that more than 99% of endogenously formed methylglyoxal can be converted by this glyoxalase system into harmless products such as lactate[164], which is present in mammalian cells[136]. It is of interest to note that the activity of the glyoxalase system is influenced by a genetic polymorphism[165] and operates under control of the nuclear factor erythroid 2-related factor 2 (Nrf2) transcription factor[166].

There are also several receptors that play a role in the detoxification of AGEs including oligosaccaharyltransferase-48 (AGE-R1), 80K-H phosphoprotein (AGE-R2) and macrophage scavenger receptors, all known to be present in mammalian cells. AGE-R1 is present on the cell surface of monocytes and macrophages and is able to bind AGEs and induce their endocytosis[119,167]. AGEs that have been endocytosed are modified in the cell by lysosomal degradation[119,168,169]. The degradation of AGEs likely includes the formation of LMM AGEs from HMM AGEs, while other studies report new intracellular formed AGEs in macrophages[170]. The LMM AGEs and their precursors are thought to be soluble in the serum and cleared by the kidney[119,171] (see section on excretion). It has also been shown that increased activation of AGE-R1 is related to increased turnover of AGEs in plasma and tissues[12]. There are studies where AGE-R1 was found able to inhibit the effects that RAGE activation has on oxidative stress and inflammatory actions by suppressing nuclear factor-kappa B (NF-κB) and mitogen-activated protein kinases (MAPK) phosphorylation. AGE-R1 expression levels can be downregulated by a long-term high AGE burden[12,172]. This has also been suggested for AGE-R2, a receptor present on T-lymphocytes[172]. AGE-R2 is a protein which has not been proven to directly bind AGEs. However, it seems to be involved in the

degradation of AGEs by the activation of intracellular signaling. Lastly, the soluble variant of RAGE, sRAGE, is thought to help prevent AGE accumulation. sRAGE is not entirely similar to RAGE as it consists merely of the extracellular parts of the receptor and is present in the circulation. This receptor is thought to bind the same ligands as RAGE[12,168]. The absence of the intracellular parts cause that the AGE binding to sRAGE does not induce the cellular signaling cascade that would be induced upon binding to RAGE, and sRAGE could thus function as a decoy receptor. The binding of AGEs to sRAGE may potentially prevent the interaction between AGEs and RAGE thus eliminating some of the activity[168]. Possible other functions of sRAGE are still unknown[173].

Some studies report on degradation of specific AGEs. Intravenous administration of for example radiolabeled pentosidine to rats resulted in a recovery of 80% of the radioactivity in urine of which only a limited amount (20%) appeared to be intact pentosidine. The authors concluded that free pentosidine is catabolized or modified in the proximal tubule and that the kidney plays a role in pentosidine degradation[174]. The nature of the degradation products, whether this process is also relevant for other AGEs and their precursors, and whether the products formed present a detoxification or contribute to AGE-associated kidney damage remains to be elucidated.

2.3.4 Excretion

Some HMM AGEs might not be fully hydrolyzed by digestive enzymes or microbiota-derived enzymes, and this may result in substantial fecal excretion. Saturation of these intestinal degradation processes upon increasing dose levels results in increased relative fecal excretion with increasing dose levels[30]. For FL efficient degradation of both its free and protein-bound form by gut microbiota has been established with, depending on the experimental set-up, almost complete degradation within a few hours[11,40,159,161,175], while degradation of other LMM and HMM AGEs and precursors by intestinal microbiota as well as the pathways involved in these degradations remain to be further characterized. The relatively high fecal excretion of up to 55% of the administered dose of FL in young children[37] has been ascribed to their different intestinal microbial communities and activity suggested to result from their lower extent of adaptation to chronic dietary intake of heat-treated proteins[30].

Once in the systemic circulation AGEs and their precursors are mainly excreted via the kidneys into urine. Especially LMM AGEs and their precursors are readily eliminated from the body by renal excretion via glomerular filtration[119,171]. The renal clearance of an intravenous dose of free CML or CEL in rats was rapid with over 87% recovery in urine within 2 hours[176]. This excretion via glomerular filtration will be less relevant for HMM AGEs[119,171]. In humans, free pyrraline and pentosidine were recovered in the urine at 50 and 60% of the dietary doses respectively, while consumption of HMM pentosidine resulted in only 2% urinary recovery of pentosidine[32]. This limited urinary recovery of the HMM AGE is likely to be (in part) due to the limited bioavailability of HMM AGEs upon dietary intake.

In a study in rats there was a trend of increasing urinary excretion of free CML with increasing dietary levels of heat processed proteins, with 4-19% of the CML present in the diet (actual form not characterized) being recovered in urine. The increasing trend made the authors

conclude that the urinary CML was preliminary of dietary origin[177]. Another study with rats, already referred to in the section on absorption, concluded that recovery of CML in urine was independent of the molecular mass of the administered CML, suggesting, in contrast to most other data, comparable ADME characteristics between LMM and HMM CML[45].

Important to note is that some studies reported that upon their excretion by glomerular filtration free CML and pentosidine and especially also peptide bound LMM AGEs could be reabsorbed in the proximal tubule[174,178–180]. Tissue accumulation and/or binding of LMM AGEs to tissue proteins corroborates to the accumulation of HMM AGEs[12] as mentioned in the section on distribution.

2.3.5 Conclusions on ADME characteristics

Altogether, most studies indicate substantial differences in the ADME characteristics of LMM AGEs and AGE precursors versus protein-bound HMM AGEs and precursors. These differences result in different kinetics of exogenous versus endogenously formed glycation products, as summarized in **Figure 2.2**. Upon oral intake exogenous HMM AGEs and precursors show limited if any bioavailability so that systemic exposure to HMM AGEs is expected to result mainly from endogenously formed AGEs. In the gastrointestinal tract exogenous HMM AGEs and precursors are degraded to LMM AGEs and precursors which can become systemically available. Once in the systemic circulation especially LMM AGEs and precursors are cleared via urinary excretion. Elimination and clearance of HMM AGEs rather depends on receptor mediated transport into cells where they can be degraded via lysosomal degradation. Endogenous HMM AGEs may result from exposure to endogenously formed or exogenously provided AGE precursors including the reactive dicarbonyls like glyoxal, methylglyoxal, or 3-deoxyglucosone, although one could also argue that these reactive AGE precursors in food may readily react with proteins and amino acids in the food matrix before being ingested. This would leave endogenous production of the reactive AGE precursors and possibly exposure to LMM glycation products as a major source for endogenous HMM AGE formation. The production of these endogenous reactive AGE precursors may be enhanced for example upon exposure to high levels of glucose[181], via degradation of FL[160], in individuals with diabetes[182–185], or upon ageing[186]. In general, interspecies and interindividual differences in toxicokinetic properties are likely to exist and remain to be characterized to a further extent.

Based on these toxicokinetic considerations, systemic and tissue levels of HMM AGEs may result mainly from endogenous formation, while LMM AGEs and precursors may originate from both endogenous and exogenous sources. Effects of dietary exogenous HMM AGEs themselves may thus be limited to the intestinal tract and/or result from their LMM intestinal degradation products.
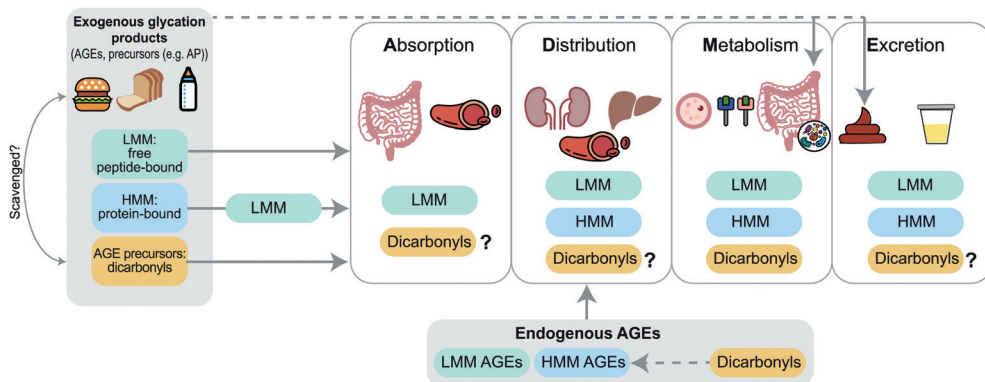
Figure 2.2. Overview of toxicokinetic characteristics of exogenous and endogenous glycation products including advanced glycation end products (AGEs) and Amadori products (AP), distinguishing between their low molecular mass (LMM) free and peptide-bound form (green), high molecular mass (HMM) protein-bound form (blue) and their reactive dicarbonyl precursors (yellow).

2.4 Toxicodynamics

The modes of action generally reported to play a role in the ultimate potential adverse health effects of AGEs include 1) dicarbonyl stress resulting in cross-linking and damage to protein structures and functions, and 2) interactions with AGE receptors (RAGEs) inducing pathways leading to adverse effects. These two pathways are of different importance for LMM AGEs and AGE precursors versus HMM AGEs. In addition, 3) toxicodynamic effects of AGEs and their precursors on gut microbiota composition and/or gut barrier integrity provide another potential link between dietary exposure to glycation products and possible pathological consequences.

2.4.1 Dicarbonyl stress resulting in cross-linking and protein damage

Early in the process of production of glycation products, dicarbonyls can be formed e.g. via decomposition of Amadori products via the Namiki pathway or as products of glycolysis. These dicarbonyls are reactive compounds. Accumulation of such dicarbonyls can not only result in AGE production but also in what is referred to as dicarbonyl stress[163], which can have negative effects on health. Dicarbonyls are able to react with body proteins and amino acids, leading to the formation of AGEs and cross-linking of proteins. Baynes and Thorpe (1999) confirmed that increased production of endogenous AGEs in diabetes is linked to increased cross-linking of body proteins[187]. Dicarbonyls have been reported to react with for example amino groups of proteins of the connective tissue matrix and the basement membranes[162,188]. The respective components are long-lived proteins so that damage formed may accumulate over time[189]. In the case of very high AGE concentrations, short-lived plasma proteins can be affected as well, such as for examples low density lipoproteins (LDL) and immunoglobulins[189].

Cross-linking of body proteins can have many physiological consequences. It results in altered structure and function of the proteins[189,190]. Additionally, the proteins are less easily degraded[190]. The AGE cross-linking of proteins such as collagen is related to an increase in stiffness in tissues that are rich in these proteins[189]. This includes arterial stiffness, stiffness in lung tissue, joints, and extracellular matrix. Stiffness in these tissues has been associated with diseases including hypertension, cataract, dementia, atherosclerosis, glomerulosclerosis, emphysema and joint pain[162]. Cross-linking of body proteins is related to complications in diabetes and increased cardiovascular risk[188].

Dicarbonyl stress has also been associated with damage in the kidney, vascular damage and accelerated atherosclerosis development[162,163,191]. Development of atherosclerosis occurs not only because of cross-linking but also because AGEs formed in the matrix of vessel walls are thought to be able to 'trap' LDL. This leads to decreased uptake and degradation of LDL in the kidney, which in turn promotes the lipoprotein accumulation and atherosclerosis[163,189]. Raj et al. (2000) also concluded that LDL, when bound to the extracellular matrix as a result of AGE formation, can be oxidized[162]. This results in the formation of toxic degradation products of LDL. These oxidized LDL particles can lead to the formation of antibodies which bind to AGEs in vessel walls, and thereby contribute to vascular inflammation and atherosclerosis[192]. In addition, dicarbonyl stress can lead to oxidative stress and inflammation and also induce carbonylation of biomolecules such as DNA, and thus damage DNA[193–195].

The reactive dicarbonyls causing protein crosslinking are precursors of AGEs that may originate from both exogenous and endogenous sources. However, given the high reactivity of these dicarbonyls it can also be foreseen that when formed in food upon heating they may be scavenged via reactions with food matrix proteins forming AGEs in the food before the food is actually consumed. Relatively low levels of dicarbonyls (0-40 mg/kg food) were indeed found in certain food products in a recently presented dietary dicarbonyl database where the three major dicarbonyls methylglyoxal, glyoxal and 3-deoxyglucosone were quantified in multiple food products. The presence of relatively lower levels of dicarbonyls in certain food products was explained by the presence of potential scavengers such as polyphenols or protein residues in the food product. However, multiple food products contained relatively high levels of dicarbonyls (40-2990 mg/kg) (i.e. cake, dried fruit, candy bars)[196]. It remains to be investigated if these dicarbonyls would be scavenged when these food products are consumed combined with other dietary compounds.

2.4.2 Interactions with receptors

Circulating AGEs can bind to AGE receptors (RAGEs) on cell surfaces. RAGEs can be found on cells in the cardiovascular system, including heart tissue, endothelial cells, white blood cells, lung tissue, neural tissue and the intestinal tract[12,197]. Following the binding of AGE to RAGE, the transcription factor, NF-κB is activated[12,109]. Activation of NF-κB leads to activation of NADPH oxidase, which increases oxidative stress, and activates an inflammatory cascade. This cascade consists of elevated expression of proinflammatory cytokines, growth factor and adhesive molecules, which are molecules that interact with leukocytes[109]. Oxidative stress also contributes to endogenous formation of AGEs. ROS involved in oxidative stress can damage proteins, possibly accompanied by the production of more AGEs[168] and increased infiltration of macrophages[198]. Besides the inflammatory response and increased oxidative

stress, the activation of NF-κB causes proliferative, fibrotic, angiogenic, thrombogenic and apoptotic reactions. These reactions can contribute to the development of cardiovascular diseases[109,163]. The combination of chronic inflammation, oxidative stress and high AGE content has been shown to promote chronic kidney disease and kidney damage[171]. Animal studies suggested that the combination of these factors can even be involved in tumor development[199].

It was found that not all AGEs have the same affinity to RAGE. Free CML and CEL do not interact with RAGE[41,49] and the presence of a polypeptide backbone was found to be required in order to interact with RAGE as tested with both synthesized LMM CML (~ 1 kDa)[41] and HMM CML (>30 kDa)[41,49,200]. The early Amadori product FL was shown to not interact with RAGE at all, not in its free, LMM or HMM form[41].

Studies on the effect of dietary AGE exposure and expression of cytokines have reported 3.5-fold increased expression of various cytokines upon providing an AGE rich diet to mice[201]. Interestingly, the heated diet induced a stronger inflammatory response than the unheated diet enriched with CML, suggesting that free AGEs may not be the AGEs responsible for induction of the inflammatory response. The involvement of RAGE in these processes was shown in a study in which RAGE knock out mice did not show production of inflammatory cytokines, endothelial dysfunction and aortic stiffening upon 9 months exposure to a diet enriched in HMM CML-BSA[202].

Finally the RAGE-dependent release of serotonin by human parietal cells *in vitro* was shown to be affected by HMM AGEs whilst free CML showed a RAGE-independent increase in serotonin release[203]. Another *in vitro* study with RAGE-expressing HEK-293 cells showed a comparable RAGE-dependent effect on cellular p38 MAP kinase activation by free and casein-linked HMM CML, although it should be noted that also non-AGE type products from heating, such as *N*-methylpyridinium, appeared able to induce this effect[204].

Other receptors interacting with AGEs include AGE-R1, AGE-R2, macrophage scavenger receptors and the soluble form of RAGE (sRAGE)[144,163]. These receptors have different functions from RAGE. As discussed in Section 2.3.3, AGE-R1, AGE-R2 and macrophage scavenger receptors are involved in endocytosis and subsequent degradation of AGEs[12,168].

It is thought that exogenous HMM AGEs, provided they can reach the systemic circulation, can bind to RAGE similarly as endogenously produced AGEs[205]. However, given the potential limited bioavailability of HMM AGEs their role in activation of the RAGE receptors may be limited compared to that of endogenously formed HMM AGEs, except in the gastrointestinal tract where RAGE expression is generally low[197] but is upregulated under pathophysiological conditions[206].

2.4.3 Alterations of gut microbiota composition and/or gut barrier integrity

A third mode of action potentially involved in the toxicodynamics of AGEs includes their effect on the gut microbiota composition and activity. Such effects may result in a decrease or increase of the abundance of specific bacteria, which in turn may have no, positive, or negative health implications, such as for example an effect on inflammation. Increasingly

links between alterations in gut microbiota composition and disease have been reported[207]. Multiple studies showed an effect of exposure to exogenous AGEs on gut microbiota composition, both in experimental animals and humans. **Table 2.1** presents an overview, and reveals that upon dietary exposure to a (heated) diet rich in AGEs several studies reported a decrease in the relative abundance of *Lactobacillus spp.*[51,151,208,209], while others showed an increase in the genus *Akkermansia*[210,211] and/or *Allobaculum*[211–213] or *Dubosiella*[151]. Effects on host health directly linked to these AGE-mediated gut microbial alterations remain to be established and understood. Such effects may potentially result from alterations in gut microbial production of short chain fatty acids (SCFAs) (**Table 2.1**)[208,211,212,214,215], or of other fecal bacterial metabolites[210,214] although evidence for such an underlying mode of action remains to be substantiated. Nevertheless, and whatever the underlying mode of action, given the important role of the gut microbiota in human health and disease[216] an AGE-mediated effect on the gut microbiota could prove to represent an additional mode of action for AGE-mediated health effects. Obviously, free AGEs and precursors, reactive dicarbonyls, dipeptide bound AGEs and precursors resulting from digestion, and HMM AGEs and precursors may all affect the gut microbiota in different ways. An important condition to further elucidate such effects is to distinguish between all these AGEs and their precursors when characterizing exposure; this information is not always provided in the studies listed in **Table 2.1**.

In addition to alterations in gut microbiota profiles[20,52], exposure to exogenous AGEs can induce other effects in the intestine. It was found that intestinal epithelial integrity was affected by exposure to dietary AGEs, as shown by altered gene expression of several tight junction proteins[210,212], potentially resulting in increased systemic exposure to exogenous (HMM) AGEs or increased systemic infiltration of bacteria and microbial metabolites or components[217]. Overall, the potential effects of exogenous dietary glycation products on the intestinal microbiota and the potential consequences for metabolite formation, intestinal inflammatory processes and barrier integrity[218], support the relevance of including the gut microbiota composition, function and dynamic (local) effects combined with intestinal translocation studies in future glycation product exposure studies[19].

Table 2.1 Alterations in gut microbial composition and metabolome due to exogenous exposure to glycation products. Abbreviations: AGE = advanced glycation endproducts; AP = Amadori product; CEL = carboxyethyllysine; CML = carboxymethyllysine; HMF = hydroxymethylfurfural; MG-H1 = N6-(5-hydro-5-methyl-4-imidazolon-2-yl)-ornithine; RCT = randomized controlled trial; LMM = low molecular mass; HMM = high molecular mass; PB = protein-bound; SCFA = short chain fatty acid; MgO = methylglyoxal; GO = glyoxal; 3-DG = 3-deoxyglucosone.

Exposure	Subject or system used	Altered bacterial taxa Increased compared to control group	Altered bacterial taxa Decreased compared to control group	Altered bacterial metabolites	Reference
In vivo human studies					
Diet high in total CML and HMF, randomized two-period crossover trial for 7 days with wash-out period	20 adolescents, fecal samples		*Lactobacillus* spp., *Enterobacteria*, ratio *Escherichia/Shigella*		51
Dietary AGE restriction for one month after habitual high AGE diet	20 peritoneal dialysis patients, RCT, fecal samples	*Alistipes indistinctus, Clostridium hathewayi, Ruminococcus gauvreauii*	*Prevotella copri, Bifidobacterium animalis*		20
In vivo studies with experimental animals					
Heated glucose-lysine added to the diet, resulting in increased APs, HMF and CML. Orally exposed for 87 days.	Rats, cecal content		Lactobacilli, total bacteria		51
Soluble LMM or HMM AGEs from bread crust added to the diet for 88 days (LMM < 5 kDa; HMM > 5 kDa)	Rats, cecal content	LMM: *Bacteroides* spp., ratio *Escherichia/Shigella* HMM: total bacteria, ratio *Escherichia/Shigella*	LMM: total bacteria, *Lactobacillus* spp., *E. rectale/C. coccoides,* HMM: *Lactobacillus* spp., *E. rectale/C. coccoides, C. leptum*	Total fecal SCFAs increased after both LMM and HMM AGE diets	208
Heated high-fat diet, for 8 weeks	apoE-/- mice, cecal content	*Firmicutes, Allobaculum, Clostridiales*	*Bacteroidetes, Rikenellaceae*		213
Glycated fish protein, orally for 14 days	Rats (Sprague-Dawley), cecal content	Actinobacteria, Verrucomicrobia, *Allobaculum, Collinsella, Ruminococcaceae_UCG-014, Lactobacillus animalis, Turicibacter, Akkermansia, Allisonella, Lachnospiraceae_UCG-006*	Fusobacteria, Deferribacteres, *Ruminococcus_gauvreauii_group, Ruminococcaceae_UCG-009, Erysipelatoclostridium*	Total fecal SCFAs were increased; cecal SCFAs were unaffected	211
CML, orally for 21 days (1.6 mg/kg bw/day)	Mice, cecal samples	*Bacteroidaceae, Odoribacteraceae, Desulfovibrionaceae, Dorea*	*Lachnospiraceae, Sutterella*		52

Exposure	Subject or system used	Altered bacterial taxa		Altered bacterial metabolites	Reference
		Increased compared to control group	Decreased compared to control group		
High AGE diet (generated by heat treatment), orally for 8 months	Mice, fecal samples	Increased: Actinobacteria, Porphyromonadaceae, Prevotellaceae, Helicobacteraceae Parabacteroides, Alloprevotella, Helicobacter, Ruminococcaceae_ UCG_014, unclassified Rhodospirallaceae	Decreased: Firmicutes, Rikenellaceae, Lachnospiraceae, Desulfovibrionaceae Desulfovibrio, Rikenellaceae_RC9_gut_ group, unclassified Lachnospiraceae, Alistipes, Lachnospiraceae_NK4A136_ group	Decrease in fecal acetate and butyrate, increase in fecal isobutyrate and isovalerate. Effects on fecal metabolome by upregulation of 36 metabolites and downregulation of 21 metabolites.	214
AGE-enriched diet (generated by replacing casein with modified, glycated casein), orally for 22 weeks	Mice, fecal samples	Lachnospiraceae Parabacteroides, Ruminococcus, Lawsonia	Muribaculaceae Lactobacillus, Prevotella, Anaerostipes, Candidatus Arthromitus,		209
High AGE diet (generated by heat treatment), orally up to 18 weeks	Rats, cecal samples	Proteobacteria, Allobaculum, Bacteroides, Desulfovibrio	Bacteroidetes, Alloprevotella, Ruminococcaceae, Lachnospiraceae, Eubacterium, Phascolarctobacterium	Decrease of the cecal SCFAs acetate and propionate.	212
Heat-treated diet, orally for 24 weeks (measured increased CML, CEL, fructosamine)	Mice, cecal samples	Helicobacteraceae, Akkermansia,	Saccharibacteria, Ruminococcus, Sutterella	Increased metabolites related to phenylalanine, tryptophan and tyrosine pathways in the cecal metabolome after heat treated diet.	210
High AGE diet (generated by heat treatment), orally for 16 weeks. Measured increase of free CML and CEL (by ELISA)	Mice (young: 3 months old; old: 15 months old), cecal samples	Young: Parabacteroides Old: Tenericutes	Young: Odoribacter	Cecal total SCFA did not differ between groups. Increased isobutyric and isovaleric acid in young mice compared to control.	215
High AGE diet (generated by heat treatment), orally for 10 weeks. Measured increase of PB CML, CEL, MG-H1, free CEL and MG-H1 and 3-DG, MGO, GO.	Mice, fecal samples	Dubosiella	Lactobacillus, Bacteroides		151

2

2.5 Discussion

The present review aimed to provide an overview of the toxicokinetics and toxicodynamics of AGEs and their precursors, distinguished based on their molecular mass, in order to evaluate the potential contribution of both endogenous and exogenous dietary glycation products on human health. **Table 2.2** presents an overview of the major differences in the toxicokinetics and toxicodynamics of endogenously formed versus exogenous glycation products. From this overview it follows that the contribution of exogenous glycation products to the potential adverse health effects may be limited for various reasons.

First of all, the systemic bioavailability of HMM AGEs and their precursors upon their oral intake may be limited. The extent to which they are degraded in the digestive track remains to be quantified and may vary for each HMM glycation product[12]. In contrast LMM AGEs and precursors present in food may become bioavailable, although for the reactive dicarbonyl precursors this may to some extent be hampered by the fact that upon their formation upon heating of food they may already react and be scavenged by amino acids and proteins present in the food matrix or diet before or when the food is actually consumed. For CML which is known to be a major AGE in heat processed foods, it was demonstrated that exposure to free CML at levels that exceeded an average dietary intake by 2 to 3 orders of magnitude resulted in an increase in tissue protein-bound CML levels to only a limited extend (less than 2-fold or not at all)[133], suggesting that at the much lower average dietary intake levels these increases may be negligible. However, it should be noted that this result may be different upon a life-long dietary exposure to AGEs. Other LMM AGEs or precursors, like for example FL may show higher levels of bioavailability but the extent to which they contribute to formation of endogenous protein-bound HMM AGEs remains to be established.

The limited systemic bioavailability of HMM AGEs and precursors may limit the contribution of exogenous glycation products to adverse effects induced via RAGE receptors, since RAGE affinity of AGEs appeared to be mainly dependent on the size of the AGE with protein- or peptide-bound CML or protein- or peptide-bound CEL interacting with RAGE, while free CML or free CEL did not[41,49]. Only in the intestinal tract orally ingested HMM AGEs may be able to activate RAGE, while for systemic effects rather endogenous formation of HMM AGEs may dominate the induction of adverse health effects via RAGE.

In addition, AGEs and their precursors, including those in their HMM form, may affect the composition and activity of the gut microbiota. This would provide another mode of action for AGE mediated effects on host health since effects on the gut microbiota are known to influence host health in both beneficial and adverse ways[216,219,220]. The importance of this mode of action in the processes underlying the potential health effects of AGEs remains to be studied to a further extent, although various studies already reported an effect of AGEs on the composition and activity of the intestinal microbiota (**Table 2.1**). Also, the relative importance of dicarbonyl stress versus the role of RAGE activation remains to be elucidated and may vary for the adverse effect under consideration.

Based on our reviewed findings we identified multiple research needs for the future. First of all, it is important that future studies invest in better characterization of the exposure

material actually tested, and of the urinary, fecal, tissue, or plasma AGE and precursors levels measured, identifying and quantifying the AGEs and precursors by analytical techniques that enable quantification of the different glycation product and of at least the HMM AGEs and precursors, LMM AGEs and precursors and dicarbonyl precursors. The absence of this information for both the test materials as well as the AGE related biomarkers and endpoints quantified hampers interpretation of the results presented and confuses the discussions on the role of exogenous AGEs as compared to endogenous AGEs in the overall health effects. This information will prove essential to quantify the respective contributions of exogenous versus endogenous glycation products to the AGE induced health effects. In addition, considering the heterogeneity of the glycation products, as also reflected in different ADME outcomes, AGEs and their precursors cannot be grouped together but specific, individual information is required for a proper evaluation, especially considering ADME properties. The use of *in vitro* models can help to increase the understanding of toxicokinetic and toxicodynamic properties of individual AGEs and precursors as *in vitro* assays provide better possibilities than *in vivo* studies to test multiple individual as well as mixtures of glycation products. LC-MS/MS based analytical techniques, such as proteomics, can be a valuable addition to further elucidate the nature of the HMM AGEs as well as of AGE modified cellular targets. Furthermore, it remains to be elucidated if reactive dietary dicarbonyls are scavenged by for example the food matrix before reaching the systemic circulation, and also to what extent they can actually become systemically available. Given the results of the present overview it seems prudent to conclude that when considering studies focusing on a role of exogenous AGEs and precursors in adverse human health effects to focus on either effects in the gastrointestinal tract (including effects on the gut microbiota) and/or effects induced by exposure to AGEs or their precursors known to be bioavailable and able to increase systemic endogenous AGE levels and/or dicarbonyl stress.

To conclude, based on the current state-of-the-art, the role of exogenous HMM AGEs and precursors seems to be restricted by their limited bioavailability to local effects on the intestine including its microbiota, unless being degraded to their LMM form. An important role is probably left for reactive dicarbonyl AGE precursors and as a consequence the endogenously formed AGEs. This implies that an important route for future research could be the role of especially reactive AGE dicarbonyl precursors and the endogenous pathways leading to their bioavailability, formation and detoxification. The direct contribution of reactive AGE dicarbonyl precursors to dicarbonyl stress and their indirect contribution to endogenous HMM AGE formation and subsequent RAGE activation remains to be further studied.

Table 2.2 Overview of main characteristics for toxicokinetics and toxicodynamics of endogenous and exogenous AGEs. Abbreviations: AGE = advanced glycation end product; LMM = low molecular mass; HMM = high molecular mass

	Endogenous glycation products	Exogenous glycation products
Toxicokinetics		
Contribute to the AGE level in the systemic circulation.	Yes	Partly, mainly for LMM AGEs and precursors and dicarbonyl precursors and for HMM AGEs and precursors upon digestive degradation to their LMM form
Can be cleared from the systemic circulation.	Yes, HMM via lysosomal degradation and LMM via glomerular filtration	Yes, mainly LMM AGEs and precursors and dicarbonyl precursors via glomerular filtration
Toxicodynamics		
Can cause damage by cross-linking.	Yes, especially the dicarbonyl precursors	Yes, especially the dicarbonyl precursors
Can cause damage by binding to RAGE.	Yes, especially the HMM AGEs	HMM AGEs only in the gastrointestinal tract or upon digestive degradation to LMM AGEs
Can affect gut microbiota composition and/or the intestinal barrier.	No	Yes, differences between LMM and HMM glycation products remain to be established
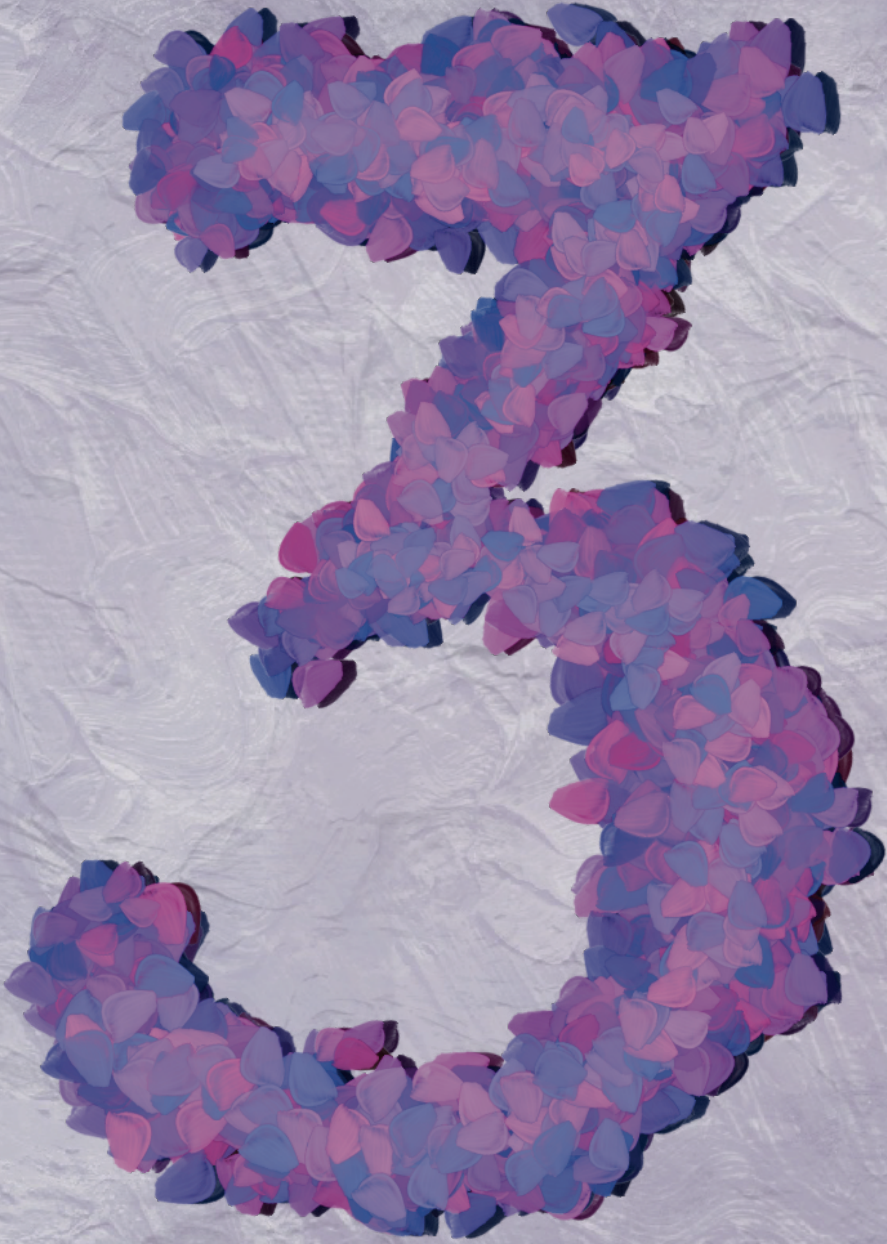
An *in vitro* model for microbial fructoselysine degradation shows substantial interindividual differences in metabolic capacities of human fecal slurries

Katja C.W. van Dongen, Meike van der Zande, Ben Bruyneel, Jacques J.M. Vervoort, Ivonne M.C.M. Rietjens, Clara Belzer, Karsten Beekmann

Abstract

Fructoselysine is formed upon heating during processing of food products, and being a key intermediate in advanced glycation end product formation considered to be potentially hazardous to human health. Human gut microbes can degrade fructoselysine to yield the short chain fatty acid butyrate. However, quantitative information on these biochemical reactions is lacking, and interindividual differences therein are not well established. Anaerobic incubations with pooled and individual human fecal slurries were optimized and applied to derive quantitative kinetic information for these biochemical reactions. Of 16 individuals tested, 11 were fructoselysine metabolizers, with V_{max}, K_m and kcat-values varying up to 14.6-fold, 9.5-fold, and 4.4-fold, respectively. Following fructoselysine exposure, 10 of these 11 metabolizers produced significantly increased butyrate concentrations, varying up to 8.6-fold. Bacterial taxonomic profiling of the fecal samples revealed differential abundant taxa for these reactions (e.g. families *Ruminococcaceae, Christenellaceae*), and *Ruminococcus_1* showed the strongest correlation with fructoselysine degradation and butyrate production ($\rho \geq 0.8$).

This study highlights substantial interindividual differences in gut microbial degradation of fructoselysine. The presented method allows for quantification of gut microbial degradation kinetics for foodborne xenobiotics, and interindividual differences therein, which can be used to refine prediction of internal exposure.

3.1 Introduction

Fructoselysine is the most abundant Amadori product in food products and is formed during heating in the processing and preparation of food products[129]. Fructoselysine is formed via the Maillard reaction by a non-enzymatic reaction between a reducing sugar (i.e. glucose) and the amino group of protein-bound or free lysine[14], as depicted in **Figure 3.1**. It occurs in a variety of food products, such as baked products, fried potatoes and infant formula[221,222], with a total daily intake in the Western diet reported to be 500 - 1,000 mg free and protein-bound fructoselysine (corresponding to 7.1-14.3 mg/kg bw/day for a 70 kg adult)[223]. The presence of fructoselysine in food raises a concern, as it is a key intermediate in the formation of the advanced glycation end product (AGE) carboxymethyllysine[224]. Also, fragmentation of fructoselysine can result in formation of reactive α-dicarbonyls (i.e. glyoxal, 3-deoxyglucosone)[14,42,43] which, in turn, can form new (protein-bound) AGEs[27,225]. AGEs have been associated with several (chronic) diseases and inflammation, such as the development of atherosclerosis, the onset of diabetes complications, and Crohn's disease[12,25,217,226,227]. Both free- and protein-bound AGEs can cause oxidative stress[228], and glycation of proteins can alter their structure and function, in addition to turning them into agonists for the receptor for AGEs (RAGE) which, upon activation, exerts pro-inflammatory responses[125,226]. While the interactions with RAGE appear to occur mainly if not only with AGEs bound to high molecular weight proteins[49,229], there is currently no consensus on which biological effects can be attributed to free AGEs or AGEs bound to low molecular weight proteins[230]. While endogenously formed AGEs are certainly an important source of internal AGE exposure, AGEs and precursors present in food have been reported to contribute significantly to the endogenous AGE and precursors pool, both in plasma and tissues[17,26,27,125,148]. A dose-dependent increase of fructoselysine has been reported in plasma, liver and kidney resulting from dietary, protein-bound fructoselysine exposure in experimental animals[30]. It is also reported that fructoselysine and several free or (peptide)bound AGEs can reach the colon as they have a low (systemic) bioavailability[15]. Free fructoselysine is transported, albeit poorly, via simple diffusion over Caco-2 monolayers *in vitro*[34] and dipeptide bound fructoselysine partially via the peptide transporter PEPT1[35]. In human volunteers fed a meal rich in protein-bound fructoselysine, only ±3% of ingested fructoselysine was excreted in urine, and only ±1% recovered in feces, implying a high degree of metabolism[129,130]. Together, this suggests that colonic microbiota metabolize the majority of ingested fructoselysine[19,129]. This is supported by *in vitro* incubations with human fecal samples[223] which show that the intestinal microbiota can metabolize fructoselysine, in addition to few specific isolated bacterial strains which are reported to be able to degrade fructoselysine, i.e. *Escherichia coli*[159], *Bacillus subtilis*[39], and *Intestinimonas butyriciproducens* AF211[40]. *I. butyriciproducens* AF211, isolated from human feces, was also shown to produce the short chain fatty acid (SCFA) butyrate from fructoselysine[40]. Butyrate, together with acetate and propionate represent the major SCFAs in the colon[231]. These gut microbial fermentation products have several important functions for (intestinal) host health[231–233], implying that fructoselysine might be converted by gut bacteria into beneficial metabolites. However, only ±10% of 65 fecal samples in the Human Microbiome Project contained *I. butyriciproducens* AF211 genes in the deep metagenome[40,67], and the other bacteria identified might only be capable of performing certain steps in this complex process, suggesting the potential existence of interindividual differences. To date, no data on the catalytic efficiencies, and interindividual

differences in gut microbial fructoselysine degradation, along with SCFA formation have been reported. In this study, an *in vitro* method was optimized and applied to derive the catalytic efficiency of fructoselysine degradation and accompanying SCFA production, to quantify interindividual differences therein, and to investigate associations with bacterial composition based on 16S rRNA amplicon sequencing.
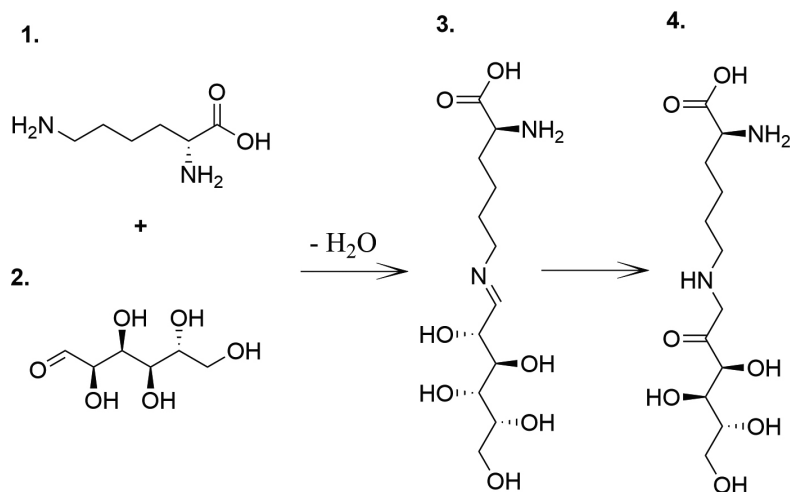

Figure 3.1 Fructoselysine (4) formation via reaction between the ε-amino moiety of lysine (1) and glucose (2), to form the so-called Schiff base (3), which subsequently undergoes an Amadori rearrangement reaction to yield fructoselysine (4).

3.2 Materials and methods

Chemicals and reagents

Fructoselysine (CAS: 21291-40-7) was purchased from Carbosynth Limited (Berkshire, UK). 3-Nitrophenylhydrazine hydrochloride (3NPH-HCl; CAS: 636-95-3), N-(3-dimethylaminopropyl)-N'-ethylcarbodiimide (EDC; CAS: 25952-53-8), pyridine anhydrous (CAS: 110-86-1), glycerol (CAS: 56-81-5), sodium propionate (CAS: 137-40-6) and sodium butyrate (CAS: 156-54-7) were purchased from Sigma-Aldrich (Steinheim, Germany). Formic acid (99-100%, analytical grade; CAS: 64-18-6) and sodium acetate anhydrous (CAS: 127-09-3) were purchased from Merck (Darmstadt, Germany). $^{13}C_6$-3-nitrophenylhydrazine hydrochloride (^{13}C-3NPH-HCl; CAS: 1977535-33-3) was obtained from Cayman Chemicals (Ann Arbor, USA). PBS was purchased from Gibco (Paisley, UK). Acetonitrile (ACN; UPLC/MS grade; CAS: 75-05-8) was obtained from BioSolve BV (Valkenswaard, the Netherlands).

Collection of human fecal samples

Fresh fecal samples were collected from 16 human individual volunteers (12 females, 4 males) aged between 24 and 64 years of Caucasian, Asian, and Hispanic demographic

origin. Volunteers were not pregnant, did not suffer from chronic gastrointestinal diseases and did not use antibiotics three months prior to donation. Fecal samples were collected fresh in fecal collection tubes and were immediately processed in an anaerobic environment (85% CO_2, 5% H_2, 10% N_2). After a four times dilution (w/v) in anaerobic storage buffer (10% glycerol in PBS), samples were filtered using a SpinCon system (Meridian Bioscience), which was centrifuged for 5 min at 3,000 xg at 10 °C. After filtration, samples were homogenized before aliquots were prepared and stored at -80 °C until further use. This study was assessed by the Medical Ethical Committee of Wageningen University and judged to not fall under the Dutch 'Medical Research Involving Human Subjects Act'. Participants granted informed consent before participation in this study.

Incubations of the fecal slurries with fructoselysine

All fecal incubations were performed under anaerobic conditions at 37˚C. Experimental conditions were optimized by assessing linearity of fructoselysine degradation over time and over the amount of pooled fecal slurry, which consisted of equal amounts of the 16 individual fecal samples. 40 µM fructoselysine was incubated with 2.5%, 5% or 10% pooled fecal slurry in anaerobic PBS, in a volume of 50 µL per Eppendorf tube in technical triplicates for 0, 20, 40, 60 and 80 minutes. 5% Fecal slurry, corresponding to 0.0125 g feces/mL, and an incubation time of 60 minutes were selected for further experiments to derive Michaelis-Menten kinetics of fructoselysine degradation of both pooled and individual human fecal slurries. These were incubated in technical duplicates with increasing fructoselysine concentrations ranging from 0-400 µM for the pooled and 0-600 µM for the individual incubations (added from 50 times concentrated aqueous stock solutions). These exposure concentrations cover the range of physiological relevant fructoselysine concentrations (81-162 µM) reached by the reported daily intake, taking into account the volume of the colon and the dilutions applied in the anaerobic incubations. For detection of SCFA formation, pooled or individual fecal slurries (5%) were incubated in technical triplicates with a final concentration of 400 µM or 600 µM fructoselysine, respectively, in parallel to the solvent control. To terminate the reactions and to precipitate proteins, particles, and microorganisms 50 µL cold ACN (1:1) were added to the incubations. The remaining mixture was vortexed, stored on ice for at least 15 minutes, and centrifuged for 15 min at 18,000 xg at 4ºC. Supernatants were further processed for fructoselysine or SCFA measurement as described below. All incubations as described above were performed 3 times.

Fructoselysine measurement

The supernatants of the incubation samples were transferred to UPLC vials and analyzed by LC-MS/MS for fructoselysine quantification using a Shimadzu Nexera XR LC-20AD SR UPLC system coupled to a Shimadzu LCMS-8040 triple quadrupole MS (Kyoto, Japan). 2 µL supernatant were injected onto a Phenomenex Polar-RP Synergi column (30 x 2 mm, 2.5 µm) at 40 ºC. The mobile phase consisted of a gradient made from ultrapure water with 0.1% (v/v) formic acid and ACN with 0.1% (v/v) formic acid at a flow rate of 0.3 mL/min. The gradient started with 95% ACN for 2.5 min, to reach 0% ACN at 4 min, and was subsequently kept at 0% ACN until 6 min, followed by a shift to 100% ACN from 6 to 7.8 min returning to 95% ACN at 8.1 min and kept at these initial conditions up to 14 min. Under these conditions fructoselysine eluted at 5.6 min. The LCMS-8040 coupled with an ESI source was used for MS/MS identification. Positive ionization for multiple reaction monitoring (MRM) mode was

used. Fructoselysine was quantified using precursor to product transition *m/z* 309.2 → 84.2 (collision energy (CE) = -31 V) which was the most intense fragment ion. MRM transitions *m/z* 309.2 → 291.1 (CE = -11 V), *m/z* 309.2 → 273.1 (CE = -15 V) and *m/z* 309.2 → 225.2 (CE = -17 V) were used as reference ions. An external calibration curve in matrix was prepared using a commercially available standard. Peak areas were integrated using LabSolutions software (Shimadzu). The amount of fructoselysine degraded during incubation was calculated and expressed in μmol/h/g feces.

SCFA measurement
SCFAs in the supernatants of the incubation samples were derivatized and subsequently measured by LC-MS/MS, based on a previously described method with minor adaptations[234]. In short, 40 μL of the supernatant was mixed with freshly prepared 20 μL 200 mM 3NPH-HCl in 50% ACN and 20 μL 120 mM EDC-6% pyridine in 50% aqueous ACN solution in small glass tubes. After mixing, the tubes were placed with a cap in a 40 ºC heating block and incubated for 30 min and afterwards placed on ice for 1 min. The mixture was diluted with 320 μL nanopure water. To 90 μL of this diluted mixture, 10 μL of ^{13}C isotope labelled derivatized SCFA standard mix (IS-SCFA mix) (prepared as described below) was added as internal standard (ISTD) to account for analytical variability. The IS-SCFA mix was created by using ^{13}C-3NPH-HCl instead of 3NPH-HCl and a mixture of the SCFAs acetate, propionate and butyrate resulting in final concentrations after derivatization of 500 μM, 400 μM and 400 μM, respectively. Further steps for the derivatization procedure were similar as described above. After the reaction, this IS-SCFA mix was aliquoted and stored at -80ºC in glass vials until use. For quantification of the SCFAs, a calibration curve was prepared by derivatizing a concentration range of a mixture of acetate, propionate and butyrate with the same procedure as described above. To 90 μL of these derivatized SCFA standards, 10 μL of the IS-SCFA mix were added which resulted in a final concentration of 50 μM for acetate-^{13}C-3NPH and 40 μM for propionate-^{13}C-3NPH and butyrate-^{13}C-3NPH.

A Shimadzu Nexera XR LC-20AD XR UPLC system coupled to a Shimadzu LCMS-8045 triple quadruple mass spectrometer (Kyoto, Japan) was used for analysis of the SCFAs. 10 μL of sample were injected onto a Phenomenex Kinetex C18 column (50 x 2.1 mm, 1.7 μm) at 40 ºC. The mobile phase consisted of a gradient made from ultrapure water with 0.1% (v/v) formic acid and ACN with 0.1% (v/v) formic acid at a flow rate of 0.6 mL/min. The gradient started with 10% ACN to reach 20% ACN at 4 min, followed by a shift to 100% ACN reached at 4.1 min, and was subsequently kept at 100% ACN until 7.5 min, returning to 10% ACN at 7.6 min and kept at these initial conditions up to 10 min. Under these conditions, acetate-3NPH and its ISTD acetate-^{13}C-3NPH eluted at 1.3 min, propionate-3NPH and its ISTD propionate-^{13}C-3NPH eluted at 2.3 min and butyrate-3NPH and its ISTD butyrate-^{13}C-3NPH at 3.9 min. The LCMS-8045 was equipped with an ESI source and used for MRM quantification in negative ion mode. The following MRM transitions from precursor to product per compound were selected for quantification: acetate-3NPH *m/z* 194.0 → 137.1 (CE=17.0 V), acetate-^{13}C-3NPH *m/z* 200.1 → 143.1 (CE=17.0 V), propionate-3NPH *m/z* 208.1 → 137.0 (CE=19.0 V), propionate-^{13}C-3NPH *m/z* 214.1 → 143.1 (CE=19.0 V), butyrate-3NPH *m/z* 222.1 → 137.0 (CE=19.0 V) and butyrate-^{13}C-3NPH *m/z* 228.1 → 143.1 (CE=19.0 V). The ratio of peak area in the unknown sample was divided by the peak area of the corresponding ISTD was used for quantification using the constructed calibration curve with ISTD IS-SCFA mix.

DNA isolation, PCR amplification of the 16S rRNA gene and sequencing

DNA from the fecal samples was isolated by applying a double bead-beating procedure in combination with the customized MaxWell® 16 Tissue LEV Total RNA Purification Kit (XAS1220; Promega Biotech AB, Stockholm, Sweden). DNA isolates were quantified and purity (OD 260/280 ratio) was assessed with a DeNovix DS-11 FX+ Spectrophotometer / Fluorometer (DeNovix Inc., Wilmington, USA) combined with the Qubit® dsDNA BR Assay Kit (Invitrogen, Carlsbad, USA). DNA isolates were further processed in triplicate PCR reactions to amplify the 16S ribosomal RNA (rRNA) V4 region of each sample combined with unique barcoded sequences to identify individual samples. PCR product formation was confirmed by gel electrophoresis and after pooling triplicate PCR products they were purified using the CleanPCR kit (CleanNA, Waddinxveen, the Netherlands). A detailed description can be found in the Supplementary materials. 200 ng of each purified barcoded sample was pooled in one library and subsequently sequenced (Illumina NovaSeq 6000, paired-end 150 bp; Eurofins Genomics Europe Sequencing GmbH, Konstanz, Germany). The 16S rRNA gene sequencing raw data has been deposited in the European Nucleotide Archive under accession number PRJEB39539.

Microbiota data analysis and processing

Sequences of the 16S rRNA gene were analyzed using NG-Tax 2.0 pipeline[235] with default settings, generating *de novo* exact match sequence clusters (ASVs; amplicon sequence variants). Taxonomy was assigned using the SILVA[236] 16S rRNA gene reference database release 132. Further data analysis was performed using R version 3.6.1. Using the Phyloseq package[237] (version 1.30.0) the OTU table with the phylogenetic tree and the metadata were constructed. OTUs with a relative abundance >0.1% in one of the individual samples were included for further data analysis. Microbiome composition plots were created using the Microbiome package (version 1.8.0)[238]. Beta diversity (Bray-Curtis dissimilarities) was assessed with Phyloseq and its statistical significance with permutational multivariate analysis of variance (PERMANOVA) applying the Adonis function (999 permutations) of Vegan package[239] version 2.5-6. Taxa present in one of the fecal samples with a relative abundance >1% were used for correlations and differential abundance testing. Spearman's rank correlation of the relative abundance data per taxa were made, with use of the Microbiome package, with the V_{max} and SCFA values obtained in the present study, and correlations ρ ≥0.5 were included. Significant correlations after false discovery rate (FDR) correction for multiple testing were indicated (p-values were set to 0.1 or 0.05). The web-based tool Linear Discriminant Analysis (LDA) Effect Size (LEfSe)[240] was used to identify differential abundance taxa based on the relative abundance between the two assigned groups (i.e. fructoselysine metabolizers and non-metabolizers) of the fecal samples. Statistically significant differentially abundant taxa (p-value was set to 0.05 or 0.01 for the Kruskal-Wallis test) with an effect size of the logarithmic LDA score > 2.0 were included.

Data analysis of fructoselysine degradation and SCFA formation

The data for the degradation of fructoselysine with increasing fructoselysine substrate concentrations were fitted to the standard Michaelis-Menten equation: $V = V_{max} * [S]/(K_m + [S])$

with [S] being the substrate concentration (µM), V_{max} (µmol/h/g feces) being the apparent maximum velocity and K_m (µM) being the apparent Michaelis-Menten constant. This was done using GraphPad Prism 5 Version 5.04 (2010) software (San Diego, CA, USA). The k_{cat} was determined as V_{max}/K_m and describes the catalytic efficiency.

For comparison of SCFA and fructoselysine concentrations in these studies, statistics between the different treatment conditions were evaluated by multiple paired t-tests or one-way ANOVA tests followed by Tukey's post-hoc test, where a criterion of a p-value lower than 0.05 was considered to be significant using Microsoft Excel 2016 or GraphPad Prism 5 Version 5.04 (2010). Structural formulae were drawn using ChemDraw 18.0.

3.3 Results

Fructoselysine degradation by the human gut microbiota using pooled fecal slurries
Fructoselysine was degraded by the human gut microbiota in the pooled fecal slurry. After optimization of the incubation conditions with respect to time and the amount of fecal slurry (**Figure 3.2**), Michaelis-Menten kinetics K_m, V_{max}, and k_{cat} (i.e. V_{max}/K_m) were determined for the pooled human fecal slurries. Optimized experimental conditions consisted of 5% fecal slurry with an incubation time of 60 minutes at which fructoselysine degradation was still linear in time and over fecal slurry concentrations (**Figure 3.2**). **Figure 3.3** shows concentration-dependent fructoselysine degradation by the pooled fecal slurries. From these data a V_{max} of 5.1 ± 0.6 µmol/h/g feces, a K_m of 88.1 ± 28.7 µM and a k_{cat} of 58.3 mL/h/g feces were derived (**Table 3.1**).

Interindividual differences in fructoselysine degradation by the human gut microbiota
Based on the results obtained for the pooled human fecal samples, kinetic parameters were determined for all 16 individual fecal slurries. Seven substrate concentrations ranging up to 5 times the K_m of the pool were used to measure the concentration-dependent degradation of fructoselysine and to derive the kinetic constants (**Figure 3.4, Table 3.1**).
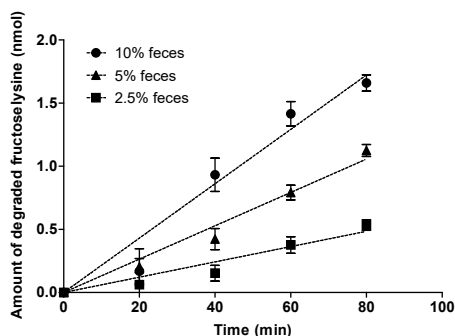

Figure 3.2 Time-dependent fructoselysine (40 µM) degradation by increasing concentrations of pooled human fecal slurry. Data points show the average±SD from 3 repeated experiments.
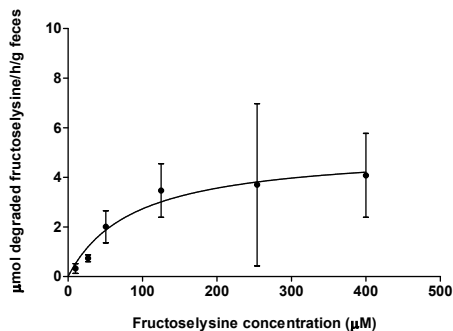
Figure 3.3 Concentration-dependent degradation of fructoselysine following anaerobic incubation of fructoselysine in 5% pooled human fecal slurry over 60 min. Data points show the average±SD from 3 repeated experiments.

Fecal slurries from 5 out of the 16 individuals showed minimal to no activity towards fructoselysine degradation (i.e. individuals 1, 10, 13, 15, 16; hereafter referred to as non-metabolizers), compared to 11 out of 16 individuals where fructoselysine degradation was observed (i.e. individuals 2, 3, 4, 5, 6, 7, 8, 9, 11, 12, 14; hereafter referred to as metabolizers). For the fecal slurries from these latter 11 individuals, interindividual differences in kinetics for fructoselysine degradation were observed, with up to 14.6-fold, 9.5-fold and 4.4-fold differences in the V_{max}, K_m and k_{cat} (i.e. V_{max}/K_m) values, respectively. Low concentrations of baseline fructoselysine were present in fecal slurries (i.e. 1-10 µM); there was no correlation between these fructoselysine concentrations and the ability to degrade fructoselysine (Supplementary materials **Figure S3.1**).
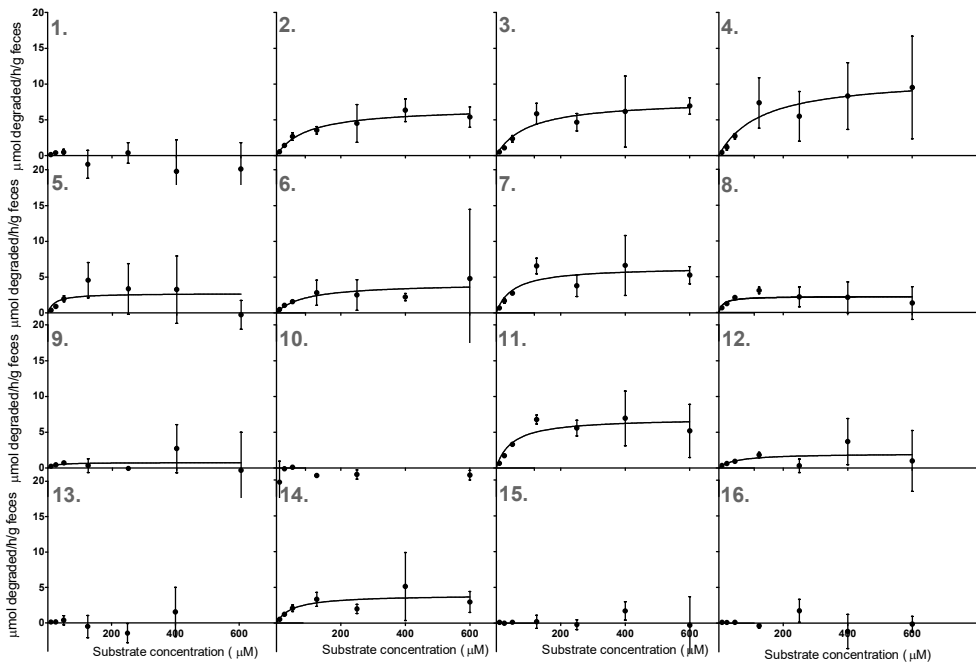
Figure 3.4 Concentration-dependent degradation of fructoselysine following anaerobic incubations of 5% fecal slurries from 16 individuals (metabolizers: red; non-metabolizers: blue). Data points show the average ± SD from 3 repeated experiments.

Table 3.1 Kinetic parameters (V_{max}, K_m and k_{cat}) of fructoselysine degradation by the human gut microbiota of pooled and individual human fecal slurries from 16 individuals studied in vitro. Data are the average from 3 repeated experiments. NA: no or minimal activity for fructoselysine degradation, of which the kinetic parameters could not be assessed.

Fecal slurry	V_{max} (μmol/h/g feces)	K_m (μM)	k_{cat} (mL/h/g feces)
Pool	5.1 ± 0.6	88.1 ± 28.7	58.3
Individual 1	NA	NA	NA
Individual 2	6.7	94.1	71.5
Individual 3	7.8	97.0	80.3
Individual 4	11.0	131.0	84.1
Individual 5	2.7	20.5	132.7
Individual 6	4.1	89.6	46.1
Individual 7	6.4	51.4	124.7
Individual 8	2.2	13.7	163.7
Individual 9	0.8	20.1	37.5
Individual 10	NA	NA	NA
Individual 11	7.0	48.5	144.1
Individual 12	2.0	53.3	37.9
Individual 13	NA	NA	NA
Individual 14	3.9	49.0	80.5
Individual 15	NA	NA	NA
Individual 16	NA	NA	NA

SCFA formation upon fructoselysine conversion by the human gut microbiota

Given that fructoselysine degradation has been described to result in SCFA formation, and predominantly butyrate[40], the changes in the levels of the SCFAs acetate, propionate and butyrate upon incubation of fecal slurries from the 16 individuals with fructoselysine were quantified. To this end, the incubations were first optimized with pooled fecal slurries for time dependent SCFA formation in incubations with and without fructoselysine (Supplementary materials **Figure S3.2**). Results obtained revealed that all three SCFAs increased in concentration over time, both in fructoselysine exposed and non-exposed fecal incubations. Compared to the corresponding control incubations with pooled fecal slurries without added fructoselysine, incubations with fructoselysine addition showed the largest increase in butyrate formation (1.49-fold) after 6 hours incubation (Supplementary materials **Figure S3.2**), and this incubation time was therefore selected for further experiments with the individual fecal slurries to quantify SCFA formation. Because SCFA formation was not assessed for linearity over time (Supplementary materials **Figure S3.2**) their formation is expressed per 6 hours of incubation. To allow comparison of SCFA formation between individuals, individual fecal slurries were incubated with a high concentration of fructoselysine (600 μM) to assure saturation of its degradation for all individuals (based on Figure 3.4), and the concentrations of butyrate, acetate and propionate were determined. Concentrations increased in the individual fecal control incubations without fructoselysine exposure (except for acetate where 5 individuals did not show an increase) during 6 hours of incubation, and addition of fructoselysine led to a significant additional increase of butyrate

and acetate (**Figure 3.5**). Interindividual differences were observed in the concentrations of butyrate, acetate and propionate determined after 6 hours of incubation in both the samples without and with added fructoselysine (Supplementary materials **Figure S3.3**).
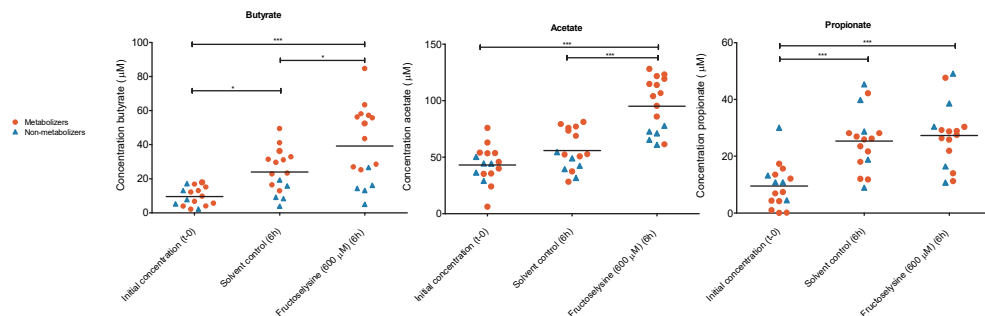

Figure 3.5 Concentrations of butyrate, acetate and propionate in 5% fecal slurries of 16 human individuals at t=0 and after 6 hours of incubation with fructoselysine (600 µM) or without (solvent control). Each symbol represents the data of one individual sample, averaged from 3 repeated experiments (metabolizers: red; non-metabolizers: blue). ANOVA was performed followed by Tukey's post-hoc test: * $p < 0.05$; ** $p < 0.01$; *** $p < 0.001$.

In all but one sample of the metabolizers (i.e. number 12) there was a significant fructoselysine-dependent increase in butyrate concentrations during 6 hours of incubation. In 8 out of the 11 metabolizers there was as significant fructoselysine-dependent increase in acetate concentrations, and only in one of them for propionate. Only in one of the 5 non-metabolizers there was a significant fructoselysine-dependent increase in SCFA concentrations (i.e. acetate; number 15) for 6 hours incubation.

Butyrate concentrations for the 11 metabolizers increased on average with 40.4 ± 17.5 µM after exposure to fructoselysine compared to 20.0 ± 8.5 µM in the solvent control during the 6 hours of incubation. For the non-metabolizers, during the 6 hours of incubation butyrate concentrations increased with 6.0 ± 2.6 µM after exposure to fructoselysine compared to 2.2 ± 0.7 µM in the solvent control (Supplementary materials **Table S3.1**).

Comparison of fructoselysine degradation and SCFA formation
To combine the results of individual fructoselysine degradation data with the formation of SCFAs, obtained V_{max} values for fructoselysine degradation were correlated to the changes in SCFA concentrations observed upon incubation with fructoselysine corrected for the level of formation in the corresponding non-exposed incubations. The fructoselysine-dependent increases in SCFA concentrations were transformed to a comparable unit as used for fructoselysine degradation (µmol formed/6 h/g feces). Linear regression revealed that fructoselysine degradation is predominantly associated with butyrate formation ($R^2 = 0.762$; **Figure 3.6**), and to a lesser extent with acetate ($R^2 = 0.236$) and propionate formation ($R^2 = 0.006$). Based on the slope of these correlations it can be inferred that on average per 1 mole of fructoselysine degraded per hour about 0.24 mole of butyrate is present in the incubation sample after 6 hours of incubation.
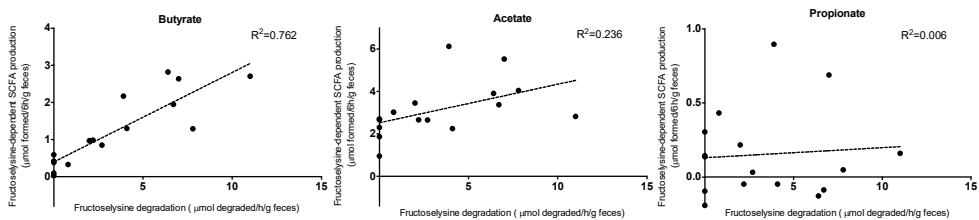
Figure 3.6 Correlation of the V_{max} for fructoselysine degradation (µmol degraded/h/g feces) and fructoselysine dependent SCFA formation corrected for the level of formation in the corresponding incubations performed without added fructoselysine determined at t=6h (µmol formed/6h/g feces), experimentally obtained using fecal slurries from 16 human individuals. For samples for which no fructoselysine degradation was observed, the V_{max} for fructoselysine degradation was set at 0.

Taxonomic profiling of the human fecal samples and its association with fructoselysine degradation and SCFA formation

To assess if the observed interindividual differences in fructoselysine degradation and SCFA formation are associated with bacterial composition, fecal samples were characterized using 16S rRNA gene sequencing. This analysis revealed that the individual fecal samples differed in the relative abundance of the top 10 taxa present at phylum and family level (Supplementary materials **Figure S3.4**). To compare the bacterial composition of metabolizers with non-metabolizers, Bray-Curtis β-diversity was assessed and showed differences in bacterial composition between samples (**Figure 3.7**). As shown in **Figure 3.7**, metabolizers and non-metabolizers did not form two clear, separate clusters. However, PERMANOVA analysis of the centroids of the two groups revealed a significant difference between metabolizers and non-metabolizers (p-value <0.01), suggesting that differences in bacterial composition between the two groups do exist, which was investigated further by differential abundance testing. This was performed by applying LEfSe. Taxa that differed significantly between metabolizers and non-metabolizers with an effect size of the logarithmic LDA score >2.0 were identified. This revealed 15 genera of 9 families that differed significantly (p-value <0.05) between the two groups (**Figure 3.8**). Three genera (*Ruminococcus_1, Christensenellaceae_R7_group, Ruminococcaceae_UCG_002*) and one family (*Christensenellaceae*) had a p-value below 0.01. These were all present in a relative abundance of on average 1-1.8% in the metabolizers and 0-0.1% in the non-metabolizers. These ratios and quantified average relative abundances for metabolizers and non-metabolizers were found to be comparable for the identified taxa *Alistipes, Lachnospiraceae ND3007* group*, Akkermansia* and *Rikenellaceae*. The significantly different family *Ruminococcaceae* was highly abundant with an average relative abundance of 24% in the metabolizers and 14% in the non-metabolizers. The significantly different family *Veilonellaceae* had an average relative abundance of 2.5% in the metabolizers versus 6% in the non-metabolizers. The significantly different phylum Proteobacteria was present with an average relative abundance of 1.2% in the metabolizers versus 2% in the non-metabolizers, while other phyla (e.g. Firmicutes, Bacteroidetes) were not significantly different between the two groups.
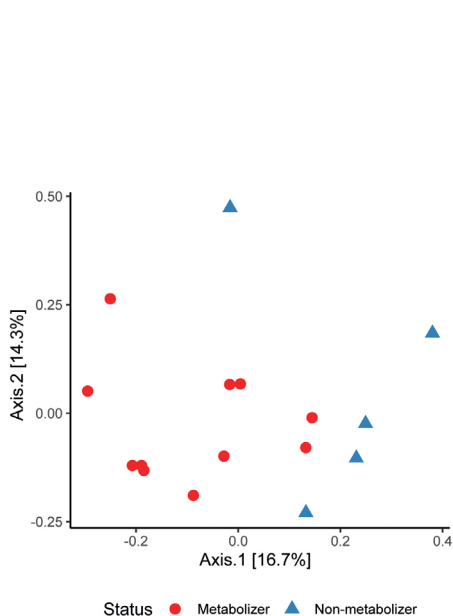
Figure 3.7 Beta diversity PCoA plot of Bray-Curtis dissimilarities of the 16 human fecal samples, divided in metabolizers (red circles) and non-metabolizers (blue triangles) based on experimentally obtained V_{max} values of fructoselysine degradation.
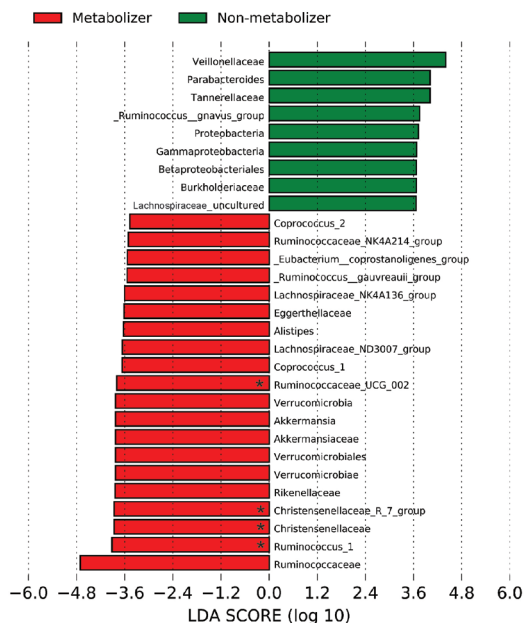
Figure 3.8 LEfSe results of the significant different taxa found by comparing the metabolizers (red) with the non-metabolizers (green), ranked to their effect size. Nomenclature is based on the highest achievable taxonomic resolution level. The log10 LDA score threshold was set to 2.0 and the alpha value was set to 0.05. The taxa which remained significantly different by lowering the alpha value to 0.01 are marked (*).

To identify possible relations between the relative abundance of taxa and the experimentally obtained V_{max} of fructoselysine degradation or the fructoselysine-dependent SCFA production, Spearman's rank correlation was performed. In **Figure 3.9** taxa correlating with one or more of the parameters with ρ ≥ 0.5 are shown. Taxa which were also identified by LEfSe analysis were labelled grey. Several taxa were found to have a correlation with one or more parameters. For example, the relative abundance of the genus *Ruminococcus_1* was correlated to V_{max} with ρ=0.81 and butyrate formation with ρ=0.80. The correlation was weaker with acetate formation (ρ=0.57) and not observed for propionate (ρ=0.19) formation. In addition, *Lachnospiraceae NK4A136_group*, *[Eubacterium] eligens group, [Eubacterium] coprostanoligenes group, Barnesiella, Ruminococcaceae UCG-002* and *Christenellaceae R-7 group* were found to have a correlation with both the V_{max} for fructoselysine degradation (ρ = 0.67 to 0.75), and butyrate formation (ρ = 0.57 to 0.79), but only a slight or no correlation with acetate formation (ρ = 0.15 to 0.51) and propionate formation (ρ = -0.22 to 0.20). This observation of a higher correlation with butyrate than with acetate or propionate formation is in line with the observed correlations between fructoselysine degradation (V_{max} values) and SCFA production shown in **Figure 3.6**, which revealed butyrate as the predominant SCFA formed upon fructoselysine degradation.

Interindividual differences in SCFA levels in human fecal samples

Quantified initial concentrations of SCFAs in the fecal samples, scaled up from measurements in the diluted fecal slurries (Supplementary materials **Figure S3.5**), differed remarkably between individuals. It was assessed if the initial SCFA concentrations are predictive for the fructoselysine-dependent or -independent SCFA formation in incubations. Correlations of the initial SCFA concentrations with the produced SCFA concentrations revealed that initial SCFA concentrations are not associated with (R^2 <0.15) and thus not predictive for fructoselysine-dependent or fructoselysine-independent SCFA formation in the fecal slurry incubations (Supplementary materials **Figure S3.6**).
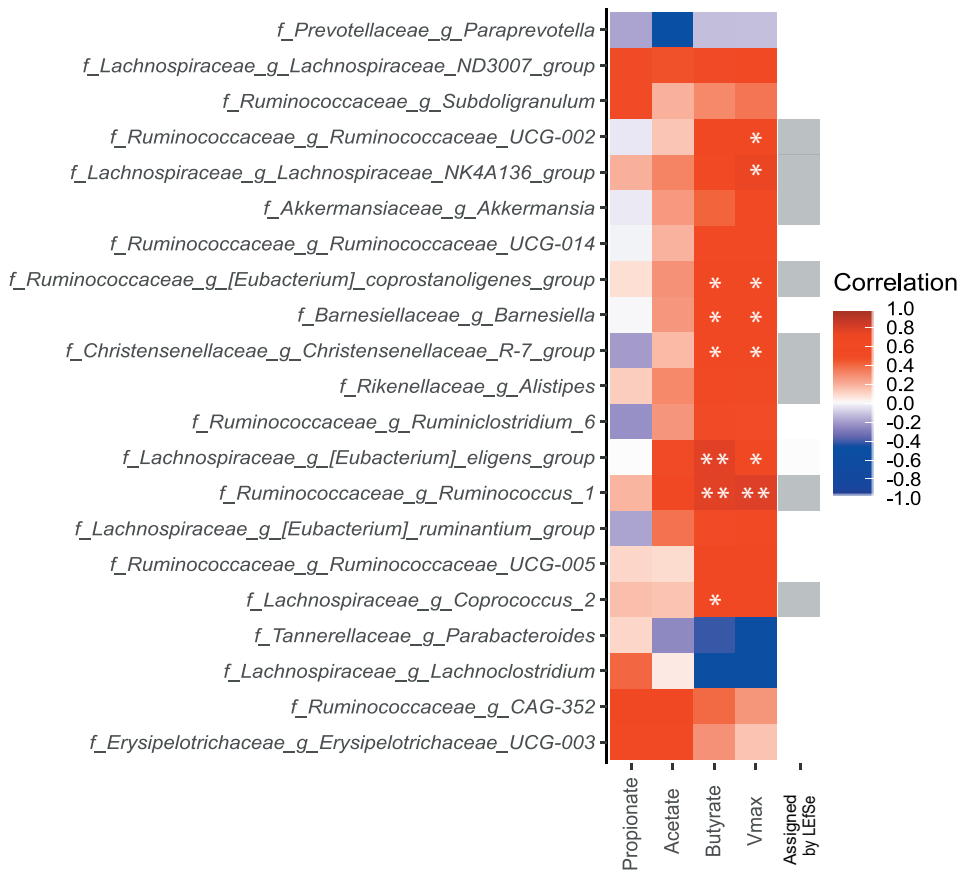
Figure 3.9 Taxa correlating with the metadata (Vmax, butyrate, acetate or propionate) of each individual (Spearman's rank correlation). Taxa with ρ ≥ 0.5 for one or more parameters (V_{max}, butyrate, acetate or propionate) are shown. Statistically significant correlations after FDR correction are marked (* if p-values < 0. 1; ** if p-value < 0.05). The intensity of the color corresponds to the correlation coefficient. Taxa also identified by LEfSe analysis are indicated with a grey box.

3.4 Discussion

In this study, human gut microbial degradation of fructoselysine and accompanying formation of SCFAs were quantified *in vitro* using anaerobic fecal incubations, which enabled the characterization of interindividual differences in this metabolic process. In line with previous observations, fructoselysine degradation by human fecal slurries was observed[223]. Optimization of the incubation conditions to define linear conditions in time and with the amount of fecal slurry enabled definition of the kinetic parameters of this degradation, both of the pooled and individual human fecal slurries. Substantial differences in fructoselysine degradation were observed between individuals, and non-metabolizers and metabolizers of fructoselysine could be identified. V_{max} and K_m values for fructoselysine degradation varied up to 14.6-fold and 9.5-fold, respectively, in the group of metabolizers. Fecal samples from 5 of the 16 individuals (i.e. 31.3%; the non-metabolizers) appeared to be unable to degrade fructoselysine. In the current study, there was no association between the amount of fructoselysine already present in feces and the ability to metabolize fructoselysine, perhaps because this first characteristic is obviously also dependent on actual fructoselysine intake, which was not assessed in this study.

For the first time, we quantified Michaelis-Menten kinetics and interindividual differences of fructoselysine degradation by the human gut microbiota, using human fecal slurries. The results can be compared to data reported by Bui et al. (2015) on interindividual differences in the presence of microbiota derived genes considered relevant for this degradation[40]. It was reported that only ±10% of the human intestinal microbial metagenomes of 65 subjects analyzed in the Human Microbiome Project[67] are equipped with genes from *I. butyriciproducens* AF211 shown to be involved in fructoselysine degradation[40]. The fact that the percentage of individuals in the present study able to degrade fructoselysine was substantially higher than 1-2 out of 16 indicates that also other genes, metabolic pathways, and/or microorganisms are likely to be involved in the degradation. Sofar, few other bacterial strains (i.e. *B. subtilis* and *E. coli*) next to *I. butyriciproducens* AF211 were shown to (partially) degrade fructoselysine[39,159]. However, in this study, application of 16S rRNA amplicon sequencing did not identify any of these three taxa in the human fecal samples, which might be due to e.g. absence of the taxa, presence in low abundance in the fecal samples, which has been reported before for *E. coli* in healthy populations[241,242], or primer choice. In general, the results of the present study provide further support for the hypothesis that additional, yet unidentified bacterial strains present in the human gut are also capable or involved in fructoselysine degradation. Several taxa were found to be positively correlated with both the V_{max} of fructoselysine degradation and fructoselysine-dependent produced butyrate formation, where *Ruminococcus_1* showed a strong correlation ($\rho \geq 0.8$) with both parameters and might be a relevant microbe for these studied reactions, as it was also assigned as a biomarker for the metabolizers in the LEfSe analysis. Species belonging to the genus *Ruminococcus_1* have been reported to ferment carbohydrates and fibers, and produce acetate and other substrates for butyrate producing species[243,244]. Other taxa for which their abundance was identified to correlate with individuals' V_{max} and butyrate formation data (*Lachnospiraceae NK4A136 group, [Eubacterium] eligens group, Barnesiella, Christenellaceae R7 group, Coprococcus_2, Alistipes*) have also been associated with SCFA production and/or carbohydrate fermentation[245–248]. Overall, the correlation

data and LEfSe analysis suggest that fructoselysine degradation seems to be performed by multiple microorganisms which would imply facilitation by a larger, coherent diversity. This is probably also a result from cross-feeding, with involvement of a large part of the microbial community, including low-abundant taxa[249].

Based on the correlation of SCFA formation with fructoselysine degradation, of the three SCFAs measured, butyrate appeared to be the preferred product of fructoselysine degradation. While propionate formation showed no correlation with fructoselysine degradation, acetate formation was weakly correlated with its degradation. Despite the low correlation of fructoselysine degradation with acetate formation, acetate showed the highest increase of the three SCFAs upon incubation with fructoselysine compared to incubations without added fructoselysine. This might be due to the fact that acetate itself is an important substrate for microbial cross-feeding, and can be formed and utilized by several other metabolic pathways occurring simultaneously in the incubations[249,250]. After the 6 hours of incubation, in the metabolizers on average 0.24 moles of butyrate were formed per mole of fructoselysine degraded per hour, based on the individuals' V_{max} values. This is less than the 3 moles of butyrate which have been reported to be potentially produced from 1 mole of fructoselysine by *I. butyriciproducens* AF211[40]. These differences may be explained by the fact that this reported 3:1 ratio was observed for single strain incubations and a long incubation time (i.e. 7 days), compared to the fecal slurries and relatively short incubation times used in the present study. In the incubations with fecal slurries, a more diverse bacterial composition may have facilitated different metabolic pathways and swift further catabolism of SCFAs formed[67]. The observed alterations in SCFA levels after fructoselysine exposure in the present study are in agreement with reports of higher SCFA levels in rat feces after exposure to fructoselysine and similar compounds[251]. It is of interest to note that there was also SCFA formation in the anaerobic fecal slurry incubations without added fructoselysine, indicating that either constituents of the fecal samples themselves or the glycerol present in the storage buffer[252] provided carbon sources to support this SCFA production by the microbiota.

Given the potential hazardous aspects of fructoselysine, the most abundant Amadori product in food[223], and the generally perceived beneficial effects of butyrate for human host health, the degradation of fructoselysine by the human gut bacteria is proposed to be a detoxification pathway, with, as shown in the present study, significant interindividual differences. While dietary fructoselysine appears to potentially form a hazard to human health, being a key intermediate in AGE formation (i.e. carboxymethyllysine) and reported to contribute to formation of reactive α-dicarbonyls *in vivo*, more insight in the adverse properties of fructoselysine and AGEs present in food, and the consequences of exposure for human health is needed. The present results will facilitate the definition of internal exposure concentrations and understanding interindividual differences therein.

The optimized *in vitro* method defined in this study can be used for quantification and assessment of interindividual differences in the metabolic capacity of the human gut microbiota. The model provides a way to quantify individual kinetic parameters relevant to absorption, distribution, metabolism and excretion (ADME) properties and can be applied to other (foodborne) chemicals or pharmaceuticals. The resulting data can be integrated

in physiologically based kinetic (PBK) models used to extrapolate *in vitro* data to *in vivo* predictions, after scaling of the fecal incubations to the entire microbial content of the gut. There is increasing awareness for the role of the intestinal microbiome in human safety and risk assessments, and a need to develop suitable models that can be incorporated in new generation toxicity testing and risk assessment moving towards the use of human-based *in vitro* models as alternatives to animal experimentation[13]. While longer, continuous culturing techniques might be required to study the effects of foodborne chemicals on the intestinal microbiome, the described methodology is an effective and efficient way to characterize the contribution of the gut microbiome to chemical toxicokinetics. In addition, interindividual differences can be quantified as shown in the present study, which indicated substantial interindividual differences in fructoselysine degradation and accompanying SCFA formation. This highlights the large interindividual differences present in the metabolic capacity of the human gut microbiota which can affect ADME properties and therewith health effects of (foodborne) chemicals in humans.

3.5 Supplementary materials

Supplemental Methods

Detailed description of methods: DNA isolation, PCR amplification of the 16S rRNA gene and sequencing

DNA from the fecal samples was isolated by transferring fecal samples to sterile bead-beating tubes containing 0.25 g zirconia beads (0.1mm) and three glass beads (2.5 mm), with 300 μL STAR buffer. The tubes containing the fecal samples were applied to bead-beating for three cycles of 1 minute, 5 m/s and incubated for 15 min on a heated shaker (95 ˚C, 900 rpm). After centrifugation (15 min at 4 ˚C, 15 000 rpm) the supernatant was transferred to sterilized Eppendorf tubes, and 200 μL STAR buffer was added to the remaining pellets and were applied to the bead-beating procedure. Afterwards, supernatants originating from one fecal sample were combined and 250 μL was applied to the customized MaxWell® 16 Tissue LEV Total RNA Purification Kit (XAS1220; Promega Biotech AB, Stockholm, Sweden). Purified DNA was eluted in 50 μL nuclease free water and the quantity and purity (OD 260/280 ratio) was assessed with DeNovix DS-11 FX+ Spectrophotometer/Fluorometer (DeNovix Inc., Wilmington, USA) and the Qubit® dsDNA BR Assay Kit (Invitrogen, Carlsbad, USA). Template DNA was diluted to 20 ng/μL and subjected to triplicate PCR reactions to amplify the 16S ribosomal RNA (rRNA) V4 region for each sample with a total volume of 35 μL per reaction. 0.7 μL Of V4 primers (515-F GTGYCAGCMGCCGCGGTAA, 806-R GGACTACNVGGGTWTCTAAT; 10 μM each) were, together with a unique barcoded primer to allow for parallel sequencing of different samples, mixed with 7 μL 5x Phusion Green HF buffer, 0.7 μL dNTPs mixture, 0.35 μL Phusion Hot start II DNA polymerase (2U/μl, ThermoScientific, the Netherlands) and 25.5 μL nuclease free water to form the master mix. Applied PCR cycling conditions consisted of a 30 second denaturation step at 98 ˚C, followed by 25 cycles of 10 seconds at 98 ˚C, 10 seconds at 50 ˚C and 10 seconds at 72 ˚C. The PCR reaction finished with an extension step of 7 min at 72 ˚C. PCR product formation was confirmed by gel electrophoresis (1% agarose gel). Triplicate PCR products per sample were pooled and subsequently purified using the CleanPCR kit (CleanNA, Waddinxveen, the Netherlands). After quantification with the Qubit® dsDNA BR Assay Kit, 200 ng of each purified barcoded sample was pooled in one library and subsequently sequenced (Illumina NovaSeq 6000, paired-end 150 bp; Eurofins Genomics Europe Sequencing GmbH, Konstanz, Germany).

Supplemental Tables

Table S3.1 Increases in SCFA concentration (µM) determined after 6h of incubation with and without 600 µM fructoselysine, compared to the initial concentration of the respective SCFAs present at time 0. Negative values indicate a decrease in concentration. Data shown are averages ± SEM from 3 repeated experiments. Variation within one group (i.e. metabolizers and non-metabolizers) is indicated with averages ± SD.

|		Butyrate (µM)		Propionate (µM)		Acetate (µM)	
	Sample number	Solvent control	Fructose-lysine (600 µM)	Solvent control	Fructose-lysine (600 µM)	Solvent control	Fructose-lysine (600 µM)
	1	2.1 ± 1.2	9.5 ± 3.9	4.4 ± 1.1	6.2 ± 1.2	-4.7 ± 5.8	29 ± 13.1
	2	24.7 ± 4.8	49 ± 5.7	25.9 ± 2.3	24.8 ± 1.0	41.3 ± 15.8	83.4 ± 13.7
	3	28.9 ± 2.5	45 ± 4.4	16 ± 3.5	16.6 ± 3.0	23.1 ± 12.3	73.6 ± 18.5
	4	25.7 ± 10.2	59.5 ± 8.4	11.9 ± 2.8	13.9 ± 2.1	15.2 ± 20.2	50.4 ± 13.9
	5	23.2 ± 3.9	33.8 ± 5.1	12.4 ± 3.0	12.8 ± 2.7	10.6 ± 15.3	43.7 ± 19.3
	6	18.3 ± 4.4	34.5 ± 2.0	12.5 ± 4.2	11.9 ± 5.3	22 ± 20.4	50 ± 27.5
	7	34.4 ± 7.4	69.6 ± 8.0	19.2 ± 3.7	17.6 ± 2.6	25.8 ± 24.7	74.6 ± 19.4
	8	10.8 ± 2.8	23.1 ± 1.8	11.8 ± 4.2	11.2 ± 3.2	22 ± 22.2	55.2 ± 20.6
	9	6 ± 1.7	10.1 ± 2.1	24.9 ± 2.3	30.3 ± 2.8	1.2 ± 12.9	38.9 ± 18.7
	10	1.6 ± 0.4	2.8 ± 1.1	8 ± 3.1	5.6 ± 3.4	-1.1 ± 18.7	10.8 ± 19.5
	11	19.3 ± 6.4	52.2 ± 10.4	17.5 ± 2.4	26.1 ± 2.6	17.6 ± 14.6	86.6 ± 21.4
	12	10.8 ± 2.0	22.9 ± 6.5	19.3 ± 3.1	22 ± 2.8	28.4 ± 19.6	71.5 ± 22.3
	13	1.4 ± 0.7	6.6 ± 2.2	15.3 ± 5.2	19.1 ± 6.8	-5.1 ± 12.0	28.2 ± 25.3
	14	18 ± 3.8	45.1 ± 5.8	10.6 ± 0.7	21.8 ± 3.8	-16.2 ± 6.2	60.3 ± 25.2
	15	3.1 ± 0.9	7.9 ± 3.1	17.9 ± 5.0	19.6 ± 4.0	-1.9 ± 24.0	26.9 ± 22.1
	16	2.8 ± 1.4	3.1 ± 1.7	26.6 ± 5.2	25.4 ± 6.4	25.4 ± 19.0	48.7 ± 25.0
All individuals (n=16)	**Average**	14.4	29.7	15.9	17.8	12.7	52.0
	SD	10.7	21.2	6.1	7.0	15.2	21.4
Metabolizers (n=11)	**Average**	20.0	40.4	16.5	19.0	17.4	62.6
	SD	8.5	17.5	5.0	6.4	10.2	16.2
Non-metabolizers (n=5)	**Average**	2.2	6.0	14.4	15.2	2.5	28.7
	SD	0.7	2.6	7.8	7.9	11.5	12.0
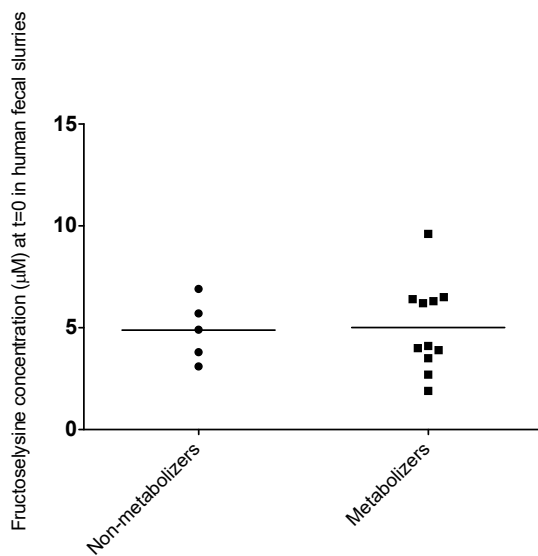
Figure S3.1 Fructoselysine concentrations (µM) quantified in 16 individual human fecal slurries grouped for non-metabolizers (n=5) and metabolizers (n=11), based on their experimentally assessed ability to degrade fructoselysine. Each data point represents one individual.
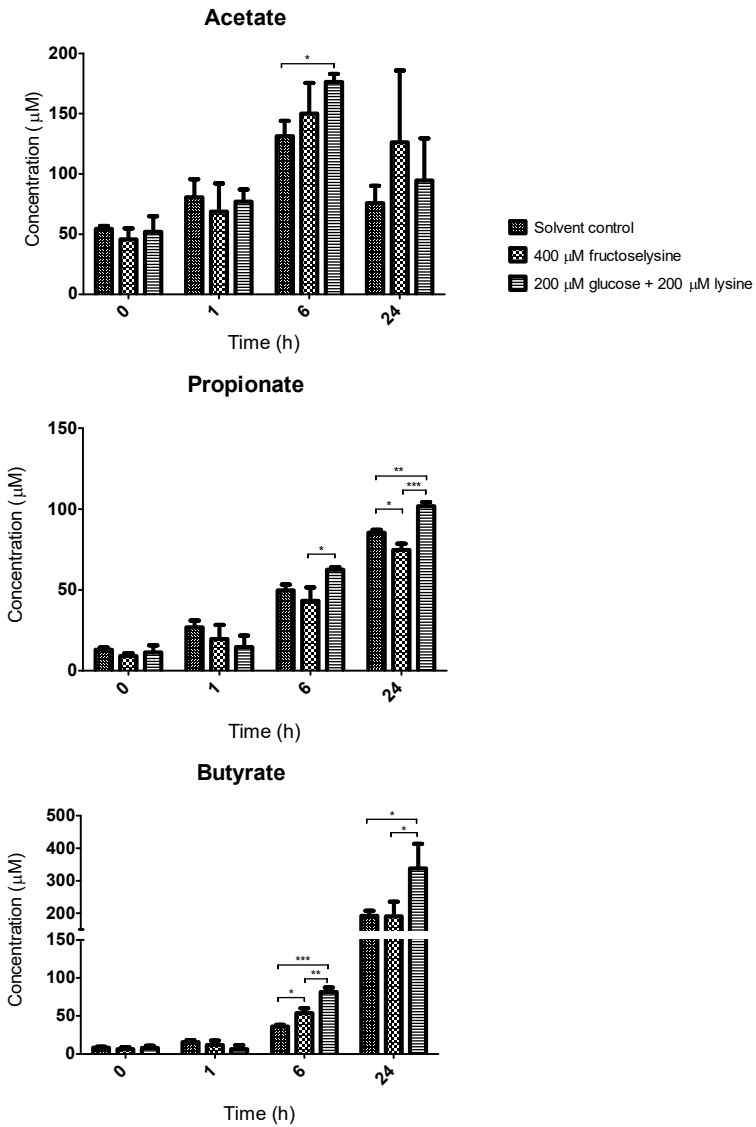
Figure S3.2 SCFA levels in pooled human fecal slurries after exposure to fructoselysine, glucose and lysine or the solvent control over time. For statistical analysis ANOVA was performed followed by Tukey's post-hoc test: * p <0.05; ** p < 0.01; *** p <0.001.
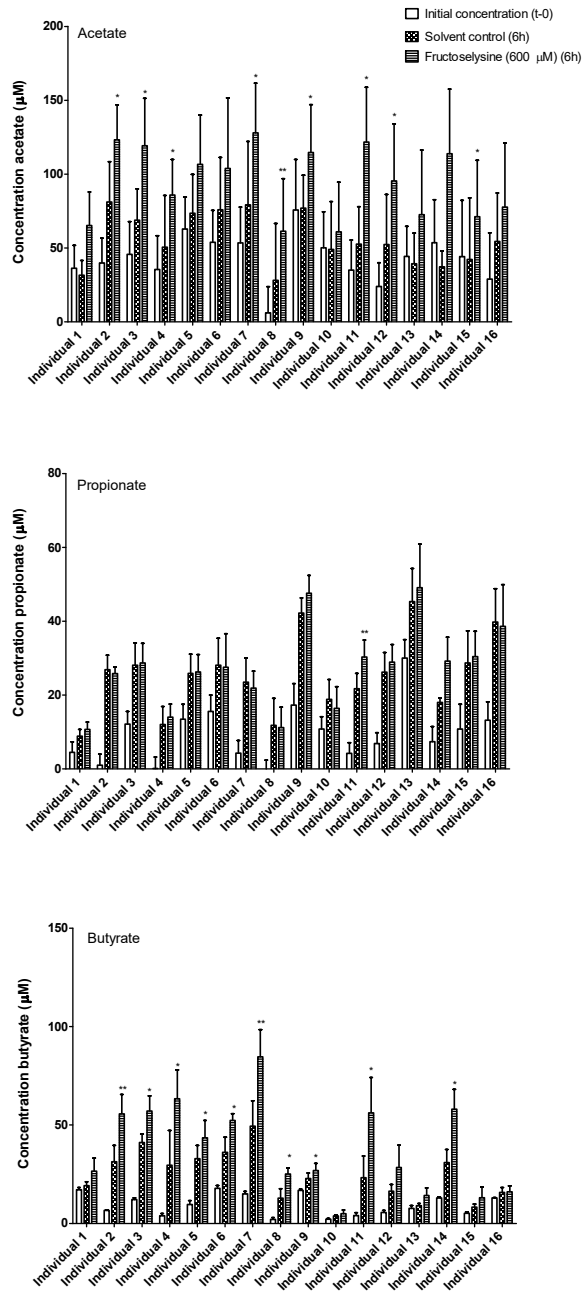
Figure S3.3 SCFA concentrations in fecal slurries at t=0 and at t=6h. Data points represent the average ± SD of 3 repeated experiments. Multiple paired t-tests were performed at 6h incubation of fructoselysine exposure (600 μM) compared to the solvent control: * p < 0.05; ** p < 0.01.
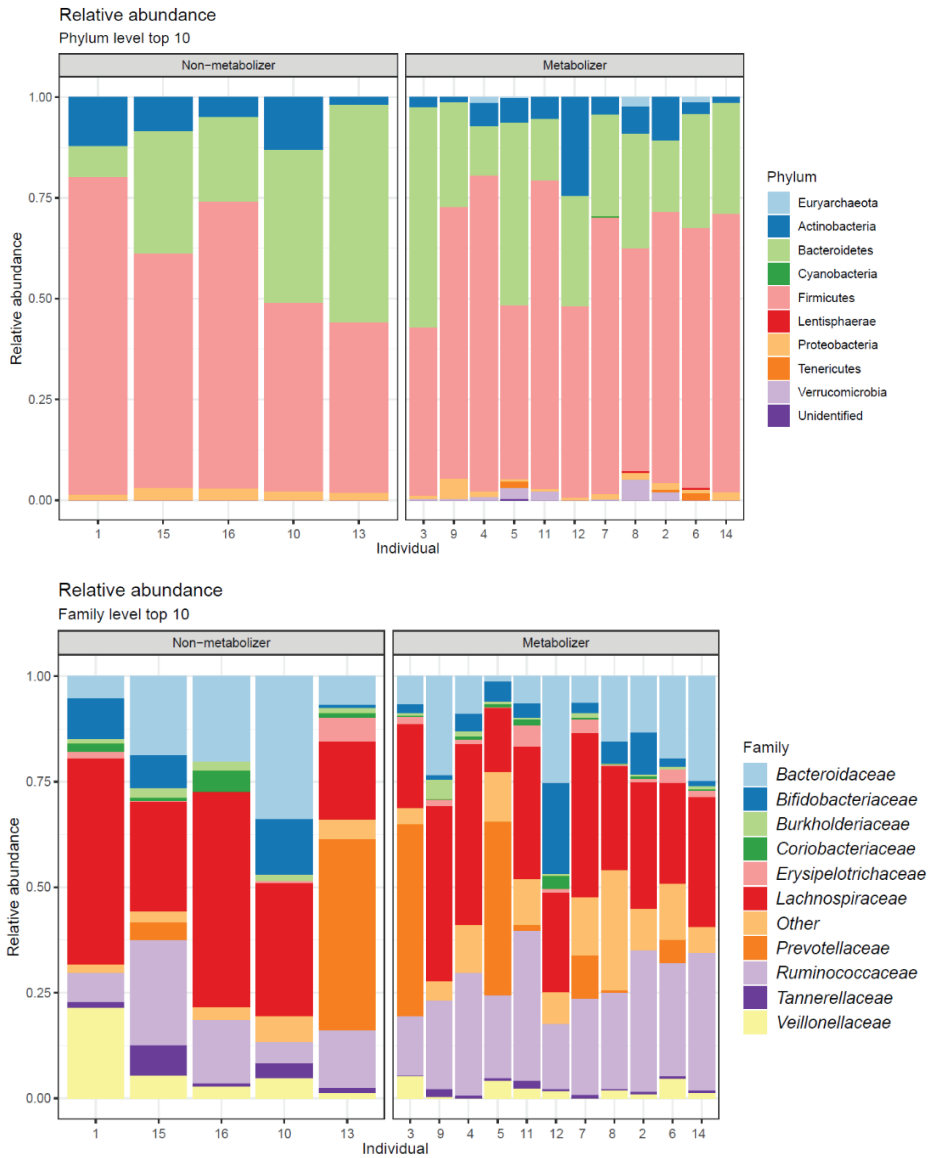
Figure S3.4 Bacterial composition plots showing the relative abundance of the top 10 taxa present both at Phylum (upper plot) or Family (lower plot) level. The individual fecal samples assessed are divided into "metabolizers" and "non-metabolizers", referring to their capability to degrade fructoselysine in this study in vitro.
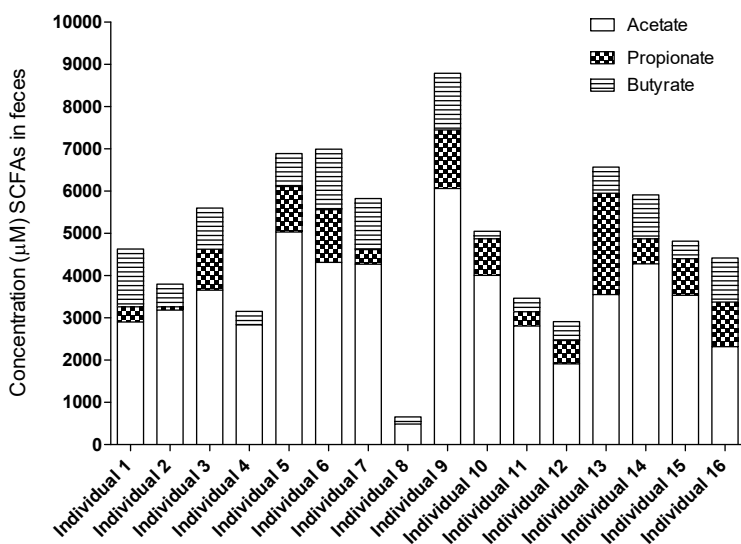
Figure S3.5 Initial concentrations (t=0) of the SCFAs acetate, propionate, and butyrate in the 16 human fecal samples, scaled up from measurements in the incubation samples.
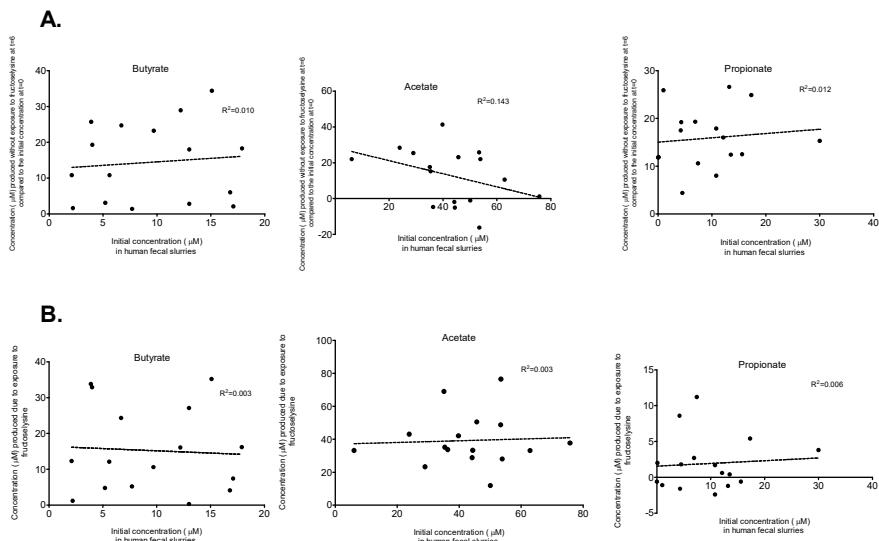
Figure S3.6 Correlation of the SCFA formation in the solvent control at t=6 compared to t=0 (A) or the fructoselysine dependent SCFA formation at t=6 (B) with the initial concentration of the SCFA found in the fecal slurry, experimentally obtained using fecal slurries from 16 human individuals.
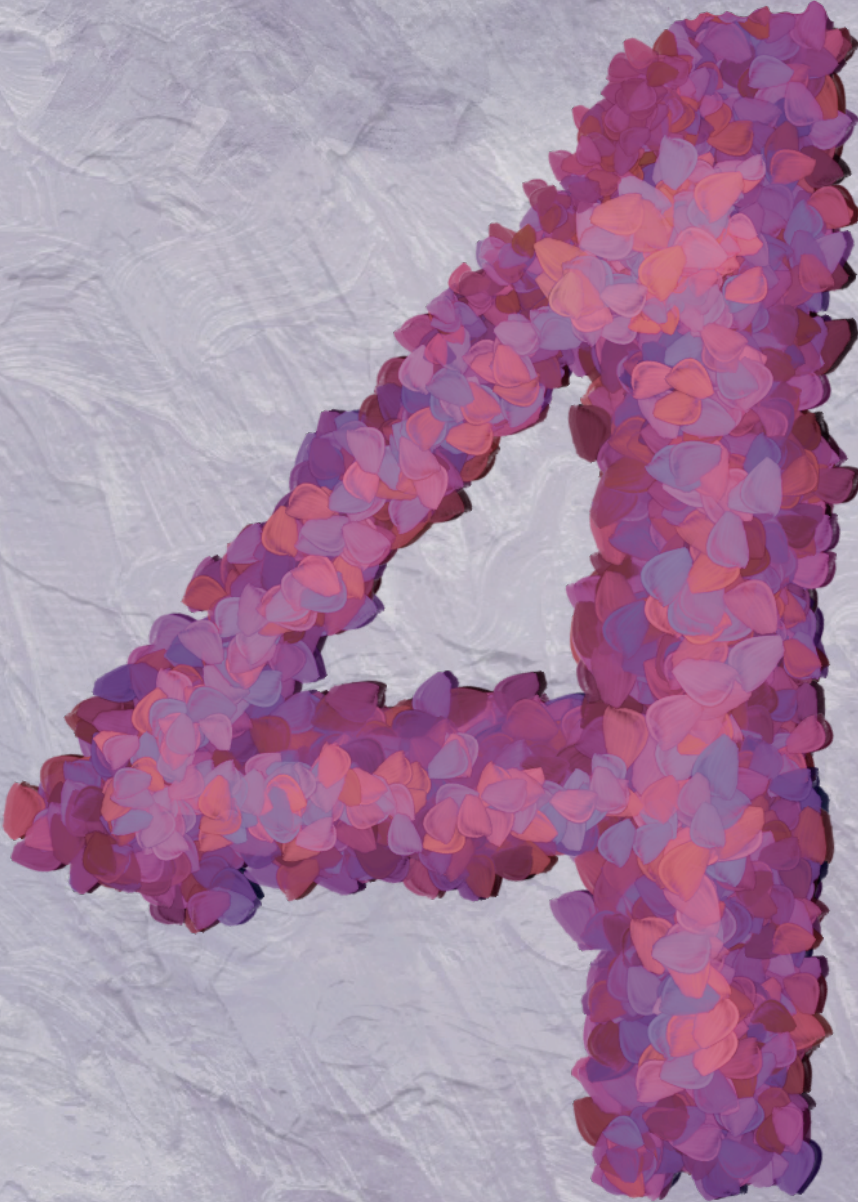
Inter- and intraindividual differences in the capacity of the human intestinal microbiome in fecal slurries to metabolize fructoselysine and carboxymethyllysine

Katja C.W. van Dongen, Clara Belzer, Wouter Bakker, Ivonne M.C.M. Rietjens, Karsten Beekmann

Abstract

The advanced glycation end product (AGE) carboxymethyllysine and its precursor fructoselysine contaminate heated, processed food products and are considered hazardous for human health. Upon dietary exposure, they can be degraded by human colonic gut microbiota, reducing internal exposure. Pronounced interindividual and intraindividual differences in these metabolic degradations were found in anaerobic incubations with human fecal slurries *in vitro*. The average capacity to degrade fructoselysine was 27.7-fold higher than that for carboxymethyllysine, and degradation capacities for these two compounds were not correlated ($R^2=0.08$). Analysis of the bacterial composition revealed that interindividual differences outweighed intraindividual differences, and multiple genera were correlated with the individuals' carboxymethyllysine and fructoselysine degradation capacities (e.g. *Akkermansia*, *Alistipes*).

The results of the present study show that the capacity for intestinal microbial degradation of these two compounds can be substantial, likely reducing internal exposure levels and thus the potential hazards related to dietary exposure of carboxymethyllysine and fructoselysine.

4.1 Introduction

Glycation products are formed during heating and processing of food products, are abundantly present in the Western diet[12,230] and include advanced glycation end products (AGEs) and their precursors such as Amadori products. They are formed by non-enzymatic glycation reactions between amino acids and reducing sugars (i.e. the Maillard reaction[104]) and can be present in food in both their protein-bound as well as in their free form[12,230]. One of the most abundant AGEs in the Western diet is carboxymethyllysine, which can be formed via rearrangement of the Amadori product fructoselysine or via reactions of reactive dicarbonyls (i.e. glyoxal and 3-deoxyglucosone) with the amino acid lysine[9,44]. Besides the presence of AGEs in the diet, they are also formed endogenously in the human body[12,230]. Dietary exposure to AGEs is reported to contribute to AGE levels in plasma[22,151,253,254] and tissues[29,133,151]. In addition, exposure to dietary AGEs has been associated with increased markers of negative health effects such as inflammation and endothelial dysfunction[23]. However, the actual contribution of dietary AGEs towards adverse health effects remains debated. In addition, alterations in gut bacterial profiles are reported to be induced by exposure to heat-treated diets which are high in AGEs[51,151,208–210,212,255]. The gut microbiota can also affect AGEs by metabolism thereof. It has been shown that human gut bacteria in fecal slurries can degrade AGEs and their precursors *in vitro*[161,223,256], with single bacterial strains reportedly able to metabolize specific AGEs such as carboxymethyllysine,[47,48] and its precursor fructoselysine[38,40]. Because of the potential hazardous effects of AGEs on human health, gut microbial metabolism could serve as a potential detoxification pathway. Furthermore it has been shown that substantial interindividual differences in human bacterial degradation of fructoselysine exist[161], and also interindividual differences in carboxymethyllysine degradation have been reported in a number of individuals[48,256].

The human gut microbiota is a complex and dynamic ecosystem with large interindividual differences in composition. The microbiota composition is mainly shaped by environmental factors (e.g. diet and lifestyle)[62], and it can change over time and, among others, following xenobiotic exposure, which can have consequences for its functioning[67]. While the most fundamental metabolic functions of the microbiota are considered to be temporally stable and conserved among individuals despite differences in composition[67], in a previous study we reported large interindividual differences in the kinetics of gut microbial degradation of fructoselysine[161]. Given the dynamic nature of the microbiota[257], and being reactive to a plethora of host and environmental factors it is of interest to also assess the temporal variability of gut microbial degradation activities. Therefore, in the present study we aim to quantify interindividual as well as intraindividual differences of gut microbial degradation of fructoselysine and carboxymethyllysine. To this end, *in vitro* anaerobic incubations with fecal samples collected from multiple individuals at different sampling times spread over 3 to 16 weeks were performed with both fructoselysine and carboxymethyllysine as substrates. Total bacterial cell load in these samples was quantified and microbial composition was characterized by 16S rRNA amplicon sequencing and correlated with the respective degradation capacities.

4.2 Materials and Methods

Chemicals and reagents

Carboxymethyllysine (CAS: 5746-04-3) and fructoselysine (CAS: 21291-40-7) were purchased from Carbosynth Limited (Berkshire, UK). D4-labelled carboxymethyllysine was purchased from Buchem BV (Apeldoorn, the Netherlands). Glycerol (CAS: 56-81-5) was purchased from Sigma-Aldrich (Steinheim, Germany). Formic acid (99-100%, analytical grade, CAS: 64-18-6) was purchased from Merck (Darmstadt, Germany). PBS was purchased from Gibco (Paisley, UK). Acetonitrile (ACN; UPLC/MS grade; CAS: 75-05-8) was obtained from BioSolve BV (Valkenswaard, the Netherlands).

Collection of human fecal samples

Fresh fecal samples were collected from 20 human volunteers (11 females, 9 males), aged between 19 and 64 years, at sampling time one (ST1). Of these individuals, 13 donated a sample again on two later occasions (8 females, 5 males, aged between 24 and 65 years old; with ≥3 weeks in-between over a total maximum period for all 3 donations of 16 weeks; corresponding to ST2 and ST3; see Supplementary Materials **Table S4.1** for the sampling times of each individual). Fecal samples were immediately processed after donation as described before[161] and stored at -80°C after a 4x dilution (w/v) in anaerobic storage buffer consisting of 10% glycerol in PBS until further use. All participants granted informed consent before participation in this study. The study design was assessed by the Medical Ethical Committee of Wageningen University and judged to not fall under the Dutch 'Medical Research Involving Human Subjects Act'.

Anaerobic incubations of fecal slurries with carboxymethyllysine and fructoselysine

Anaerobic incubations with human fecal slurries and fructoselysine or carboxymethyllysine were performed as previously described[161]. In short, pooled or individual human fecal slurries were mixed with anaerobic PBS and carboxymethyllysine or fructoselysine. 50 μL of this mixture were divided over Eppendorf tubes and incubated at 37°C for the required duration, after which reactions were stopped by addition of 50 μL ice-cold ACN, and stored on ice for >15 min. All handlings were performed inside an anerobic chamber (85% N_2, 10% CO_2 and 5% H_2)(Bactron EZ anaerobic chamber). Samples were centrifuged at 15,000 x g for 15 min at 4 °C, and resulting supernatants were used for subsequent analysis by LC-MS/MS.

Optimization of experimental conditions for the incubations of human fecal slurries and fructoselysine was previously described[161], resulting in anaerobic incubations of one hour with 5% individual fecal slurry in PBS (i.e. 0.0125 g/mL) with a final, saturating concentration of 125 μM fructoselysine. For carboxymethyllysine degradation, experimental conditions were optimized with pooled human fecal samples containing equal amounts of 20 individual human fecal samples collected at ST1. With this pooled fecal slurry, experimental conditions were optimized to achieve linear degradation of carboxymethyllysine over increasing percentage of fecal slurry and over time (Supplementary Materials **Figure S4.1A**). Subsequent anaerobic incubations of individual fecal samples were performed with 20% individual human fecal slurries in PBS (i.e. 0.05 g/mL) for 3 hours with a final, saturated

substrate concentration of 80 μM carboxymethyllysine (Supplementary Materials **Figure S4.1B**). All experiments were performed in at least technical duplicates and were repeated three times.

Quantification of fructoselysine and carboxymethyllysine by LC-MS/MS
80 μL supernatants of the anaerobic fecal slurry incubations were transferred into LC-MS/MS vials. In addition, for carboxymethyllysine, 10 μL of 120 μM aqueous D4-carboxymethyllysine was added as internal standard. Fructoselysine and carboxymethyllysine concentrations were quantified using a Shimadzu Nexera XR LC-20AD SR UPLC system coupled to a Shimadzu LCMS-8040 triple quadrupole MS (Kyoto, Japan). The LCMS-8040 coupled with an ESI source was used for MS/MS identification. Positive ionization for multiple reaction monitoring (MRM) mode was used. For fructoselysine, 2 μL of supernatant were injected onto a Phenomenex Polar-RP Synergi column (30 x 2 mm, 2.5 μm), at which fructoselysine eluted at 5.6 min and was quantified using the precursor to product transition m/z 309.2 > 84.2 (collision energy (CE) = -31 V), which was the most intense fragment ion, as previously described[161]. For carboxymethyllysine, 1 μL of supernatant was injected onto a Waters Acquity BEH Amide column (2.1 x 100 mm, 1.7μm) at 40 °C. The mobile phase consisted of a gradient made from solvent A (i.e. ultrapure water with 0.1% formic acid (v/v)) and solvent B (i.e. ACN with 0.1% formic acid (v/v)). The gradient started with 75% B, to reach 12.5% B at 5 min and was subsequently kept at 12.5% B until 11 min, followed by a shift to reach 95% B at 12 min, which was kept stable until 17 min before returning to the initial start conditions at 18 min keeping these conditions up to 24 min. The initial flow of 0.3 mL/min was decreased to 0.15 mL/min from 5 to 5.5 min, and remained 0.15 mL/min up to 11 min before returning to the initial flow of 0.3 mL/min at 17 min. Under these conditions, carboxymethyllysine and D4-carboxymethyllysine eluted at 4.6 min. Carboxymethyllysine was quantified using the precursor to product transition m/z 204.9 > 84.2 (CE = -21 V). MRM transitions m/z 204.9 > 130.2 (CE = -12 V) and m/z 204.9 > 56.1 (CE = -39 V) were used as reference ions. D4-carboxymethyllysine was quantified using the MRM transition m/z 208.9 > 88.1 (CE = -21 V), while MRM transitions m/z 208.9 > 134.2 (CE = -12 V) and m/z 208.9 > 56.1 (CE = -42 V) were used as reference ions. External calibration curves were prepared in the same way as described for the unknown samples for quantification of concentrations present in the samples. Peak areas were integrated using LabSolutions software (Shimadzu). The amount of degraded fructoselysine or carboxymethyllysine during incubation was calculated and expressed in μmol degraded/g feces/hour and μmol degraded/1×10^{12} bacterial cells/hour.

Bacterial taxonomic profiling by 16S rRNA gene amplicon sequencing
DNA was isolated from the fecal slurries using a bead-beating procedure in combination with the customized MaxWell® 16 Tissue LEV Total RNA Purification Kit (XAS1220; Promega Biotech AB, Stockholm, Sweden). DNA isolates underwent triplicate PCR reactions of the 16S ribosomal RNA (rRNA) gene V4 region (515-F; 806-R) with a library approach as described before[151,161]. PCR products were purified, pooled and sequenced (Illumina NovaSeq 6000, paired-end, 70 bp; Eurofins Genomics Europe Sequencing GmbH, Konstanz, Germany).

Total bacterial load by qPCR
To quantify the total bacterial load in each individual fecal slurry, quantitative PCR (qPCR) was performed based on a previously described method[258]. Triplicate qPCR reactions

consisted of 1 µL DNA isolate (1 ng/µL) and 9 µL reaction mixture (composed of 62.5% iQ SYBR Green Supermix, 2.5% forward primer (10 µM), 2.5% reverse primer (10 µM) and 32.5% nuclease free water. The following set of primers for total bacterial 16S rRNA genes were used: 1369-F (5'-CGG TGA ATA CGT TCY CGG-3') and 1492-R (5'-GGW TAC CTT GTT ACG ACT T-3'). A purified DNA isolate of *Escherichia coli* was used to create a standard curve to facilitate quantification. The amplification program started at 95 °C for 10 min, followed by 40 cycles of denaturing at 95 °C for 15 sec, annealing at 60 °C for 30 sec and elongation at 72°C for 15 sec. The program ended with a melt curve from 60 °C to 95 °C. A CFX-384 Touch Real-Time PCR detection system (Bio-Rad, California, USA) was used. Data analysis was performed with the CFX manager (Bio-Rad). Quantified copy numbers of total 16S rRNA genes/g fecal sample were divided by the average 16S rRNA genes per bacterium (i.e. 4.2[259]) and thus transformed to total bacterial load/g fecal sample.

Data analysis

Sequences of the 16S rRNA gene were analyzed using NG-Tax 2.0 pipeline with default settings[235], generating *de novo* exact match sequence clusters (ASVs; amplicon sequence variants). The SILVA 16S rRNA gene reference database[236] release 132 was used to assign taxonomy. R (version 4.0.2) was used for further data analysis, using the Phyloseq package[237] (version 1.34.0) to combine the ASV table with the phylogenetic tree and metadata. A relative abundance cut-off of 0.1% of a taxa in one of the individual samples was used to include ASVs for further analyses, unless mentioned otherwise. When desired, relative abundance data were transformed into absolute abundance data by multiplying the relative abundance of a taxa within one sample with the corresponding total bacterial load/g fecal sample, as quantified by qPCR. The Microbiome package[238] (version 1.12.0) was used to create composition plots of the top taxa present in the samples, sorted with hierarchical clustering based on Bray-Curtis beta diversity dissimilarities using the average linkage approach using all taxa present in the samples. Belonging dendrograms were created with the packages Phyloseq[237], Stats and Ape[260] (version 5.4.1). Spearman's rank correlations of fructoselysine and carboxymethyllysine degradation with microbial taxa which were present at a relative abundance of >1% in one of the samples and glomerated at genus level were made. *P* values were adjusted for multiple testing with the Benjamini & Hochberg false discovery rate using the Microbiome package[238].

Quantified amounts of degraded fructoselysine and carboxymethyllysine of three repeated experiments were averaged and standard deviations were calculated using GraphPad Prism 5.0. Individual amounts of degraded fructoselysine and carboxymethyllysine were corrected for the applied weight of feces used in the incubations and/or the total bacterial cell load per gram feces and expressed per hour. For the latter, the percentage of total substrate degraded was quantified using the total substrate added relative to the average total bacterial cell load set as 100%. Outliers were identified using IBM SPSS Statistics version 25 using a multiplier of 3.0. Statistically significant differences in the amount of fructoselysine or carboxymethyllysine degraded per sampling time were assessed with an ANOVA test combined with a Tukey's multiple comparison post-hoc test. Unless otherwise stated, results were found to be statistically significant when *P*-values were <0.05.

4.3 Results

Interindividual and intraindividual differences in gut microbial carboxymethyllysine degradation profiles in vitro

Interindividual differences in carboxymethyllysine degradation were investigated for all collected individual fecal samples, i.e. 20 individual fecal samples donated at a first sampling time (i.e. ST1) and fecal samples donated by 13 of these 20 individuals at two other sampling times (i.e. ST2 and ST3). Anaerobic incubations were performed with individual human fecal slurries based on optimized experimental conditions (i.e. with final concentrations of 0.05 g feces/mL and 80 µM of carboxymethyllysine; see Supplementary Materials **Figure S4.1**). The amount of carboxymethyllysine degraded per hour was expressed relative to the total bacterial load in the samples as quantified by qPCR, which were in line with literature[261] (for bacterial load of samples see Supplementary Materials **Figure S4.2**; for carboxymethyllysine degradation per g feces see Supplementary Materials **Figure S4.3**). For individual 1, ST1 was assessed as being an outlier and thus excluded from further analyses. Overall, the degradation capacities of the individual fecal slurries tested ranged from no or minimal carboxymethyllysine degradation to a maximum of 0.83 µmol carboxymethyllysine degradation/1×10^{12} bacterial cells/h (Individual 5, ST2), the latter resulting in 65% of the added substrate being degraded under the experimental conditions applied. Average carboxymethyllysine degradation for the different sampling times for the 13 individuals that donated 3 times were not significantly different and were in the same range, i.e. 0.09 (ST1), 0.3 (ST2) and 0.15 (ST3) µmol carboxymethyllysine degradation/1×10^{12} bacterial cells/h (**Figure 4.1**), resulting in 7%, 24% and 12% of the added substrate being degraded under the experimental conditions applied, respectively.
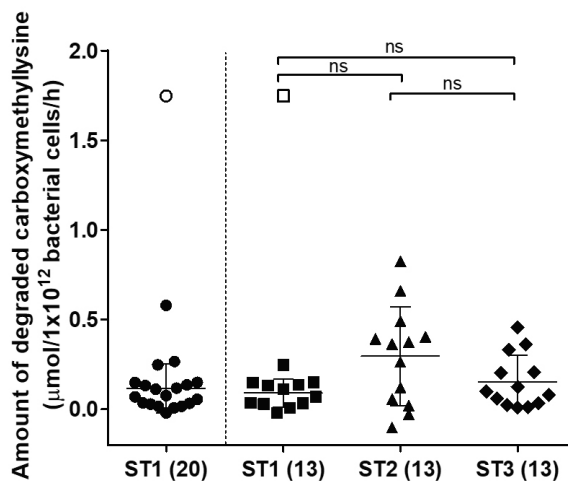

Figure 4.1 Amount of carboxymethyllysine degraded after anaerobic incubation of individual human fecal samples (0.05 g/ml final concentration) with 80 µM carboxymethyllysine, expressed per hour. ST1, ST2 and ST3 indicate different sampling times, and the number in brackets refers to the number of individuals who donated at these different sampling times. For ST1 this is a total of 20 individuals, whereof 13 individuals donated at two additional sampling times, which are separately visualized in the second column ST1(13). Scatter dots indicate average values of three independent experiments for each individual fecal sample. Center bars and whiskers indicate mean values with the standard deviation. Open symbols refer to an identified outlier. N.s. refers to not statistically significant.

Intraindividual variability in carboxymethyllysine degradation capacities were further quantified for the 13 individuals who donated at ST1, ST2 and ST3, as shown in **Figure 4.2**. The capacity to degrade carboxymethyllysine differed within most individuals over time. As such, several individuals were not always able to degrade carboxymethyllysine (i.e. Individuals 2, 4, 7, 10, 11, 12) while other individuals mainly showed differences in the amount being degraded (i.e. Individuals 1, 3, 5, 6, 8, 9, 13). The largest absolute difference of carboxymethyllysine being degraded was for individual 5 with a difference of 0.68 µmol/1×10^{12} bacterial cells/h between sampling time ST1 and ST2, corresponding to a difference of 54% of the added substrate being degraded under the experimental conditions applied. Almost no difference of carboxymethyllysine degradation between different sampling times was detected for individual 4 between sampling times ST2 and ST3 (with a negligible difference of 0.002 µmol/1×10^{12} bacterial cells/h).

When expressing the degradation per gram feces instead of bacterial load (see Supplementary Materials **Figure S4.3**), inter- and intraindividual differences ranged from no to minimal carboxymethyllysine degradation to a maximum of 0.48 µmol carboxymethyllysine/g feces/h being degraded, the latter resulting in 91% of the added substrate being degraded under the experimental conditions applied. Comparing the amount of bacterial cells/g feces with the amount of degraded carboxymethyllysine/g feces/h confirms that there is no correlation between the absolute number of bacteria in the samples and the ability to degrade carboxymethyllysine ($R^2=0.059$; see Supplementary Materials **Figure S4.4A**).
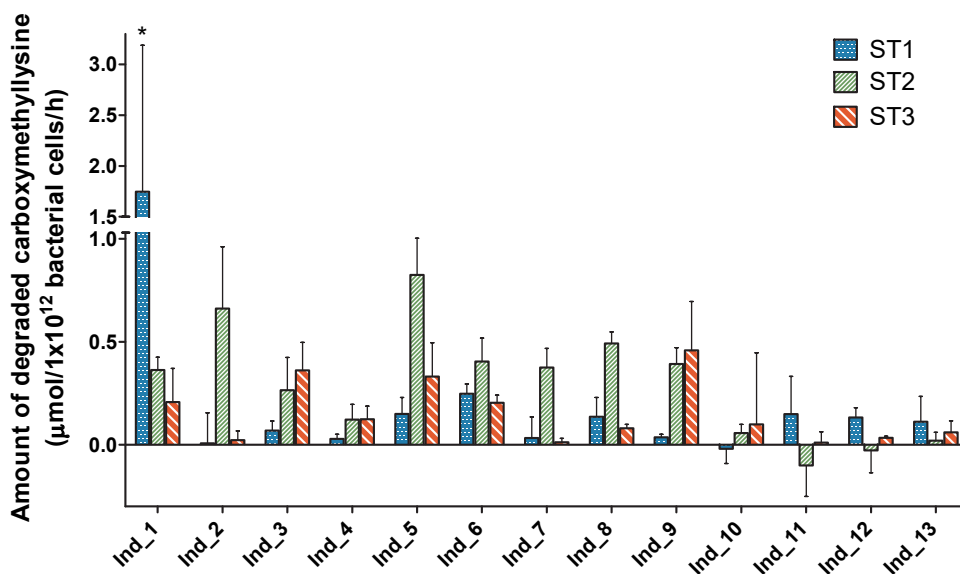

Figure 4.2 Intraindividual differences in degradation of carboxymethyllysine upon anaerobic incubations with individual human fecal slurries (final concentration of 0.05 g/mL), shown for 13 individual donors sampled at three sampling times (i.e. ST1, ST2 and ST3). The data represent the average ± SD of three repeated experiments. * Refers to Ind 1 ST1 which was assessed as an outlier.

Interindividual differences and intraindividual differences in fructoselysine human gut microbial degradation profiles in vitro

To allow comparison of carboxymethyllysine degradation to degradation of its precursor fructoselysine, interindividual and intraindividual differences in fructoselysine degradation were quantified using previously optimized experimental conditions[161] at a saturated substrate concentration of fructoselysine (i.e. with final concentrations of 0.0125 g feces/mL and 125 µM of fructoselysine) using the same individual human fecal samples as for carboxymethyllysine. The amount of fructoselysine degraded per hour was expressed relative to the total bacterial load in the samples as quantified by qPCR (for bacterial load of samples see Supplementary Materials **Figure S4.2**; for fructoselysine degradation per g feces see Supplementary Materials **Figure S4.5**). The value from Individual 1, ST1 was assessed as an outlier and therefore excluded from further analyses. Overall, interindividual differences in the degradation capacity of the individual fecal slurries tested ranged from no or only minimal degradation to 19.63 µmol fructoselysine degradation/1×10^{12} bacterial cells/h (Individual 10, ST3), the latter resulting in 82.5% of the added substrate being degraded under the experimental conditions applied. Average fructoselysine degradation for the different sampling times for the 13 individuals that donated 3 times were not statistically significantly different and were in the same range, i.e. 4.8 (ST1), 5.3 (ST2) and 4.4 (ST3) µmol/1×10^{12} bacterial cells/h (**Figure 4.3**), resulting in 20%, 22% and 18% of the added substrate being degraded under the experimental conditions applied, respectively.

Intraindividual variability in fructoselysine degradation capacities were further quantified within the 13 individuals who donated at ST1, ST2 and ST3, as shown in **Figure 4.4**. The capacity to degrade fructoselysine differed within most individuals over time; all samples from Individual 7 degraded no or only very little fructoselysine, and two individuals showed a relatively stable capacity to degrade fructoselysine for all three sampling times (i.e. Individuals 4 and 5). The largest absolute difference of fructoselysine being degraded was within individual 10 with a difference of 17.5 µmol/1×10^{12} bacterial cells/h between sampling times ST2 and ST3, corresponding to a difference of 74% of the added substrate being degraded under the experimental conditions applied. Almost no absolute difference in degraded fructoselysine between different sampling times was detected for individual 12 between sampling times ST1 and ST2 (with a difference of 0.01 µmol/1×10^{12} bacterial cells/h).
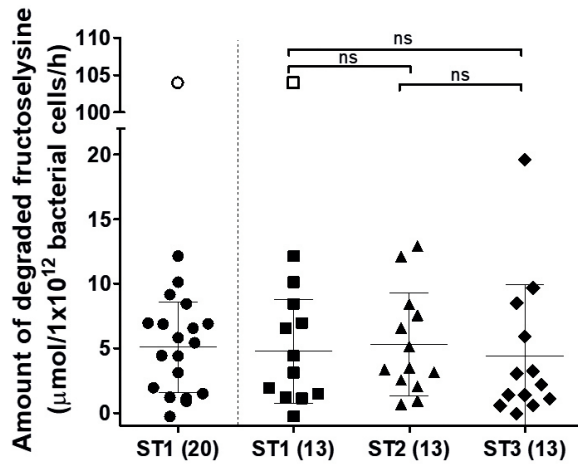
4

Figure 4.3 Amount of fructoselysine degraded after anaerobic incubation of individual human fecal samples (0.0125 g/mL final concentration) with 125 μM fructoselysine per hour. ST1, ST2 and ST3 indicate different sampling times, and the number in brackets refers to the number of individuals who donated at these different sampling times. For ST1 this is a total of 20 individuals, whereof 13 individuals donated at two additional sampling times, which are separately visualized in the second column ST1(13). Scatter dots indicate average values of three independent experiments. Center bars and whiskers indicate mean values with the standard deviation. Open symbols refer to an identified outlier. N.s. refers to not statistically significant.
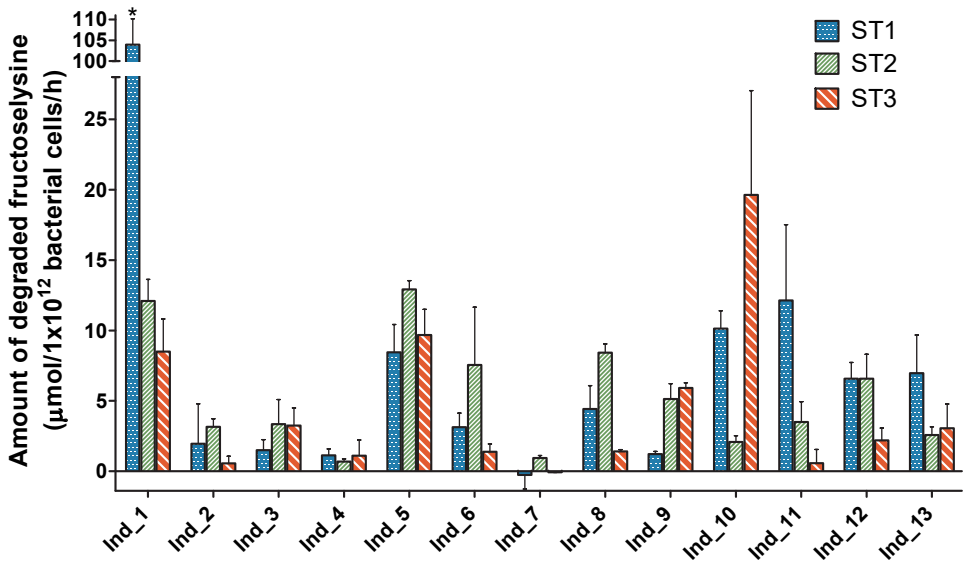
Figure 4.4 Intraindividual differences in degradation of fructoselysine upon anaerobic incubations with individual human fecal slurries (final concentration of 0.0125 g/mL), shown for 13 individual donors sampled at three sampling times (i.e. ST1, ST2 and ST3). The data represent the average ± SD of three repeated experiments * Refers to Ind 1 ST1 which was identified to be an outlier.

When expressing fructoselysine degradation per gram feces instead of bacterial load (see Supplementary Materials **Figure S4.5**), inter- and intraindividual differences ranged from no to minimal fructoselysine degradation to a maximum of 5.4 µmol fructoselysine/g feces/h being degraded, resulting in 54% of the added substrate being degraded under the experimental conditions applied. Comparing the amount of bacterial cells/g feces with the amount of degraded fructoselysine/g feces/h confirms that there is no correlation between the absolute number of bacteria in the samples and the ability to degrade fructoselysine (R^2=0.002; see Supplementary Materials **Figure S4.4B**).

Comparison of carboxymethyllysine and fructoselysine degradation

Figure 4.5 presents a linear regression analysis of the amount of fructoselysine and carboxymethyllysine degraded/$1x10^{12}$ bacterial cells/h. This reveals that there is no correlation between the capability to microbially degrade fructoselysine and carboxymethyllysine for all individual collected fecal samples (R^2=0.084 for degradation/$1x10^{12}$ bacterial cells/h, see **Figure 4.5**; for degradation/g feces/h R^2=0.253, see Supplementary Materials **Figure S4.6**). Overall, fructoselysine was degraded faster than carboxymethyllysine (i.e. on average 27.7-fold faster when expressed relative to the bacterial load; 23.4-fold faster when expressed per gram feces). Regarding intraindividual differences, fructoselysine and carboxymethyllysine showed comparable relative variability amongst all sampled individuals (CV = 85% for fructoselysine; CV = 112% for carboxymethyllysine; n=45).
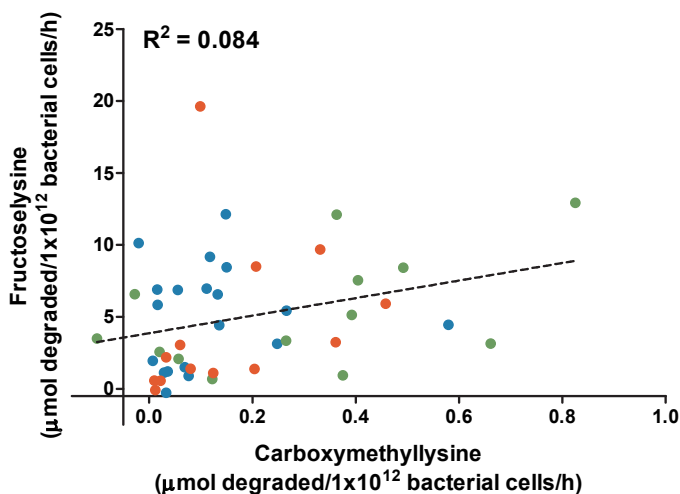
Figure 4.5 Linear regression between the amount of fructoselysine and carboxymethyllysine degraded during anaerobic incubations with individual human fecal slurries. A total of 45 individual donated fecal samples were included consisting of 19 individuals (sample ST1) whereof 13 individuals donated at two additional sampling times (i.e. ST2 and ST3). Blue circles refer to ST1; green circles to ST2; red circles to ST3. Individual 1, ST1 was excluded from the analysis as it was assessed as an outlier.

Assuming a total transit time in the colon of 24 hours[262] and a total fecal mass of 128 grams per 24 hours[263] the experimentally obtained *in vitro* average degradation capacities of all individuals can be extrapolated to the *in vivo* situation. This analysis can reveal whether the

estimated daily intake (EDI) of carboxymethyllysine and fructoselysine, amounting to 0.3 mg/kg bw/day for carboxymethyllysine and 7.1-14.3 mg/kg bw/day for fructoselysine[223], can be completely degraded in the colon (see Supplementary Materials **Table S4.2**). For carboxymethyllysine 18 of the 46 tested fecal samples had degradation capacities too low to completely degrade the estimated daily intake, and 11 of the 20 donors who donated a fecal sample (once or more) had degradation capacities too low to completely degrade the EDI at one or more sampling times. For fructoselysine, depending on the level of intake, 8-20 of the 46 tested fecal samples had degradation capacities too low to completely degrade the EDI. 4-10 Of the 20 donors who donated a fecal sample (once or more) had degradation capacities too low to completely degrade the EDI at one or more sampling times (see Supplementary Materials **Table S4.2**).

Interindividual and intraindividual differences in human gut microbial composition
Bacterial taxonomic profiling by 16S rRNA amplicon sequencing revealed interindividual and intraindividual differences in bacterial composition of the collected fecal samples. Bray-Curtis beta diversity dissimilarities (Supplementary Materials **Figure S4.7**) show a variance of 19.7% on the first PCoA axis and a variance of 12.9% on the second PCoA axis. This is in line with literature[264], indicating that the variation observed in the cohort of this study is representative. Composition plots of the absolute abundance of the main taxa at phylum and family level (**Figure 4.6**) and genus level (Supplementary Materials **Figure S4.8**) combined with hierarchical clustering of Bray-Curtis beta diversity dissimilarities of the full dataset indicate, with some exceptions, that most individuals clustered together over their three sampling times. This indicates that interindividual differences in overall microbial composition of the collected samples seem to be larger than intraindividual differences, as reported in literature[261,265,266]. Firmicutes appeared to be the highest abundant phylum present in most samples followed by Bacteroidetes. The families *Lachnospiraceae, Ruminococcaceae* and for some individuals *Prevotellaceae, Bacteroidaceae* or *Bifidobacteriaceae* accounted for the largest abundance of the microbial taxa present in the collected samples. Supplementary Materials **Figure S4.9** shows relative abundance data at phylum, family and genus level.

Associations of bacterial taxa with carboxymethyllysine and fructoselysine degradation profiles
To explore potential relationships between specific bacterial genera and carboxymethyllysine or fructoselysine degradation, a Spearman's rank correlation analysis was performed with genera present with a relative abundance >1% in one of the individual fecal samples. Based on absolute bacterial abundances as quantified via total bacterial cell load, multiple genera showed a statistically significant correlation to carboxymethyllysine and/or fructoselysine degradation expressed per gram feces/h (**Figure 4.7**). The following genera showed a positive correlation with fructoselysine degradation, ordered by increasing adjusted *P*-value: *Akkermansia* (ρ = 0.49; *P*-value = 0.029), *Megasphaera* (ρ = 0.43; *P*-value = 0.085), *Eubacterium_ruminantium_group* (ρ = 0.42; *P*-value = 0.085) and *Bifidobacterium* (ρ = 0.41; *P*-value = 0.088). Fructoselysine degradation correlated negatively to *Sutterella* (ρ = 0.52; *P*-value = 0.028). Carboxymethyllysine degradation was positively correlated with *Alistipes* (ρ = 0.49; *P*-value = 0.028) and *Akkermansia* (ρ = 0.47; *P*-value = 0.031). Detailed correlation plots of all statistically significant correlations are provided in the Supplementary Materials **Figure S4.10**, while all genera correlated were additionally visualized in a heatmap in Supplementary Materials **Figure S4.11**.
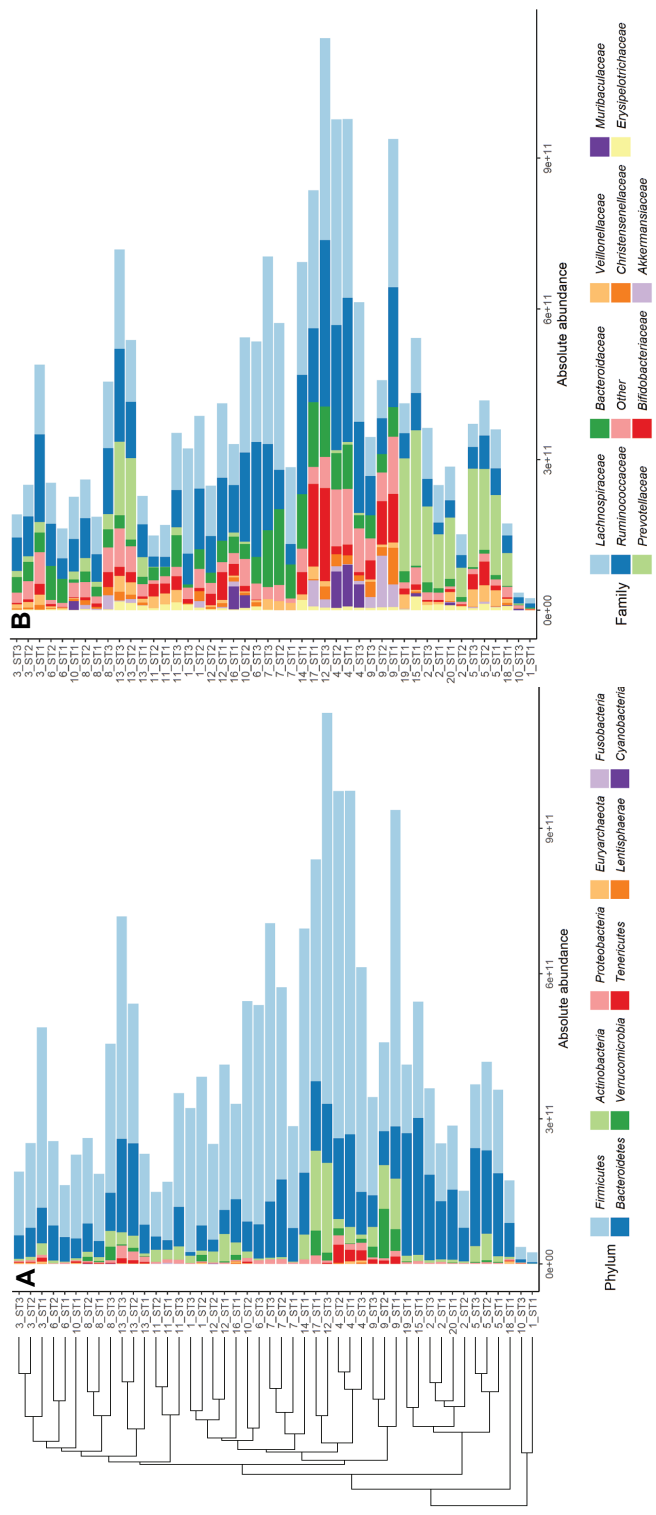
Figure 4.6 Absolute abundance of microbial taxa, assessed with 16S rRNA amplicon sequencing and qPCR, present in the individual fecal samples (y-axis labels consist of subject number and sampling time). The top 10 taxa present at Phylum (panel A) and Family (panel B) level are provided, sorted based on hierarchical clustering of Bray-Curtis dissimilarities using the average linkage approach with all taxa included.
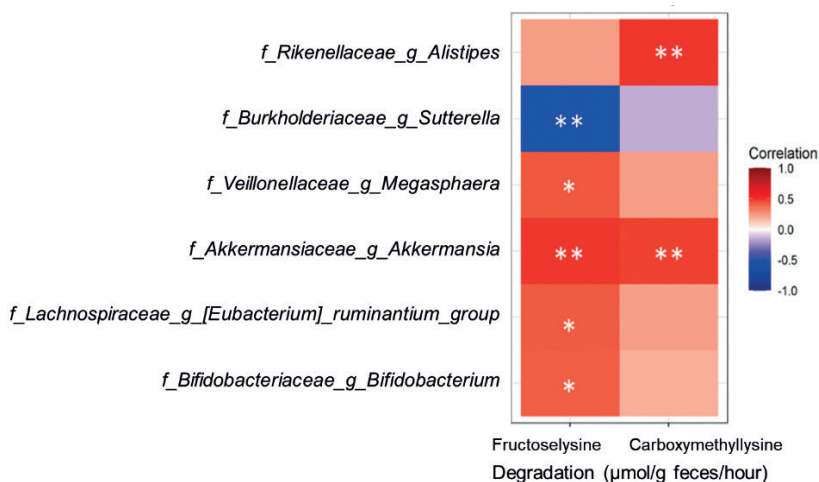
Figure 4.7 Spearman's rank correlation analysis of bacterial genera with the amount of degraded fructoselysine and carboxymethyllysine per gram feces per hour. Bacterial genera present with a relative abundance >1% in one of the individual fecal samples were included and were transformed into absolute abundance (using quantified total bacterial cell load by qPCR). Only taxa with one or more statistically significant correlation after correction for multiple testing (FDR) were included in this heatmap, and indicated as follows: ** P-value < 0.05; * P-value <0.1.

4.4 Discussion

In this study we report interindividual and intraindividual differences in gut microbial degradation of the AGE carboxymethyllysine and its precursor fructoselysine (**Figure 4.9**). We show that fructoselysine is more readily degraded than carboxymethyllysine, and there appears to be no correlation between the degradation of the two.

Upon application of *in vitro* anaerobic incubations with individual human fecal slurries, pronounced interindividual differences in this microbial degradation capacity were found for both fructoselysine and carboxymethyllysine, ranging from no degradation at all to almost complete degradation of the substrates, added at saturating concentrations, under the employed experimental conditions. Interindividual differences in these microbial degradation capacities have been previously reported in literature as well, although for a lower number of individuals, of which the experimentally obtained microbial degradation capacities were largely in line with our results[161,223]. The substantial intraindividual differences for fructoselysine and carboxymethyllysine quantified in this study are, to the best of our knowledge, the first reported. Thus, this information on temporal variability within these degradation capacities, elucidated by analysis of fecal samples collected at different sampling times (3-16 weeks in between), could not be compared to studies in literature.

Interindividual differences and the (in)ability to microbially degrade fructoselysine has been discussed previously[40], where the gene code yhfQ, coding for fructoselysine kinase involved

in bacterial degradation of fructoselysine[40], was identified and shown to be present in the fecal metagenomes of only some individuals (~10%)[40,67]. Via this pathway, fructoselysine can be phosphorylated into fructoselysine-6-phosphate[40] which can be further metabolized by microbes and in some cases yield short chain fatty acids (SCFAs) from it[40]. However, the interindividual differences in the presence of this gene (yhfQ) only partially explain the quantified interindividual differences in fructoselysine degradation in the present study (since 95% of the tested fecal samples degraded the added fructoselysine at least to some extent). Another gene code coding for fructoselysine kinase has been identified as well (i.e. frlD[39,159]), which is involved in microbial degradation of fructoselysine as well. Little has been reported about microbial degradation pathways of carboxymethyllysine. It is hypothesized that degradation pathways involve decarboxylase, oxidase or 5-aminopentanamidase[267]. However, this remains to be further investigated and confirmed.

Despite fructoselysine being a precursor for carboxymethyllysine, there was no correlation in the ability to microbially degrade the two substrates. Also, fructoselysine was degraded more efficiently than carboxymethyllysine as has been reported before[223], which, taken together, emphasizes that different metabolic pathways possibly present in different microbes are involved. In addition to this, the more efficient fructoselysine degradation might also be partly explained by a generally higher dietary exposure to fructoselysine (intake ± 7.1-14.3 mg/kg bw/day) compared to carboxymethyllysine (intake ± 0.3 mg/kg bw/day)[223] and a potentially resulting microbial adaptation. This exposure-induced metabolic capacity is also proposed in a study where a small set of fecal metagenomes of breast fed and formula fed infants was analyzed for the presence of enzymes known to be involved in fructoselysine metabolism[268]. Infants who consumed more formula, which, unlike breast milk, contains high levels of fructoselysine, had a higher expression of those degrading enzymes in their feces[269], indicating that pathways involved in fructoselysine metabolism can be induced by exposure. The observed intraindividual differences in this study imply that possibly also in adults fructoselysine degradation activities might be driven by exposure. However, this remains to be further investigated, for example upon controlled dietary changes.

The observed inter- and intraindividual differences in degradation activities of the substrates are possibly partly due to differences in the abundances of specific bacterial species. A potential role was identified for the genera *Akkermansia*, *Megasphaera*, *Bifidobacterium* and *Eubacterium_ruminantum_group* in fructoselysine degradation, while for carboxymethyllysine degradation the genera *Alistipes* and *Akkermansia* might be involved based on our experimental results. In literature, multiple bacteria have been reported to be involved in fructoselysine degradation (i.e. *Intestinimonas butyriciproducens, Bacillus subtilis, Escherichia coli*[39,40,159]) and carboxymethyllysine degradation (i.e. *Escherichia coli, Oscillibacter, Cloacibacillus evryenis*[47,267]). The variety of bacteria identified in literature and the present study indicates that probably multiple bacteria in an ecosystem are responsible for the differences in microbial degradation activities instead of one specific bacteria.

Some metabolites formed upon bacterial carboxymethyllysine degradation have been identified (i.e. 5-(carboxymethylamino)pentanoic acid, 2-amino-6-(formylmethylamino) hexanoic acid, carboxymethyl-cadaverine and N-carboxymethyl-Δ[1]-piperideinium ion)[47,267], however this accounted for <10% of the concentrations of carboxymethyllysine actually being

degraded. This reveals that probably other, currently unknown metabolites are also formed upon carboxymethyllysine degradation. Possible SCFA formation has been hypothesized however in the present study we could not experimentally confirm this (data not shown), partly due to high SCFA background levels in the fecal slurries of our experimental set-up. For fructoselysine, the SCFA butyrate has been shown to be an important metabolite formed by *I. butyriciproducens*[40] and butyrate production also correlated with fructoselysine degradation by human fecal slurries[161]. Future studies on metabolite formation upon carboxymethyllysine and fructoselysine degradation are recommended to identify whether this degradation actually is a detoxification pathway, as metabolites formed might be systemically available and can mediate effects of the gut microbiota on host health[270].

Inter- and intraindividual differences in fructoselysine and carboxymethyllysine gut microbial degradation can potentially affect internal exposure levels, as not all individual tested fecal slurries were able to completely degrade the intake at the level of the EDI when extrapolating the *in vitro* obtained data to the *in vivo* situation. Quantification of interindividual differences in toxicokinetic data with the presented *in vitro* model might thus, depending on the research question, be a valuable contribution to human-based *in vitro* methodologies of modern toxicological risk assessment strategies, as it can add to host metabolism. Altogether the results of the present study show that the capacity for intestinal microbial degradation of these two compounds can be substantial, likely reducing internal exposure levels and thus the potential hazards related to dietary exposure of carboxymethyllysine and fructoselysine.
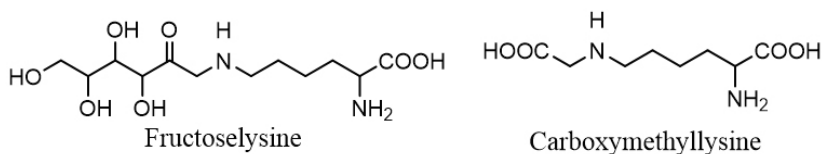

Figure 4.9 Chemical structures of fructoselysine and carboxymethyllysine presented in their free form.

Acknowledgements

4.5 Supplementary Materials

Supplemental Tables

Table S4.1 Fecal collection sampling times per individual. Fecal samples were collected at three sampling times (i.e. ST1, ST2 and ST3) of which ST1 is referred to as the first sampling time and indicated as week 0. The Δt shows the number of weeks the sample was donated compared to ST1.

Individual	ST2 (Δt compared to ST1 in weeks)	ST3 (Δt compared to ST1 in weeks)
1	9	12
2	3	6
3	3	16
4	3	6
5	6	9
6	6	9
7	3	6
8	3	6
9	6	9
10	3	6
11	3	9
12	3	9
13	3	6

Table S4.2 Calculation of scaling the in vitro determined degradation parameters to the in vivo situation

	Daily intake (mg/kg bw)	Daily intake (µmol)[a]	In vitro degradation capacities per hour[b,c]	In vitro degradation capacities per 24 hours[b,d]	In vivo degradation capacity (µmol)[e]	% Of transit time for complete degradation of the daily intake[e]	Number of incomplete degradations out of 46 individuals[h]	Number of incomplete degradations out of 20 individuals[i]
Fructose lysine[f]	7.1-14.3	1612.1-3246.8	1.64	39.44	5048.13	31.9-64.3	8-20	4-10
Carboxymethyllysine[g]	0.3	102.8	0.07	1.69	216.01	47.6	18	11

[a] Assuming an average body weight for adults of 70 kg[271].
[b] Expressed as µmol/g feces/h.
[c] Degradation capacities were experimentally obtained in the present study and represent the average of all tested fecal samples excluding the outlier Individual 1 ST1.
[d] Transformed to total transit time in the colon which equals 24 hours[262].
[e] A total fecal mass of 128 grams per 24 hours was assumed[263]
[f] Molecular weight is 308.3 g/mol.
[g] Molecular weight is 204.2 g/mol.
[h]Number of individual collected fecal samples tested (n=46) with degradation activities[b] too low to completely degrade the daily intake[a]
[i]Number of individuals who donated a fecal sample at least once (n=20) with one or more sampling times (i.e. ST1, ST2 and/or ST3) with degradation activities[b] too low to completely degrade the daily intake[a]
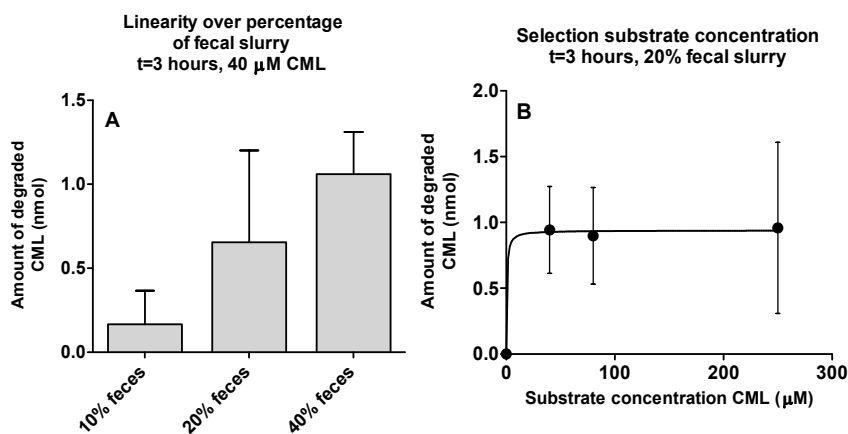
Supplemental Figures

Figure S4.1 Optimization of experimental conditions using pooled human fecal slurries. Linearity of carboxymethyllysine (CML) degradation over percentage of fecal concentration at 3 hours of anaerobic incubation with 40 µM CML (A) and selection of a saturated substrate concentration of CML (µM) at 3 hours incubation using 20% pooled human fecal concentration.
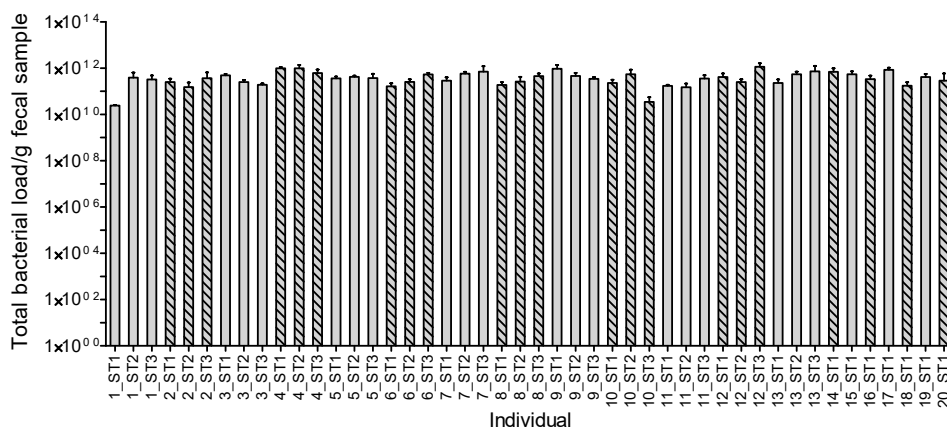

Figure S4.2 Total bacterial cell load per gram fecal sample, as collected per individual (indicated by initial numbers on x-axis labels) at different sampling times (i.e. ST1, ST2 and ST3). Total bacterial cell load was determined by qPCR, and data represent the average ± SD of three technical replicates.
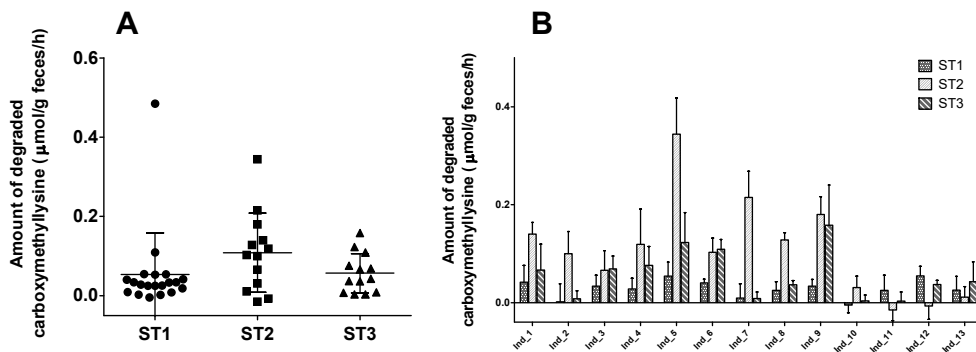
Figure S4.3 Amount of carboxymethyllysine degraded after anaerobic incubation of individual human fecal samples (0.05 g/ml final concentration) with 80 µM carboxymethyllysine, expressed per hour. ST1, ST2 and ST3 indicate different sampling times, ST1 includes 20 individual donated fecal samples, ST2 and ST3 each 13 individually donated fecal samples. Scatter plots (A) show general spread in the populations with the center bars of the scatter dots indicating mean values while whiskers indicate the SD. Bar plot (B) shows intraindividual differences in carboxymethyllysine degradation of 13 individual donors sampled at the three sampling times. All data points represent average values of three independent experiments.
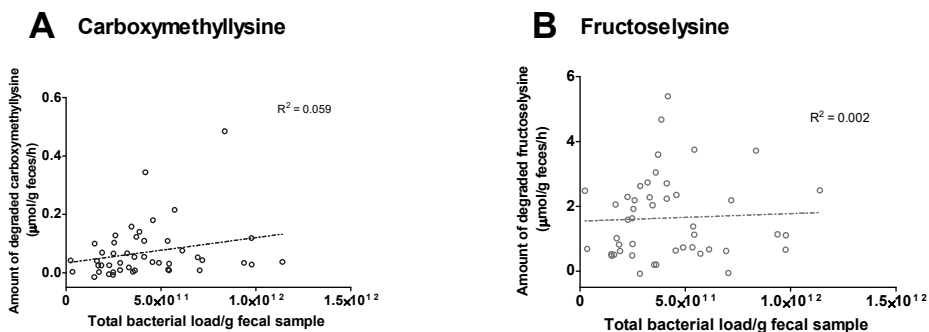

Figure S4.4 Amount of degraded carboxymethyllysine (A) and fructoselysine (B) per hour of anaerobic incubation per gram feces correlated to the total bacterial load per gram fecal sample of each individual tested. Data points of the degradation represent an average value of three independent experiments.
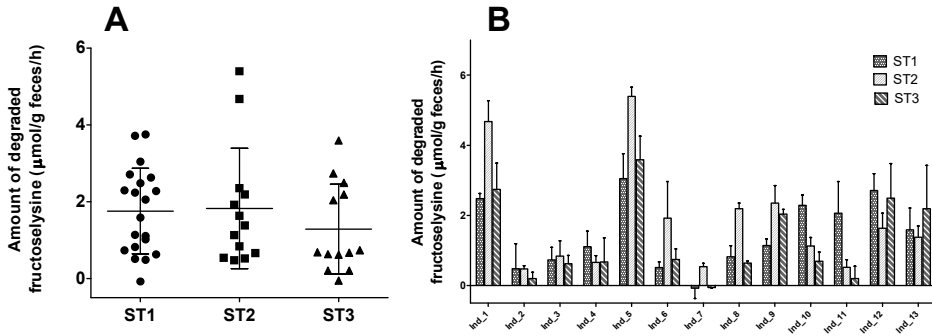
Figure S4.5 Amount of fructoselysine degraded after anaerobic incubation of individual human fecal samples (0.0125 g/mL final concentration) with 125 µM fructoselysine per hour. ST1, ST2 and ST3 indicate different sampling times; ST1 includes 20 individual donated fecal samples, ST2 and ST3 each 13 individually donated fecal samples. Scatter plots (A) show general spread in the populations with the center bars of the scatter dots indicating mean values while whiskers indicate the SD. Bar plot (B) shows intraindividual differences in fructoselysine degradation of 13 individual donors sampled at the three sampling times. All data points represent average values of three independent experiments.
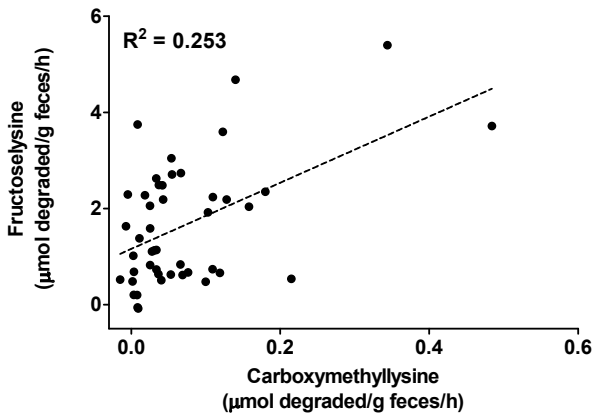

Figure S4.6 Linear regression between the amount of fructoselysine and carboxymethyllysine being degraded by anaerobic incubations with individual human fecal slurries, presented as µmol degraded/g feces per hour. A total of 46 samples were included consisting of 20 individuals (sampling time ST1) whereof 13 individuals donated additionally twice more a fecal sample (sampling times ST2 and ST3).
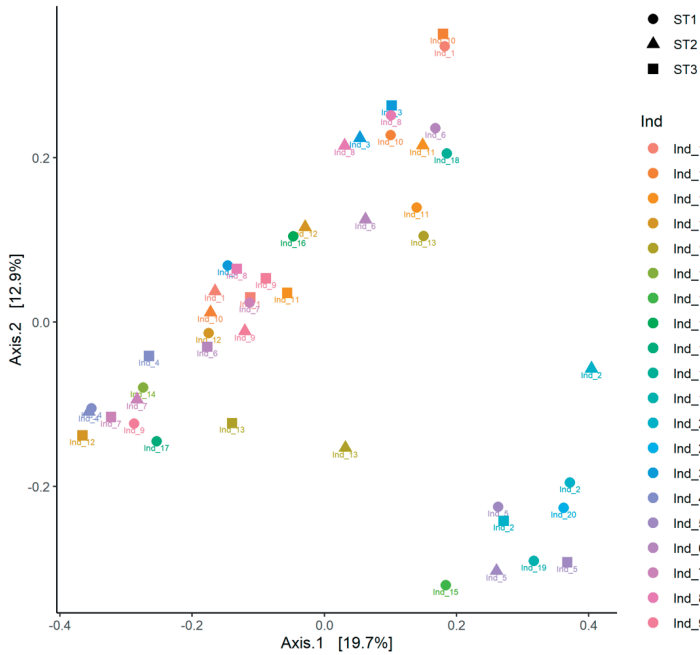
Figure S4.7 PCoA plot of Bray-Curtis beta diversity dissimilarities of 20 individual (Ind) collected human fecal samples (i.e. ST1), of which 13 individuals donated at two additional sampling times (i.e. ST2, ST3). Each data point represents one fecal sample, labelled and colored with the individual number and the different symbols refer to the three sampling times.
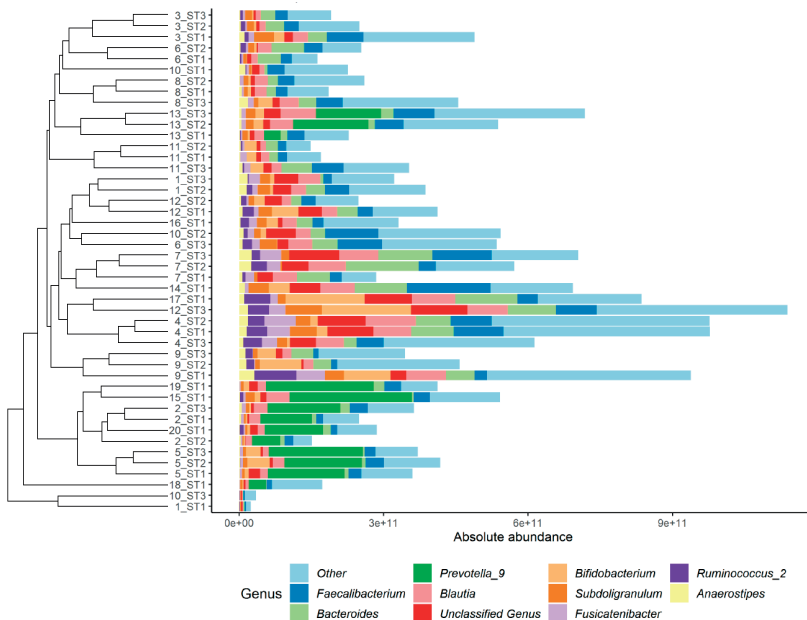

Figure S4.8 Absolute abundance of microbial taxa, assessed with 16S rRNA sequencing and qPCR, present in the individual fecal samples (y-axis labels consist of subject number and sampling time). The top 10 taxa present at genus level are shown, sorted based on hierarchical clustering of Bray-Curtis dissimilarities using the average linkage approach with all taxa included.

Figure S4.9 Relative abundance of microbial taxa, assessed with 16S rRNA sequencing, present in the individual fecal samples (y-axis labels consist of subject number and sampling time). The top 10 taxa present at phylum, family and genus level are shown, sorted based on hierarchical clustering of Bray-Curtis dissimilarities using the average linkage approach with all taxa included.
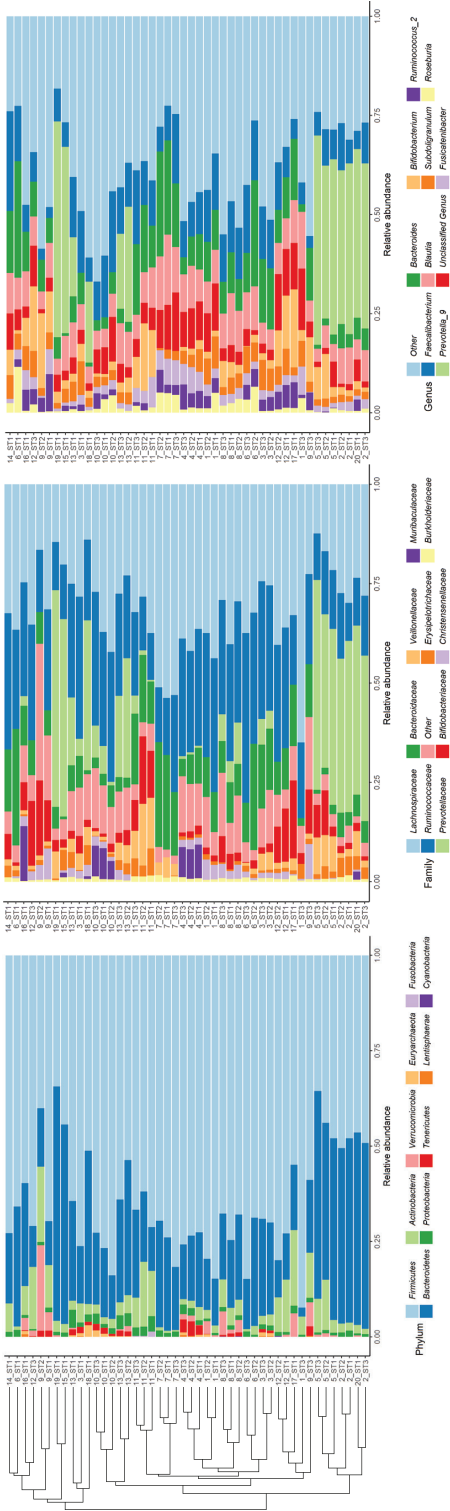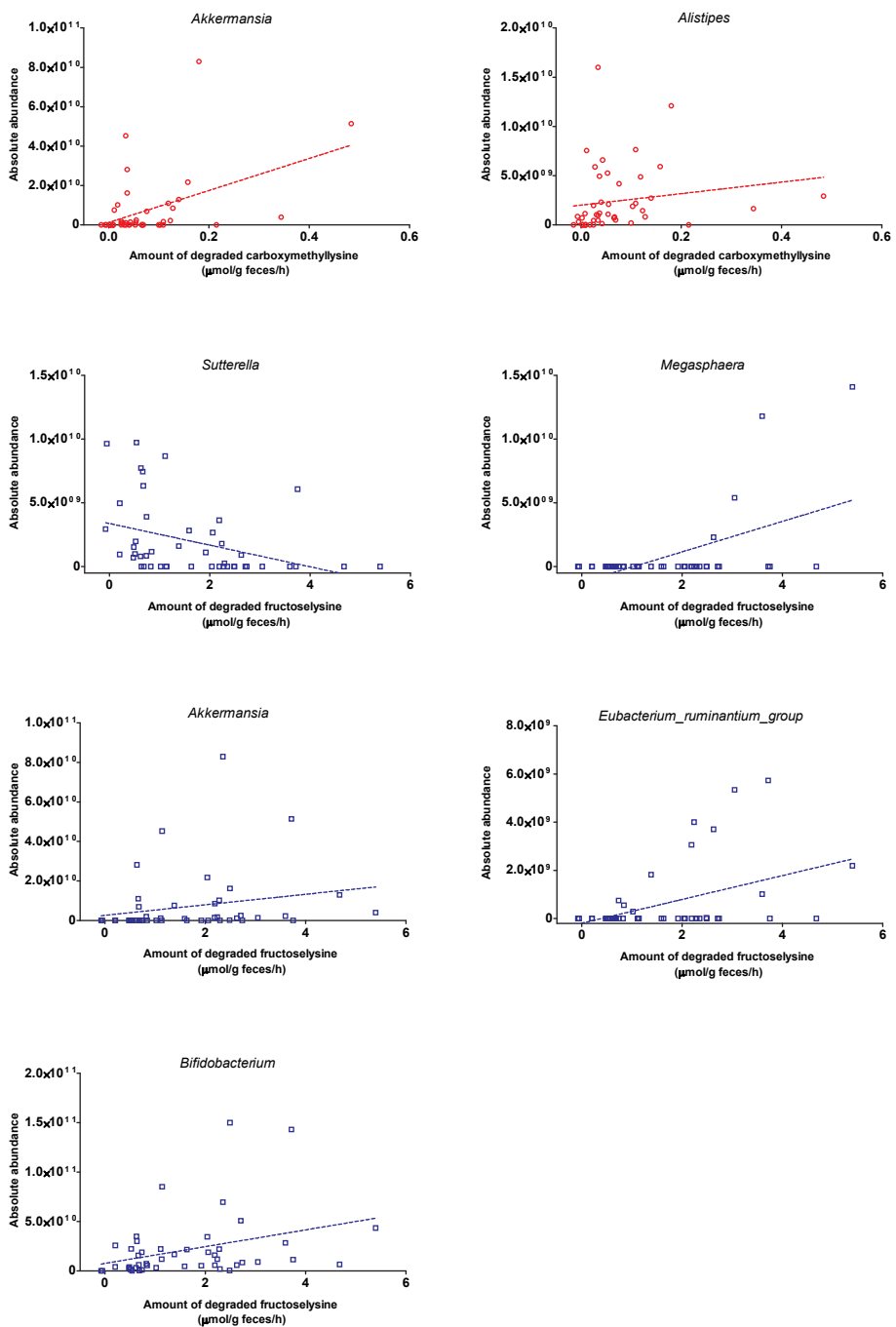
Figure S4.10 Detailed correlation plots of the statistically significant correlated genera with carboxymethyllysine (red) and fructoselysine (blue) degradation.
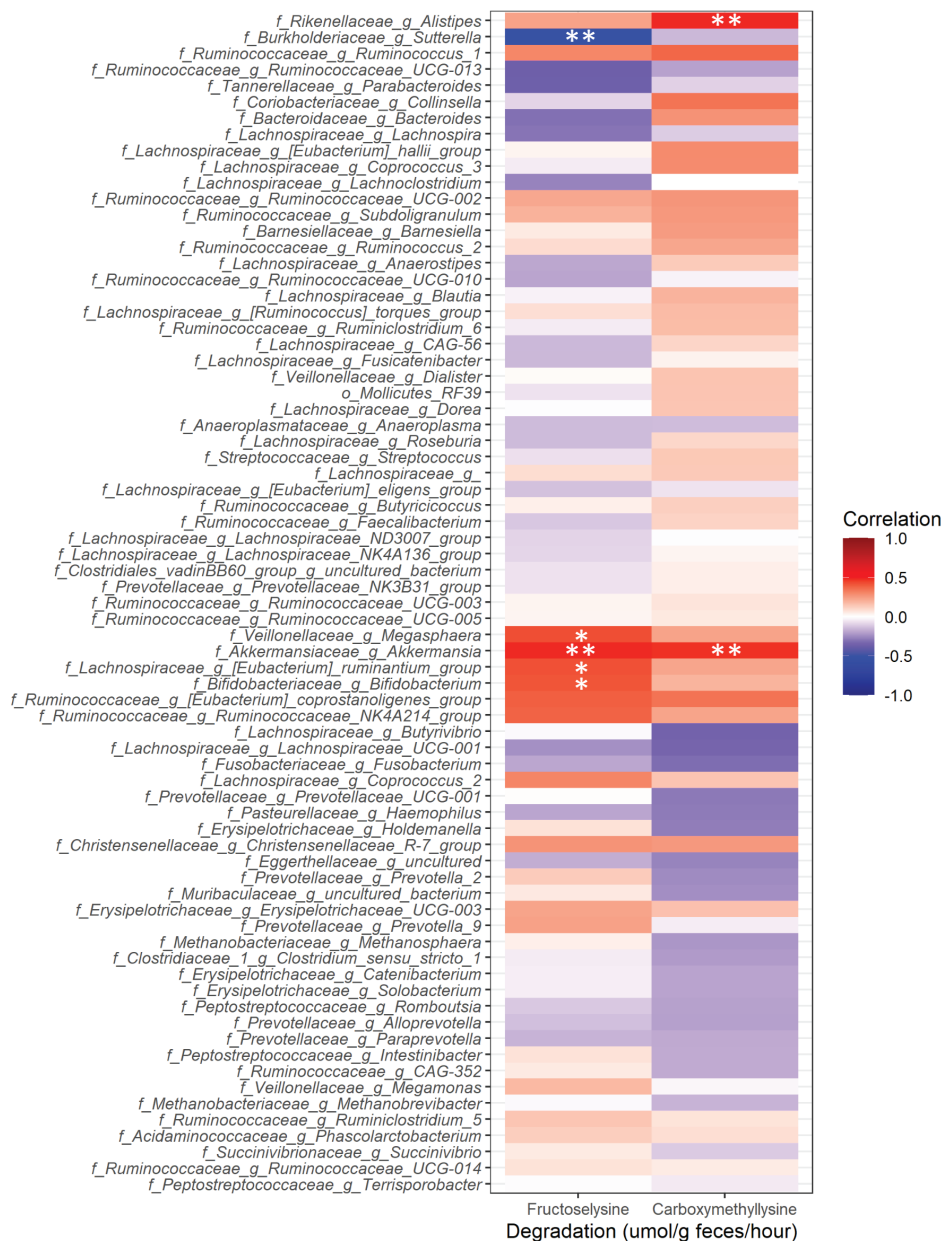
Figure S4.11 Spearman's rank correlation analysis of bacterial genera with the amount of degraded fructoselysine and carboxymethyllysine as quantified per gram feces used in the incubation system, expressed per hour. Bacterial genera present with a relative abundance >1% in one of the fecal samples were included and were transformed into absolute abundance (using quantified total bacterial cell load by qPCR). Statistically significant correlations after correction for multiple testing (FDR) were indicated as follows: ** p-value < 0.05; * p-value <0.1.
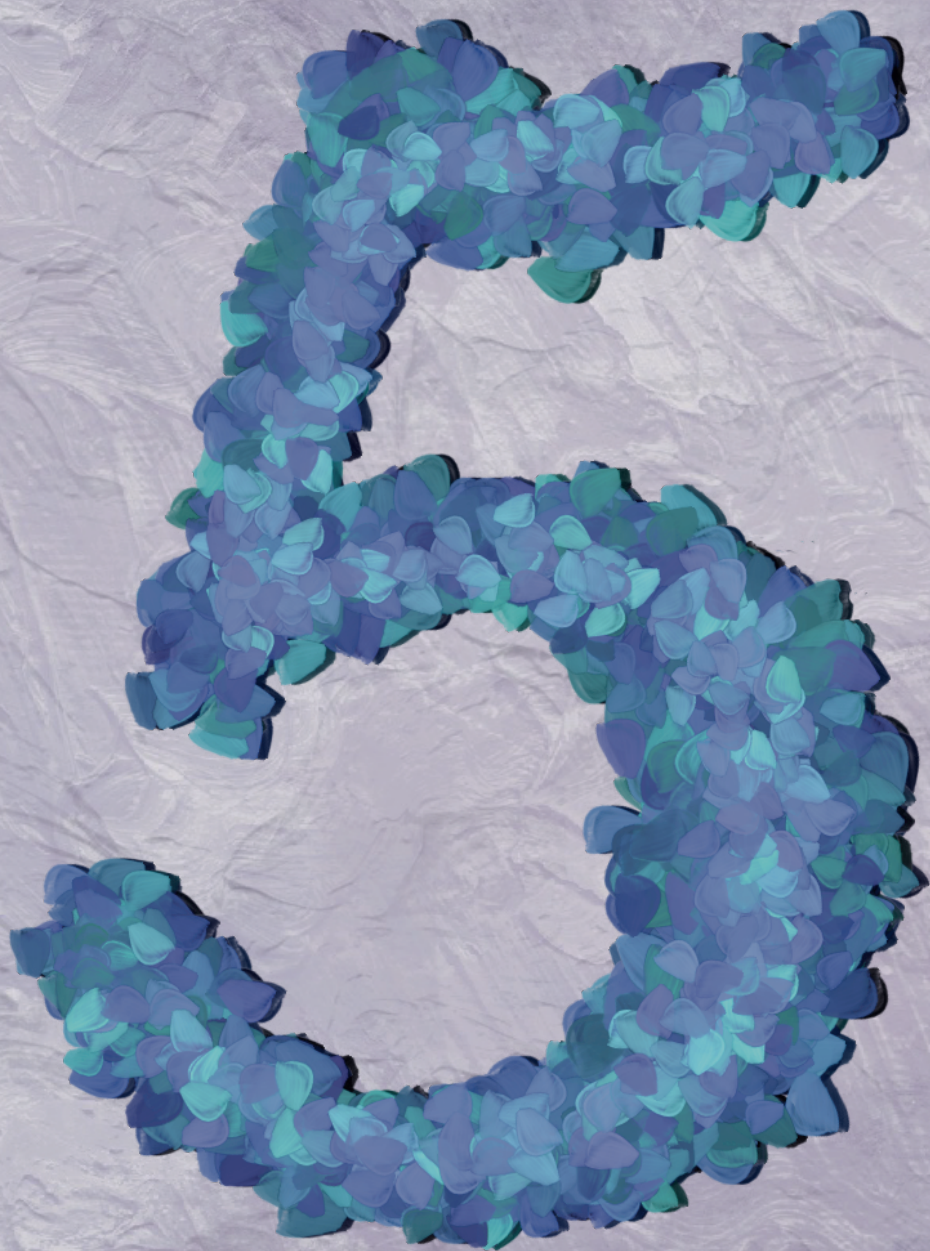
Differences in gut microbial fructoselysine degradation activity between breast-fed and formula-fed infants

Katja C.W. van Dongen, Athanasia Ioannou, Sebastiaan Wesseling, Karsten Beekmann, Clara Belzer

Abstract

The Amadori product fructoselysine is formed upon heating of food products and present in high amounts in infant formula while being almost absent in breast milk. The human gut microbiota can degrade fructoselysine for which interindividual differences have been described for adults. The aim of this study is to compare functional differences in microbial fructoselysine degradation between breast-fed (BF) and formula-fed (FF) infants, in view of their different diets and resulting different fructoselysine exposures.

First, a publicly available metagenomic dataset with metagenome assembled genomes (MAGs) from infant fecal samples was analyzed and showed that query genes involved in fructoselysine degradation (frlD/yhfQ) were abundantly present in multiple taxa in fecal samples from both BF and FF infants, with a higher prevalence in the FF infants compared to the BF infants. Next, fecal samples from exclusively BF and FF infants were collected and anaerobically incubated with fructoselysine. Both groups were able to degrade fructoselysine, however the fructoselysine degradation activity was significantly higher by fecal samples from FF infants compared to fecal samples from BF infants. No significant differences in microbiota composition between the two groups were found.

All together the current study provides evidence that the infant gut microbiota of both BF and FF infants is able to degrade fructoselysine and that infant formula feeding, leading to increased dietary fructoselysine exposure, seems to result in an increased fructoselysine degradation activity in the gut microbiota of infants. This indicates that the infant gut microbiota adapts towards dietary fructoselysine exposure.

Keywords: in vitro model; infant formula; infant gut microbiota; metagenome assembled genomes; blastp; AGEs; adaptation

List of abbreviations: AGE advanced glycation end product; **ASV** amplicon sequence variant; **BF** breast-fed; **CCA** canonical correspondence analysis; **CE** collision energy; **EDI** estimated daily intake; **FF** formula-fed; **LEfSe** linear discriminant analysis (LDA) effect size; **LC** liquid chromatography; **MAGs** metagenome assembled genomes; **MRM** multiple reaction monitoring; **MS** mass spectrometry; **PBS** phosphate-buffered saline.

5.1 Introduction

During the heating of food products, glycation products can be formed. These include the Amadori product fructoselysine, a precursor for the advanced glycation end product (AGE) carboxymethyllysine, which is produced via the non-enzymatic Maillard reaction from glucose and lysine residues during heating[14,272]. Depending on the nature of the lysine residue, free, peptide-bound and/or protein-bound fructoselysine can be formed. During the production process of infant formula, extensive heating is applied to ensure microbial safety by which also high levels of fructoselysine are formed[273–275]. In human breast milk, in contrast, fructoselysine is (almost) absent with ~239-fold lower levels compared to infant formula[87]. The question has been raised whether the fructoselysine degradation activity of infant gut microbiota adapts to these different exposure levels of fructoselysine due to the type of nutrition. It is known, for example, that the gut microbiota of formula-fed (FF) infants is distinct from that of breast-fed (BF) infants both with respect to its composition as well as its metabolic capacity[61,79,276,277]. In line with these observations, the aim of this study was to explore the ability of the infant gut microbiota to adapt towards different diets (BF or FF) with respect to their different levels of dietary derived fructoselysine.

Upon ingestion, fructoselysine can reach the colon and interact with gut microbiota[129,130], resulting in its degradation as shown by *in vitro* fermentations with human fecal slurries[161,223] and with single bacterial strains[39,40,278]. In adults interindividual differences in microbial fructoselysine degradation have been reported[161]. An identified key enzyme in bacterial fructoselysine degradation is fructoselysine 6-kinase (encoded by frlD/yhfQ) which catalyzes ATP-dependent phosphorylation of fructoselysine into fructoselysine 6-phosphate, which can subsequently be converted into lysine and glucose 6-phosphate (**Figure 5.1**)[39,40,278]. The genes coding for the kinase (frlD/yhfQ) were identified in multiple microbes (i.e. *Bacillus subtilis, Escherichia coli, Intestinimonas butyriciproducens*[39,40,278]) and seems to be essential for bacterial fructoselysine degradation[279].

In FF infants aged 3 months, fecal fructoselysine excretion was reported to be 15.7 µmol/g feces while being absent in similar-aged BF infants[269]. The latter can be explained due to the absence of fructoselysine in breast milk, while the reported levels of fructoselysine in the feces of FF infants indicate that not all dietary exposed fructoselysine was absorbed or degraded by the gut microbiota. The composition of breast milk differs from infant formula in several ways[280], including differences in fructoselysine levels. The gut microbiota can adapt towards dietary exposure, and in this study, it was investigated whether the ability of the infant gut microbiota to degrade fructoselysine also adapts towards different dietary fructoselysine exposure levels as part of different diets. To this end, a comparison in metagenomic differences and similarities of fructoselysine degradation genes between BF and FF infants was made with a publicly available metagenomic dataset[61,281]. In addition, BF and FF infant fecal samples were collected and compared for bacterial composition and *in vitro* metabolic activity to degrade fructoselysine. Fructoselysine levels were quantified in the infant formula of the FF infants to explore if differences in the consequent dietary fructoselysine exposure correlated with individuals' fructoselysine degradation activities.
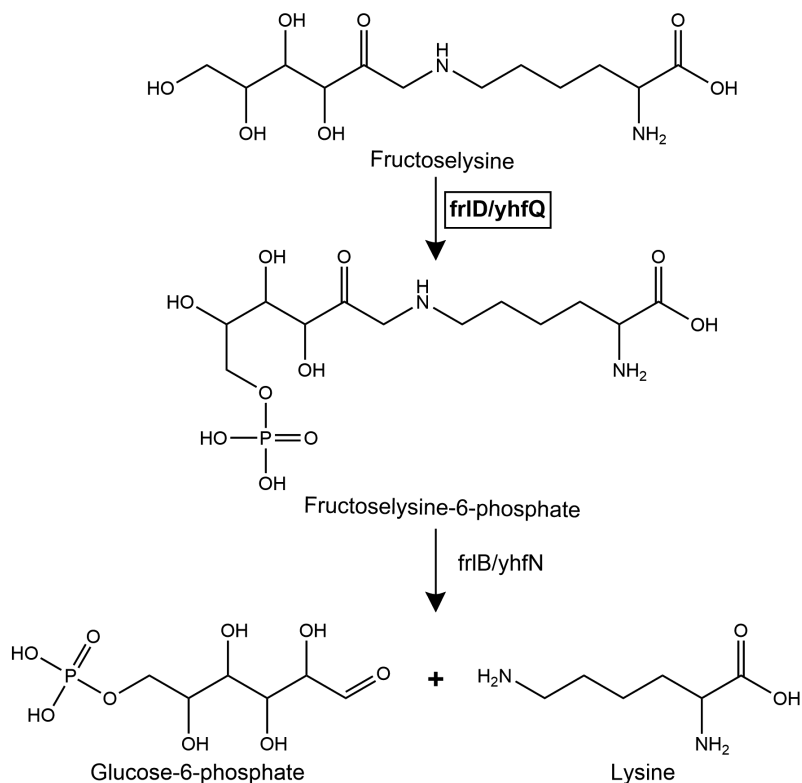
Figure 5.1 Pathway of fructoselysine degradation with identified genes involved. frlD/yhfQ encodes for fructoselysine kinase while frlB/yhfN encodes for fructosamine-6-phosphate deglycase.

5.2 Materials and Methods

Chemicals and reagents

Fructoselysine was purchased from Carbosynth Limited (Berkshire, UK). Glycerol, acetone, leucine aminopeptidase, pepsin, prolidase, pronase E and Tris were purchased from Sigma-Aldrich (Zwijndrecht, The Netherlands). *n*-Hexane was from VWR international (Amsterdam, The Netherlands). Formic acid (99-100%, analytical grade) was purchased from Merck (Darmstadt, Germany). Phosphate-buffered saline (PBS) was obtained from Gibco (Paisley, UK). Methanol and acetonitrile (ACN), both in UPLC/MS grade were purchased from BioSolve BV (Valkenswaard, The Netherlands).

Metagenomic dataset analysis

Metagenome Assembled Genomes (MAGs)[281] were filtered for the infant sequences of a publicly available dataset[61]. The latter include metagenomic data from infants that are a few days, four months and twelve months old from various feeding backgrounds and birth modes. The nucleotide sequences were translated into amino acid sequences also based

on protein-coding gene prediction, using 'Prodigal'[282] (version 2.6.3) in normal mode using default parameters. The MAGs were concatenated and transformed into a database with the use of the 'makeblastdb' command of the 'blast'[283] (version 2.11.0) module. 'Blastp' was performed for the sequences presented in Supplementary Materials **Table S5.1** against the created MAGs database. The taxonomy of the MAGs was based on the GTDB database[284]. Hits were filtered for evalue < 1E-15, which resulted in no removal of hits. No other filtering was performed on the hits meaning that the hits are not necessarily functional proteins.

The aligned hits of 'blastp' were retrieved in fasta files using the 'seqinr' package in R (version 4.0.2). Sequences were parsed for unique sequences per sequence, query gene and species name to avoid repetition in results. Alignment of amino acid sequences was performed with the build-in MUSCLE tool of MEGA (version 7.0.26) with default parameters. Aligned sequences were trimmed to equal lengths to avoid false divergence due to unequal lengths. The phylogenetic trees were created with the iqtree module (version 1.6.12). The Maximum-Likelihood model was used with the LG matrix[285] for 2 classes, empirical amino acid frequencies and FreeRates heterogeneity. The phylogenetic trees were further annotated with the iTOL software (version 6.3.2)[286]. Prevalence of the query genes per feeding mode at 4 months were calculated by dividing the number of subjects per species, query and feeding mode by the total number of subjects per feeding mode multiplied by 100. Subjects with a feeding mode not assessed at 4 months were removed for this purpose.

Collection and processing of infant fecal samples
Infant fecal samples were collected and stored individually and assigned a random number. Parents from the infants granted informed consent before participation in this study. The study design was assessed by the Medical Ethical Committee of Wageningen University and judged not to fall under the Dutch 'Medical Research Involving Human Subjects Act'. Fecal samples were collected from infants aged between 1 and 6 months who were either exclusively BF or FF (prior to introduction of solid foods), who did not receive antibiotics (when applicable up to 3 months prior to donation) and were born via vaginal childbirth. Fecal samples were scooped from the diaper into a sterile 50 mL filter top tube, which was directly stored in a BD GasPak™ EZ Anaerobe gas generating pouch system with indicator (BD, Maryland, USA) and transferred to the fridge (± 4°C). In addition, for the FF infants a scoop of formula powder was collected. Within 24 hours, the fecal sample was further processed to fecal slurry under anaerobic conditions and stored at -80°C after a 4x dilution (w/v) in anaerobic storage buffer (10% (v/v) glycerol in PBS; 0.25 g feces/mL) as described before[161].

In vitro **anaerobic incubations with fecal slurries**

Anaerobic incubations with the collected fecal slurries –individual or pooled– with fructoselysine were performed as previously described[161]. In short, two pools were created, containing equal amounts of either all FF infant fecal slurries or either all BF infant fecal slurries. 5% (v/v) Fecal slurry (final concentration of 0.0125 g feces/mL) from both pools were incubated in PBS for 0, 0.5, 1, 1.5, 2, 3 and 4 hours with fructoselysine at 430 μM under anaerobic conditions. These experimental conditions were based on previous research

using adult human fecal slurries[161] and taking into account background fructoselysine concentrations in the pooled fecal samples of the FF infants so that the final concentration of fructoselysine was similar for the incubations with FF and BF samples.

Based on the pooled and previous results[161], 5% (v/v) of infant fecal slurry (final concentration of 0.0125 g feces/mL) was found appropriate to study interindividual differences with all individual fecal slurries. To this end, background fructoselysine concentrations were quantified in these individual fecal slurries by LC-MS/MS as was done for the pool. The fecal slurries were subsequently incubated with a final concentration of 430 µM fructoselysine for 0, 2, 3 and 4 h. After the desired incubation time, reactions were terminated by addition of ice-cold ACN (1:1) and the samples were stored on ice for at least 15 min. All handlings were performed inside an anaerobic chamber (85% N_2, 10% CO_2 and 5% H_2, Bactron EZ anaerobic chamber). Samples were centrifuged at 15,000 x g for 15 min at 4°C, and fructoselysine concentrations in the supernatants were analyzed by LC-MS/MS. All anaerobic incubations were performed in technical duplicates and were repeated at least three times.

Sample preparation of collected infant formula samples
Both protein-bound and free fructoselysine were quantified in the collected infant formula samples based on the procedure of Hegele et al.[8].

Total fructoselysine levels were quantified upon digestion. After weighing 1 g of milk powder, 10 mL of 0.02N HCl was added, and the milk suspension was weighed again. After mixing the suspension repeatedly for at least 15 minutes at room temperature, 50 µL of the milk suspension was transferred to an Eppendorf cup containing 950 µL 0.02N HCl. The remaining milk suspension was reserved for protein determination, using the Pierce™ BCA Protein Assay kit (Thermo Fisher Scientific, Illinois, USA), according to manufacturer's instructions.

To the milk suspension 18 µL of pepsin was added (1 mg/mL in 0.02N HCl) and the sample was subsequently incubated for 1 h at 37°C. This was repeated, and followed by an addition of 250 µL 2M Tris (pH 8.2) and 15 µL pronase E (1 mg/mL in 2M Tris (pH 8.2)) after which the sample was incubated for 1 h at 37°C. Again, 15 µL pronase E solution was added followed by incubation for 1 h at 37°C. Subsequently, 20 µL leucine aminopeptidase (7 U/mL in H_2O) and 10 µL prolidase (105 U/mL in 2M Tris (pH 8.2)) were added and the sample was incubated for 24 h at 37°C. In the final step 15 µL pronase E was added and the incubation was continued for another 1 h at 37°C. The samples were stored at -20°C until sample preparation for the LC-MS/MS. After thawing, the samples were centrifugated (15,000 x g for 30 min) and 500 µL of the supernatant was further prepared for LC-MS/MS as described below. An additional aliquot of each sample was spiked with fructoselysine for peak identification in the LC-MS/MS measurement.

Infant formula was prepared for free fructoselysine quantification as follows. In short, 1 gram of milk powder was weighed in a Greiner tube and 10 mL of nanopure H_2O was added to the powder and the milk solution was weighed again. After mixing the suspension repeatedly during at least 15 minutes at room temperature, 1 mL of milk suspension was transferred to another 15 mL Greiner tube and weighed again. 10 mL of ice-cold acetone/MeOH (1:1, v/v) was added, after which the sample was vortexed and stored at -20°C for 1 h. After thawing,

the sample was centrifugated (2,000 x g, 5 min) and the supernatant was transferred to a glass tube. The supernatant was evaporated slowly under a flow of nitrogen gas while the tube was put in a heat block set at lukewarm. The dry remnant was resuspended in 1.4 mL nanopure H_2O followed by adding 1.4 mL n-hexane. After vortexing the mixture thoroughly, it was kept at room temperature for 1 h until the separation between the two phases was sharp and clear, upon which the hexane fraction was removed. Then 500 µL of the water fraction was aliquoted and stored at -20°C until sample preparation for LC-MS/MS carried out as described hereafter. An additional aliquot of each sample was spiked with fructoselysine for peak identification in the LC-MS/MS measurement.

Prior to LC-MS/MS measurement, samples were filtered. To this end, Nanosep 3K Omega Filters of Pall Corporation (VWR international) were washed 5 times with nanopure H_2O combined with a centrifugation step (12,000 x g, 2 min) before filtering the samples. Nanopure H_2O was removed from the filter and the filter was transferred to a clean Eppendorf tube and loaded with 200 µL sample. After repeated centrifugation at 12,000 x g for 1 min at least 100 µL filtered sample was collected. The digestion filtrates were 25 times diluted in nanopure H_2O and the free analyte filtrates were undiluted. All filtrates were subsequently analyzed by LC-MS/MS. Preparation and measurement of the infant formula samples was repeated three times.

LC-MS/MS method and data processing to quantify fructoselysine in infant fecal slurries and infant formula samples

Fructoselysine concentrations were quantified using a Shimadzu Nexera XR LC-20AD SR UPLC system coupled to a Shimadzu LCMS-8040 triple quadrupole MS (Kyoto, Japan) for the anaerobic incubation samples, or coupled to a Shimadzu LCMS-8045 triple quadrupole MS (Kyoto, Japan) for the infant formula samples. The MS coupled to an ESI source was used for MS/MS identification, using positive ionization for multiple reaction monitoring (MRM), as previously described[161]. 1 µL of either a milk or fecal incubation sample was injected onto a Phenomenex Polar-RP Synergi column (30 x 2 mm, 2.5 µm) at 40°C. The mobile phase consisted of a gradient made from solvent A (i.e., ultrapure H_2O with 0.1% formic acid (v/v)) and solvent B (i.e., ACN with 0.1% formic acid (v/v)) at a flow rate of 0.3 mL/min. The gradient started with 95% ACN for 2.5 min, to reach 0% ACN at 4 min, and was subsequently kept at 0% ACN until 6 min, followed by a shift to 100% ACN from 6 to 7.8 min returning to 95% ACN at 8.1 min and kept at these initial conditions up to 14 min. Fructoselysine eluted at 5.6 min. The precursor to product transition m/z 309.2 > 84.2 (collision energy (CE) = -31 V) was used for quantification, while the transitions m/z 309.2 > 291.1 (CE = − 11 V), m/z 309.2 > 273.1 (CE = − 15 V) and m/z 309.2 > 225.2 (CE = − 17 V) were used as reference ions. Calibration curves of pure fructoselysine were used for quantification of fructoselysine present in the samples. Peak areas were integrated using LabSolutions software (Shimadzu).

The amount of degraded fructoselysine during the anaerobic incubations was expressed in µmol degraded/g feces and also in µmol degraded/$1x10^{11}$ bacterial cells, or additionally relative to the duration of incubation, unless stated otherwise. Regarding the infant formula samples, quantified free fructoselysine was subtracted from the total fructoselysine quantified in the infant formula upon digestion to quantify the protein-bound fructoselysine levels. Protein-bound and free fructoselysine levels in infant formula were expressed per

mg protein in the infant formula. Data of three repeated experiments were averaged and standard deviations were calculated with GraphPad Prism 5.0. Outliers were identified per feeding mode and time point using IBM SPSS Statistics version 25 using a multiplier of 3.0. When applicable, results were considered to be statistically significant when *P*-values were <0.05.

DNA isolation, 16S rRNA amplicon sequencing, qPCR and data processing
DNA was isolated from the fecal samples with a bead-beating procedure combined with the customized MaxWell® 16 Tissue LEV Total RNA Purification Kit (XAS1220; Promega Biotech AB, Stockholm, Sweden). The V4 region (515-F; 806-R)[287,288] of the 16S ribosomal RNA (rRNA) gene was amplified by triplicate PCR reactions combined with a library approach as described before[161]. PCR products were purified, pooled and sequenced (Illumina NovaSeq 6000, paired-end; Eurofins Genomics Europe Sequencing GmbH, Konstanz, Germany).

With quantitative PCR (qPCR) reactions, the total bacterial load in each individual fecal slurry was quantified. Triplicate qPCR reactions were performed based on a previously described method[258], where 1 µL DNA isolate (1 ng/µL) was mixed with 9 µL reaction mixture (containing 62.5% iQ SYBR Green Supermix, 2.5% forward primer (10 µM), 2.5% reverse primer (10 µM) and 32.5% nuclease free water). The total 16S rRNA gene was amplified with the following primer set: 1369-F (5'-CGG TGA ATA CGT TCY CGG-3') and 1492-R (5'-GGW TAC CTT GTT ACG ACT T-3'). A standard curve was made with purified DNA isolate from *Escherichia coli* for quantification. The amplification program started at 95°C for 10 min, followed by 40 cycles of denaturing at 95°C for 15 sec, annealing at 60°C for 30 sec and elongation at 72°C for 15 sec, to end with a melt curve from 60°C to 95°C, using a CFX-384 Touch Real-Time PCR detection system (Bio-Rad, California, USA). The CFX manager was used for data analysis. Quantified copy numbers of total 16S rRNA genes/g fecal sample were divided by the average 16S rRNA genes per bacterium (i.e. 4.2[259]) and further transformed to total bacterial load/g fecal sample.

Sequences of the 16S rRNA gene were further processed with the NG-Tax 2.0 pipeline with default settings[235], generating *de novo* exact match sequence clusters (ASVs; amplicon sequence variants). Taxonomy was assigned with the SILVA 16S rRNA gene reference database release 132[236]. Data were further analyzed with R (version 4.0.2). The ASV table was combined with the phylogenetic tree and metadata using the Phyloseq package[237] (version 1.34.0). Taxa present in at least one of the samples with a relative abundance >0.1% were included for further analyses, unless mentioned otherwise. By multiplying the relative abundance of a taxa within one sample with the corresponding total bacterial load as quantified by qPCR, absolute abundance data were created. Relative and absolute abundance plots of the top taxa were created with the Microbiome package[238] (version 1.12.0). Bray-Curtis beta diversity was assessed with the Phyloseq package. Canonical correspondence analysis (CCA) was performed with the Vegan package[239] with feeding mode and age used as constraining factors. Spearman's rank correlations of fructoselysine degradation with microbial taxa present at a relative abundance of >0.1% in at least one of the samples and glomerated at genus and phylum level were made. *P* values were adjusted for multiple testing with the Benjamini & Hochberg false discovery rate using the Microbiome package[238]. The web-

based tool to perform linear discriminant analysis (LDA) effect size (LEfSe) analysis[240] was used to identify differential abundant taxa as previously described[161]. Results were found to be statistically significant when *P*-values were <0.05.

5.3 Results

Metagenomic differences and similarities of fructoselysine degradation genes between fecal samples from BF and FF infants

To assess if fecal samples from BF and FF infants differ in their metabolic potential to degrade fructoselysine, a metagenomic dataset analysis was done with the metagenomes of a publicly available dataset[61,281]. For this purpose, the main focus was on the frlD/yhfQ genes (**Figure 5.1**) which were shown to be crucial for fructoselysine degradation, which is catalyzed by the corresponding enzyme[279].

The MAGs of fecal samples from BF and FF infants included in the dataset showed multiple hits with the query genes (frlD/yhfQ) and were grouped on phylogenetic basis to retrieve insight in which bacterial taxa might harbor these genes and could potentially be involved in fructoselysine degradation (iTol tree Supplementary Figure **S5.1**). Especially a great diversity of taxa of the phylum Firmicutes appeared to be relevant, and to a lesser extent Actinobacteria, while only a few taxa of the phyla Proteobacteria and Bacteroidetes appeared to be potentially involved in fructoselysine degradation. For some genera a diversity of species belonging to the same overarching genus appeared to be potentially involved, as was the case for e.g., *Clostridium spp., Blautia spp., Collinsella spp.* and others. This diversity of species indicates the possible necessity to increase resolution in order to identify differences in bacterial composition between the two groups. The genes involved in the second degradation step as shown in **Figure 5.1** (frlB/yhfN) were also redundant in multiple species part of different overarching genera and phyla as shown in the phylogenetic tree (iTol tree Supplementary materials **Figure S5.2**).

When only including the data of the BF, FF and mixed-fed 4 months old infants of the dataset[61], analysis revealed that the queries of frlD/yhfQ genes were present in multiple bacterial species and redundant in all diet groups. However, subject prevalence data (i.e. the number of subjects per feeding mode having a hit of the query genes per bacterial species) revealed that the query genes were in general present in a larger proportion of the microbiota of subjects in the FF infants, followed by those from the mixed feeding infants while they were lowest for the microbiota derived from the BF infants (**Figure 5.2**).

Bacterial composition of collected fecal samples from BF and FF infants

The individual fecal samples collected in the present study were analyzed for their bacterial composition by 16S rRNA amplicon analysis. In total 20 infant fecal samples were collected consisting of 10 exclusively BF infants (aged between 8-21 weeks, average 16 weeks) and 10 exclusively FF infants (aged between 7-21 weeks, average 13 weeks). The individuals of the two feeding modes did not result in two distinct clusters based on Bray-Curtis beta diversity dissimilarities (Supplementary materials **Figure S5.3**), indicating that the overall fecal bacterial composition did not differ between the two groups (FF and BF infants).
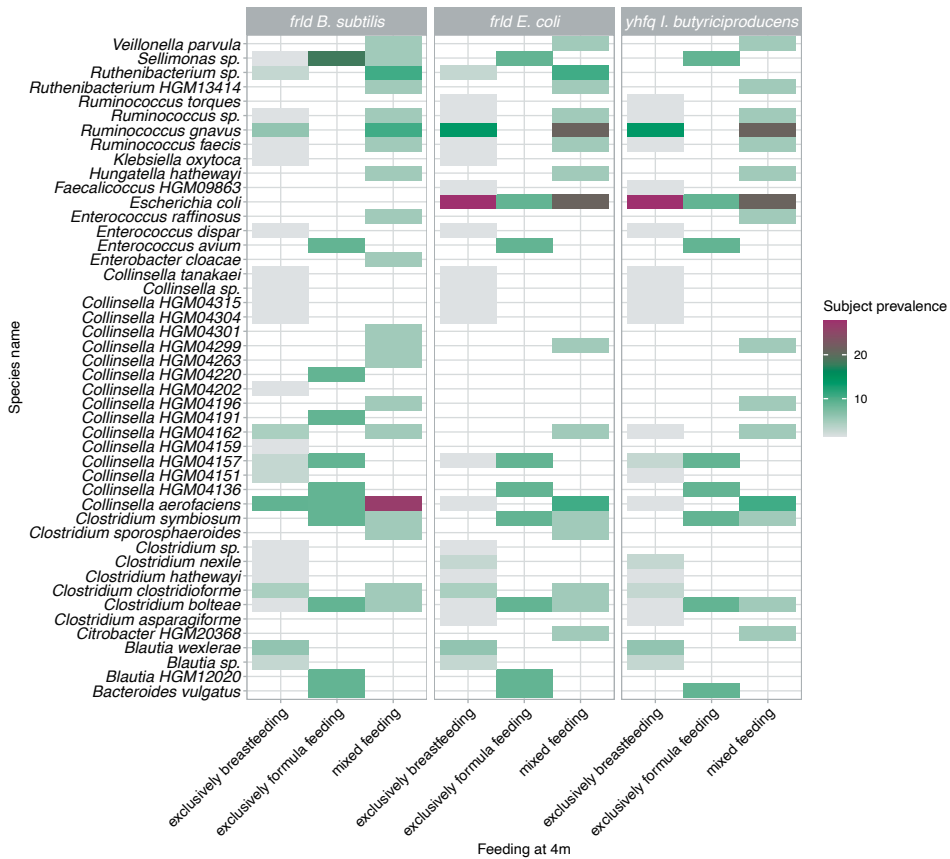
Figure 5.2 Heatmap of hits of the query genes against the included metagenome assembled genomes (MAGs), for infants aged 4 months. Subject prevalence indicates the percentage of subjects that have a hit of each query per bacterial species (y-axis) and feeding mode of infants (x-axis).

To see whether this was the case for specific bacterial taxa, bacterial composition plots were created at both phylum and genus level (for absolute abundances see **Figure 5.3**; for relative abundance plots see Supplementary materials **Figure S5.4**). This revealed that for most individuals, especially the genus *Bifidobacterium* was present in the individual fecal samples, which belongs to the phylum Actinobacteria, while for two individuals this genus was absent so these are considered as possible outliers (Individual 15 and 19). LEfSe analysis was performed to indicate differential abundant taxa between the two feeding modes, but no taxa were shown to be significantly different between the two groups with a LDA effect size > 2.0 (data not shown). This indicates that the feeding mode is, for this group of infants, not the main driver determining the variance in microbiota composition. This was confirmed by CCA analysis (canonical correspondence analysis) where age and feeding mode both did significantly explain some variation in the microbiota composition (adjusted *P*-values <0.05) but only for 8.7% and 6.8%, respectively (Supplementary materials **Figure S5.5**).
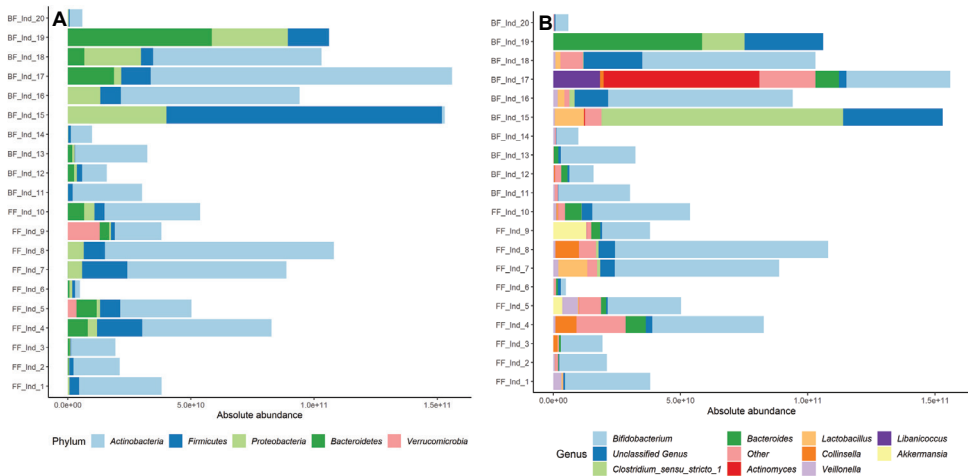
Figure 5.3 Absolute abundance of microbial taxa, assessed with 16S rRNA amplicon sequencing and qPCR, present in fecal samples either exclusively breast-fed (BF) or formula-fed (FF) infants. The top 10 taxa present at phylum (panel A) and genus (panel B) level are shown. Y-axis labels indicate feeding mode and subject number.

Differences in fructoselysine degradation activities between BF and FF infant fecal samples *in vitro*

As the metagenomic dataset analysis revealed that fructoselysine degradation query genes were more prevalent in FF infants, it was investigated whether *in vitro* fructoselysine degradation activities by the collected fecal samples were also higher for the FF infants compared to the BF infants. First, pooled fecal slurries of both BF and FF infants were incubated anaerobically with fructoselysine up to four hours. The amount of fructoselysine degraded was corrected for the total bacterial cell load per gram feces as quantified by qPCR (for individuals' total bacterial load see Supplementary Materials **Figure S5.6**). Both groups were able to degrade fructoselysine, but the fructoselysine degradation was significantly and on average about 6-fold higher in FF infants compared to the BF infants from 1.5 hours incubation onwards (*P*-value < 0.05) (degradation expressed per 1×10^{11} bacterial cells see **Figure 5.4**; degradation expressed per gram feces see Supplementary Materials **Figure S5.7**). For the first two hours of anaerobic incubation both groups seemed to have a lag phase. The largest absolute difference in fructoselysine degradation between FF and BF infants was observed at t=4 hours and amounted to 24.4 µmol/1×10^{11} bacterial cells.

To assess whether interindividual differences in the fructoselysine degradation capacity of the BF and FF infant fecal samples exist, all infant fecal samples collected were incubated individually under the same experimental conditions for 2, 3 and 4 hours. Amounts of degraded fructoselysine were calculated per individual (see Supplementary Figure **S5.8**). Based on the feeding mode the amounts of degraded fructoselysine were compared per time point (expressed per 1×10^{11} bacterial cells (**Figure 5.5**) and expressed per gram feces (Supplementary Materials **Figure S5.9**). Identified outliers were excluded from further analyses (i.e. BF individual 12 at all time points, BF individual 20 at t=2h, FF individual 6 at t=4h). Comparing the two feeding modes at the different time points revealed that on group

level, fecal samples from FF infants degraded on average significantly more fructoselysine compared to fecal samples from BF infants with an absolute difference of 14.9, 26.1 and 20.2 μmol/1x10^{11} bacterial cells at t=2, t=3 and t=4 hours, respectively ($P < 0.05$). Interindividual differences in the fructoselysine degradation activities were observed in both feeding modes as shown in **Figure 5.5**, resulting in overlap in the range for the degradation capacity of the microbiota of the individuals from the two groups. This implies that it is not possible to distinguish between BF and FF infants based on *in vitro* obtained fructoselysine degradation activities on an individual level, while on average group level it is.
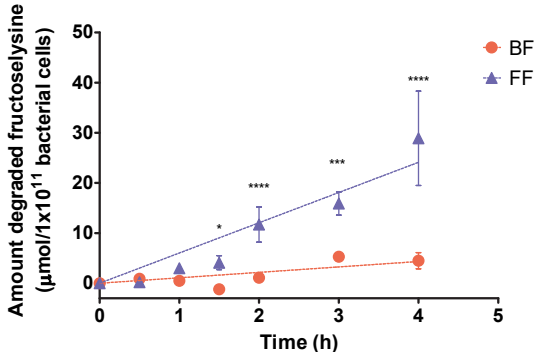

Figure 5.4 Amount of degraded fructoselysine upon anaerobic incubation of fructoselysine (in a final substrate concentration of 430 μM at t=0h) with pooled fecal slurries (final fecal concentration 0.0125 g/mL) of infants exclusively breast-fed (BF) or formula-fed (FF), containing 10 infant fecal samples per feeding mode per pool. Data points represent the average ± SD of three repeated experiments. Differences between the BF and FF results were assessed for statistical significance per time point by a 2-way ANOVA followed by Bonferroni post-hoc test: * p-value <0.05; ** p-value < 0.01; *** p-value < 0.001; **** p-value < 0.0001.
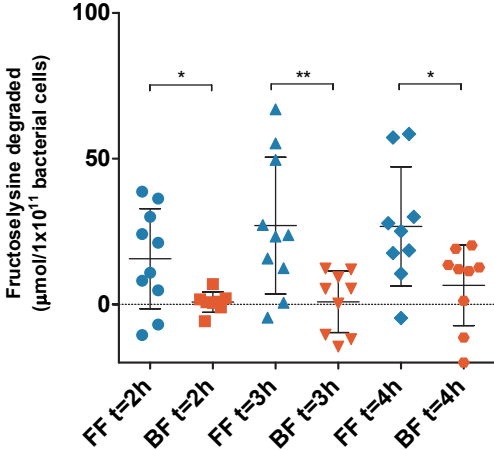

Figure 5.5 Amount of degraded fructoselysine by individual fecal samples from exclusively breast-fed (BF) or formula-fed (FF) infants quantified at each anaerobic incubation time point (i.e. 2, 3 or 4 hours). Scatter dots indicate average values of three independent experiments for each individual fecal sample. Center bars indicate average values while whiskers indicate the standard deviation. Whether the values of the two feeding modes were significantly different for each respective incubation time was evaluated with an unpaired t-test: * p-value < 0.05; ** p-value < 0.01. Identified outliers were excluded.

To assess whether the interindividual differences in fructoselysine degradation activity of the FF infants could be explained by different levels of fructoselysine in their collected infant formula powder, protein-bound and free fructoselysine levels were quantified (**Figure 5.6**). This revealed that in the formula powder the protein-bound proportion of fructoselysine (ranging from 107 – 342 μg/mg protein) was four orders of magnitude higher compared to the proportion of free fructoselysine (ranging from 21 - 68 ng/mg protein), and the quantified protein-bound levels were somewhat higher than previous reported data in literature[275]. However, the interindividual differences in fructoselysine degradation activity of the FF infant fecal samples could not be explained by the protein-bound fructoselysine levels in the respective infant formula samples as the correlation between these parameters was not strong (R^2=0.4; Supplementary Materials **Figure S5.10**).
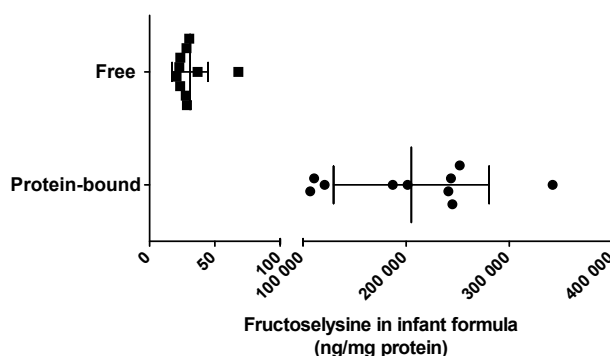

Figure 5.6 Amount of fructoselysine quantified in collected infant formula samples analyzed in both free and protein-bound form of fructoselysine per mg protein present in the infant formula. Data points represent average values of three repeated analyses of one infant formula sample.

The high levels of fructoselysine in the infant formula were also reflected in the fecal fructoselysine excretion levels with an average of 11.6 μmol/g feces for the FF infants (Supplementary Materials **Figure S5.11**), a result which is in line with literature[269]. The presence of a substantial amount of fructoselysine in the fecal samples collected from the FF infants indicates that the microbiota of the FF infants cannot degrade all fructoselysine ingested with the formula. This conclusion is corroborated by extrapolation of the *in vitro* degradation activities of the FF infants to the *in vivo* situation and comparing these to the estimated daily intake (EDI) as quantified based on the detected fructoselysine levels in infant formula. Only 28.6% of the amount of ingested fructoselysine originating from intake at the respective EDI, was estimated to be degraded by the obtained average degradation activity detected in the fecal samples from FF infants (Supplementary Materials **Table S5.2**). However, these results need to be interpreted with some caution as they are based on average values, estimations and assumptions (e.g. daily fecal weight).

To determine whether specific bacterial taxa present in the infant fecal samples were associated with fructoselysine degradation, a Spearman's rank correlation analysis was performed with taxa present in a relative abundance >0.1% in at least one of the individual fecal samples when transformed to absolute abundance glomerated at phylum (**Figure 5.7**)

or genus (Supplementary materials **Figure S5.12**) level. This analysis revealed that the phylum Bacteroidetes was shown to be significantly correlated with the amount of fructoselysine degraded (for BF: ρ = 0.85; adjusted *P*-value = 0.018) while no genus was significantly correlated.
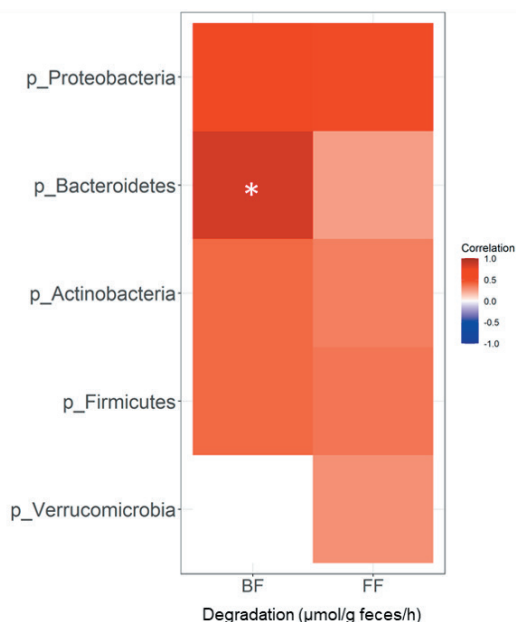

Figure 5.7 Spearman's rank correlation analysis of bacterial taxa at phylum level with the amount of degraded fructoselysine per gram feces per hour. This degradation rate represents the average degradation rate of the three measured incubation time points per individual fecal sample. Bacterial taxa present with a relative abundance >0.1% in one of the individual fecal samples were included and transformed into absolute abundance (using quantified total bacterial cell load by qPCR). P-values were adjusted for multiple testing by FDR and indicated as follows: * P-value < 0.05.

5.4 Discussion

In the present study, we show that the diet of infants affects the efficiency of the infant gut microbiota to degrade dietary derived fructoselysine. Fecal samples collected from FF infants showed a higher *in vitro* activity for microbial degradation of fructoselysine compared to the samples from BF infants. Search against a publicly available metagenome dataset revealed that sequences homologous to the ones of the functional genes involved in fructoselysine degradation are widely present in MAGs of both BF and FF infants, but with a higher prevalence in FF infants. The homologous sequences have a varying identity percentage to the query genes meaning functionality cannot be guaranteed, however, they were redundant amongst multiple bacterial species. Overall, the present study showed that fecal samples of infants exposed to different diets (i.e. breast milk and infant formula) resulting in different dietary fructoselysine exposures, differed in their microbial

fructoselysine degradation activity. The microbial fructoselysine degradation activity was on average 6-fold higher for the pooled fecal samples from the FF infants compared to the pooled fecal samples from the BF infants.

Fructoselysine is a food process contaminant formed upon heating and processing of food products, and is highly present in infant formula due to the heating processes applied during production[273–275]. The high levels of fructoselysine in infant formula are in contrast to the low to no levels of fructoselysine in human breast milk[87]. This has been confirmed by the large differences in fecal excretion of fructoselysine by the two feeding groups as observed in the present study and reported in literature[269]. This large difference in dietary fructoselysine exposure between BF and FF infants was accompanied by a higher microbial fructoselysine degradation activity of the fecal slurries from the FF infants, although the fecal slurries of the BF infants were also able to degrade fructoselysine. This is in line with the metagenomic dataset analysis as we observed sequences homologous to the relevant genes in question (frlD/yhfQ) also in the BF infant fecal samples, although with a lower corresponding prevalence as compared to the FF infant fecal samples. However, our observations are not completely in agreement with a previous study where two inoculates of BF infant fecal samples were unable to degrade fructoselysine, while two FF infants were able to do so[268].

In the present study the bacterial composition of the collected fecal samples did not differ significantly between the BF and FF infants, possibly as a higher resolution might be needed to characterize differences in their bacterial composition as also indicated upon the metagenomic dataset analysis. Similar to these observations, the interindividual differences in microbial fructoselysine degradation activity of both the BF and FF infant fecal samples could not be explained by differential abundance of specific bacterial genera, indicating that identical bacteria might be capable of multiple functionalities depending on the compounds they ferment and that multiple bacteria could be potentially involved. This is in line with the results of the metagenomic dataset analysis focused on the frlD/yhfQ genes, coding for a kinase, essential for microbial fructoselysine degradation[279]. The homologous sequences were widely present in different genera that are part of different phyla, both in the fecal data of BF and FF infants of the metagenomic dataset. In addition, at species level the sequences were found in different species that were part of the same overarching genus, indicating that differences in potential fructoselysine degradation activities can go up to at least species level. In line with the higher *in vitro* fructoselysine degradation activity of the fecal samples from the FF infants compared to the BF infant fecal samples, the potential genes involved in fructoselysine degradation (i.e. frlD/yhfQ) were found in a higher prevalence in feces from FF infants compared to that from BF infants. A previous study found genes involved in fructoselysine metabolism in metagenomes of most of the FF infants (56%) and only in some BF infants (10%)[268]. However, in this previous study the complete fructoselysine metabolism pathway was considered[40] while the analysis of the present study focused on the first step in the fructoselysine degradation.

The results combined show that the potential fructoselysine degradation function is redundant in the metagenomes of both BF and FF infant fecal samples, but that fecal samples collected from FF infants, which have been exposed to fructoselysine through their diet, showed a higher fructoselysine degradation activity *in vitro* compared to fecal samples from

BF infants. This suggests that direct dietary exposure might be responsible for an increase in activity of the microbes involved, which might also -at least partly- explain interindividual differences in fructoselysine degradation observed with adult human fecal samples[161].

The fructoselysine degradation activity of the FF infants (average 3.42 µmol/h/g feces) was comparable to the average of 16 individual adults (3.4 µmol/h/g feces) as shown in our previous study[161]. However, based on these degradation rates and the daily defecation rates, it was calculated that, due to the high fructoselysine intake by FF infants, only 28.6% of the estimated daily fructoselysine intake was expected to be microbially degraded. This estimation of incomplete fructoselysine degradation is supported by the quantified levels of fructoselysine still being present in the collected fecal samples of the FF infants. This incomplete fructoselysine degradation implies a direct exposure to fructoselysine in the intestine of the infants. Whether this can affect local intestinal health remains to be further investigated, as well as whether subsequent fructoselysine exposure affects microbial composition itself. In the present study the microbial composition of the collected fecal samples did not differ between the BF and FF infants, while diets high in AGEs have previously been reported to affect fecal microbiota composition[51,151]. However, it remains unclear whether those reported alterations can be exclusively attributed to the different AGE levels in the provided diets.

In summary, a metagenomic dataset analysis revealed that particular genes involved in microbial fructoselysine degradation were present in fecal samples from both BF and FF infants, although with a higher prevalence in the fecal samples from the FF infants. Additional collected fecal samples from FF infants appeared to show a higher fructoselysine degradation activity *in vitro* compared to the collected fecal samples from BF infants, an observation that can likely be ascribed to relatively higher dietary fructoselysine exposure of the gut microbiota from the FF infants. This suggests that, at least for the AGE precursor fructoselysine, the (infant) gut microbiota can adapt towards exposures via the environment through e.g., the diet.

Acknowledgements

5.5 Supplementary materials

Supplemental tables

Table S5.1 Sequences used for blastp against the created MAGs (metagenome assembled genomes) database

Abbreviation	Origin	Protein name	GenBank Accession No.	Reference
frlD	*Escherichia coli* str. K-12 substr. MG1655	Fructoselysine kinase	NP_417833.1	[278]
frlD	*Bacillus subtilis* subsp. Subtilis str. 168	Fructoselysine kinase	NP_391137.1	[39]
yhfQ	*Intestinimonas butyriciproducens* str. AF211	Fructoselysine kinase	ALP93343.1	[40]
frlB	*Bacillus subtilis* subsp. Subtilis str. 168	Fructosamine-6-phosphate deglycase	NP_391141.1	[39]
frlB	*Escherichia coli* str. K-12 substr. MG1655	Fructosamine-6-phosphate deglycase	NP_417830.4	[278]
yhfN	*Intestinimonas butyriciproducens* str. AF211	Fructosamine-6-phosphate deglycase	ALP93345.1	[40]

Table S5.2 Calculation of scaling the in vitro determined degradation parameters to the in vivo situation

	Average fructoselysine in tested formula samples (mg/g protein)	Daily intake (mg per 24h)[a]	Daily intake (μmol per 24h)[b]	Average in vitro degradation capacities (μmol/g feces/h)[c]	In vivo degradation capacity in 24h (μmol)[d]	% Of daily intake can be degraded in 24h
Formula-fed infants	205.1	2744.8	8903.0	3.42	2544.5	28.6

[a] Assuming 9.7% protein content per gram infant formula powder, 6 scoops each 4.6 g per bottle, 5 bottles a day. Based on 'Nutrilon Zuigelingenvoeding 1' online guidelines.
[b] Molecular weight is 308.3 g/mol.
[c] Degradation capacities were experimentally obtained in the present study and represent the averaged individual degradation rates per feeding group which were assessed by averaging the three measured incubation time points per individual fecal sample of all tested fecal samples per feeding group
[d] Transformed by assuming a daily fecal mass of 31g over 24h[289,290].
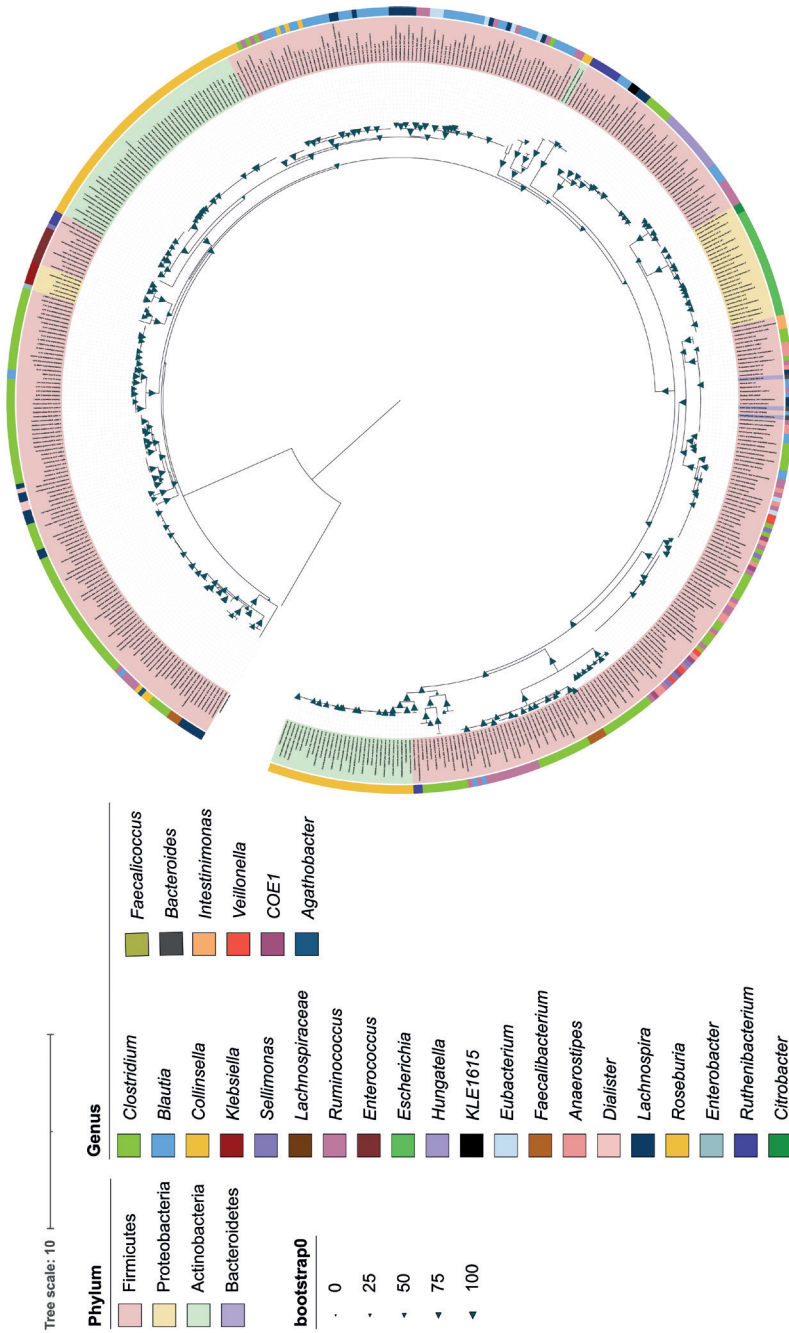
Supplemental figures

Figure S5.1 iTol phylogenetic tree of the genes frlD and yhfQ, responsible for the degradation of fructoselysine into fructoselysine-6-phosphate. Bacterial taxa with frlD/yhfQ genes at phylum and genus level are highlighted in assigned colors. Species are mentioned at tree edges.

Figure S5.2 iTol phylogenetic tree of the genes frlB and yhfN, responsible for further metabolism of fructoselysine-6-phosphate. Bacterial taxa with frlB/yhfN genes at phylum and genus level are highlighted in assigned colors. Species are mentioned at tree edges.
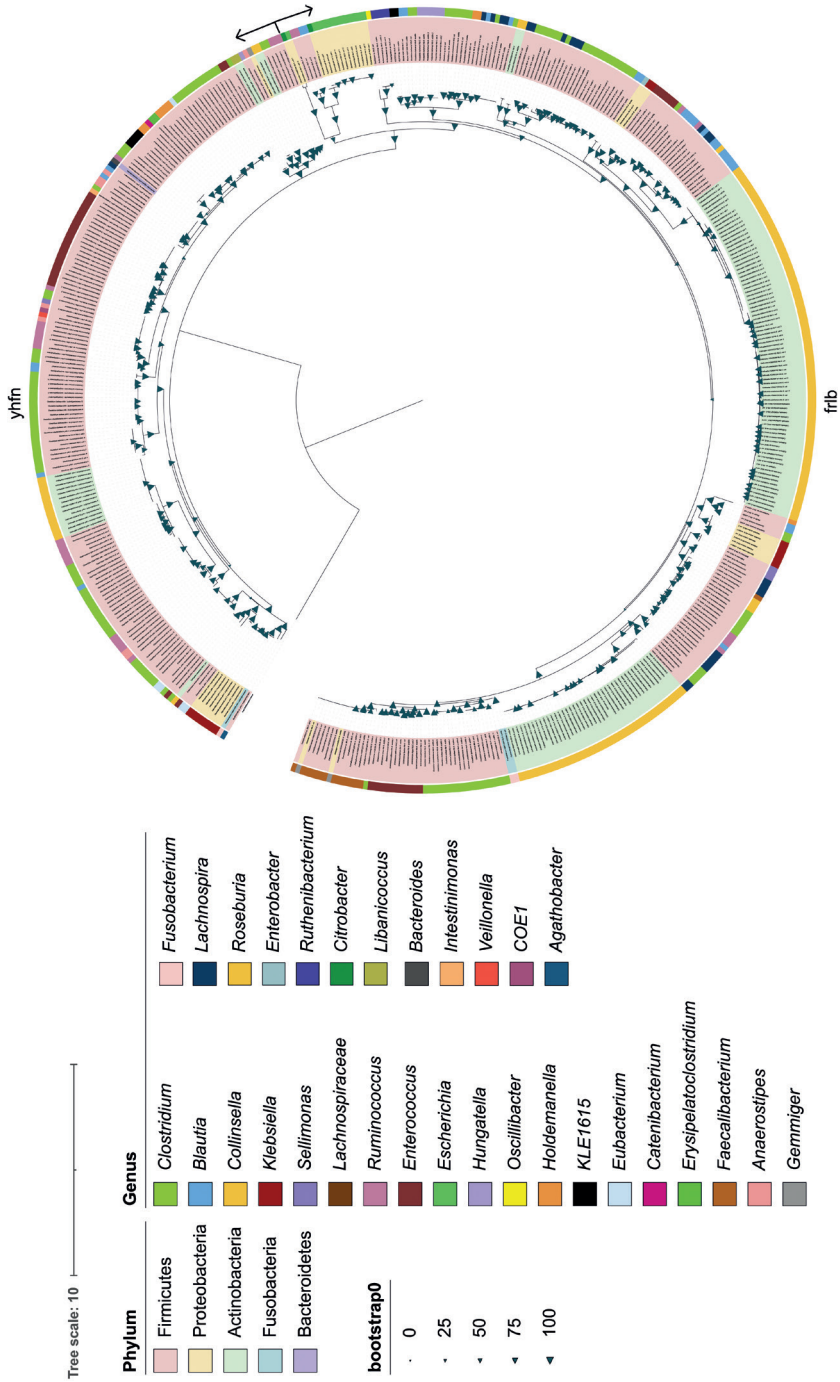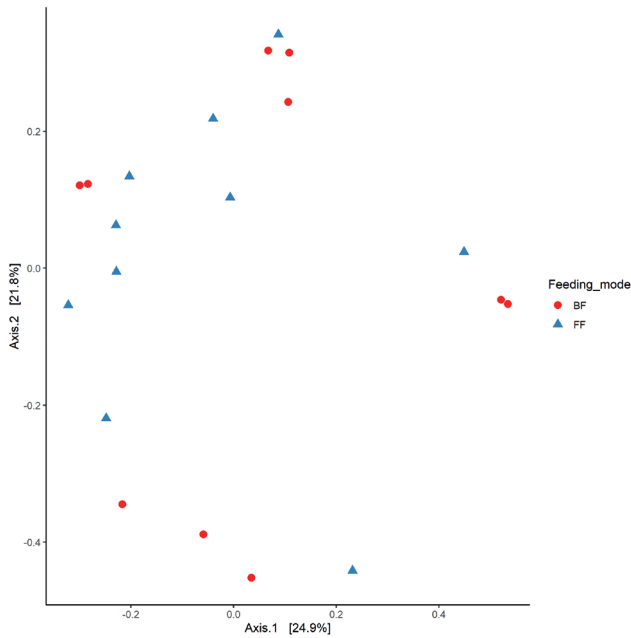
Figure S5.3 PCoA plot of Bay-Curtis beta diversity dissimilarities of 20 individual fecal samples of exclusively breast-fed (BF; red circles) or formula-fed (FF; blue triangles) infants.
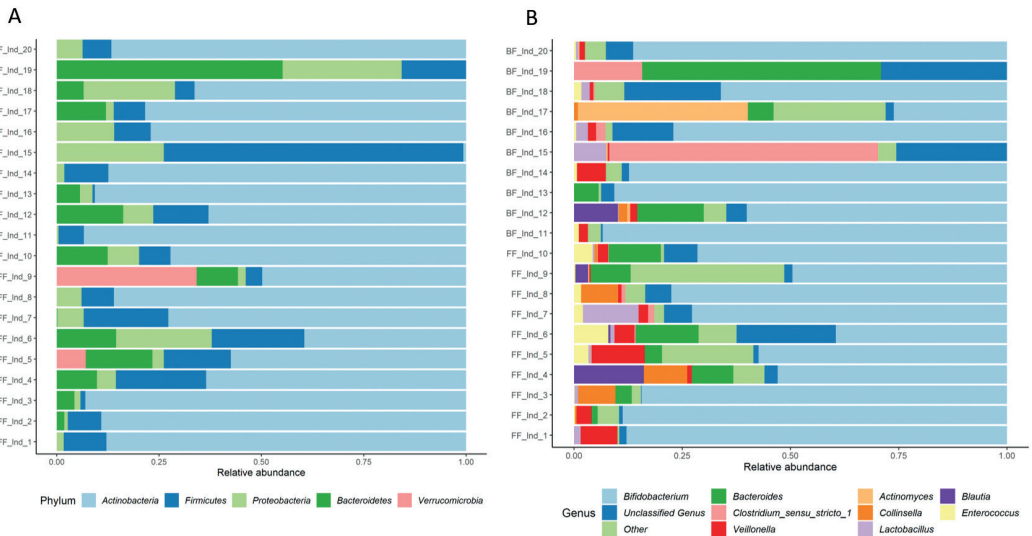

Figure S5.4 Relative abundance of microbial taxa, assessed with 16S rRNA amplicon sequencing and qPCR, present in infant fecal samples either exclusively breast-fed (BF) or formula-fed (FF). The top 10 taxa present at phylum (panel A) and genus (panel B) level are shown. Y-axis labels consist of feeding mode and subject number.
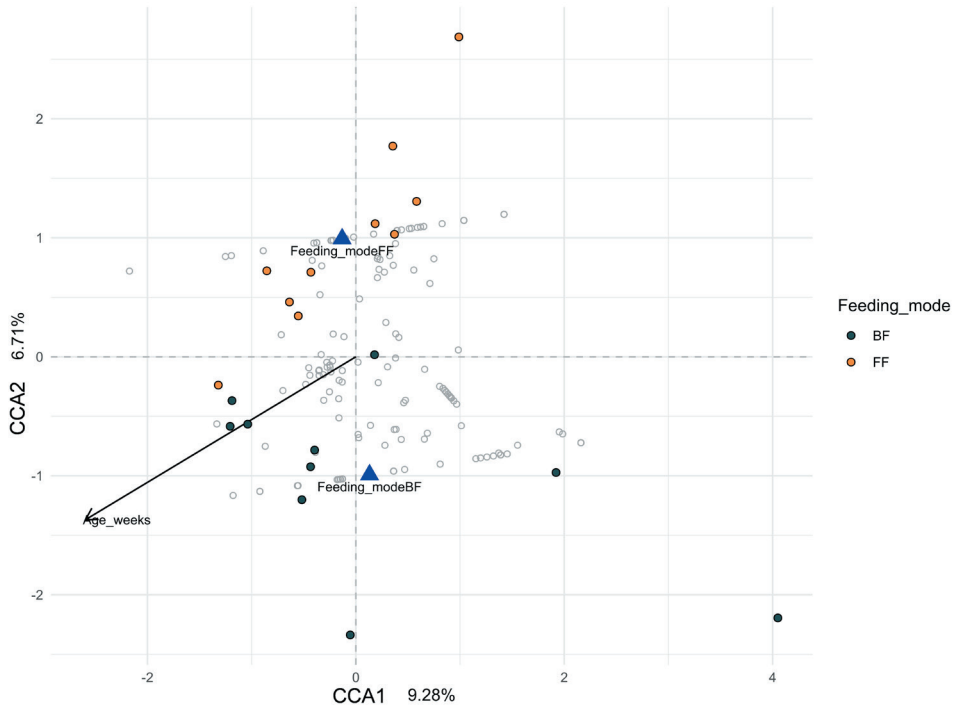
Figure S5.5 Canonical correspondence analysis (CCA). Grey open circles represent bacterial taxa; closed circles represent the infant fecal samples (black breast-fed BF; orange formula-fed FF); blue triangles represent the centroids of the FF and BF infant fecal samples. Axis percentages represent the percentage of variation explained only by the constraining variables (i.e., feeding mode and age).
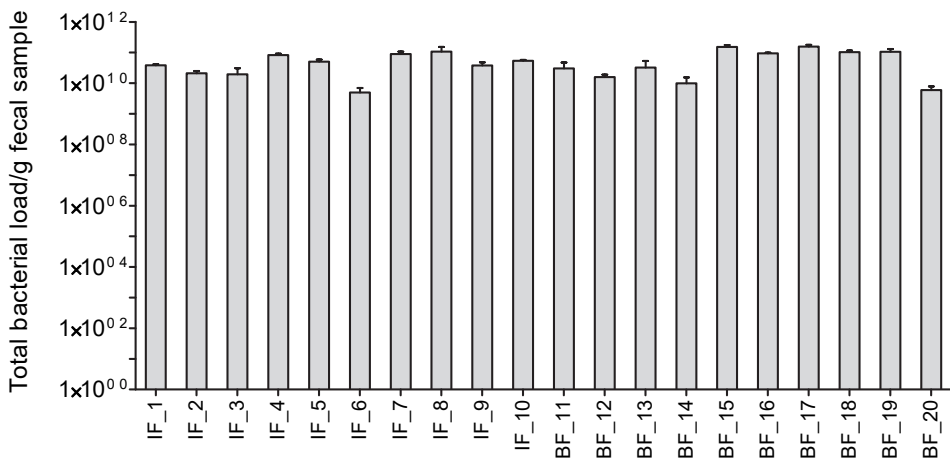

Figure S5.6 Total bacterial cell load per gram fecal sample, as collected per individual for both feeding groups (FF formula-fed; BF breast-fed). Total bacterial cell load was determined by qPCR and data represent the average ± SD of three technical replicates.

Figure S5.7 Amount of degraded fructoselysine upon anaerobic incubation of fructoselysine (final substrate concentration 430 μM) with pooled fecal slurries (final fecal concentration 0.0125 g/mL) of infants exclusively breast-fed (BF) or formula-fed (FF), containing 10 infant fecal samples per feeding mode. Data points represent the average ± SD of three independent repeated experiments. Differences between the BF and FF results were assessed for statistical significance per time point by a 2-way ANOVA followed by Bonferroni post-hoc test: * p-value <0.05; ** p-value < 0.01; *** p-value < 0.001; **** p-value < 0.0001.
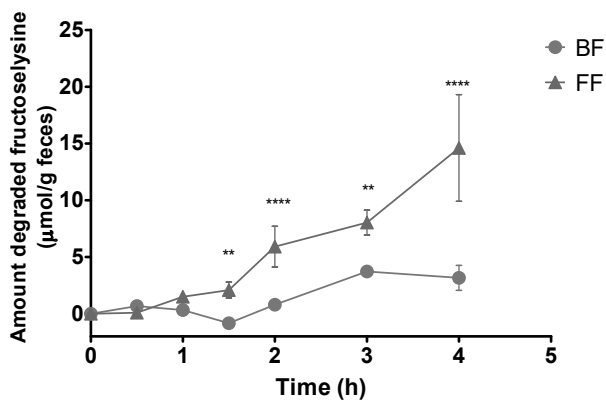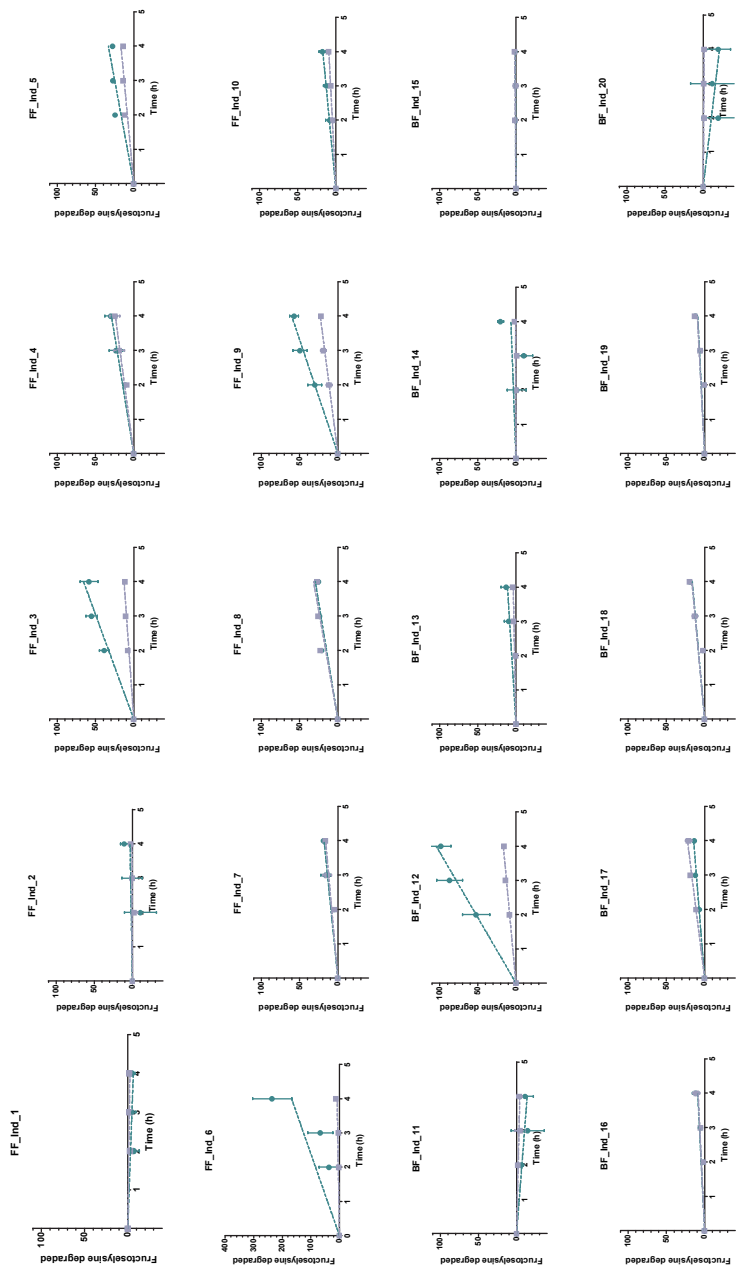
Figure S5.8 Amount of degraded fructoselysine upon anaerobic incubation of fructoselysine (final substrate concentration 430 µM) with individual fecal slurries (final fecal concentration 0.0125 g/mL) of infants exclusively breast-fed (BF) or formula-fed (FF), containing 10 infant fecal samples per feeding mode. Data points represent the average ± SD of three independent repeated experiments. Dotted lines represent the slope.
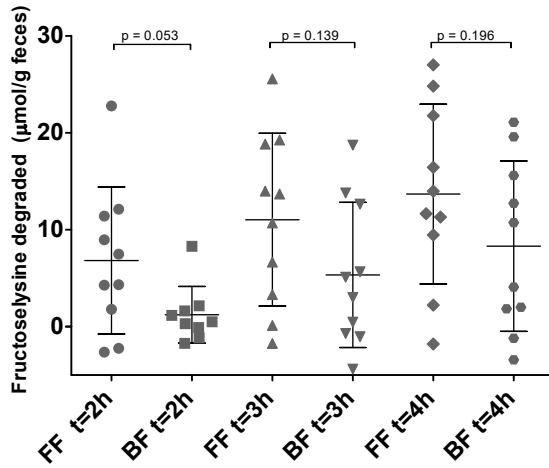
Figure S5.9 Amount of degraded fructoselysine by individual fecal samples from exclusively breast-fed (BF) or formula-fed (FF) infants quantified at each anaerobic incubation time point (i.e. 2, 3 or 4 hours). Scatter dots indicate average values of three independent experiments for each individual fecal sample. Center bars indicate average values while whiskers indicate the standard deviation. Whether the values of the two feeding modes were significantly different for each respective incubation time was evaluated with an unpaired t-test. Identified outliers were indicated with an open symbol and excluded for further analyses.
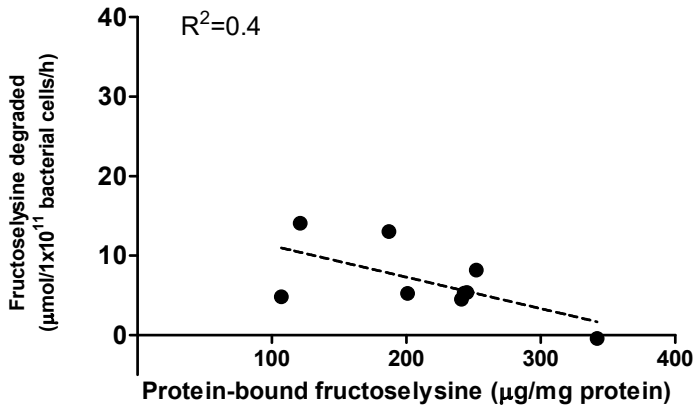
Figure S5.10 Correlation of amount of degraded fructoselysine of formula-fed infants and protein-bound fructoselysine levels in their infant formula. The rate of fructoselysine degradation represents the average degradation rate per individual of the three measured incubation time points.
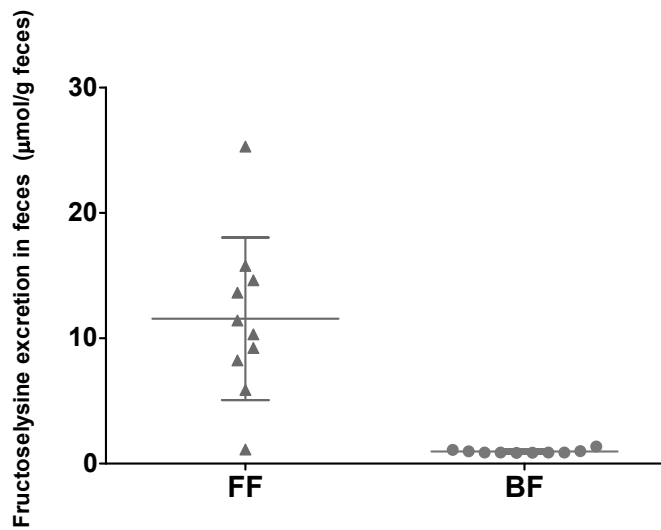
Figure S5.11 Fructoselysine fecal excretion in exclusively formula-fed (FF) or breast-fed (BF) infant fecal samples.
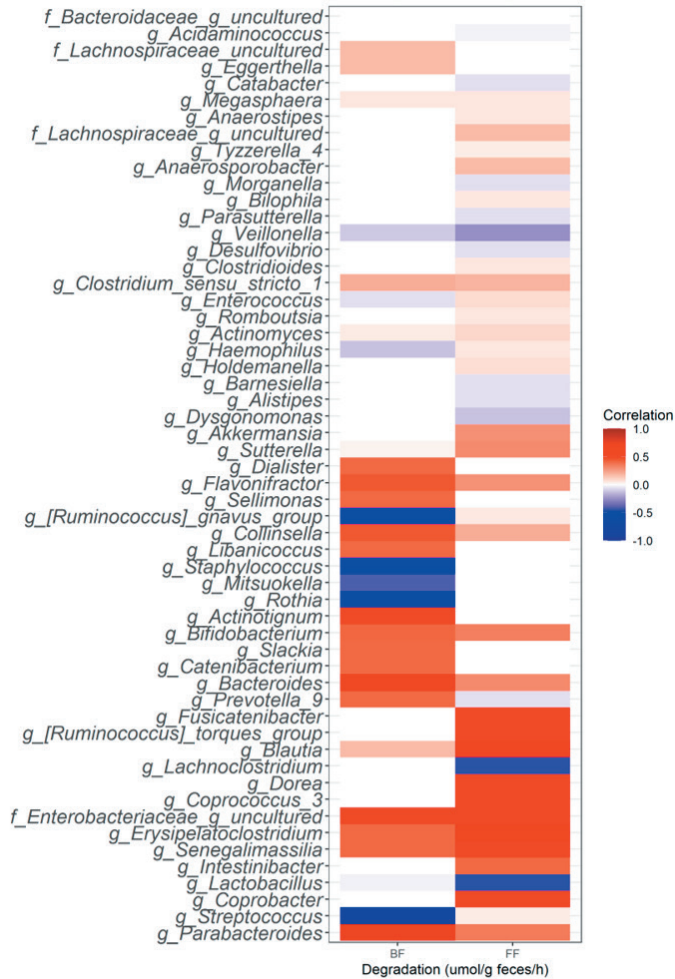
Figure S5.12 Spearman's rank correlation analysis of bacterial taxa at genus level with the amount of degraded fructoselysine per gram feces per hour. This degradation rate represents the average degradation rate of the three measured incubation time points per individual fecal sample. Bacterial genera present with a relative abundance >0.1% in one of the individual fecal samples were included and transformed into absolute abundance (using quantified total bacterial cell load by qPCR). P-values were adjusted for multiple testing by FDR.

Dietary advanced glycation endproducts (AGEs) increase their concentration in plasma and tissues, result in inflammation and modulate gut microbial composition in mice; evidence for reversibility

Katja C.W. van Dongen*, Armand M.A. Linkens*, Suzan M.W. Wetzels, Kristaan Wouters, Tim Vanmierlo, Marjo P.H. van de Waarenburg, Jean L.J.M. Scheijen, Willem M. de Vos, Clara Belzer#, Casper G. Schalkwijk#

*,# These authors contributed equally

Abstract

Scope: Dietary advanced glycation endproducts (AGEs) are associated with negative biological effects, possibly due to accumulation in plasma and tissues and through modulation of inflammation and gut microbiota. Whether these biological consequences are reversible by limiting dietary AGE intake is unknown.

Methods and results: Young healthy C57BL/6 mice were fed a standard chow (n=10) or a baked chow high AGE-diet (n=10) (~1.8-6.9 fold increased protein-bound Nε-(carboxymethyl) lysine (CML), Nε-(1-carboxyethyl)lysine (CEL), and Nδ-(5-hydro-5-methyl-4-imidazolon-2-yl)-ornithine (MG-H1)) for 10 weeks or a switch diet with baked chow for 5 weeks followed by 5 weeks of standard chow (n=10). We assessed accumulation of AGEs in plasma, kidney, and liver and measured inflammatory markers and gut microbial composition. After 10 weeks of baked chow, a substantial panel of AGEs were increased in plasma, liver, and kidney. These increases were normalized after the switch diet. The inflammatory z-score increased after the baked chow diet. Gut microbial composition differed significantly between groups, with enriched *Dubosiella spp.* dominating these alterations.

Conclusion: A high AGE-diet led to an increase of AGEs in plasma, kidney, and liver and to more inflammation and modification of the gut microbiota. These effects were reversed or discontinued by a diet lower in AGEs.

List of abbreviations: AGEs Advanced glycation endproducts; **ASV** amplicon sequence variants; **CEL** Nε-(1-carboxyethyl)lysine; **CML** Nε-(carboxymethyl)lysine; **CRP** c-reactive protein; **FDR** false discovery rate; **GO** glyoxal; **IQR** interquartile range; **LDA** linear discriminant analysis; **LEfSe** LDA effect size; **LOD** limit of detection; **MG-H1** Nδ-(5-hydro-5-methyl-4-imidazolon-2-yl)-ornithine; **MGO** methylglyoxal; **PERMANOVA** permutational multivariate analysis of variance; **RCT** randomized controlled trial; **rRNA** ribosomal RNA; **3DG** 3-deoxyglucosone

6.1 Introduction

Advanced glycation endproducts (AGEs) are abundantly present in processed food products and may contribute to beneficial effects on flavor, smell, and shelf life[291]. These dietary AGEs are formed during the non-enzymatic reaction between free amino acids and reducing sugars, via the so-called Maillard reaction[104]. There is increasing evidence in humans and animals that consumption of dietary AGEs contribute to AGEs measured in plasma[26,292] and organs[293] and that a diet high in dietary AGEs in humans has negative biological effects, such as low-grade inflammation, endothelial dysfunction, and insulin resistance[294]. However, it is currently unknown whether AGE accumulation in tissues and the negative biological effects associated with a high AGE diet are reversible. Furthermore, how dietary AGEs are involved in the aforementioned biological effects remains poorly understood. Dietary AGEs may exert their biological effects, at least partly, through modulation of the gut microbiota composition, which in turn is increasingly recognized to play a fundamental role in the pathophysiology of obesity, diabetes, and cardiovascular disease[295]. Although there are some discrepancies, several animal studies have shown that a heat-treated diet high in dietary AGEs can modulate gut microbiota composition[210,296–299]. However, the effects on inflammatory markers or increases in protein-bound and free AGE levels in plasma and/or tissues were not addressed in all of these studies. Furthermore, it is currently unknown whether changes in gut microbiota composition following a high AGE diet are reversible.

In light of the above, we hypothesized that mice fed a high dietary AGE diet for 10 weeks show increased blood and tissue AGEs, increased inflammatory markers, and different microbiota composition as compared to mice fed a standard dietary AGE diet. In addition, we studied whether changes following the high dietary AGE diet were reversible by implementing a switch after 5-weeks of high dietary AGE diet to the standard dietary AGE diet for 5 subsequent weeks.

6.2 Material and methods

Animal studies
To obtain a high AGE diet, a standard rodent chow (ssniff, Soest, Germany) was baked at 160 °C for two hours (hereafter referred to as "baked chow"). 9-week-old female C57BL/6/OlaHsd mice were randomly divided in three cages in groups of 10 (**Figure 6.1**). After a one-week acclimatization period, the mice were divided in three groups fed either standard chow (n=10), baked chow high in dietary AGEs (n=10), or a "switch diet" (n=10) for 10 weeks. In the switch diet group, mice were first fed the baked chow diet for 5 weeks, and subsequently the standard chow diet for 5 weeks. All diets were provided ad-libitum. Fecal and blood samples were collected after the 1-week acclimatization period. Blood samples were collected after 5 weeks of dietary intervention, while fecal samples were collected every 2.5 weeks. At the end of the 10-week dietary intervention, all mice were sacrificed by anesthetic overdose and plasma, liver and kidneys, and feces (from the rectum) were collected. To test whether accumulation of AGEs in organs after a high dietary AGE diet are reversible, two extra groups of 10 mice were allocated to either 5 weeks of the standard chow diet or 5 weeks of the baked chow diet under the same conditions as mentioned above. At the end of the 5-week

dietary intervention, all mice were sacrificed. All experiments were approved by the local ethical committee for animal experiments of Hasselt University and performed according to institutional guidelines (matrix 201503).
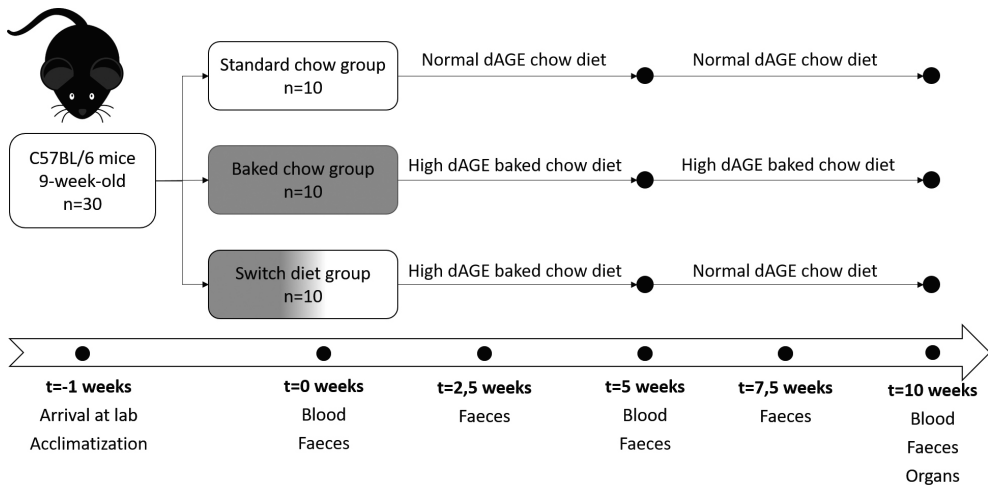

Figure 6.1 Design of the main study. dAGE: dietary AGE.

Advanced glycation end products and oxoaldehyde measurements

AGEs were measured in chow diets, plasma, liver, and kidney. AGEs in plasma were measured as this reflects uptake of dietary AGEs from the gastrointestinal tract. We chose to measure AGEs in liver and kidney as these are major organs and are highly susceptible to AGE accumulation and AGE-induced damage[300,301]. Livers and kidneys were homogenized using a Mini-bead beater homogenizer (Biospec) and 250 μl sodium phosphate buffer (0.1 M) supplemented with protease inhibitor (Roche) and 0.02% Triton-x (Sigma-Aldrich). Free- and protein-bound AGEs Nε-(carboxymethyl)lysine (CML), Nε-(1-carboxyethyl)lysine (CEL), and Nδ-(5-hydro-5-methyl-4-imidazolon-2-yl)-ornithine (MG-H1) were analyzed in plasma, liver, and kidney homogenates by LC-MS/MS after extraction as described in detail before[7,302]. Additionally, free-, protein-bound AGEs and the oxoaldehydes (also referred to as dicarbonyls) methylglyoxal (MGO), glyoxal (GO) and 3-deoxyglucosone (3DG) were analysed in pulverized animal diets as described previously[303].

Inflammation markers

IFN-γ, IL-10, IL-6, KC/GRO, and TNF-α were measured in plasma using MSD V-PLEX multiplex assay platforms (Meso Scale Diagnostics, Rockville, MD, U.S.A.). C-reactive protein (CRP) was measured using mouse CRP ELISA DuoSet kit (R&D system, Minneapolis, Minn, U.S.A.). For IFN-γ and IL-6, some samples were below the limit of detection (LOD) (<0.12 pg/ml for IFN-γ, n=3, <3 pg/ml for IL-6, n=14). These missing values were substituted by half the LOD, a commonly used method[304] (thus 0.06 pg/ml for IFN-γ and 1.5 pg/ml for IL-6).

Microbial 16S rRNA sequencing

DNA was isolated from the fecal pellets using a bead-beating procedure in combination with the customized MaxWell® 16 Tissue LEV Total RNA Purification Kit (XAS1220; Promega Biotech AB, Stockholm, Sweden) as described before[305]. Triplicate PCR reactions of the 16S ribosomal RNA (rRNA) gene V4 region (515-F GTGYCAGCMGCCGCGGTAA, 806-R GGACTACNVGGGTWTCTAAT; 10 μM each) were applied to the template DNA isolates (20 ng/μL) with a unique barcoded sequences library approach to identify individual fecal pellets with a total volume of 35 μL per reaction. Formed PCR products were qualitatively confirmed and purified as described before[305]. 200 ng of each sample was pooled after quantification with the Qubit® dsDNA BR Assay Kit and subsequently sequenced (Illumina NovaSeq 6000, paired-end, 150 bp; Eurofins Genomics Europe Sequencing GmbH, Konstanz, Germany). The 16S rRNA gene sequencing raw data has been deposited in the European Nucleotide Archive (ENA) under accession number PRJEB41378.

Microbiota data processing and analysis

Sequences of the 16S rRNA gene were analyzed using the NG-Tax 2.0 pipeline[235] with default settings, which generates *de novo* exact match sequence clusters: amplicon sequence variants (ASVs). ASVs with a relative abundance below 0.1% were removed and the threshold for taxonomic assignment was set at 80%. The SILVA 16S rRNA gene reference database release 132[236] was used to assign taxonomy. The program R (version 3.6.1) was used for further data analysis. The Phyloseq package[237] (version 1.30.0) was applied to combine the ASV table with the phylogenetic tree and the metadata. ASVs with a relative abundance >0.1% in one of the individual samples were included for further data analysis. Bray-Curtis dissimilarities (beta-diversity) were assessed with the Phyloseq package. Relative abundance composition plots at phylum and genus level were created using the Microbiome package[238]. The web-based tool Linear Discriminant Analysis (LDA) Effect Size (LEfSe)[240] was used to identify differential abundant taxa between the diet groups per sampling week. Spearman's rank correlations of microbial compositional data, glomerated at genus level, with relevant clinical data were performed with the associate function of the Microbiome package[238] (version 1.8.0). Therefore, subsets of each sampling week were created and taxa with a relative abundance >1% in one of the samples were included.

Statistical analysis

Analyses were conducted using SPSS version 25 for Windows (IBM Corporation, Armonk, NY, USA). AGE and oxoaldehyde content of standard and baked chow are presented as mean ± SD, and comparisons of AGE and oxoaldehyde content of standard and baked chow diets were tested using the two-tailed unpaired Students T-test. Comparisons between free and protein-bound AGEs in plasma and tissues and inflammatory markers between groups were performed using the Mann-Whitney-U test. Free and protein-bound AGEs in plasma and tissues and inflammatory markers are presented as median [IQR] due to skewed distributions. To increase statistical efficiency and reduce multiple testing when correlating inflammatory markers to the microbiota data, an inflammatory z-score was calculated by combining TNF-α, IFN-γ, KC/GRO, IL-6 and the inverse of IL-10 (1/IL-10) as described previously[306]. To this end, first, z-scores for all individual parameters were calculated as follows: (individual value minus whole study population mean value)/ whole study population SD, thus resulting in a standardized variable ranging from approximately -2.5 to + 2.5 SD with a mean of 0. Second, as these individual z-scores share the same unit, they were averaged, resulting

in one single inflammation score, which was subsequently standardized. Permutational multivariate analysis of variance (PERMANOVA) of microbial beta diversity was assessed by application of the Adonis function (999 permutations) of Vegan package[239] (version 2.5-6). LEfSe analysis revealed differential abundant taxa if the *P* value of the non-parametric Kruskal-Wallis test between two diet groups was <0.05 and the effect size of the logarithmic LDA score >2.0. *P* values of correlations of microbial taxa with clinical data were adjusted for multiple testing using the Benjamini & Hochberg false discovery rate (FDR). All analysis were considered statistically significant with *P* values <0.05 unless otherwise stated.

6.3 Results

Increased levels of AGEs in chow after baking
To assess the effect of baking on chow diets, we compared free and protein-bound AGEs, and oxoaldehyde content between standard chow and baked chow. While levels of free CEL and MG-H1 increased after the baking procedure (34%, *p* < 0.05, and 266%, *p* < 0.01, respectively), free CML decreased after the baking procedure (-54%, *p* < 0.05) (**Figure 6.2**). In contrast, levels of protein-bound AGEs in chow were uniformly and significantly increased following the baking procedure: 299% for protein-bound CML (*p* < 0.001), 691% for CEL (*p* < 0.001) and 182% for MG-H1 (*p* < 0.001) (**Figure 6.2**). Likewise, levels of oxoaldehydes were also significantly increased following the baking procedure: 108% for MGO (*p* < 0.05), 53% for GO (*p* < 0.05) and 379% for 3DG (*p* < 0.001) (**Figure 6.2**).

Mice fed baked chow ate less than mice fed standard chow, but weight gain was similar
To test whether weight gain over 10 weeks in young mice was different after the consumption of a baked chow diet, standard chow diet, or the switch diet, we determined food intake and weight at baseline and after 10 weeks. Mice fed the baked chow diet for 10 weeks ate less than mice fed the standard chow diet or switch diet: 2.96 g/day, 3.77 g/day, and 3.13 g/day, respectively (**Table 6.1**). In line with this, body weight was higher after 10 weeks of standard chow compared to baked chow or the switch diet, with median (g) [IQR] of 23.4 [22.2;24.1], 21.1 [20.5;21.2], and 21.8 [20.3;22.5], respectively. However, body weight of mice fed the baked chow diet was already lower at baseline as compared to mice fed the standard chow diet, thus percentage weight gain was not different between mice fed standard chow, baked chow, or the switch diet after 10 weeks, with median (%) [IQR] of 22 [19;29], 19 [15;22], and 17 [16;23], respectively (**Table 6.1**).
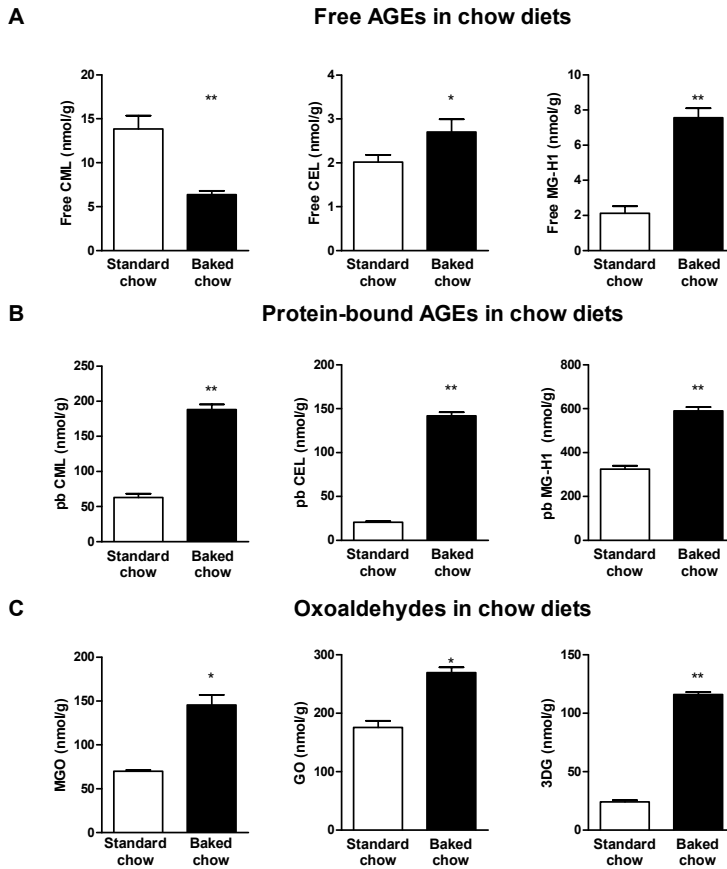
Figure 6.2 Free AGEs (A), protein-bound AGEs (B), and oxoaldehydes (C) in standard chow and baked chow, as analyzed by UPLC-MS/MS. CML: Nε-(carboxymethyl) lysine. CEL: Nε-(1-carboxyethyl)lysine. MG-H1: Nδ-(5-hydro-5-methyl-4-imidazolon-2-yl)-ornithine. MGO: methylglyoxal. GO: glyoxal. 3DG: 3-deoxyglucosone. pb: protein-bound. For free and protein-bound AGEs, bars and error bars indicate mean and SD of 5 samples per diet. For oxoaldehydes, bars and error bars indicate mean and SD of 2 samples per diet. * indicates p < 0.05

Table 6.1 Mice characteristics

	Standard Chow	Baked Chow	Switch Diet	P standard vs baked	P standard vs switch	P Baked vs switch
Weight baseline (g)	19.1 [17.9-19.5]	18.0 [17.1-18.2]	18.1 [16.4-19.3]	0.019	0.165	0.481
Weight sacrifice (g)	23.4 [22.2-24.1]	21.1 [20.5-21.2]	21.8 [20.3-22.5]	0.001	0.004	0.481
Weight gain (g)	4.2 [3.5-5.2]	3.3 [2.8-3.8]	3.1 [2.9-4.1]	0.043	0.035	0.796
Weight gain (%)	22 [19-27]	19 [15-22]	17 [16-23]	0.218	0.123	1.000
Food intake (g/day)	3.77	2.96	3.13			

Sample size n = 10 per group. Weight is presented as median [IQR]. Food intake was measured for each group as whole, thus statistical differences between groups cannot be computed. Significant differences (p < 0.05) are shown bold.

A baked chow diet increases both free and protein-bound AGEs in plasma

To assess the impact of the chow diets on the level of AGEs after 10 weeks, we compared free and protein-bound AGEs in plasma between groups. All free AGEs in plasma were higher after baked chow compared to standard chow, with median (nmol/L) [IQR] of 536 [406;795] vs. 355 [332;430], p = 0.004 for CML, 228 [129;374] vs. 118 [86;135], p = 0.011, for CEL, and 242 [89;303] vs. 76 [61;102], p = 0.019 for MG-H1 (**Figure 6.3A**). Results for protein-bound AGEs in plasma were similar, except for MG-H1. After 10 weeks of the baked chow diet, protein-bound CML and CEL in plasma were higher compared to the standard chow diet, with median (nmol/L) [IQR] of 853 [805;919] vs. 561 [542;599], p < 0.001, and 311 [227;345] vs. 207 [183;235] p = 0.011, respectively. Protein-bound MG-H1 in plasma was lower after baked chow compared to standard chow: 1464 [1377;1506] vs. 1630 [1502;1911], p = 0.011 (**Figure 6.3B**).

A baked chow diet increases AGEs in liver and kidneys, but mainly in the free form

We next determined the difference in AGE levels in organs after 10 weeks of the baked chow or standard chow diet. In liver, free CML and MG-H1, but not CEL, were higher after baked chow compared to standard chow, with median (nmol/g of protein) [IQR] of 8.0 [7.2;8.5] vs. 5.4 [4.9;5.7] for CML (p < 0.001), 2.3 [1.6;3.3] vs. 0.8 [0.8;0.9] for MG-H1 (p < 0.001), and 8.0 [7.4;8.7] vs. 8.1 [6.8;9.6] for CEL (p = 0.730) (**Figure 6.3C**). Contrarily, protein-bound AGEs in liver were not different, although there was a trend for increased protein-bound CML in liver after baked chow compared to standard chow: 21 [20;22] vs. 18 [17;21] for CML (p = 0.063), 44 [39;46] vs. 41 [37;44] for CEL (p = 0.393), and 24 [21;28] vs. 25 [23;33] for MG-H1 (p = 0.436) (**Figure 6.3D**). In kidney, free AGEs were higher after baked chow compared to standard chow, although the difference in free CML did not reach statistical significance: 224 [143;284] vs. 161 [119;179] for CML (p = 0.052), 114 [67;147] vs. 48 [37;57] for CEL (p < 0.001), and 17 [8;26] vs. 5 [5;6] for MG-H1 (p = 0.001) (**Figure 6.3E**). In contrast, protein-bound CML in kidney, but not CEL or MG-H1, was higher in kidney after baked chow compared to standard chow: 26 [24;29] vs. 22 [19;24] for CML (p<0.001), 19 [18;22] vs. 21 [17;22] for CEL (p = 0.796), and 28 [22;44] vs. 31 [25;36] for MG-H1 (p = 0.971) (**Figure 6.3F**).
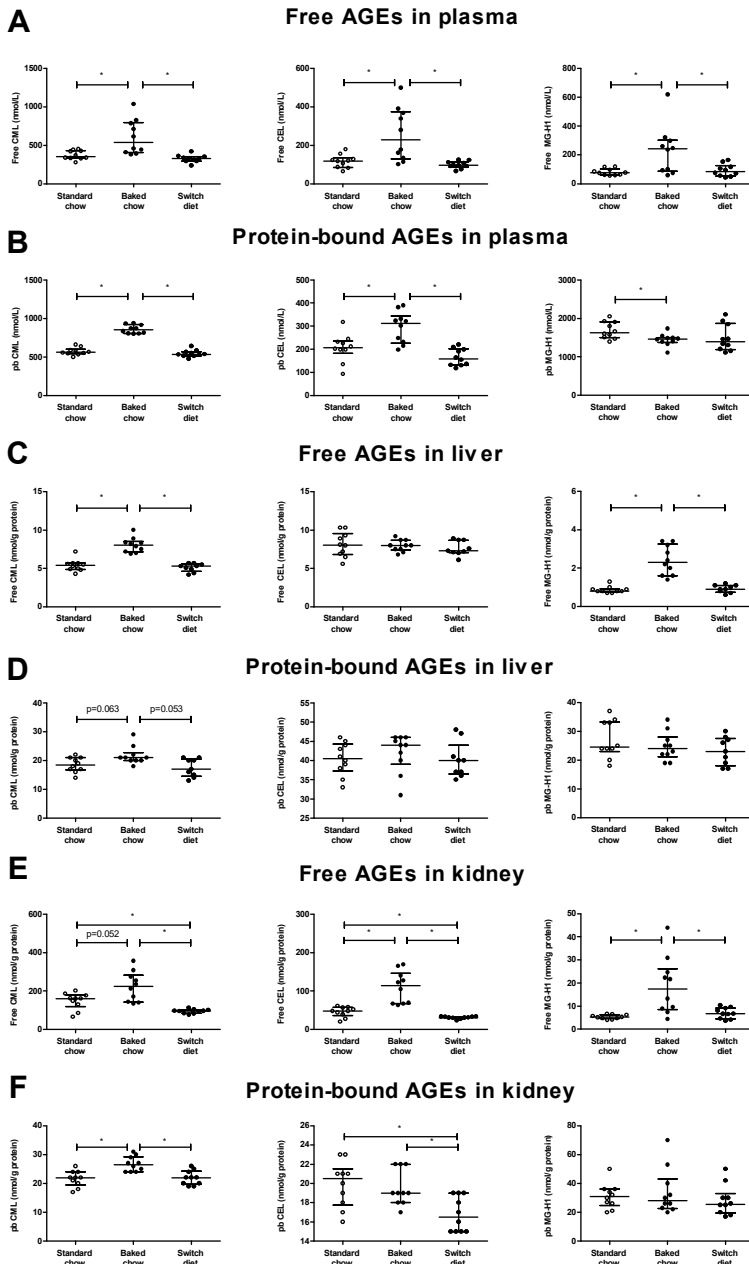
Figure 6.3 Free and protein-bound AGEs in plasma (A,B), liver (C,D), and kidney (E,F) of mice after 10 weeks of standard chow, baked chow, and the switch diet, as analyzed by UPLC-MS/MS. CML: Nε-(carboxymethyl)lysine. CEL: Nε-(1-carboxyethyl)lysine. MG-H1: Nδ-(5-hydro-5-methyl-4-imidazolon-2-yl)-ornithine. pb: protein-bound. Center bars of scatter dots indicate median values while whiskers indicate inter quartile range. * indicates p<0.05 for the difference between chow diets. N = 10 for all groups, except for free and protein-bound AGEs in liver for the switch diet group, where n = 9.

The accumulation of AGEs in plasma and organs after a baked chow diet is reversible

We next studied whether the accumulation of AGEs after a baked chow diet can be reversed by a standard chow diet. We first assessed whether AGEs in plasma and organs were already increased after 5 weeks of the baked chow diet. In general, all free and protein-bound AGEs were increased in plasma, kidney, and liver of mice fed the baked chow diet for 5 weeks compared to mice fed the standard chow diet for 5 weeks (Supplementary material **Figure S6.1**). However, protein-bound MG-H1 in plasma was not significantly different between mice fed the baked chow diet for 5 weeks compared to the standard chow diet, with median (nmol/g of protein) [IQR] of 1599 [1487;2128] vs. 1484 [1371;1704]. In addition, free CEL was lower and protein-bound MG-H1 was not different in liver of mice fed the baked chow diet compared to the standard chow diet: 8.3 [8.0;8.9] vs. 9.6 [8.8;10.4] , p = 0.007 and 25.3 [21.5;28.9] vs. 26.5 [24.9;30.8], p = 0.280, respectively. The accumulation of AGEs in plasma, kidney and liver after 5 weeks of a baked chow diet were reversible, as most AGEs in plasma, liver, and kidney were significantly decreased after the switch to standard chow (**Figure 6.3A-F**). Remarkably, free CML, free CEL, and protein-bound CEL in kidney were even lower after the switch diet as compared to 10 weeks of standard chow, with median (nmol/g of protein) [IQR] of 96 [85;102] vs. 161 [119;179], p = 0.011, 31 [29;33] vs. 48 [37;57], p = 0.015, and 16 [15;19] vs. 21 [17;22], p = 0.009, respectively (**Figures 6.3E and 6.3F**).

A baked chow diet affects some markers of inflammation

To assess whether inflammation is increased after a baked chow diet compared to a standard chow diet, a panel of inflammatory markers were analyzed individually. TNF-α, IFN-γ, KC/GRO, CRP, and IL-6 were not different after 10 weeks of baked chow or standard chow (**Figure 6.4A**). However, the anti-inflammatory cytokine IL-10 was significantly lower after baked chow compared to standard chow: 9.4 pg/ml [8.5;10.4] vs. 12.8 pg/ml [10.1;14.8], p = 0.011 (**Figure 6.4A**). We next combined the inflammatory markers into an overall inflammatory z-score that also included IL-10. The inflammatory z-score was higher after 10 weeks of baked chow than after 10 weeks of standard chow, with median (SD) [IQR] of 0.37 [-0.13;1.31] vs. -0.39 [-1.05;0.20], p = 0.029 (**Figure 6.4B**). Then we determined whether the increase in inflammation after a baked chow diet could be reversed by a standard chow diet. We first assessed whether inflammatory markers in plasma were already increased after 5 weeks of the baked chow diet. In contrast to AGEs in plasma and organs, inflammatory markers in plasma and the inflammatory z-score were not already increased after 5 weeks of baked chow compared to 5 weeks of standard chow (Supplementary materials **Figure S6.2**). In fact, plasma TNFα was lower after 5 weeks of baked chow compared to 5 weeks of standard chow, with median (pg/ml) [IQR] of 5.85 [5.16-6.39] vs. 7.50 [6.48;8.42], p = 0.017. Although inflammatory markers in plasma were not already increased after 5 weeks of baked chow, the subsequent increase in inflammatory markers after 10 weeks of baked chow could be prevented by the switch to standard chow, with inflammatory z-score median [IQR] 0.37 [-0.13;1.31] vs -0.41 [-0.81;0.26], p = 0.034 (**Figure 6.4B**).

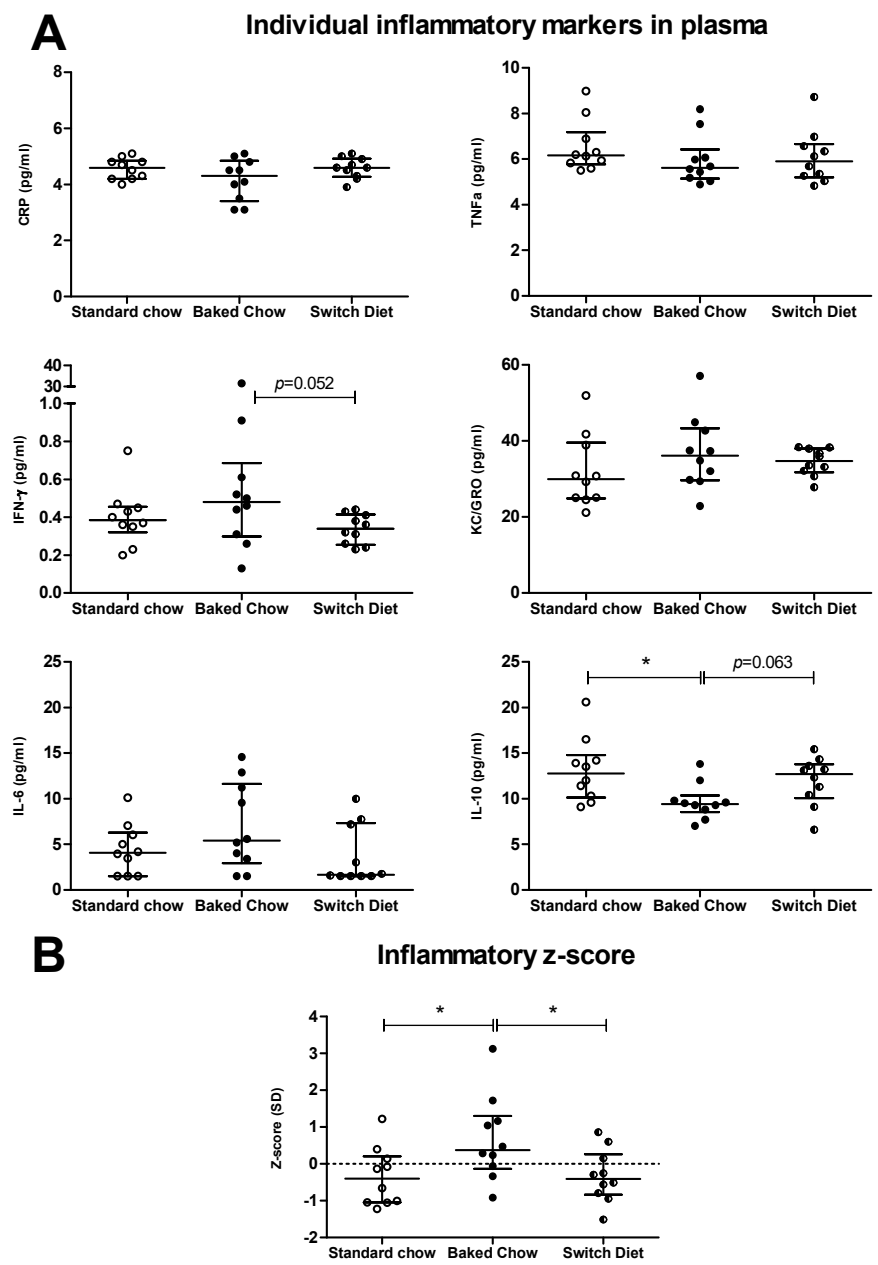**Figure 6.4** Inflammatory mediators in plasma of mice after 10 weeks of standard chow, baked chow, and the switch diet. A: individual inflammatory mediators. B: Inflammatory z-score consisting of TNF-α, IFN-γ, KC/GRO, IL-6, and IL-10. Center bars of scatter dots indicate median values while whiskers indicate inter quartile range. * indicates p < 0.05 for the difference between chow diets. N = 10 for all groups.

Gut microbial composition is altered after feeding a baked chow diet, and is reversible

Based on Bray-Curtis beta diversity dissimilarity distances, differences in overall microbial composition were shown in principal coordinate analysis (PCoA) plots from week 7.5 onwards (**Figure 6.5**). Where in week 5 almost all samples were still distributed over the four quadrants (Axis 1 = 23.2%, Axis 2 = 13.5%), in week 7.5 the fecal samples from the mice fed the baked chow diet almost all clustered together in the bottom left quadrant, while almost all fecal samples from the standard chow diet clustered together in the upper right quadrant (Axis 1 = 23.6%, Axis 2 = 12%). The fecal samples from the mice fed the switch diet were distributed over the two upper quadrants and were located in between the samples of the baked chow and the standard chow diet. In week 10 the fecal samples of the mice fed the baked chow and the standard chow diet again were distributed over opposite quadrants, while the samples of the mice fed the switch diet were located in between these two diet groups, as expected (Axis 1 = 26.2%, Axis 2 = 23%). It should be noted that in week 10 not all fecal pellets were collected for each group (n=6 for the baked chow group; n=4 for the standard chow group; n=2 for the switch group). Further PERMANOVA analysis revealed that the provided diet explained a statistically significant ($p < 0.001$) variation in microbial composition from week 5 onwards with 19.5% variance explained by the diet in week 5, 22.9% in week 7.5 and 35.2% in week 10. Bray-Curtis dissimilarities of week 0 and week 2.5 were not statistically significant. Their corresponding PCoA plots are shown in the supplementary materials (Supplementary materials **Figure S6.3**).
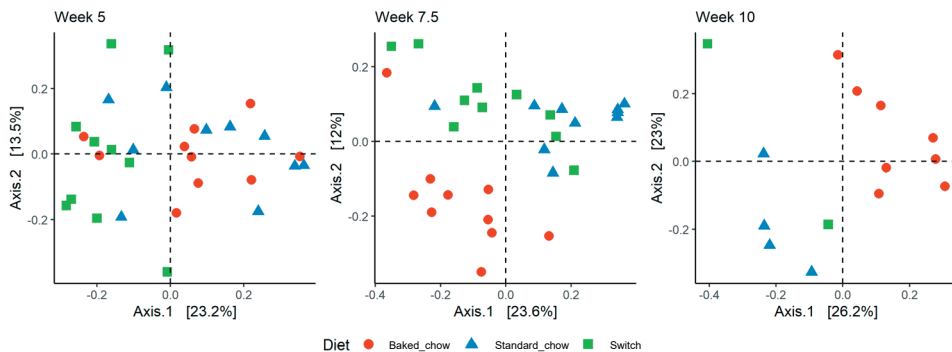
Figure 6.5 Principal coordinate analysis plots (PCoA) of Bray-Curtis' beta-diversity dissimilarities of the fecal pellets per week. Each data point represents one fecal pellet of an individual mouse and labelled per diet (red circles for baked chow diet; blue triangles for the standard chow diet; green squares for the switch diet).

Relative abundance composition plots both on phylum level and genus level per sampling week showed differences between the different diet groups (Supplementary materials **Figure S6.4**), especially at genus level. In order to identify taxa which contributed to observed differences in microbial composition between the diet groups as assessed with Bray-Curtis dissimilarities, LEfSe analysis of the microbiota composition was performed per sampling week from week 5 onwards. Differential abundant taxa were identified after comparing the microbial composition of the baked chow with the standard chow (**Figure 6.6**) and the switch with the standard chow (Supplementary materials **Figure S6.5**), and were visualized in

cladograms (circular phylogenetic trees). Comparing the baked chow with the standard chow revealed that at week 5, six genera (i.e. *Olsenella, Ruminococcaceae_UCG_009, Dubosiella, Turicibacter, Parasutterella* and *Akkermansia* with respective average relative abundances (%) of 0.7, 0.1, 3.6, 0.5 and 3.2) and four families (i.e. *Atopobiaceae, Erysipelotrichaceae, Burkholderiaceae, Akkermansiaceae*) were enriched after the baked chow diet and three genera (i.e. *Clostridiales_vadinBB60_group_uncultured, Roseburia* and *Faecalibaculum* with respective average relative abundances (%) of 0.1, 4.5 and 1.0) and one family (i.e. *Clostridiales_vadinBB60_group*) was enriched after consumption of standard chow. At week 7.5, twelve genera (i.e. *Bifidobacterium, Rikenella, Eubacterium_xylanophilium_group, Lachnoclostridium, Roseburia, Ruminiclostridium_5, Ruminococcaceae_uncultured, Ruminococcaceae_UCG_009, Ruminococcaceae_UCG_014, Dubosiella, Faecalibaculum, Desulfovibrio* with respective average relative abundances (%) of 0.2, 0.3, 0.1, 0.6, 1.5, 0.3, 1.1, 0.1, 0.3, 13.1, 0.2 and 1.7) and three families (i.e. *Bifidobacteriaceae, Erysipelotrichaceae* and *Desulfovibrionaceae*) were assigned as enriched taxa for the baked chow group, while for the standard chow diet five genera (i.e. *Bacteroides, Muribaculaeae_uncultured, Muribaculum, Lactobacillus* and *Marvinbryantia* with respective average relative abundances (%) of 1.2, 46.5, 1.2, 10.5 and 0.7) and four families (i.e. *Bacteroidaceae, Muribaculaceae, Lactobacillaea* and *Clostridiales_vadinBB60_group*) were enriched. The analysis performed at week 10 identified four genera (i.e. *Clostridium_sensu_stricto_1, Dubosiella, Turicibacter* and *Parasutterella* with respective average relative abundances (%) of 0.6, 26.2, 0.9 and 0.7) and three families (i.e. *Clostridiaceae_1, Erysipelotrichaceae* and *Burkholderiaceae*) to be enriched for the baked chow diet, while for the standard chow diet five genera (*i.e. Bacteroides, Lactobacillus, Lachnospiraceae_UCG_004, Oscillibacter* and *Ruminiclostridium* with respective average relative abundances (%) of 1.2, 22.5, 0.1, 0.4 and 0.7) and two families (*i.e. Bacteroidaceae, Lactobacillaceae*) were identified to be enriched.
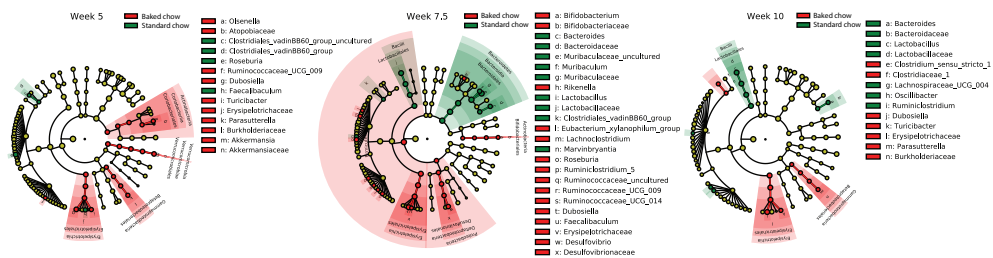
Figure 6.6 LEfSe results of the significant different taxa found by comparing the mice with the baked chow diet (red) to the standard chow diet (green), sampled in week 5 (n = 10 per group), 7.5 (n = 10 per group) and week 10 (baked chow: n = 6; standard chow: n = 4). Nomenclature was based on the highest achievable taxonomic resolution level. The alpha value was set to 0.05 and the log10 LDA score threshold to 2.0.

The microbiota of baked chow-fed mice was found to be consistently enriched in the genus *Dubosiella*, while that of mice fed the standard chow diet were enriched in *Lactobacillus* and *Bacteroides* from week 7.5 onwards. The highest number of identified taxa after LEfSe analysis were found in week 7.5 which could be explained by the fact that in week 10 not all fecal pellets were collected for each group (n=6 for the baked chow group; n=4 for the

chow group; n=2 for the switch group), while for week 7.5 fecal pellets from all mice (n=10 per group) were collected and subsequently analyzed for its microbial composition. LEfSe analysis of the switch diet with the standard chow diet (Supplementary materials **Figure S6.5**) resulted in the highest number of enriched taxa in week 5 which decreased to week 7.5 and further to week 10. In week 10 only three genera (i.e. *Dubosiella, Turicibacter* and *Ileibacterium* with respective average relative abundances (%) of 2.9, 3.7 and 12.4) were shown to be higher abundant in the switch diet. This indicates that the microbial composition as affected by the baked chow diet is a diet-dependent reversible change.

Gut microbiota composition data are associated with clinical parameters

To assess whether gut microbiota composition was associated with other measured outcomes (i.e. AGE plasma and tissue levels, inflammatory markers), Spearman's rank correlations were determined after 5 and 10 weeks for mice fed the baked chow and the standard chow diet (**Figure 6.7**). In week 5, the genera *Olsenella* and *Turicibacter* showed a statistically significant positive correlation with free plasma CML levels (*Olsenella*: $\rho=0.769$, $p = 0.008$; *Turicibacter*: $\rho=0.686$, $p = 0.030$) and CEL (*Olsenella*: $\rho=0.711$, $p = 0.024$; *Turicibacter*: $\rho=0.671$, $p = 0.031$). In week 10, no bacterial taxa were statistically significantly correlated with the other outcomes after correction for multiple testing, possibly due to less fecal pellets being collected at week 10. However, in week 10 several taxa showed a trend towards a high positive or negative correlation ($\rho>0.7$ or $\rho<-0.7$) with these outcomes. As such, *Dubosiella* showed a high positive correlation with free kidney CEL levels ($\rho=0.719$), *Lachnospiraceae* NK4A136 group with CRP levels in plasma ($\rho=0.709$), *Alloprevotella* with protein-bound MG-H1 in plasma ($\rho=0.755$), *Rikenellaceae* RC9 gut group with protein-bound MG-H1 levels in the kidney ($\rho=0.745$) and *Alistipes* with plasma CRP levels ($\rho=0.709$). On the other hand, *Rikenellaceae* RC9 gut group showed a high negative correlation with free CML in the liver ($\rho=-0.729$), *Muribaculaceae* uncultured bacterium with free CML and CEL in plasma ($\rho=-0.797$ and -0.825), protein-bound CML in plasma ($\rho=-0.755$), free CML in the liver ($\rho=-0.753$), and free CML and MG-H1 in the kidney ($\rho=-0.748$ and -0.783). *Muribaculum* showed high negative correlations with free CML and CEL in plasma, and free MG-H1 in plasma and kidney ($\rho=-0.797$, -0.825, -0.718, and -0.734, respectively).

Since not all fecal pellets were collected at week 10, an additional Spearman's rank correlation analysis was performed using the microbial composition data of week 7.5 with other measured outcomes determined at week 10 (Supplementary materials **Figure S6.6**). This revealed multiple statistically significant correlations. *Dubosiella* showed a positive correlation with free MG-H1 in liver ($\rho=0.754$, $p = 0.018$), free CML in liver ($\rho=0.683$, $p =0.078$), protein-bound CML in plasma ($\rho=0.796$, $p =0.014$) and free CEL in kidney ($\rho=0.771$, $p =0.014$). *Desulfovibrio* showed a positive correlation with free MG-H1 levels in the liver ($\rho=0.667$, $p =0.098$). On the other hand, *Muribaculum* showed a negative correlation with free MG-H1 both in liver ($\rho=-0.777$, $p =0.014$) and kidney ($\rho=-0.715$, $p =0.040$). *Marvinbryantia* showed a negative correlation with protein-bound CEL in plasma ($\rho=-0.744$, $p =0.021$). Although statistically significant results differed between Spearman's rank correlations using microbiota composition data from week 7.5 or week 10, the overall trend in found correlations was comparable.

Bacteroides and *Lactobacillus* showed a time-dependent increase from week 5 to week 10 towards negative correlations with free and protein-bound AGE levels in plasma and tissues, while *Dubosiella* showed a time-dependent increase towards positive correlations with free and protein-bound AGE levels in plasma and tissues. These results are in line with the taxa identified in the LEfSe analysis.
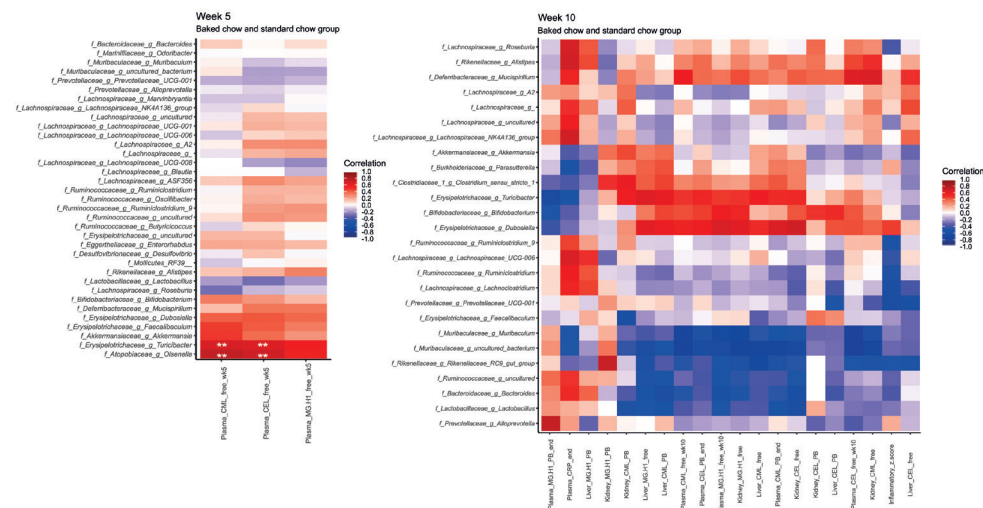

Figure 6.7 Heatmaps of Spearman's rank correlation coefficient of relative abundance microbial composition data with relevant clinical parameters per sampling week, of mice in the baked chow and standard chow group. Bacterial taxa with a relative abundance >1% in one of the samples were included. Statistically significant correlations after adjustment for multiple testing are marked with * (p < 0.1) or ** (p < 0.05). Nomenclature was based on the highest achievable taxonomic resolution level. pb: protein-bound.

6.4. Discussion

Here, we show that consumption of a baked diet containing high levels of AGEs leads to an increase of AGEs in plasma, kidney, and liver and to a reduction of circulating IL-10 in addition to changes in gut microbiota composition in young mice. These effects were reversible or discontinued by switching the high AGE diet to a diet with lower levels of AGEs. AGEs are generated in foods during various preparation methods involving dry heat, such as baking, grilling, frying, and toasting. Indeed, we saw a marked increase of the AGEs CML, CEL and MG-H1 after the baking of chow diet at 160 °C for two hours. Although food intake was lower in mice receiving the baked chow diet in comparison to the standard chow diet, total AGE intake was still increased in mice fed the baked chow diet. In line with this, free CML, CEL, and MG-H1 in plasma were higher in mice receiving the baked chow diet compared to mice receiving the standard chow diet. Although both free (CEL and MG-H1) and protein-bound (CML, CEL, and MG-H1) AGEs were increased in chow diets after baking, the uptake of dietary AGEs into the circulation is likely to depend mainly on digestion and absorption of protein-bound AGEs. It was previously shown that absorption of AGEs *in vitro* takes place

mainly in the form of dipeptides, instead of free amino acid AGEs[35]. In addition, levels of protein-bound AGEs in baked chow were approximately 30-80 fold higher than levels of free AGEs. In line with this, the increase in free plasma CML after the baked chow diet occurred in absence of an increase in free CML in baked chow.

Surprisingly, protein-bound CML and CEL in plasma were also higher, while protein-bound MG-H1 was lower in mice receiving the baked chow diet compared to mice receiving the standard chow diet. As such, we would not expect a direct increase in plasma protein-bound AGEs following the high AGE baked chow diet. This would be in line with our previous data in humans showing that the free form of AGEs in plasma, but not the protein-bound form, is associated with dietary AGE intake in participants of the CODAM study[26]. However, randomized controlled trials (RCTs) in humans are still inconclusive as there are reports of both an increase in protein-bound AGEs in plasma[22] and no change[307] after a high-AGE diet. This distinction is important, as the origin of both forms of AGEs is different, and it has implications for their biological effects, for example as free AGEs do not have affinity for the receptor for AGEs (RAGE)[49,308,309].

We also observed some surprising findings in organs of mice fed the baked chow diet. While we observed higher levels of most free AGEs in liver and kidney in these mice, we also observed higher protein-bound CML in kidney. Direct evidence for dietary AGE accumulation in organs is already available in animal models, but free- and protein-bound AGEs have not been assessed simultaneously[30,293,310,311]. Tessier et al. used ^{13}C-labeled CML to discriminate between dietary and endogenous CML and found that dietary CML accumulated in several organs of mice, but they could not discriminate between free and protein-bound CML due to low quantities of tissue being available[293]. The increase in protein-bound CML and CEL in plasma and protein-bound CML in kidney of mice fed the baked chow diet in the present study could be the result from indirect effects of dietary AGEs. It has previously been shown that dietary CML and MGO-modified albumin lead to significant increases of NF-κB and RAGE in kidneys of piglets and white adipose tissue respectively[311,312]. As such, protein-bound AGEs in plasma and tissues may reflect increased endogenous formation of AGEs, and not a direct uptake of dietary AGEs. In addition, we also measured reactive precursors of AGEs in the chow diet, which were increased upon heating. The increased levels of these reactive oxoaldehydes in baked chow diet may give rise to increased endogenous levels of protein-bound AGEs.

In line with the increase in AGEs in plasma and tissue, we observed reduced levels of circulating IL-10 in mice fed the baked chow diet as compared to mice fed the standard chow diet. Also driven by this, the inflammatory z-score was significantly higher after the baked chow diet compared to the standard chow diet. In line with our findings, Rajan et al. observed a significant increase in expression of several pro-inflammatory cytokines in 12-week old mice after a 6-month dietary intervention with baked chow diet[313] and Mastrocola et al. also observed a decrease in IL-10 after feeding a high AGE diet for 22 weeks in 4-week old mice[298]. Although with the current data we cannot provide insights in the origin of increased inflammation following the baked chow diet, the increase in protein-bound CML in kidney is suggestive of involvement of the kidneys. Future studies could provide insight in a potential direct link between increased protein-bound levels in a specific tissue with the

origin of observed inflammation. Nonetheless, the increase in inflammation after the baked chow diet may provide some insight into the mechanisms behind the biological effects of dietary AGEs. Circulating IL-10 levels are lower in obese insulin resistant individuals and treatment with IL-10 improves lipid-induced insulin resistance[314]. As such, the decrease in circulating IL-10 after the baked chow diet could potentially contribute to the decrease in insulin sensitivity observed in humans after a high-AGE diet[307]. However, in humans, the increase in inflammation after a high-AGE diet is observed in some RCTs[315] but not all[16] and deserves further investigation.

To our knowledge, we are the first to show that the accumulation of AGEs in plasma and organs after a diet high in dietary AGEs is reversible. We showed that most AGEs in plasma, kidney, and liver were already increased after 5 weeks of the baked chow diet and that this accumulation of AGEs is fully reversible, by switching the diet to standard chow for 5 subsequent weeks. Although reversibility may be expected for AGEs in plasma, as they are rapidly cleared by the kidneys[316], the latter does not necessarily apply to dietary AGEs accumulating in organs. We can currently only speculate on how dietary AGEs are transported into organs, if they end up in the intra- or extracellular matrix, and if glycated proteins (i.e. protein-bound AGEs) show different protein turnover rates. For example, the extracellular space is less subjected to protein turnover[317]. Additionally, glycated proteins in food have been reported in some studies to show resistance to enzymatic breakdown in the gastrointestinal tract[318] and this could also potentially apply to enzymatic protein turnover. Inflammation, on the other hand, was not already increased after 5 weeks of the baked chow diet. Although mice fed the switch diet showed decreased inflammation compared to mice fed the baked chow diet for 10 weeks, we cannot speak of true reversibility. Nonetheless, dietary AGEs have been associated with negative biological effects in humans[294], but also several negative clinical outcomes, such as insulin resistance[307], weight gain[319], and vertebral fractures[320]. Therefore, the important finding of reversibility of AGE accumulation in plasma and organs may have beneficial implications for those whom ingest a diet high in AGEs to lower the dietary AGE-associated negative biological effects and clinical outcomes. Furthermore, the observation of reversible AGE accumulation after modulation of dietary AGEs also further strengthens their causal link.

Next to effects of baked chow diets on AGE levels in plasma and tissues and inflammatory markers, the baked chow diet also altered the gut microbiota composition of mice compared to the standard chow diet. From week 5 onwards significant effects of the baked chow diet on the gut microbiota composition were observed by assessing Bray-Curtis dissimilarities. Interestingly, statistically significant effects on gut microbiota composition were earlier observed (i.e. week 5) compared to effects on the inflammatory z-score and IL-10 levels in plasma (i.e. week 10). In the baked chow group, the genus *Dubosiella* was consistent enriched. *Dubosiella* was recently isolated from mice[321], and has not been associated with specific functions before. However, *Dubosiella* belongs to the family *Erysipelotrichaceae* and was found to be related to *Allobaculum stercoricanis*[321]. The genus *Allobaculum spp*. was increased in relative abundance in two animal studies after a glycated or high AGE diet[211,297], which might imply a specific genera-cluster or family as a potential target for a high AGE diet. Interestingly, this does not corroborate with previous findings by Yang et al. (2020) who found an enrichment in the order *Erysipelotrichales* after the control diet instead of

the high AGE diet. However, no specific genus was identified and it is relevant to note that old mice (15-month-old) were studied[299]. On the other hand, *Lactobacillus* and *Bacteroides* were consistent enriched in the standard chow group, corresponding to a relative decrease in the baked chow group, which corroborates partially or fully with earlier findings showing a contraction in *Lactobacillus spp.* or *Bacteroides spp.*[208,210,296–298,322]. However, not all animal studies found this contraction in *Lactobacillus spp.* or *Bacteroides spp.*[299], indicating the need for multiple studies to derive clear and consistent conclusions regarding effects on gut microbiota composition.

In week 5, the genera *Olsenella* and *Turicibacter* showed a positive statistically significant correlation with free CML and CEL in plasma, while in week 10 no statistically significant correlations were found after correction for multiple testing. This could be explained by the higher number of parameters involved in the correlations of week 10 compared to week 5. Overall, *Dubosiella* showed high correlations with most parameters measured at week 10, and was included in statistical significant positive correlations when applying microbiota composition data from week 7.5 instead of week 10. Our data suggests that *Dubosiella spp.* are associated with a diet high in AGE levels. However, further work is required to identify the function or role of *Dubosiella spp.* in order to explain this link with AGEs. A hypothesized explanation of the enrichment of *Dubosiella spp.* in the baked chow diet group is the utilization of AGEs as a substrate by the bacterium. Multiple bacterial strains were reported in literature to degrade CML. For example *Cloacibacillus evryvenis*[323], isolated from human feces, and *Escherichia coli* strains[324] were shown to degrade CML *in vitro*, which proves the ability of specific gut bacteria to utilize an AGE.

An attempt was made to investigate whether the effects of the baked chow diet on gut microbial composition were reversible by including the switch diet group. The results of both the Bray-Curtis dissimilarities and LEfSe analysis indicated that the trend of changing microbiota composition due to the baked chow diet is reversible. In week 10, LEfSe analysis identified 3 genera (i.e. *Dubosiella, Turicibacter* and *Ileibacterium*) to be enriched in the switch diet group. These findings suggest that minor differences in microbiota composition between the standard chow and the switch diet were still observed, which can be explained by the fact that the gut microbiota requires time to adapt towards a new diet composition. It could be that a 5-week dietary intervention of the standard chow diet after 5 weeks of the baked chow diet was too short to completely adapt and consequently forming a comparable microbiota composition as in the 10-week standard chow diet group.

Our study has several strengths. Protein-bound and free AGEs were measured both in the chow diets as well as in plasma and organs of mice with the highly specific gold standard UPLC-MS/MS technique. To our knowledge, we are the first to concurrently measure both forms of AGEs in both the experimental diet and tissue compartments. In addition, the validity of our findings is increased by inclusion of a control group and the switch group. Also, inclusion of the switch group enables us to show that changes in AGE accumulation following a high AGE diet are reversible in nature. Moreover, it is important to highlight that the chow baking conditions were not substantially different from the conditions used

in other studies, and while AGE levels in the baked chow diet were increased, they still represented realistic dietary levels. Finally, we used very young, healthy mice without any underlying disease.

Our study also has several limitations. Primarily, we cannot rule out that the baking procedure has had effects on chow other than increasing AGEs, such as decreasing vitamin bioavailability or increasing acrylamide formation. Additionally, mice weighed less at the end of the study after the baked chow diet compared to the standard chow diet, and food intake was lower of mice in the baked chow diet group. However, percentual increase of weight did not differ between groups, and in addition bacterial taxa associated with weight loss, such as *Allobaculum*[325] or *Akkermansia muciniphila*[326], were not showing a similar trend towards lower weight in the baked chow diet group. If anything, lower food intake in the baked chow group reduced exposure to dietary AGEs and lead to underestimations of their effects. Finally, our observations of reversible AGE accumulation in kidney and liver may not be extrapolated to other organs. Likewise, our findings in mice cannot be directly extrapolated to humans, as species differences exist in for example metabolic rate and dietary habits, as also in gut microbiota composition[327].

In summary, intake of dietary AGEs results in reversible elevated levels of AGEs in plasma and organs and alterations in the gut microbiota composition with a change in the inflammatory profile of healthy young mice. Randomized controlled trials on the effects of dietary AGEs on gut microbiota in humans are needed.

6

Acknowledgements

6.5 Supplementary materials
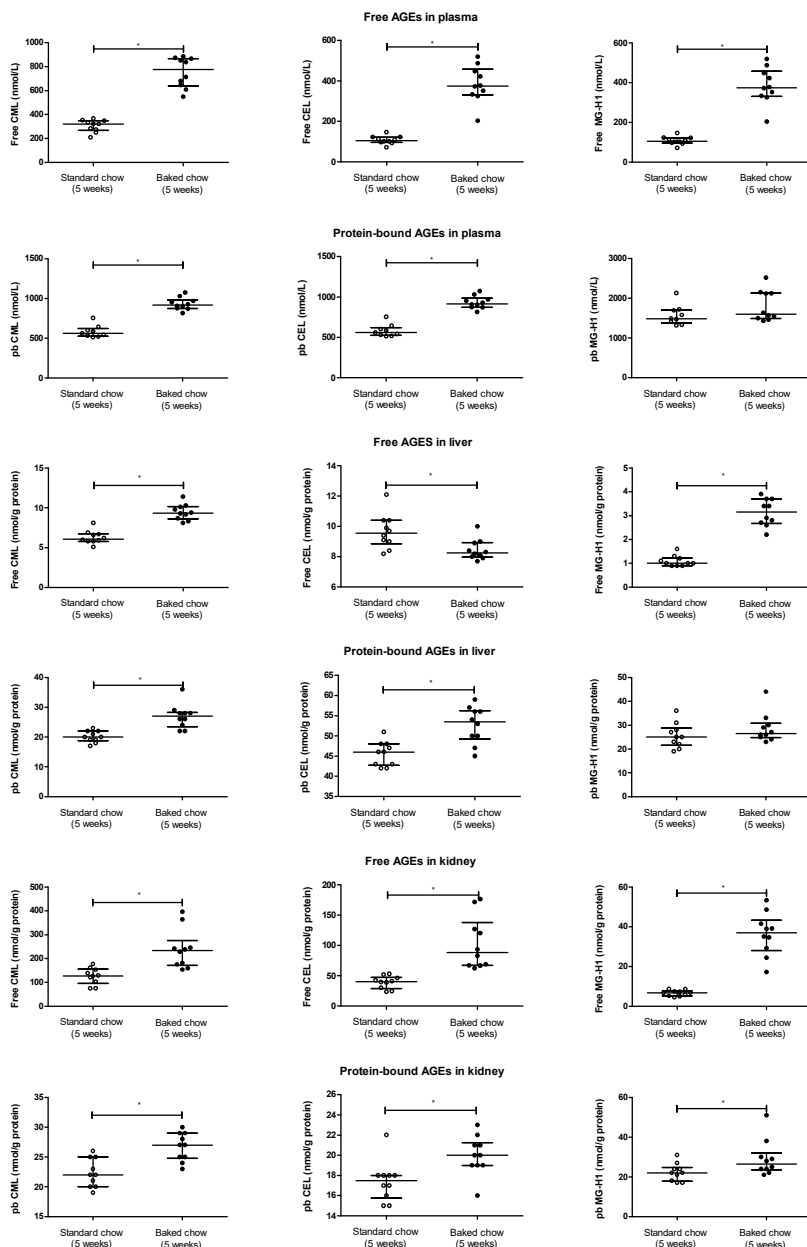
Figure S6.1 Free and protein-bound AGEs in plasma, kidney and liver of mice after 5 weeks of the standard chow diet or baked chow diet. CML: Nᵉ-(carboxymethyl)lysine. CEL: Nᵉ-(1-carboxyethyl)lysine. MG-H1: Nᵟ-(5-hydro-5-methyl-4-imidazolon-2-yl)-ornithine. pb: protein-bound. Center bars of scatter dots indicate median values while whiskers indicate inter quartile range. * indicates p<0.05 for the difference between chow diets. n = 10 for both groups, except for plasma protein-bound AGEs in the standard chow group, where n = 9.
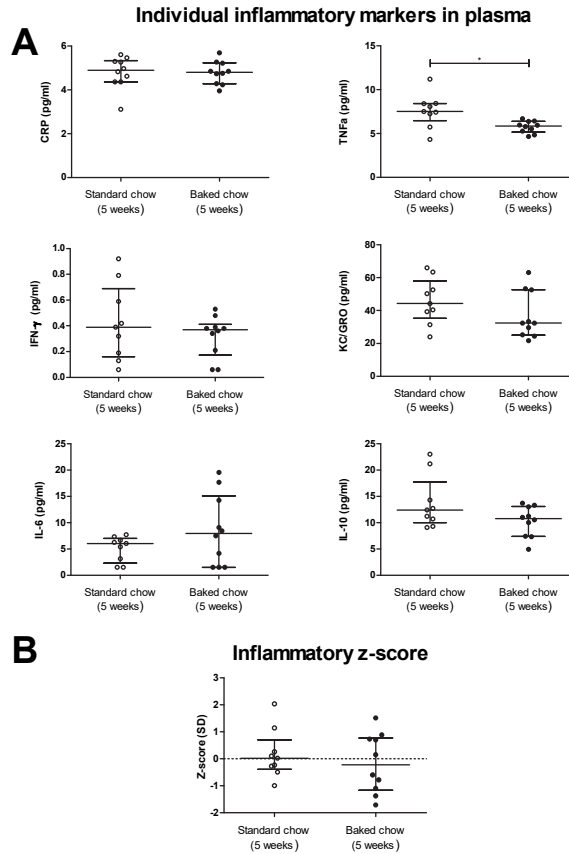
Figure S6.2 Inflammatory mediators in plasma of mice after 5 weeks of standard chow or baked chow. **A:** individual inflammatory mediators. **B:** Inflammatory z-score consisting of TNF-α, IFN-γ, KC/GRO, IL-6, and IL-10. Center bars of scatter dots indicate median values while whiskers indicate inter quartile range. * indicates p<0.05 difference between chow diets. N = 9 for the standard chow group, n = 10 for the baked chow group.
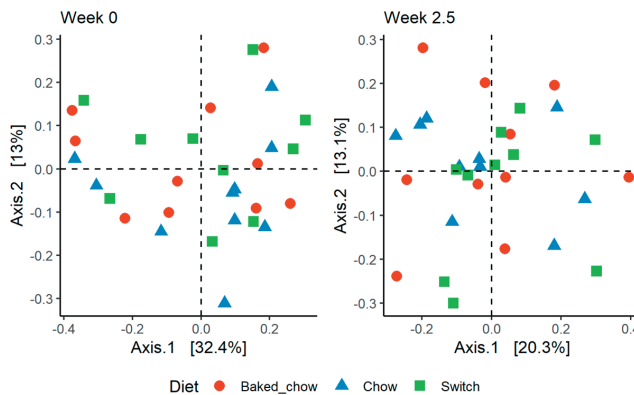
Figure S6.3 Principal coordinate plots (PCoA) of Bray-Curtis' beta diversity dissimilarities of the fecal pellets for week 0 and week 2.5. Each data point represents one fecal pellet of an individual mouse and labelled per diet (red circles for baked chow diet; blue triangles for the standard chow diet; green squares for the switch diet).
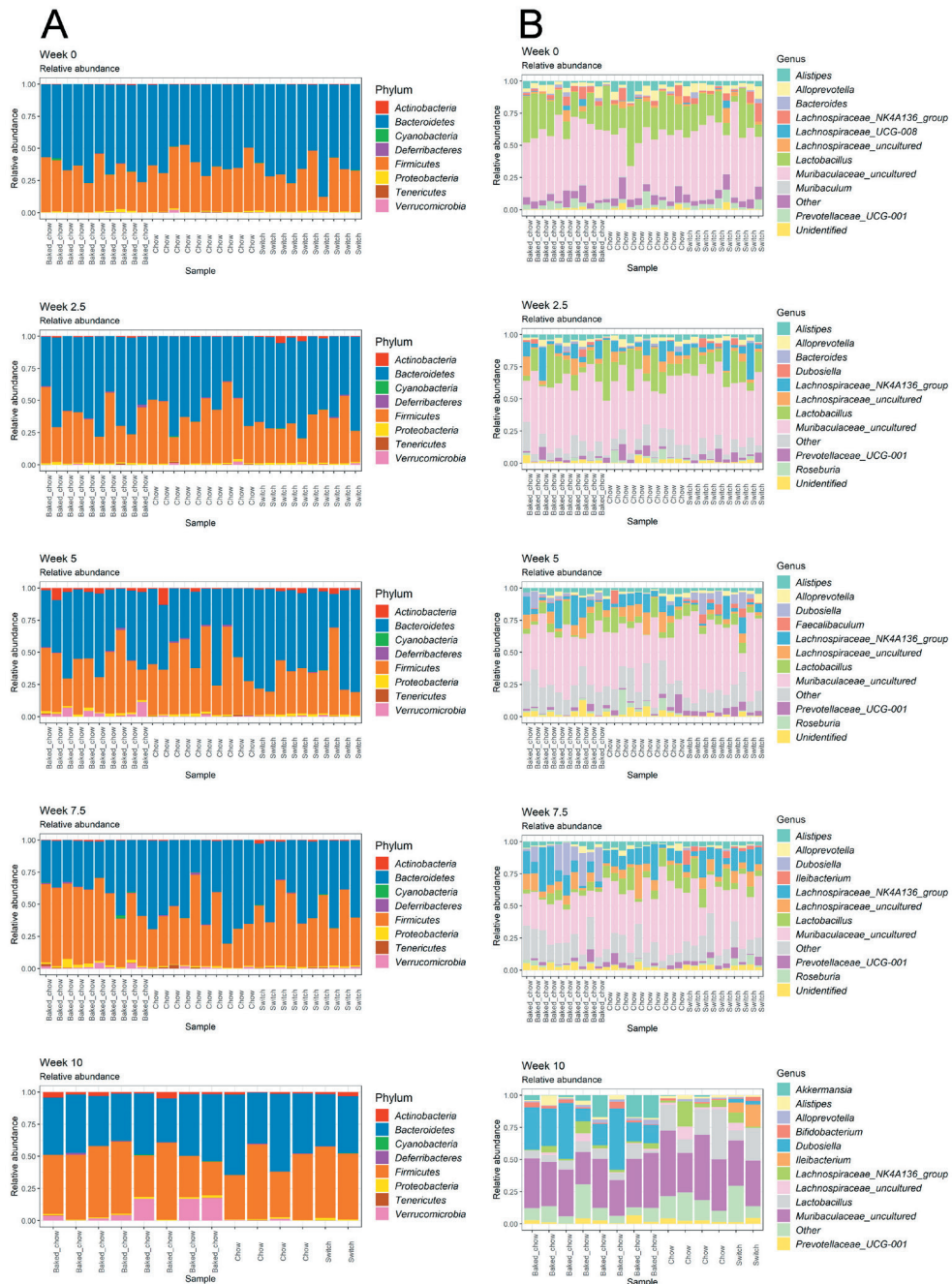
Figure S6.4 Bacterial composition plots with the relative abundance of the top 11 taxa at phylum (panel A) and genus level (panel B) of each sampling week; taxa are labelled as "other" refer to taxa not present in this top 11. The x-axis represents the mice sampled per diet group (baked chow diet; standard chow diet; switch diet).
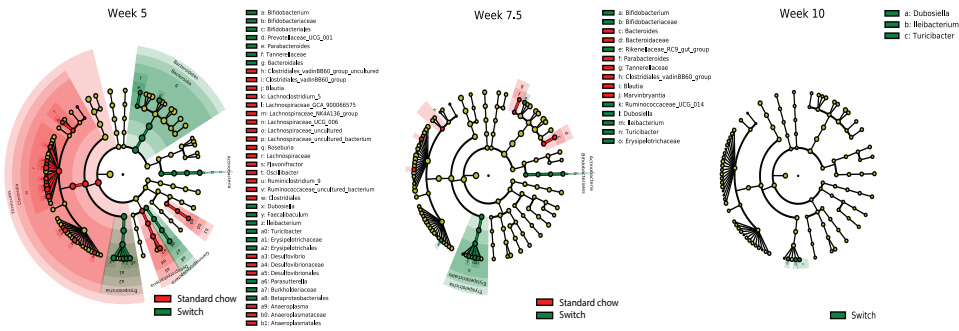
Figure S6.5 LEfSe results of the significant taxa found by comparing the mice with the switch diet (red) to the standard chow diet (green), sampled in week 5, 7.5 and 10. Nomenclature was based on the highest achievable taxonomic resolution level. The alpha value was set to 0.05 and the log10 LDA score threshold to 2.0.
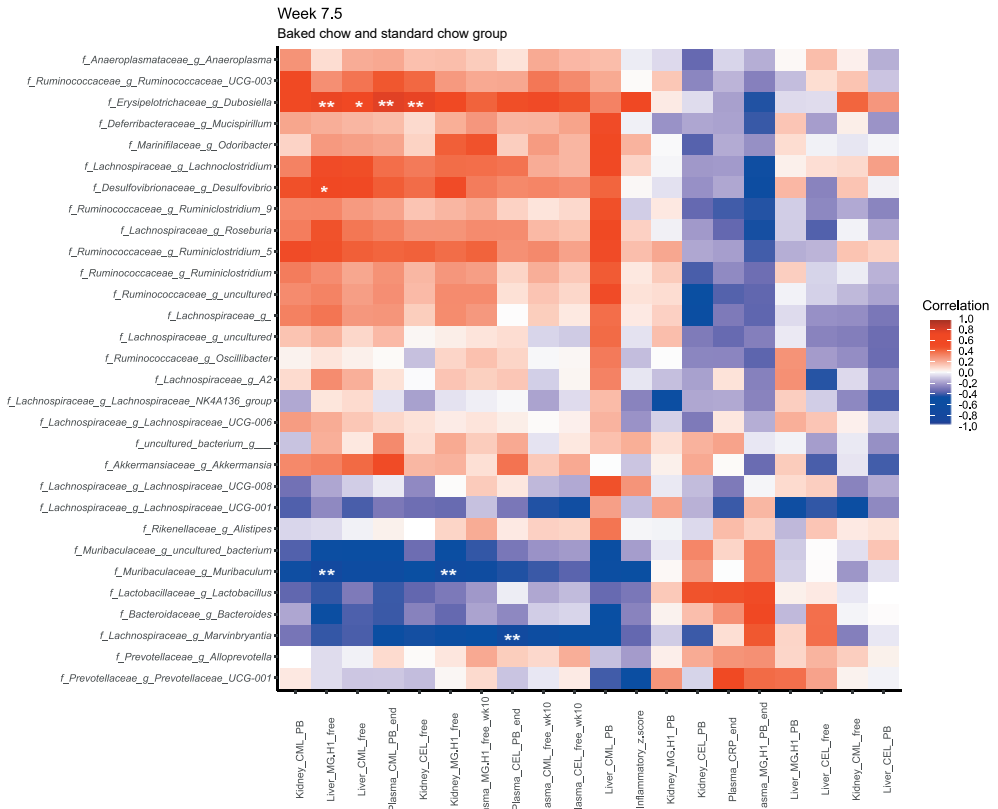
Figure S6.6 Heatmap of Spearman's rank correlation coefficient of relative abundance microbial composition data of week 7.5 with relevant clinical parameters measured at week 10, of mice in the baked chow and standard chow group. Bacterial taxa with a relative abundance >1% in one of the samples were included. Statistically significant correlations after adjustment for multiple testing are marked with * (p<0.1) or ** (p<0.05). pb: protein-bound.
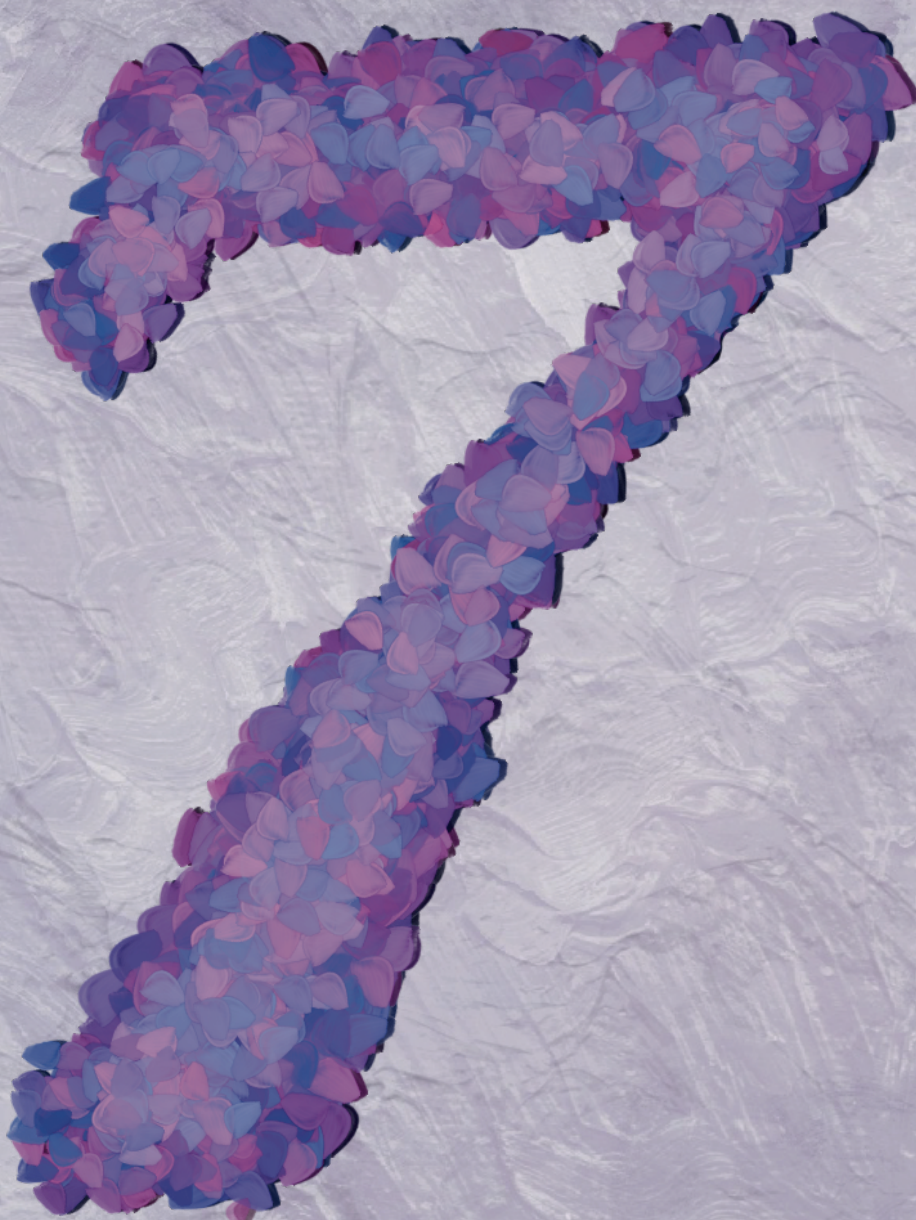
General discussion

7.1 Overview of the results and main findings

Glycation products comprise advanced glycation end products (AGEs) and their precursors such as the Amadori product fructoselysine, and are a heterogenous group of compounds formed non-enzymatically upon heating of food products in a reaction between amino-acid residues and reducing sugars, or via reactive dicarbonyls, as described in **Chapter 1**. As such, high levels of especially protein-bound AGEs and free AGEs and their precursors can be found in food products, often derived from lysine and arginine residues. Upon ingestion part of the dietary low molecular mass (LMM) free AGEs or precursors can be taken up and enter the systemic circulation, while another fraction can reach the colon and interact with gut microbiota. High molecular mass (HMM) protein-bound AGEs and precursors are not easily or not at all taken up by intestinal cells and they probably do not directly contribute to plasma levels of protein-bound AGEs[108]. After ingestion, they are digested in the intestinal tract, releasing among others LMM AGEs and precursors, or reach the colon where they can also interact with the gut microbiota. Besides arising from exposure to dietary glycation products (called exogenous exposure as they are formed outside the body), glycation products can also be formed inside the body (called endogenous exposure). While following the same pathways of formation as exogenous glycation products, formation of endogenous glycation products is slower due to the lower (physiological) temperatures. Adverse health effects have been associated with the presence of AGEs inside the body[23–25], however, the contribution of exogenous glycation products to the level of endogenously detected AGEs and the accompanying effects on health are debated as further discussed in Section **7.2.1** below. In **Chapter 2** of the thesis an overview of the similarities and differences of exogenous and endogenous AGEs and their precursors, both in their kinetics as well as their potential role in induction of adverse health effects is presented. The distinction between LMM glycation products, HMM glycation products and the dicarbonyl precursors was emphasized as they differ in their toxicokinetic and toxicodynamic properties. Indeed, the bioavailability of exogenous LMM AGEs and their precursors, and possibly the reactive dicarbonyl precursors, seems to be higher than the bioavailability of HMM AGEs, of which the bioavailability appears to be limited. Yet, especially the HMM AGEs seem to activate the AGE receptor (RAGE), which is considered to be the first step in a relevant mode of action, inducing inflammation and oxidative stress that appear to underly at least some of the adverse health effects associated with AGEs[12]. LMM AGEs and precursors do not seem to bind to RAGE, but can possibly contribute to endogenous HMM AGE formation. Furthermore, LMM AGEs and their precursors appear to be cleared from the systemic circulation by urinary excretion, leading to a debate on their contribution to the adverse health effects. Unabsorbed exogenous LMM AGEs and precursors and exogenous HMM AGEs -possibly partly cleaved into LMM AGEs in the upper intestinal tract- are hypothesized to possibly induce local effects on the intestinal tissues (e.g. intestinal barrier integrity) and interact with the gut microbiota. This can result in the alteration of microbial composition which can possibly underly associated adverse health effects, although causal relations remain to be established as further discussed in Section **7.2.3** below. On the other hand, the gut microbiota itself can also contribute to metabolism of AGEs and precursors and degrade these exogenous compounds.

To gain insight in the metabolism of glycation products by the gut microbiota, an *in vitro* model with human fecal slurries was optimized in **Chapter 3**. Using this model, the Michaelis-Menten kinetic parameters (i.e. V_{max}, K_m and kcat) for gut microbial degradation of the LMM precursor fructoselysine were determined for 16 individuals. Fructoselysine is an Amadori product formed from glucose and lysine and is a key intermediate in the formation of the AGE carboxymethyllysine. The results showed that in the population of donors of fecal samples, there are microbial non-metabolizers and microbial metabolizers of fructoselysine, with the microbial metabolizers showing interindividual differences in the kinetic parameters. These interindividual differences can contribute to overall differences in ADME (absorption, distribution, metabolism and excretion)-characteristics of fructoselysine. The amount of degraded fructoselysine was associated with formation of the short chain fatty acid (SCFA) butyrate, which is considered a beneficial bacterial metabolite for intestinal and human health. Multiple bacterial taxa were positively correlated with fructoselysine degradation which raised the question whether genes involved in bacterial fructoselysine degradation are widespread amongst different taxa, which is amongst others further investigated in **Chapter 5**. Overall, the *in vitro* model is considered suitable to study gut microbial degradation of fructoselysine and interindividual differences therein, as further discussed in Section **7.2.2** below, and was used for further studies described in this thesis.

Besides interindividual differences in composition[67] and specific metabolic activities of the gut microbiota[64], temporal variability and thus intraindividual differences are also inherent to the dynamic aspects of the gut microbiota[328]. In **Chapter 4** it was investigated whether, in addition to interindividual differences, these intraindividual differences are also evident for microbial degradation of fructoselysine, as well as for the LMM AGE carboxymethyllysine. Carboxymethyllysine can be formed by rearrangement of fructoselysine or by reaction of the dicarbonyls glyoxal or 3-deoxyglucosone with lysine residues. 20 Individuals donated a fecal sample of which 13 individuals donated two additional fecal samples (with an interval of ≥3 weeks between sampling times), enabling the quantification of temporal variability. Pronounced interindividual and intraindividual differences were found for both fructoselysine and carboxymethyllysine degradation, representative for the challenging dynamic properties of the gut microbiota, as further discussed in Section **7.2.4** below. In addition, the average capacity to microbially degrade fructoselysine compared to carboxymethyllysine was much higher (27.7-fold) and the capacities were not correlated, showing the need for toxicokinetic data of individual AGEs and precursors as probably different pathways and bacteria govern the metabolism. Indeed, also for the results obtained in **Chapter 4**, multiple bacteria were positively correlated with the ability of an individual to degrade carboxymethyllysine and/or fructoselysine (e.g. *Akkermansia spp.* and *Alistipes spp.*) of which causal relations remain to be established as further discussed in Section **7.2.3** below. The results of this study further showed that average degradation capacities of both fructoselysine and carboxymethyllysine would be sufficient to completely degrade amounts consumed upon exposure at the level of the estimated daily intake (EDI). The data obtained in this chapter described inter- and intraindividual differences in microbial degradation of a foodborne AGE and its precursor and will be further discussed in Sections **7.2.2** and **7.2.4**.

It was hypothesized that the differences in average degradation capacities between fructoselysine and carboxymethyllysine as well as the observed inter- and intraindividual

differences might be a result of microbial adaptation to dietary exposure. To gain more insight in the effect of dietary exposure on specific gut microbial activities, the capacity to degrade fructoselysine of fecal samples collected from breast-fed (BF) and formula-fed (FF) infants was compared in **Chapter 5**. Breast milk generally contains no or only minute amounts of fructoselysine, unlike infant formula which contains high levels of fructoselysine due to the heating applied during production procedures[87]. First, fructoselysine degradation capacities were compared between the two feeding groups by searching for genes involved in fructoselysine degradation (i.e. frlD and yhfQ) in the metagenome assembled genomes (MAGs) of a publicly available dataset including data for fecal samples of both BF and FF infants[61,281]. The query genes linked to fructoselysine degradation were found in both the BF and FF infants and were redundant in multiple bacterial species, implying a widespread presence of these genes. However, in FF infants the prevalence of the involved genes (frlD/yhfQ) was higher compared to the BF infants. Further, bacterial taxonomic profiling of additional infant fecal samples collected from both exclusively BF and exclusively FF infants revealed no significant differences in overall bacterial composition between the two feeding groups. Nevertheless, anaerobic incubations with the collected infant fecal slurries revealed that samples from FF infants degraded higher amounts of fructoselysine compared to samples from BF infants. Together this shows that, at least for fructoselysine, the infant gut microbiota seems to be able to adapt towards environmental exposures, in this case the diet. This links again to the dynamic aspects of the gut microbiota as further discussed in Sections **7.2.4** and **7.2.5** below.

This dynamic aspect of the gut microbiota was also observed in **Chapter 6** where mice were exposed to a baked chow (shown to be higher in the AGEs carboxymethyllysine, carboxyethyllysine and MG-H1, especially in their HMM form) or a standard chow up to 10 weeks. Bacterial composition was assessed in the collected fecal samples at multiple time points, which showed significant differences between different feeding regimens. Especially *Dubosiella spp.* was increased in the baked chow group. In the switch group (i.e. 5 weeks of baked chow diet followed by 5 weeks of the standard chow diet) these differences in bacterial composition seemed to be reversible, as the baked chow diet affected bacterial composition but –at least in this study– this seemed to be reversed when returning to the standard chow diet. This seems to illustrate a bacterial adaptation to the diet. Whether this altered gut microbiota composition can have consequences for host health remains to be established, as further discussed in Sections **7.2.3** and **7.2.5** below. Another important finding of this study was that the three analyzed AGEs (i.e. carboxymethyllysine, carboxyethyllysine and MG-H1) accumulated in plasma (both in their free and protein-bound form), liver (mainly in their free from) and kidney (both in their free and protein-bound form). These levels returned to levels comparable to the controls upon returning to the standard chow diet. This indicates that accumulation of these AGEs due to dietary exposure might be reversible upon returning to a diet lower in AGEs, at least in mice, which is possibly relevant for adverse health effects due to dietary exposure.

Overall, the research presented in this PhD thesis provided novel insights but also raised several items, which deserve further discussion as presented in the following sections.

7.2 General discussion and future perspectives

In this section, the research conducted in this thesis will be discussed and placed in a wider perspective. First of all, in Section **7.2.1** research considering the effects of dietary AGEs and their precursors on human health will be discussed, how literature data can be interpreted and that exogenous AGE exposure needs to be evaluated relative to endogenous AGE production. In Section **7.2.2** the applied *in vitro* model using human anaerobic fecal incubations is discussed. The use of fecal samples, the applicability domain of the model and how to extrapolate the obtained *in vitro* data to the *in vivo* situation deserves further attention. In this thesis, associations between microbiota composition and other outcomes were made. The use of these associations and how to move to a causal relation is discussed in Section **7.2.3**. In general, the research conducted in this thesis touches upon several aspects of dietary and gut microbiological research, such as the dynamic aspects of the gut microbiota, which will be discussed from a toxicological perspective in Section **7.2.4**. Finally, in Section **7.2.5**, future research perspectives covering dietary glycation product research related to human health are presented.

7.2.1 Effects of dietary glycation products on human health

Multiple studies report increased AGE levels in plasma and/or tissues upon increased exposure to dietary AGEs and their precursors[26,27,125] and multiple adverse health effects have been reported to be induced by or associated with intake of exogenous and/or increased levels of endogenous AGEs, including e.g. cardiovascular diseases[16], diabetes[17], effects on gut microbiota composition[19,20] and on the intestine[18]. However, there is no general consensus on whether dietary AGEs and their precursors contribute to these adverse health effects. This can be partially attributed to difficulties in characterization of the glycation products and resulting exposure in available human and animal studies, which complicates the interpretation of reported results. Another important reason for the lack of consensus is that -besides being present in foods- AGEs and their precursors can also be formed endogenously (i.e. inside the human body), which makes it a challenge to distinguish between effects attributed to exogenous or endogenous glycation products. These aspects were already addressed to some extent in **Chapter 2** and will be further discussed in this section.

Characterization of glycation products
First of all, it needs to be considered that glycation products are a heterogenous group of compounds which include AGEs and precursors such as the Amadori product fructoselysine, and thus can have different toxicokinetic properties (as also shown in **Chapters 2**, **4** and **6**) and probably also different toxicodynamic properties (as also presented in **Chapter 2**). Accordingly, it is important to properly characterize the glycation products to which study objects are exposed. This can be achieved by use of LC-MS/MS techniques. However, in many studies (in humans, animals and *in vitro*) unspecific methods are used such as for example ELISA (enzyme-linked immunosorbent assay) assays, where one antibody is used to measure the heterogenous group of AGEs while the recognized epitopes often remain unknown[10], or methods based on immunofluorescence while not all glycation products exhibit fluorescence properties[329]. Often a sum measure to quantify AGEs (i.e. 'total AGE content') is used, often using one AGE as surrogate for all, such as carboxymethyllysine,

instead of chemically characterizing individual AGEs and their precursors[10]. In addition, no distinction is made between LMM and HMM glycation products with these methods, while they have different toxicokinetic and toxicodynamic properties as also evaluated in **Chapter 2**. Individual characterization of the different types of glycation products is important to adequately characterize exposure via the diet or to characterize the endogenous levels in biological matrices (i.e. AGE levels in plasma and other biological fluids, tissue homogenates and secretions). Since in many studies this has not been done, the reported results are difficult to interpret. Specific chemical analytical methods such as targeted LC-MS/MS approaches, combined with sample preparation to liberate the HMM AGEs and precursors (e.g. hydrolysis, enzymatic digestion), can characterize individual glycation products[8]. This method is currently the state-of-the-art to use[10], and is useful for known AGEs and precursors. Considering the heterogeneity of the glycation products and the presence of probably many unknowns, other untargeted analytical techniques can be of possible use as further discussed in section **7.2.5** below.

Dietary exposure to AGEs and their precursors in human and animal studies
Another source of uncertainty can be found in the exposure conditions themselves. Especially in human trials but also in e.g. rodent studies (as in **Chapter 6**), a heated diet is often used as a source of dietary AGEs. The applied heating procedures can have possible drawbacks on many other aspects of the diet such as vitamin content, formation of other process related contaminants such as acrylamide, PAHs (polycyclic aromatic hydrocarbons), furans, potentially interfering with the observed biological effects[330]. On the other hand, in some cases diets applied to decrease intake of dietary glycation products are evaluated as 'virtually free of Maillard compounds'[32,136] by avoidance of certain food products (e.g. baked and roasted food products), without any further analytical assessments. In addition, especially for human intervention trials, dietary AGE exposure assessment is often done with a database approach where dietary AGE exposure is estimated based on food intake of the participants and a database containing measured AGE levels in food products[7]. However, also within product groups differences in quantified glycation product levels exist and home-cooking procedures can also introduce formation of AGEs and their precursors. Thus, measuring duplicate diet studies would be preferred over studies in which exposure is determined based on this estimation procedure using food questionnaires and default glycation product levels in food. Furthermore, some human trials did not assess compliance to the intervention, did not control for caloric intake or nutritional value when comparing a diet high or low in AGEs, and in case of cross-over designs, carry-over effects were not always controlled[16,149,331]. Of course, when designing intervention trials or other *in vivo* studies, especially including human subjects, choices need to be made as these interventions are in general costly and resources are typically not unlimited. However, the above-mentioned factors causing inaccuracies and uncertainties make the studies difficult to interpret or compare and thus to reach a consensus on the possible risk of dietary AGEs and their precursors.

Exogenous versus endogenous glycation products
To elucidate if dietary, exogenous AGEs and their precursors contribute to effects associated with the AGEs in the human body, a first step is to quantify their relative contribution. Once in the human body, exogenous AGEs and their precursors are expected to have the same

mode of action as endogenous glycation products, when they are the exact same type. To understand associations between AGE levels in biological matrices (i.e. AGE levels in plasma and other biological fluids, tissue homogenates and secretions), health effects and dietary AGE and precursor exposure data, and to see whether effects observed can be attributed to exogenous or endogenous AGEs and precursors, it is essential to elucidate the kinetic fate of endogenous and exogenous glycation products. As discussed in **Chapter 2**, when doing this a distinction should be made between LMM and HMM AGEs. In addition, this evaluation needs to be done for individual compounds as the heterogeneity of the AGEs and their precursors can also result in differences in their toxicokinetic characteristics, like observed in **Chapter 4** and **6**.

Toxicokinetics of LMM and HMM AGEs have been reviewed in **Chapter 2**. In case of absorption some discrepancies between *in vitro* data (e.g. Caco-2 transwell culture data) and *in vivo* data exist, as in *in vivo* studies exogenous exposure to AGEs and their precursors result in their entering the systemic circulation at least partially, while *in vitro* studies describe for some LMM AGEs and precursors limited uptake[29,36]. Thus, at least part of the dietary exposed exogenous AGEs and precursors can be absorbed as also shown in **Chapter 6**, where both LMM and HMM AGEs were found to be increased in the systemic circulation of mice upon a baked chow diet high in the measured AGEs carboxymethyllysine, carboxyethyllysine and MG-H1, which were present in the diet mainly in their HMM form. When entering the systemic circulation, it is also of use to know how and where these AGEs deposit: in plasma, tissues or organs, intra- or extracellular. In **Chapter 6** both LMM and HMM AGEs ended up especially in plasma and kidney (carboxymethyllysine, carboxyethyllysine) which seemed to reflect only a temporary increase which appeared to be associated to the exposure diet as shown by introducing the switch diet. In **Chapter 2** it was concluded, based on the toxicokinetic and toxicodynamic data available, that the effects of exogenous HMM AGEs and precursors seem to be limited to local effects on the gut microbiota and intestine due to their relatively low bioavailability, unless being digested into their LMM form, while LMM AGEs and precursors once absorbed can be cleared by renal excretion. Thus, whether the increased levels of HMM AGEs detected in the systemic circulation and tissues analyzed in **Chapter 6** originate as such from the diet, or are formed at an increased level upon exposure to a diet high in HMM AGEs but also in their dicarbonyl precursors, and/or result from degradation of the dietary HMM AGEs to LMM AGEs that upon absorption gives rise to increased formation of endogenous HMM AGEs, remains to be elucidated.

When assessing the risk for dietary AGEs and their precursors, dicarbonyl precursors are important to consider as well. Dicarbonyls are also present in the diet[196] and can also be produced endogenously. The dicarbonyls (e.g. methylglyoxal, glyoxal, 3-deoxyglucosone) are, as explained earlier, important reactive precursors in the formation of AGEs. The (dietary) dicarbonyls can thus again, like other dietary components (such as artificial sweeteners[332]) or diets having a high glycemic load[333], enhance endogenous formation of AGEs or possibly induce other biological effects. Thus, as indicated above, the significantly higher level of dicarbonyls in the baked chow diet as compared to the chow diet in **Chapter 6**, may have contributed to the higher endogenous HMM AGE levels. The possible relevance of these reactive dietary dicarbonyls will be further discussed in section **7.2.5**.

Interactions between exogenous, dietary glycation products and the gut microbiota
From toxicokinetic data available, it is clear that at least part of the exogenous dietary AGEs and their precursors reach the gut microbiota. Experimentally obtained data presented in this thesis (**Chapter 3, 4, 5**) show that –at least for fructoselysine and carboxymethyllysine– if not absorbed, they can be degraded by the human gut microbiota, which was estimated (as further discussed in Section **7.2.2**) to result on average in almost a complete degradation when intake would be at the level of the EDI. However, inter- and intraindividual differences in the degradation of these two model glycation products by the human gut microbiota were found. It is also of interest to note that the microbial degradation of the dietary LMM AGEs and their precursors can lead to formation of metabolite production that may have secondary effects, either positive or negative, on host health[40,47,54,267] as shown for fructoselysine degradation which was associated with butyrate production (**Chapter 3**). The metabolic pathways involved and potential biological effects of the metabolites formed from dietary glycation products remain of interest for future studies. In addition, it is relevant to further elucidate whether exogenous glycation product-exposure induced effects on the microbiota composition -as also shown in mice in **Chapter 6**- are a potential mode of action and contribute to effects, adverse or beneficial, on human health or rather only represent an adaptation of the gut microbiota to the diet (as hypothesized in **Chapter 5**) or both. How to additionally study interactions between dietary glycation products with the gut microbiota related to human health will be further discussed in Sections **7.2.4** and **7.2.5**.

Overall, it is clear that there are several challenges regarding interpretation of the results of dietary glycation product-induced adverse health effect studies, and at this point no definite conclusion can be given whether dietary AGEs and their precursors causally affect or link with specific human health effects. Future research perspectives on this aspect will be further discussed in Section **7.2.5**.

7.2.2 Applicability domain of anaerobic fecal incubations and *in vitro* to *in vivo* extrapolation

The data shown in this thesis as obtained by the use of anaerobic *in vitro* fecal incubations have been used to quantify inter- and intraindividual differences in gut microbial metabolic activities. The *in vitro* model used (i.e. small anaerobic batch incubations with human fecal slurries and the substrate of interest in PBS) is a simple and fast model which is shown to be useful to study kinetics of gut microbial metabolism of foodborne substrates for different individuals. A similar set-up has been shown suitable to also study interspecies differences in gut microbial metabolism of foodborne mycotoxins[334,335]. However, as for all *in vitro* models, this model represents a specific aspect of an overall complex physiological process, and for the application and extrapolation of the data to humans *in vivo* certain assumptions have to be made; these, as well as other (dis)advantages of the model compared to other (*in vitro*) methodologies are discussed in more detail in this paragraph.

The use of fecal samples
For the *in vitro* model of the present thesis, fecal samples were used as a source of gut microbial communities based on the premise that this is sufficiently representative of the colonic microbiota as previously reported[89–91]. The intestinal tract harbors microbiota which can differ between, for example, its upper and lower parts[336]. These differences include

microbial densities and composition, along with differences in e.g. pH, oxygen and available nutrients[337]. Fecal samples have been widely used to represent colonic fermentations and have a major advantage of being relatively easy to sample with relatively low discomfort for the subject. Nevertheless, it would be ideal to take samples directly from the intestine itself, potentially even enabling characterization of metabolism in different parts of the GI tract. This can be done with for example naso- and oro-intestinal catheters[88], a luminal brush, or sampling from ileostomy patients[338]. However, these methods are invasive, time and cost intensive and often require prior to the procedure a bowel preparation (cleansing) with corresponding effects on the gut microbiota[338]. New developments in this field have been made and ingestible sampling devices are promising[339] but still several challenges need to be overcome before these methods can be used on a larger scale[338]. When shown to be effective, this will pave way for new developments in gut microbiota research, providing insights in the role of the different microbiota communities in different parts of the intestinal tract.

Fermentation models
The *in vitro* anaerobic incubations of the fecal slurries in PBS performed in this thesis were all of short duration time (<6 hours) and thus considered static fermentations. This was done with the intention to retain the microbiota composition as close as possible to the original sample and is considered an advantage for gut microbial toxicokinetic studies. In addition, the selected set up remained as easily accessible as other *in vitro* toxicokinetic models, which are widely used and proven to be useful (e.g. incubations with human liver microsomes and S9 fractions)[340–342]. On the other hand, more complex continuous multi-stage fermentation models exist, such as the SHIME (Simulator of the Human Intestinal Microbial Ecosystem), the TIM-2 model (TNO intestinal model-2) and other larger fermentation systems[343]. These fermentation systems can also be inoculated with fecal samples. With nutrient supply and including different external conditions in multiple compartments, various parts of the intestine can be mimicked[343–346]. Between the set-up of these multi-stage models differences exist as well (e.g. in the included segments of the gastro intestinal tract)[343], but stable and sufficiently reproducible bacterial communities are produced as reported[344,347]. These continuous models could prove to be more suitable to study the effects of exogenous compounds on the gut microbiota (i.e. toxicodynamics) *in vitro*, compared to static batch fermentations as used in this thesis. However, the complexity of continuous models and time- and cost-intensiveness would make these models less preferred over the static batch fermentations to study toxicokinetics and/or for studies including multiple individuals. Another interesting option would be to combine both types of models, by using a continuous model to expose a stable microbial community to a substance of interest, and use a sample from the formed, possibly perturbated community to further study kinetic reactions of interest with small batch fermentations. In this way both toxicodynamic and toxicokinetic properties of the gut microbiota can possibly be studied. However, this remains to be further investigated. Another available method is applying defined synthetic microbial communities instead of fecal samples, which consist of a consortium of selected bacteria which are known to be present in the gut[348]. In this way, fermentation conditions are more controlled[343] which might be useful e.g. for comparing effects of different foodborne components. However,

considering the large interindividual differences in the gut microbiota and that still many bacteria in the gut are not identified yet would make this a less preferred model to obtain an overall overview of the effects on and of the intestinal microbiota.

Extrapolating the obtained in vitro data to the in vivo situation
Overall, the presented *in vitro* model is suitable to study individual gut microbial reaction kinetics. The application of this *in vitro* model fits within the New Approach Methodologies (NAMs) for toxicity testing[349], and considering the metabolic potential of the gut microbiota reportedly being comparable to the liver[350] it is a relevant *in vitro* model which can be applied in modern 21st century toxicity testing strategies. To use the obtained *in vitro* kinetic data for the *in vivo* situation, the data need to be extrapolated. When combining this with data originating from other *in vitro* and *in silico* models, ADME properties of a foodborne chemical of interest can be described in a physiologically based kinetic (PBK) model. PBK models have been shown useful to describe *in vivo* kinetics of a compound of interest[99] and may include a gut microbiota compartment to predict *in vivo* plasma C_{max} or AUC (area under the curve) levels taking metabolism by the gut microbiota into account[100,101]. In this thesis, *in vivo* gut microbial degradation was estimated based on the obtained *in vitro* data by using the following assumption. As such, the amount of degraded substrate per gram feces was calculated for a total, average defecation mass of 128 g/day[263] assuming to come from a total of 24 hours transit time, and thus considered to represent the total colonic microbiota content per individual adult. For infants this was 31 g per 24 hours[289,290]. However, it should be noted that with this approach, an average is used while large interindividual differences for defecation mass have been reported[263].

The *in vitro* model presented in this thesis has been used to describe and quantify the AGE degradation activities by the human gut microbiota as a whole ("what happened"). This showed to be a suitable approach to study inter- and intraindividual differences in gut microbial degradation activities. In addition, the obtained individual degradation activities were associated to multiple bacteria present in the used fecal samples as characterized by 16S rRNA amplicon sequencing. This was done to gain more insight in the bacteria involved in these microbial reactions ("who did it"). However, to fully understand and explain these associations, and to move to a causal relation, extra steps should be taken in addition to the applied strategy in this thesis. This will be further discussed in the following Section **7.2.3**.

7.2.3 Moving from association to causation in gut microbiological research
In this thesis, microbial composition as assessed by 16S rRNA amplicon sequencing was correlated to other study outcomes. To gain insight in possible roles of specific bacteria in the metabolic conversions studied, microbial degradation activities of fructoselysine and carboxymethyllysine were correlated to the bacterial composition of the used fecal samples (**Chapters 3, 4, 5**). In **Chapter 6** the aim was to explore whether specific members of the gut microbiota were associated with accumulation of AGEs in plasma and organs of the host induced upon dietary exposure to a heated diet high in AGEs. The value of the obtained associations and possible next steps to move towards identifying causal relations will be discussed in this section, and the associations with toxicokinetic and toxicodynamic endpoints will be addressed separately.

Gut microbial metabolism of foodborne substances can be relevant from a toxicological perspective. However, to increase understanding of the gut microbial ecology (and the functioning of that "organ") it would also be useful to identify which microbes are involved or possibly even responsible for these metabolic activities and via which pathways and mechanisms compounds of interest are converted by the gut microbiota. Therefore, associations were made of the rates of fructoselysine or carboxymethyllysine degradation with the microbial composition data obtained via 16S rRNA amplicon sequencing. This resulted in identification of multiple bacteria showing a high correlation to the amounts of degraded substrate during the course of the measurements, which can serve as a first step in identifying microbes involved in these reactions. However, several shortcomings are inherent to 16S rRNA amplicon sequencing. For example, the analysis lacks functional annotation[91], the assigned taxonomy depends on the used database[235] and only a region of the genome is sequenced. In addition, only bacteria present in a relative abundance of >0.1% in one of the analyzed samples were included for the association analyses, possibly resulting in scarce genera to go unnoticed. Furthermore, inherent to associations is that these can be confounded. Thus, the obtained associations alone will not provide a definite answer to "who did it" and more steps are necessary to identify a causal relation between bacteria and functional processes, when this knowledge is desired. A possible way forward is for example performing enrichments of fecal slurries with the substrate of interest over a longer time period including multiple transfers, combined with molecular or other -omics approaches to gain insight in the underlying mechanisms of the microbe(s) that is (are) thus preselected. For fructoselysine, this was done in an elegant way by Bui et al.[40] who identified *Intestinimonas butyriciproducens* AF211 to grow efficiently on fructoselysine as a substrate. This microbe was found able to degrade fructoselysine and metabolize it into SCFAs (butyrate and acetate). With a proteomics approach key steps in this metabolic pathway were identified. This approach can provide useful mechanistic information on a specific function by a bacterium isolated from the human gut. However, identification of one single metabolic functional microbe does probably not cover all degradation activities measured with the anaerobic fecal incubations, as in **Chapter 5** it was shown that the potential of a specific function (in this case fructoselysine degradation genes) was redundantly present amongst multiple species. In addition, studying one single bacterium does not provide information on its functioning in the gut microbial ecosystem, where e.g. cross-feeding mechanisms or other microbe-microbe interactions are shown to be of high importance.

The associations reported in **Chapter 6** aimed to explore whether specific bacteria of the altered gut microbiota composition were associated with toxicokinetic or toxicodynamic effects on the host (i.e. accumulation of AGEs in biological matrices, induction of inflammation markers) induced by a heated diet high in AGEs. Similarly, in literature numerous studies report associations between gut microbiota composition and a certain host phenotype (e.g. a diseased state)[351]. Often it remains unclear whether the gut microbiota composition predisposes the associated host phenotype or the other way around, or if the relation is causal at all[352]. Moving from an association to an understood causal relation would be relevant to increase understanding of the role of the gut microbiota (composition) in host health. This would be relevant information in order to evaluate for example toxicodynamic effects by foodborne compounds on the gut microbiota, to identify biomarkers in human feces for a certain diseased state and when moving towards a (dietary) therapeutical

approach. The challenging dynamic and individual aspects inherent to the gut microbiota complicate this shift towards establishing a causal relation especially in research focusing on humans. Probably a combination of *in vitro, in vivo* and human studies is necessary to prove a causal relationship. For example, combining information from a rodent gnotobiotic model (i.e. germ-free model or with known, possible humanized colonized microbes) with e.g. -omics techniques focusing on different informational levels, *in vitro* host-microbe studies and human based associations can be elucidated as the approach is able to provide information from several perspectives in different *in vivo* and *in vitro* systems. Another possible option would be to focus on mechanistic underpinning of an outcome via occurring key events based on e.g. *in vitro* and *in silico* methods, establishing a certain "outcome pathway", like done in the field of toxicology (adverse outcome pathways; AOPs)[353,354]. Although AOPs assume a linear direction, and thus do not include e.g. feedback loops[353], use of such a systematic approach to assess health effects mediated via the gut microbiota could be of use.

Another complicating challenge when correlating gut microbiota to a host phenotype is that the host phenotypes reported to correlate with the gut microbiota are often multifactorial diseases which evolve over a longer period of time (e.g. inflammatory bowel disease, obesity, diabetes type 2, Alzheimer's disease). This is also often the case for research studying adverse or beneficial health effects of dietary compounds. An additional challenge for dietary research is that the dietary compounds in question –like the glycation products– are difficult to test individually as they are part of a complex mixture of AGEs and precursors present in a complete diet, in contrast to e.g. pharmacological compounds such as antibiotics which are easier to investigate individually. The challenges and perspectives for studying dietary-microbiological interactions from a toxicological perspective will be discussed in the following Section **7.2.4**.

7.2.4 Dietary and gut microbiological research from a toxicological perspective
A lot of research has been conducted to assess interactions of dietary components with the gut microbiota and (human) host health. Also in the field of toxicology the gut microbiota is receiving increased attention[13,58]. The gut microbiota has the ability to metabolize exogenous compounds (e.g. foodborne compounds, pharmaceuticals), as also shown in this thesis. In addition, the gut microbiota plays an important role in human health which can be affected via an alteration of composition and/or function (often referred to as dysbiosis)[59]. This can affect human health and possibly cause disease. As dysbiosis can be induced by exogenous exposure, there is a potential role for dietary glycation compounds in toxicology. However, if and to what extent these compounds pose a risk and how this can be evaluated remains to be established[13]. Nevertheless the results of the present thesis reveal that when considering the toxicity of dietary glycation products the role of the gut microbiota should be taken into account. This, however, brings several challenges. These will be discussed in this section, with emphasis on dietary AGEs and their precursors.

First of all, temporal intraindividual variability in gut microbial activity was observed in **Chapter 4**, in addition to interindividual differences. This difference is relevant for toxicokinetics as it can play a role in microbial degradation activities as established for fructoselysine and carboxymethyllysine (**Chapter 4**). Consequently, this metabolism by the

gut microbiota can possibly affect the systemic uptake of a compound and thus internal exposure levels. In **Chapter 4** intraindividual differences were observed within a period of 3-16 weeks, and were hypothesized to be induced by, among others, differences in dietary exposure to the substrate prior to fecal sampling, as supported by results of **Chapter 5**. These relatively quick adaptations of the gut microbiota were also reflected in the alterations of the gut microbiota composition in mice upon a 5-week baked chow diet high in AGEs, which seemed to be reversible following a control diet for 5 subsequent weeks (**Chapter 6**). It is known that diet is an important environmental factor shaping the gut microbiota, and this can possibly affect toxicokinetics, as shown for fructoselysine and carboxymethyllysine in the present thesis.

In addition to the observed inter- and intraindividual variability, it is relevant to study different age groups in dietary-microbiological research from a toxicological perspective. For example, diets of infants differ from adults and consequently also can affect the gut microbiota in a different way. In **Chapter 5**, breast milk and infant formula having different contents of fructoselysine as consumed by BF and FF infants resulted in different *in vitro* fructoselysine microbial degradation activities between the infants fed by these two different feeding modes. In addition, calculations revealed that the EDI of fructoselysine by FF infants was unlikely to be completely degraded; on average only 29% of the fructoselysine amount provided by intake at the level of the EDI was estimated to be degraded based on the rates of fructoselysine by the respective fecal samples. This was in contrast to adults for whom at an intake at the level of the EDI on average all estimated dietary fructoselysine was estimated to be degraded. This difference could mainly be explained by the different EDIs, with FF infants on a bodyweight basis consuming approximately 30-fold higher levels of fructoselysine compared to adults. It was also of interest to note that fecal samples from BF infants were able to degrade fructoselysine as well, even without substantial dietary fructoselysine exposure through breast milk[87]. This indicates that (part of) the enzymes involved in fructoselysine degradation may be multifunctional and/or constitutively expressed for other reasons. However, this remains to be further investigated.

In order to study toxicodynamic effects of foodborne or other exogenous compounds on the gut microbiota it is important to establish a relevant adverse effect that can be quantified. Dysbiosis is often used to refer to an altered bacterial composition[59]. However, the definition of a "normal" or healthy gut microbiota is not set in stone and can be difficult to define, also because of the inter- and intraindividual differences present. Furthermore, it can be argued whether microbial composition alone is sufficient and informative enough to assess dysbiosis and potential health consequences. Bacterial composition and function are not necessarily related[67], and thus to assess toxicodynamic effects on the gut microbiota based on bacterial metabolites (e.g. present in the feces such as SCFAs) might be a more suitable outcome measure. For example, a metabolomic pattern or biomarker metabolite which reflects or is known to initiate an adverse health effect of possible toxicological concern can possibly be used to evaluate (the chances on) a toxicodynamic effect. The fecal metabolome provides a functional readout of the gut microbiota and reflects the interplay between the diet, gut microbiota and the host[91,355], and can thus possibly be of use to represent the interplay between the gut microbiota and the host[91]. As such, the fecal metabolome has been found useful to study antibiotic-induced effects in rats and metabolite alterations

were detected equally well in feces as in cecum content[89]. A heated diet high in AGEs induced effects on the cecal metabolome in mice and altered the level of phenylalanine, tryptophan and tyrosine metabolites as previously reported[210]. In another study multiple metabolic pathways (related to e.g. amino acid and energy metabolism) were altered in the mice fecal metabolome upon exposure to a heated diet high in AGEs compared to a diet low in AGEs[255]. The extent, however, to which these changes can be considered adverse towards host health remains to be elucidated. Providing a potential promising endpoint, studying exogenously-induced effects on the fecal metabolome needs further investigation, including establishments of proper dose-response behavior. In addition to further facilitate the application of studying the fecal metabolome, guidelines or standardization of outcome measures and study set ups (both *in vitro* and *in vivo*) are needed to enable comparison. For example for *in vivo* studies, it is known that the microbial composition of mice is -besides being different from humans- affected by multiple factors, including the animal vendor, strain or stock, environmental factors such as housing and of course the diet[356]. This should be standardized as much as possible or at least considered. For *in vitro* studies, human-based assays can be used but in addition also should be standardized in terms of e.g. set-up, incubation conditions to be applied, number of different individuals to be included, and relevant outcome measures.

In toxicology, there is increasing attention for the role of the gut microbiota. As described above, several aspects and challenges are important to consider when studying dietary-microbiological interactions from a toxicological perspective and can be helpful in providing direction for microbiological-dietary research from a toxicological perspective. Considering the dietary AGEs and their precursors, it has been shown that the gut microbiota can be involved in toxicokinetics and possibly in toxicodynamics as well. However, information is lacking to evaluate whether exposure to these dietary glycation products poses a risk to human health, also because the relative importance of the dietary exposure relative to endogenous formation remains to be elucidated, and more research is needed on the possible underlying pathways and modes of action. Future research perspectives on this aspect are further discussed in the following Section **7.2.5**.

7.2.5 Future research perspectives for the potential effects of dietary glycation products on human health

Toxicokinetics

To understand whether dietary glycation product exposure poses a risk to human health, internal exposure resulting from exogenous exposure needs to be assessed and compared with endogenous formation levels (as discussed in section **7.2.1**). AGEs and their precursors are a heterogenous group of compounds including HMM and LMM forms, and also reactive precursors like the dicarbonyls, and more work should be done on evaluating the toxicokinetics of all these individual glycation products. For many compounds that are part of the heterogenous group of glycation products (**Chapter 1**, **2**), information on e.g. absorption from the intestine is partially or completely lacking. *In vitro* intestinal barrier models with e.g. Caco-2 cells or intestinal organoids[357] can be of use to quantify intestinal absorption rates and compare these between the different AGEs and their precursors. In addition, gut microbial degradation activities of multiple individual glycation products which have not been evaluated yet, such as carboxyethyllysine and MG-H1, can be quantified with the *in*

vitro model presented in this thesis (as shown for fructoselysine and carboxymethyllysine in **Chapters 3, 4** and **5**). When also assessing *in vitro* digestion of individual glycation products in the upper intestinal tract up to the small intestine, such as previously done with the TIM-1 model (TNO intestinal model 1 covering the upper gastrointestinal tract)[139], a completer picture of what happens in the complete gastrointestinal tract can be provided.

When absorbed, it would be relevant to know whether and to what extent urinary excretion occurs to evaluate possible accumulation *in vivo*. Human studies can also address this question[358], but with *in vitro* models there is the advantage that one individual glycation product can be tested without interference of other possible confounding dietary components. In addition *in vitro* approaches allow testing of more compounds in a relatively easy and fast way. It should be noted that for kidney clearance, an impaired or diseased model can be useful to include since kidney failure (e.g. as a complication of diabetes) impairs kidney function and can affect urinary excretion of AGEs and their precursors[300,359]. For example, in diabetic subjects with impaired kidney function, altered levels of urinary excretion of AGEs were reported[360,361].

When absorbed and not excreted, AGEs and precursors can accumulate in organs as reported for the kidney and the liver[148,362]. In some cases accumulation of both LMM and HMM AGEs have been reported, like in **Chapter 6**. However, whether this can be attributed to direct exogenous exposure or via (indirect) endogenous formation remains to be elucidated. Mechanistic *in vitro* studies can be of use combined with e.g. uptake studies with different cell types to elucidate whether absorbed exogenous AGEs and precursors can enter the cells or stimulate endogenous formation in another way. Isotope-labelled *in vivo* studies are also useful to determine whether accumulation in e.g. tissues and organs is a result of exogenous exposure or rather the result of elevated endogenous formation, as previously shown in literature[29]. Isotope labelled HMM carboxymethyllysine was orally administered to mice and resulted in carboxymethyllysine accumulation with the highest levels in kidney, intestine and lungs[29].

In addition, when levels of glycation products are quantified with LC-MS/MS often only a few individual compounds are included. However, more glycation products exist with possible different ADME characteristics. A possible approach to identify these could include untargeted metabolomics approaches[363] or proteomics[364]. These analytical techniques can be applied to characterize the applied dietary exposure as well as to characterize biological matrices (e.g. plasma and secretions), and possibly result in better understanding of the presence and distribution of the different AGEs and their precursors and accompanying health effects. Finally, insight in the potential scavenging of reactive dicarbonyls by dietary components and/or intestinal content seems relevant as well.

Toxicodynamic effects
Besides studying metabolism of glycation products by the gut microbiota, an additional step forward to further understand health effects induced by exogenous AGEs and their precursors would be to further study possible toxicodynamic effects on the gut microbiota. As shown in **Chapter 6** and in literature, a heated diet which also contained increased dietary AGEs altered microbiota composition. Whether this can result in secondary

adverse (or beneficial) health effects remains uncertain. Like discussed in Sections **7.2.3** and **7.2.4**, additional outcome measures and study set-ups are necessary to investigate a causal relation and to understand involved mechanisms. To elaborate on that, an *in vitro* alternative to study this would be to expose (fecal) microbial communities to individual glycation products, collect supernatants containing possibly formed bioactive metabolites and subsequently expose *in vitro* cell models to this mixture, incorporating an intestinal barrier, to study secondary health effects.

Toxicodynamic effects exerted on or via the gut microbiota can be one possible underlying mode of action for the various diseases where a role of AGEs has been suggested, in addition to for example binding to RAGE and elevated dicarbonyl stress[12]. Defining relevant outcome measures and to identify the underlying mode of actions of individual LMM and HMM AGEs and their precursors in the various diseases where a role of AGEs has been suggested remains a topic of further investigation. *In vitro* methods can possibly be of use to further elucidate this and to provide mechanistic information[365]. Other dietary compounds of high interest are the reactive dicarbonyls as further discussed in the following section.

A potential role for reactive dicarbonyls
As discussed in Section **7.2.1**, other characteristics of the diet like a high glycemic load[333] or the presence of other dietary components such as reactive dicarbonyls, which are AGE precursors, can also result in AGE formation or pose a risk for human health themselves. Elevated *in vivo* levels can lead to dicarbonyl stress[366] which due to the reactive properties of the dicarbonyls can lead to AGE formation upon reacting with amino acid moieties of a protein[367], resulting in cross-linking of proteins and modification of DNA[368–370].

In **Figure 7.1**[371] it is shown that the three major dicarbonyls methylglyoxal, glyoxal and 3-deoxyglucosone can activate the nuclear factor erythroid 2-related factor 2 (Nrf2)-pathway in a concentration-dependent manner, in contrast to LMM carboxymethyllysine (data not shown), as tested in the Nrf2-CALUX (chemically activated luciferase expression) assay[372]. Methylglyoxal appeared to be the strongest Nrf2 inducer, followed by 3-deoxyglucosone and finally glyoxal. Nrf2 is a transcription factor playing a vital role in the Nrf2-electrophile responsive element (EpRE) signaling pathway which regulates expression of defense mechanisms, including glutathione production. The glyoxalase system, active in detoxification of especially the dicarbonyls methylglyoxal, glyoxal[366], is dependent on glutathione which can bind to methylglyoxal and glyoxal non-enzymatically or via glutathione-S-transferases[373,374]. 3-Deoxyglucosone is reported to be mainly detoxified via NADPH dependent aldo-keto reductases[375]. Despite the presence of cellular dicarbonyl detoxification mechanisms, dicarbonyls present in the human body were suggested to play a role in the development of multiple disorders (e.g. diabetes, cardiovascular diseases, neurodegenerative diseases)[376] and their high intrinsic electrophilic reactivity raises the need for risk assessment of the dicarbonyls. Since dicarbonyls can be formed both endogenously and exogenously as explained in **Chapter 1** and **2**, the question arises, like for AGEs, whether exogenous dietary dicarbonyls pose a risk for human health relative to the endogenous dicarbonyls. A recent study presented a database with 223 foods and drinks with quantified levels of methylglyoxal, glyoxal and 3-deoxyglucosone enabling the performance of an exposure assessment for dietary dicarbonyls and estimated the dietary intake to be ~9, ~3 and

7

~3 mg/day for 3-deoxyglucosone, methylglyoxal and glyoxal, respectively[196]. As also discussed in **Chapter 2**, some studies show that the dietary dicarbonyls are absorbed[137], however based on the limited data available this seems to differ between dicarbonyls[136] as dietary exposure of methylglyoxal to human volunteers did not seem to affect urinary excretion while for 3-deoxyglucosone dietary exposure did seem to increase urinary 3-deoxyglucosone levels[136,137]. When exposed through the diet, it is conceivable that dicarbonyls in the diet are scavenged by other dietary compounds (e.g. amino acids, phenolic compounds, thiol moieties of proteins) before reaching the intestinal tract or even before being ingested due to their high reactivity. Also inside the intestinal tract it is conceivable that they react with other compounds originating from the diet or the body inside the intestine[367] and possibly affect the gut microbiota or the intestinal cells[138]. A comparison of their reactivity towards different scavenging materials (e.g. amino acids, glutathione, other food-derived compounds) would be relevant information to evaluate their bioavailability, similar to what has been done for melanoidins[377]. Overall, the risk of exogenous dietary dicarbonyls should be evaluated in view of both dicarbonyl stress as well as endogenous AGE production. Furthermore, since LMM AGEs and precursors such as fructoselysine can degrade again into dicarbonyls (3-deoxyglucosone and glyxoal[375,378]), dietary exposure to these precursors should also be considered when evaluating the hazards or risks of dietary dicarbonyls. Clearly absence of all this information hampers current risk assessment on dietary AGEs and their precursors.
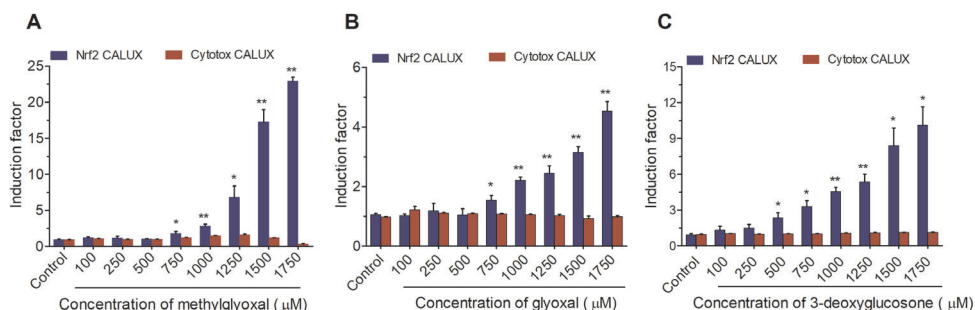

Figure 7.1 Induction of Nrf2-mediated luciferase gene expression in the Nrf2-CALUX assay (blue bars) and in the control Cytotox-CALUX assay (red bars) by methylglyoxal (A), glyoxal (B) and 3-deoxyglucosone (C). Data bars represent a mean value of three independent replicate experiments, while error bars represent the SEM. Statistically significant induction was evaluated with a Student's t-test and was indicated as following: * $p < 0.05$ and ** $p < 0.01$. CALUX: chemically activated luciferase expression. BDS (Amsterdam) is acknowledged for the use of the U2OS Cytotox and Nrf2 CALUX cells. This data was experimentally obtained and is presented in Zheng, L., van Dongen, K.C.W. et al., 2022.

7.3 Overall conclusion

Glycation products comprise AGEs and their precursors and are a heterogenous group of compounds that include compounds such as fructoselysine and carboxymethyllysine, the model compounds of the present thesis. Studying their toxicokinetics and toxicodynamics holds several challenges, especially also because they are present in exogenous sources as well as formed endogenously. How and in which form (i.e. LMM or HMM) test substances are applied in *in vivo* and in *in vitro* studies needs to be much better characterized, in order to facilitate interpretation and comparison of study results. This will help to evaluate the toxicokinetics of AGEs and their precursors as well as to identify the underlying modes of actions in the various suggested diseases that have been related to AGEs and their precursors, which still needs further elucidation. Thus, to firmly establish the possible hazards and risk of exogenous dietary AGEs and their precursors requires further investigations.

In this thesis, bi-directional interactions between glycation products and the gut microbiota have been studied. Inter- and intraindividual differences in microbial degradation activities of fructoselysine and carboxymethyllysine were elucidated and quantified. The *in vitro* method using anaerobic fecal incubations was shown to be useful to study *in vitro* microbial degradation kinetics of these (foodborne) compounds. Microbial adaptation towards dietary exposure seemed to occur as shown by the results on fructoselysine degradation activities in incubations with fecal sample from BF and FF infants, and by the putative reversible altered microbiota composition in mice upon returning to the control diet after being exposed to a heated chow diet high in AGEs. To what extent this dynamic aspect of the gut microbiota affects the ultimate hazards and risks of dietary exogenous AGEs and their precursors remains an interesting topic for future research. It also remains to be established to what extent the dietary exogenous AGEs and their precursors as compared to the endogenous formation of AGEs add to the overall exposure, and what dietary components can drive this endogenous formation. The results of the present study reveal that dietary AGEs do influence the endogenous levels and may influence the gut microbiota. Better quantification of qualitative and quantitative kinetic and dynamic characteristics of individual AGEs and precursors appears essential for adequate future hazard and risk evaluation.
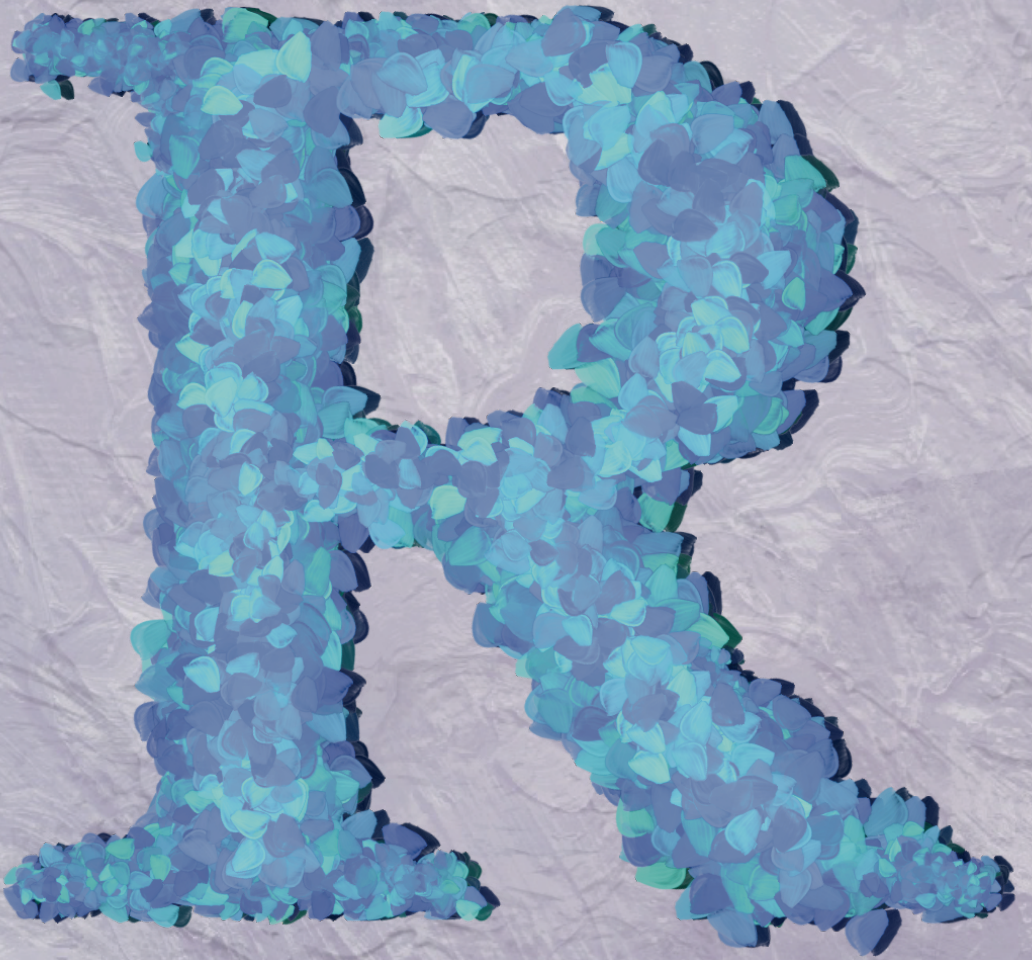
7

References

1. Bengoa, J. M. Food Transitions in the 20th-21st Century. *Public Health Nutr.* **2001**, *4* (6A), 1425–1427. https://doi.org/10.1079/PHN2001232.

2. Cordain, L.; Eaton, S. B.; Sebastian, A.; Mann, N.; Lindeberg, S.; Watkins, B. A.; O'Keefe, J. H.; Brand-Miller, J. Origins and Evolution of the Western Diet: Health Implications for the 21st Century. *Am. J. Clin. Nutr.* **2005**, *81* (2), 341–354. https://doi.org/10.1093/AJCN.81.2.341.

3. He, J.; Evans, N. M.; Liu, H.; Shao, S. A Review of Research on Plant-Based Meat Alternatives: Driving Forces, History, Manufacturing, and Consumer Attitudes. *Compr. Rev. Food Sci. Food Saf.* **2020**, *19* (5), 2639–2656. https://doi.org/10.1111/1541-4337.12610.

4. Knorr, D.; Augustin, M. A. Food Processing Needs, Advantages and Misconceptions. *Trends Food Sci. Technol.* **2021**, *108*, 103–110. https://doi.org/10.1016/J.TIFS.2020.11.026.

5. Benford, D.; Ceccatelli, S.; Cottrill, B.; DiNovi, M.; Dogliotti, E.; Edler, L.; Farmer, P.; Fürst, P.; Hoogenboom, L.; Katrine Knutsen, H.; Lundebye, A.-K.; Metzler, M.; Mutti, A.; Schouten, L. J.; Schrenk, D.; Vleminckx, C. Scientific Opinion on Acrylamide in Food. *EFSA J.* **2015**, *13* (6), 4104. https://doi.org/10.2903/J.EFSA.2015.4104.

6. Knutsen, H. K.; Alexander, J.; Barregård, L.; Bignami, M.; Brüschweiler, B.; Ceccatelli, S.; Cottrill, B.; Dinovi, M.; Edler, L.; Grasl-Kraupp, B.; Hogstrand, C.; Hoogenboom, L.; Nebbia, C. S.; Oswald, I. P.; Petersen, A.; Rose, M.; Roudot, A. C.; Schwerdtle, T.; Vleminckx, C.; Vollmer, G.; Chipman, K.; De Meulenaer, B.; Dinovi, M.; Mennes, W.; Schlatter, J.; Schrenk, D.; Baert, K.; Dujardin, B.; Wallace, H. Risks for Public Health Related to the Presence of Furan and Methylfurans in Food. *EFSA J.* **2017**, *15* (10), e05005. https://doi.org/10.2903/J.EFSA.2017.5005.

7. Scheijen, J. L. J. M.; Clevers, E.; Engelen, L.; Dagnelie, P. C.; Brouns, F.; Stehouwer, C. D. A.; Schalkwijk, C. G. Analysis of Advanced Glycation Endproducts in Selected Food Items by Ultra-Performance Liquid Chromatography Tandem Mass Spectrometry: Presentation of a Dietary AGE Database. *Food Chem.* **2016**, *190*, 1145–1150. https://doi.org/10.1016/J.FOODCHEM.2015.06.049.

8. Hegele, J.; Buetler, T.; Delatour, T. Comparative LC–MS/MS Profiling of Free and Protein-Bound Early and Advanced Glycation-Induced Lysine Modifications in Dairy Products. *Anal. Chim. Acta* **2008**, *617* (1–2), 85–96. https://doi.org/10.1016/J.ACA.2007.12.027.

9. Vistoli, G.; De Maddis, D.; Cipak, A.; Zarkovic, N.; Carini, M.; Aldini, G. Advanced Glycoxidation and Lipoxidation End Products (AGEs and ALEs): An Overview of Their Mechanisms of Formation. *Free Radic. Res.* **2013**, *47* (1), 3–27. https://doi.org/10.3109/10715762.2013.815348.

10. Hellwig, M.; Humpf, H.-U.; Hengstler, J.; Mally, A.; Vieths, S.; Henle, T. Quality Criteria for Studies on Dietary Glycation Compounds and Human Health. *J. Agric. Food Chem.* **2019**, *67*, 11307–11311. https://doi.org/10.1021/acs.jafc.9b04172.

11. Hellwig, M.; Bunzel, D.; Huch, M.; Franz, C. M. A. P.; Kulling, S. E.; Henle, T. Stability of Individual Maillard Reaction Products in the Presence of the Human Colonic Microbiota. *J. Agric. Food Chem.* **2015**, *63* (30), 6723–6730. https://doi.org/10.1021/acs.jafc.5b01391.

12. Poulsen, M. W.; Hedegaard, R. V.; Andersen, J. M.; de Courten, B.; Bügel, S.; Nielsen, J.; Skibsted, L. H.; Dragsted, L. O. Advanced Glycation Endproducts in Food and Their Effects on Health. *Food Chem. Toxicol.* **2013**, *60*, 10–37. https://doi.org/10.1016/J.FCT.2013.06.052.

13. Merten, C.; Schoonjans, R.; Di Gioia, D.; Peláez, C.; Sanz, Y.; Maurici, D.; Robinson, T. Editorial: Exploring the Need to Include Microbiomes into EFSA's Scientific Assessments. *EFSA J.* **2020**, *18* (6). https://doi.org/10.2903/j.efsa.2020.e18061.

14. Yaylayan, V. A.; Huyghues-Despointes, A.; Feather, M. S. Chemistry of Amadori Rearrangement Products: Analysis, Synthesis, Kinetics, Reactions, and Spectroscopic Properties. *Crit. Rev. Food Sci. Nutr.* **1994**, *34* (4), 321–369. https://doi.org/10.1080/10408399409527667.

R

15. Liang, Z.; Chen, X.; Li, L.; Li, B.; Yang, Z. The Fate of Dietary Advanced Glycation End Products in the Body: From Oral Intake to Excretion. *Crit. Rev. Food Sci. Nutr.* **2019**. https://doi.org/10.1080/10408398.2019.1693958.

16. Baye, E.; De Courten, M. P. J.; Walker, K.; Ranasinha, S.; Earnest, A.; Forbes, J. M.; De Courten, B. Effect of Dietary Advanced Glycation End Products on Inflammation and Cardiovascular Risks in Healthy Overweight Adults: A Randomised Crossover Trial. *Sci. Rep.* **2017**, *7* (1), 1–6. https://doi.org/10.1038/s41598-017-04214-6.

17. Vlassara, H.; Palace, M. R. Diabetes and Advanced Glycation Endproducts. *J. Intern. Med.* **2002**, *251* (2), 87–101. https://doi.org/10.1046/j.1365-2796.2002.00932.x.

18. Van Der Lugt, T.; Opperhuizen, A.; Bast, A.; Vrolijk, M. F. Dietary Advanced Glycation Endproducts and the Gastrointestinal Tract. https://doi.org/10.3390/nu12092814.

19. Snelson, M.; Coughlan, M. T. Dietary Advanced Glycation End Products: Digestion, Metabolism and Modulation of Gut Microbial Ecology. *Nutrients*. MDPI AG January 22, 2019, p 215. https://doi.org/10.3390/nu11020215.

20. Yacoub, R.; Nugent, M.; Cai, W.; Nadkarni, G. N.; Chaves, L. D.; Abyad, S.; Honan, A. M.; Thomas, S. A.; Zheng, W.; Valiyaparambil, S. A.; Bryniarski, M. A.; Sun, Y.; Buck, M.; Genco, R. J.; Quigg, R. J.; He, J. C.; Uribarri, J. Advanced Glycation End Products Dietary Restriction Effects on Bacterial Gut Microbiota in Peritoneal Dialysis Patients; a Randomized Open Label Controlled Trial. *PLoS One* **2017**, *12* (9), e0184789. https://doi.org/10.1371/journal.pone.0184789.

21. Tessier, F. J.; Birlouez-Aragon, I. Health Effects of Dietary Maillard Reaction Products: The Results of ICARE and Other Studies. *Amino Acids* **2012**, *42* (4), 1119–1131. https://doi.org/10.1007/s00726-010-0776-z.

22. Birlouez-Aragon, I.; Saavedra, G.; Tessier, F. J.; Galinier, A.; Ait-Ameur, L.; Lacoste, F.; Niamba, C. N.; Alt, N.; Somoza, V.; Lecerf, J. M. A Diet Based on High-Heat-Treated Foods Promotes Risk Factors for Diabetes Mellitus and Cardiovascular Diseases. *Am. J. Clin. Nutr.* **2010**, *91* (5), 1220–1226. https://doi.org/10.3945/ajcn.2009.28737.

23. Nowotny, K.; Schröter, D.; Schreiner, M.; Grune, T. Dietary Advanced Glycation End Products and Their Relevance for Human Health. *Ageing Res. Rev.* **2018**, *47*, 55–66. https://doi.org/10.1016/J.ARR.2018.06.005.

24. Gill, V.; Kumar, V.; Singh, K.; Kumar, A.; Kim, J.-J. Advanced Glycation End Products (AGEs) May Be a Striking Link Between Modern Diet and Health. *Biomolecules* **2019**, *9* (12), 888. https://doi.org/10.3390/biom9120888.

25. Sergi, D.; Boulestin, H.; Campbell, F. M.; Williams, L. M. The Role of Dietary Advanced Glycation End Products in Metabolic Dysfunction. *Mol. Nutr. Food Res.* **2020**, 1900934. https://doi.org/10.1002/mnfr.201900934.

26. Scheijen, J. L. J. M.; Hanssen, N. M. J.; van Greevenbroek, M. M.; Van der Kallen, C. J.; Feskens, E. J. M.; Stehouwer, C. D. A.; Schalkwijk, C. G. Dietary Intake of Advanced Glycation Endproducts Is Associated with Higher Levels of Advanced Glycation Endproducts in Plasma and Urine: The CODAM Study. *Clin. Nutr.* **2018**, *37* (3), 919–925. https://doi.org/10.1016/j.clnu.2017.03.019.

27. Koschinsky, T.; He, C.-J.; Mitsuhashi, T.; Bucala, R.; Liu, C.; Buenting, C.; Heitmann, K.; Vlassara, H. Orally Absorbed Reactive Glycation Products (Glycotoxins): An Environmental Risk Factor in Diabetic Nephropathy. *Proc. Natl. Acad. Sci.* **1997**, *94* (12), 6474–6479. https://doi.org/10.1073/pnas.94.12.6474.

28. Uribarri, J.; Cai, W.; Sandu, O.; Peppa, M.; Goldberg, T.; Vlassara, H. Diet-Derived Advanced Glycation End Products Are Major Contributors to the Body's AGE Pool and Induce Inflammation in Healthy Subjects. *Ann. N. Y. Acad. Sci.* **2005**, *1043* (1), 461–466. https://doi.org/10.1196/annals.1333.052.

29. Tessier, F. J.; Niquet-Léridon, C.; Jacolot, P.; Jouquand, C.; Genin, M.; Schmidt, A.-M.; Grossin, N.; Boulanger, E. Quantitative Assessment of Organ Distribution of Dietary Protein-Bound ^{13}C-Labeled N[ε]-Carboxymethyllysine after a Chronic Oral Exposure in Mice. *Mol. Nutr. Food Res.* **2016**, *60* (11), 2446–2456. https://doi.org/10.1002/mnfr.201600140.

30. Somoza, V.; Wenzel, E.; Weiß, C.; Clawin-Rädecker, I.; Grübel, N.; Erbersdobler, H. F. Dose-Dependent Utilisation of Casein-Linked Lysinoalanine, N(Epsilon)-Fructoselysine and N(Epsilon)-Carboxymethyllysine in Rats. *Mol. Nutr. Food Res.* **2006**, *50* (9), 833–841. https://doi.org/10.1002/mnfr.200600021.

31. Erbersdobler, H. F. The Biological Significance of Carbohydrate-Lysine Crosslinking during Heat-Treatment of Food Proteins. *Adv. Exp. Med. Biol.* **1977**, *86B*, 367–378.

32. Förster, A.; Kühne, Y.; Henle, T. Studies on Absorption and Elimination of Dietary Maillard Reaction Products. *Ann. N. Y. Acad. Sci.* **2005**, *1043* (1), 474–481. https://doi.org/10.1196/annals.1333.054.

33. Erbersdobler, H. F.; Faist, V. Metabolic Transit OfAmadori Products. *Nahrung/Food* **2001**, *45* (3), 177–181. https://doi.org/10.1002/1521-3803(20010601)45:3<177::AID-FOOD177>3.0.CO;2-A.

34. Grunwald, S.; Krause, R.; Bruch, M.; Henle, T.; Brandsch, M. Transepithelial Flux of Early and Advanced Glycation Compounds across Caco-2 Cell Monolayers and Their Interaction with Intestinal Amino Acid and Peptide Transport Systems. *Br. J. Nutr.* **2006**, *95* (6), 1221–1228. https://doi.org/10.1079/BJN20061793.

35. Hellwig, M.; Geissler, S.; Matthes, R.; Peto, A.; Silow, C.; Brandsch, M.; Henle, T. Transport of Free and Peptide-Bound Glycated Amino Acids: Synthesis, Transepithelial Flux at Caco-2 Cell Monolayers, and Interaction with Apical Membrane Transport Proteins. *ChemBioChem* **2011**, *12* (8), 1270–1279. https://doi.org/10.1002/cbic.201000759.

36. Hellwig, M.; Matthes, R.; Peto, A.; Löbner, J.; Henle, T. N-ε-Fructosyllysine and N-ε-Carboxymethyllysine, but Not Lysinoalanine, Are Available for Absorption after Simulated Gastrointestinal Digestion. *Amino Acids* **2014**, *46* (2), 289–299. https://doi.org/10.1007/s00726-013-1501-5.

37. Niederwieser, A.; Giliberti, P.; Matasovic, A. N(ε)/1 Deoxyfructosyl/ Lysine in Urine after Ingestion of a Lactose Free, Glucose Containing Milk Formula. *Pediatr. Res.* **1975**, *9* (11), 867–867. https://doi.org/10.1203/00006450-197511000-00090.

38. Wiame, E.; Delpierre, G.; Collard, F.; Van Schaftingen, E. Identification of a Pathway for the Utilization of the Amadori Product Fructoselysine in *Escherichia Coli*. *J. Biol. Chem.* **2002**, *277* (45), 42523–42529. https://doi.org/10.1074/jbc.M200863200.

39. Wiame, E.; Duquenne, A.; Delpierre, G.; Van Schaftingen, E. Identification of Enzymes Acting on α-Glycated Amino Acids in *Bacillus Subtilis*. *FEBS Lett.* **2004**, *577* (3), 469–472. https://doi.org/10.1016/j.febslet.2004.10.049.

40. Bui, T. P. N.; Ritari, J.; Boeren, S.; De Waard, P.; Plugge, C. M.; De Vos, W. M. Production of Butyrate from Lysine and the Amadori Product Fructoselysine by a Human Gut Commensal. *Nat. Commun.* **2015**, *6*, 1–10. https://doi.org/10.1038/ncomms10062.

41. Xie, J.; Reverdatto, S.; Frolov, A.; Hoffmann, R.; Burz, D. S.; Shekhtman, A. Structural Basis for Pattern Recognition by the Receptor for Advanced Glycation End Products (RAGE). *J. Biol. Chem.* **2008**, *283* (40), 27255–27269. https://doi.org/10.1074/jbc.M801622200.

R

42. Brings, S.; Fleming, T.; Freichel, M.; Muckenthaler, M. U.; Herzig, S.; Nawroth, P. P. Dicarbonyls and Advanced Glycation End-Products in the Development of Diabetic Complications and Targets for Intervention. *Int. J. Mol. Sci.* **2017**, *18* (5). https://doi.org/10.3390/ijms18050984.

43. Henle, T. Protein-Bound Advanced Glycation Endproducts (AGEs) as Bioactive Amino Acid Derivatives in Foods Review Article. *Amino Acids* **2005**, *29*, 313–322. https://doi.org/10.1007/s00726-005-0200-2.

44. Glomb, M. A.; Monnier, V. M. Mechanism of Protein Modification by Glyoxal and Glycolaldehyde, Reactive Intermediates of the Maillard Reaction. *J. Biol. Chem.* **1995**, *270* (17), 10017–10026. https://doi.org/10.1074/jbc.270.17.10017.

45. Poulsen, M. W.; Andersen, J. M.; Hedegaard, R. V.; Madsen, A. N.; Krath, B. N.; Monošík, R.; Bak, M. J.; Nielsen, J.; Holst, B.; Skibsted, L. H.; Larsen, L. H.; Dragsted, L. O. Short-Term Effects of Dietary Advanced Glycation End Products in Rats. *Br. J. Nutr.* **2016**, *115* (4), 629–636. https://doi.org/10.1017/S0007114515004833.

46. Delgado-Andrade, C.; Tessier, F. J.; Niquet-Leridon, C.; Seiquer, I.; Pilar Navarro, M. Study of the Urinary and Faecal Excretion of N ε-Carboxymethyllysine in Young Human Volunteers. *Amino Acids* **2012**, *43* (2), 595–602. https://doi.org/10.1007/s00726-011-1107-8.

47. Hellwig, M.; Auerbach, C.; Müller, N.; Samuel, P.; Kammann, S.; Beer, F.; Gunzer, F.; Henle, T. Metabolization of the Advanced Glycation End Product N -ε-Carboxymethyllysine (CML) by Different Probiotic E. Coli Strains. *J. Agric. Food Chem.* **2019**, *67* (7), 1963–1972. https://doi.org/10.1021/acs.jafc.8b06748.

48. Bui, T. P. N.; Troise, A. D.; Fogliano, V.; de Vos, W. M. Anaerobic Degradation of *N* -ε-Carboxymethyllysine, a Major Glycation End-Product, by Human Intestinal Bacteria. *J. Agric. Food Chem.* **2019**, *67* (23), 6594–6602. https://doi.org/10.1021/acs.jafc.9b02208.

49. Kislinger, T.; Fu, C.; Huber, B.; Qu, W.; Taguchi, A.; Yan, S. Du; Hofmann, M.; Yan, S. F.; Pischetsrieder, M.; Stern, D.; Schmidt, A. M. N(ε)-(Carboxymethyl)Lysine Adducts of Proteins Are Ligands for Receptor for Advanced Glycation End Products That Activate Cell Signaling Pathways and Modulate Gene Expression. *J. Biol. Chem.* **1999**, *274* (44), 31740–31749. https://doi.org/10.1074/jbc.274.44.31740.

50. van der Lugt, T.; Weseler, A.; Gebbink, W.; Vrolijk, M.; Opperhuizen, A.; Bast, A.; Van der Lugt, T.; Weseler, A. R.; Gebbink, W. A.; Vrolijk, M. F.; Opperhuizen, A.; Bast, A. Dietary Advanced Glycation Endproducts Induce an Inflammatory Response in Human Macrophages in Vitro. *Nutrients* **2018**, *10* (12), 1868. https://doi.org/10.3390/nu10121868.

51. Seiquer, I.; Rubio, L. A.; Peinado, M. J.; Delgado-Andrade, C.; Navarro, M. P. Maillard Reaction Products Modulate Gut Microbiota Composition in Adolescents. *Mol. Nutr. Food Res.* **2014**, *58* (7), 1552–1560. https://doi.org/10.1002/mnfr.201300847.

52. Aljahdali, N.; Gadonna-Widehem, P.; Delayre-Orthez, C.; Marier, D.; Garnier, B.; Carbonero, F.; Anton, P. M. Repeated Oral Exposure to N ε-Carboxymethyllysine, a Maillard Reaction Product, Alleviates Gut Microbiota Dysbiosis in Colitic Mice. *Dig. Dis. Sci.* **2017**, *62* (12), 3370–3384. https://doi.org/10.1007/s10620-017-4767-8.

53. Carding, S.; Verbeke, K.; Vipond, D. T.; Corfe, B. M.; Owen, L. J. Dysbiosis of the Gut Microbiota in Disease. *Microb. Ecol. Health Dis.* **2015**, *26* (1), 26191. https://doi.org/10.3402/mehd.v26.26191.

54. Krautkramer, K. A.; Fan, J.; Bäckhed, F. Gut Microbial Metabolites as Multi-Kingdom Intermediates. *Nat. Rev. Microbiol.* **2020**, *19* (2), 77–94. https://doi.org/10.1038/s41579-020-0438-4.

55. O'hara, A. M.; Shanahan, F. The Gut Flora as a Forgotten Organ. *EMBO Rep.* **2006**, *7* (7), 688–693. https://doi.org/10.1038/sj.embor.7400731.

56. Koppel, N.; Maini Rekdal, V.; Balskus, E. P. Chemical Transformation of Xenobiotics by the Human Gut Microbiota. *Science (80-.).* **2017**, *356* (6344), eaag2770. https://doi.org/10.1126/science. aag2770.

57. Sommer, F.; Anderson, J. M.; Bharti, R.; Raes, J.; Rosenstiel, P. The Resilience of the Intestinal Microbiota Influences Health and Disease. *Nat. Rev. Microbiol. 2017 1510* **2017**, *15* (10), 630–638. https://doi.org/10.1038/nrmicro.2017.58.

58. Licht, T. R.; Bahl, M. I. Impact of the Gut Microbiota on Chemical Risk Assessment. *Curr. Opin. Toxicol.* **2019**, *15*, 109–113. https://doi.org/10.1016/J.COTOX.2018.09.004.

59. Brüssow, H. Problems with the Concept of Gut Microbiota Dysbiosis. *Microb. Biotechnol.* **2020**, *13* (2), 423–434. https://doi.org/10.1111/1751-7915.13479.

60. Yatsunenko, T.; Rey, F. E.; Manary, M. J.; Trehan, I.; Dominguez-Bello, M. G.; Contreras, M.; Magris, M.; Hidalgo, G.; Baldassano, R. N.; Anokhin, A. P.; Heath, A. C.; Warner, B.; Reeder, J.; Kuczynski, J.; Caporaso, J. G.; Lozupone, C. A.; Lauber, C.; Clemente, J. C.; Knights, D.; Knight, R.; Gordon, J. I. Human Gut Microbiome Viewed across Age and Geography. *Nature*. Nature Publishing Group June 14, 2012, pp 222–227. https://doi.org/10.1038/nature11053.

61. Bäckhed, F.; Roswall, J.; Peng, Y.; Feng, Q.; Jia, H.; Kovatcheva-Datchary, P.; Li, Y.; Xia, Y.; Xie, H.; Zhong, H.; Khan, M. T.; Zhang, J.; Li, J.; Xiao, L.; Al-Aama, J.; Zhang, D.; Lee, Y. S.; Kotowska, D.; Colding, C.; Tremaroli, V.; Yin, Y.; Bergman, S.; Xu, X.; Madsen, L.; Kristiansen, K.; Dahlgren, J.; Jun, W. Dynamics and Stabilization of the Human Gut Microbiome during the First Year of Life. *Cell Host Microbe* **2015**, *17* (5), 690–703. https://doi.org/10.1016/j.chom.2015.04.004.

62. Rothschild, D.; Weissbrod, O.; Barkan, E.; Kurilshikov, A.; Korem, T.; Zeevi, D.; Costea, P. I.; Godneva, A.; Kalka, I. N.; Bar, N.; Shilo, S.; Lador, D.; Vila, A. V.; Zmora, N.; Pevsner-Fischer, M.; Israeli, D.; Kosower, N.; Malka, G.; Wolf, B. C.; Avnit-Sagi, T.; Lotan-Pompan, M.; Weinberger, A.; Halpern, Z.; Carmi, S.; Fu, J.; Wijmenga, C.; Zhernakova, A.; Elinav, E.; Segal, E. Environment Dominates over Host Genetics in Shaping Human Gut Microbiota. *Nat. 2018 5557695* **2018**, *555* (7695), 210–215. https://doi.org/10.1038/nature25973.

63. Sousa, T.; Paterson, R.; Moore, V.; Carlsson, A.; Abrahamsson, B.; Basit, A. W. The Gastrointestinal Microbiota as a Site for the Biotransformation of Drugs. *Int. J. Pharm.* **2008**, *363* (1–2), 1–25. https://doi.org/10.1016/J.IJPHARM.2008.07.009.

64. Spanogiannopoulos, P.; Bess, E. N.; Carmody, R. N.; Turnbaugh, P. J. The Microbial Pharmacists within Us: A Metagenomic View of Xenobiotic Metabolism. *Nat. Rev. Microbiol.* **2016**, *14* (5), 273–287. https://doi.org/10.1038/nrmicro.2016.17.

65. Sommer, F.; Bäckhed, F. The Gut Microbiota — Masters of Host Development and Physiology. *Nat. Rev. Microbiol.* **2013**, *11* (4), 227–238. https://doi.org/10.1038/nrmicro2974.

66. Bernstein, C. N.; Burchill, C.; Targownik, L. E.; Singh, H.; Roos, L. L. Events Within the First Year of Life, but Not the Neonatal Period, Affect Risk for Later Development of Inflammatory Bowel Diseases. *Gastroenterology* **2019**, *156* (8), 2190-2197.e10. https://doi.org/10.1053/J. GASTRO.2019.02.004.

67. Huttenhower, C.; Gevers, D.; Knight, R.; et al. Structure, Function and Diversity of the Healthy Human Microbiome. *Nature* **2012**, *486* (7402), 207–214. https://doi.org/10.1038/nature11234.

68. Gilbert, J. A.; Blaser, M. J.; Caporaso, J. G.; Jansson, J. K.; Lynch, S. V.; Knight, R. Current Understanding of the Human Microbiome. *Nat. Med. 2018 244* **2018**, *24* (4), 392–400. https:// doi.org/10.1038/nm.4517.

R

69. Fassarella, M.; Blaak, E. E.; Penders, J.; Nauta, A.; Smidt, H.; Zoetendal, E. G. Gut Microbiome Stability and Resilience: Elucidating the Response to Perturbations in Order to Modulate Gut Health. *Gut*. BMJ Publishing Group March 1, 2021, pp 595–605. https://doi.org/10.1136/gutjnl-2020-321747.

70. Bhalodi, A. A.; Van Engelen, T. S. R.; Virk, H. S.; Wiersinga, W. J. Impact of Antimicrobial Therapy on the Gut Microbiome. *J. Antimicrob. Chemother.* **2019**, *74* (Supplement_1), i6–i15. https://doi.org/10.1093/JAC/DKY530.

71. Jin, J.; Beekmann, K.; Ringø, E.; Rietjens, I. M. C. M.; Xing, F. Interaction between Food-Borne Mycotoxins and Gut Microbiota: A Review. *Food Control* **2021**, *126*, 107998. https://doi.org/10.1016/J.FOODCONT.2021.107998.

72. Derrien, M.; Alvarez, A. S.; de Vos, W. M. The Gut Microbiota in the First Decade of Life. *Trends Microbiol.* **2019**, *27* (12), 997–1010. https://doi.org/10.1016/J.TIM.2019.08.001.

73. Dogra, S.; Sakwinska, O.; Soh, S.-E.; Ngom-Bru, C.; Brück, W. M.; Berger, B.; Brüssow, H.; Karnani, N.; Lee, Y. S.; Yap, F.; Chong, Y.-S.; Godfrey, K. M.; Holbrook, J. D. Rate of Establishing the Gut Microbiota in Infancy Has Consequences for Future Health. *https://doi.org/10.1080/19490976.2015.1078051* **2015**, *6* (5), 321–325. https://doi.org/10.1080/19490976.2015.1078051.

74. Korpela, K.; de Vos, W. M. Antibiotic Use in Childhood Alters the Gut Microbiota and Predisposes to Overweight. *Microb. Cell* **2016**, *3* (7), 296. https://doi.org/10.15698/MIC2016.07.514.

75. Korpela, K.; de Vos, W. M. Early Life Colonization of the Human Gut: Microbes Matter Everywhere. *Curr. Opin. Microbiol.* **2018**, *44*, 70–78. https://doi.org/10.1016/J.MIB.2018.06.003.

76. Guaraldi, F.; Salvatori, G. Effect of Breast and Formula Feeding on Gut Microbiota Shaping in Newborns. *Front. Cell. Infect. Microbiol.* **2012**, *2*, 94. https://doi.org/10.3389/fcimb.2012.00094.

77. Sillner, N.; Walker, A.; Lucio, M.; Maier, T. V.; Bazanella, M.; Rychlik, M.; Haller, D.; Schmitt-Kopplin, P. Longitudinal Profiles of Dietary and Microbial Metabolites in Formula- and Breastfed Infants. *Front. Mol. Biosci.* **2021**, *8*, 490. https://doi.org/10.3389/FMOLB.2021.660456/BIBTEX.

78. Bazanella, M.; Maier, T. V.; Clavel, T.; Lagkouvardos, I.; Lucio, M.; Maldonado-Gòmez, M. X.; Autran, C.; Walter, J.; Bode, L.; Schmitt-Kopplin, P.; Haller, D. Randomized Controlled Trial on the Impact of Early-Life Intervention with Bifidobacteria on the Healthy Infant Fecal Microbiota and Metabolome. *Am. J. Clin. Nutr.* **2017**, *106* (5), 1274–1286. https://doi.org/10.3945/AJCN.117.157529.

79. Ma, J.; Li, Z.; Zhang, W.; Zhang, C.; Zhang, Y.; Mei, H.; Zhuo, N.; Wang, H.; Wang, L.; Wu, D. Comparison of Gut Microbiota in Exclusively Breast-Fed and Formula-Fed Babies: A Study of 91 Term Infants. *Sci. Reports 2020 101* **2020**, *10* (1), 1–11. https://doi.org/10.1038/s41598-020-72635-x.

80. World Health Organization. *Global Nutrition Targets 2025: Breastfeeding Policy Brief.*; 2014.

81. Le Doare, K.; Holder, B.; Bassett, A.; Pannaraj, P. S. Mother's Milk: A Purposeful Contribution to the Development of the Infant Microbiota and Immunity. *Front. Immunol.* **2018**, *9*, 361. https://doi.org/10.3389/fimmu.2018.00361.

82. Vandenplas, Y.; Berger, B.; Carnielli, V. P.; Ksiazyk, J.; Lagström, H.; Luna, M. S.; Migacheva, N.; Mosselmans, J. M.; Picaud, J. C.; Possner, M.; Singhal, A.; Wabitsch, M. Human Milk Oligosaccharides: 2'-Fucosyllactose (2'-FL) and Lacto-N-Neotetraose (LNnT) in Infant Formula. *Nutr. 2018, Vol. 10, Page 1161* **2018**, *10* (9), 1161. https://doi.org/10.3390/NU10091161.

83. Vandenplas, Y.; De Greef, E.; Veereman, G. Prebiotics in Infant Formula. *https://doi.org/10.4161/19490976.2014.972237* **2015**, *5* (6), 681–687. https://doi.org/10.4161/19490976.2014.972237.

84. Boudry, G.; Charton, E.; Le Huerou-Luron, I.; Ferret-Bernard, S.; Le Gall, S.; Even, S.; Blat, S. The Relationship Between Breast Milk Components and the Infant Gut Microbiota. *Front. Nutr.* **2021**, *8*, 87. https://doi.org/10.3389/FNUT.2021.629740/BIBTEX.

85. Akkerman, R.; Faas, M. M.; de Vos, P. Non-Digestible Carbohydrates in Infant Formula as Substitution for Human Milk Oligosaccharide Functions: Effects on Microbiota and Gut Maturation. *https://doi.org/10.1080/10408398.2017.1414030* **2018**, *59* (9), 1486–1497. https://doi.org/10.1080/10408398.2017.1414030.

86. Xie, Y.; van der Fels-Klerx, H. J.; van Leeuwen, S. P. J.; Fogliano, V. Dietary Advanced Glycation End-Products, 2-Monochloropropane-1,3-Diol Esters and 3-Monochloropropane-1,2-Diol Esters and Glycidyl Esters in Infant Formulas: Occurrence, Formulation and Processing Effects, Mitigation Strategies. *Compr. Rev. Food Sci. Food Saf.* **2021**, *20* (6), 5489–5515. https://doi.org/10.1111/1541-4337.12842.

87. Martysiak-Zurowska, D.; Stolyhwo, A. Content of Furosine in Infant Formulae and Follow-on Formulae. *Polish J. Food Nutr. Sci.* **2007**, *57* (2), 185–190.

88. Ph van Trijp, M.; Wilms, E.; Ríos-Morales, M.; Masclee, A. A.; Brummer, R. J.; Witteman, B. J.; Troost, F. J.; Hooiveld, G. J. Using Naso- and Oro-Intestinal Catheters in Physiological Research for Intestinal Delivery and Sampling in Vivo: Practical and Technical Aspects to Be Considered. *Am. J. Clin. Nutr.* **2021**, *114* (3), 843–861. https://doi.org/10.1093/AJCN/NQAB149.

89. Behr, C.; Sperber, S.; Jiang, X.; Strauss, V.; Kamp, H.; Walk, T.; Herold, M.; Beekmann, K.; Rietjens, I. M. C. M.; van Ravenzwaay, B. Microbiome-Related Metabolite Changes in Gut Tissue, Cecum Content and Feces of Rats Treated with Antibiotics. *Toxicol. Appl. Pharmacol.* **2018**, *355*, 198–210. https://doi.org/10.1016/j.taap.2018.06.028.

90. Visconti, A.; Le Roy, C. I.; Rosa, F.; Rossi, N.; Martin, T. C.; Mohney, R. P.; Li, W.; de Rinaldis, E.; Bell, J. T.; Venter, J. C.; Nelson, K. E.; Spector, T. D.; Falchi, M. Interplay between the Human Gut Microbiome and Host Metabolism. *Nat. Commun. 2019 101* **2019**, *10* (1), 1–10. https://doi.org/10.1038/s41467-019-12476-z.

91. Zierer, J.; Jackson, M. A.; Kastenmüller, G.; Mangino, M.; Long, T.; Telenti, A.; Mohney, R. P.; Small, K. S.; Bell, J. T.; Steves, C. J.; Valdes, A. M.; Spector, T. D.; Menni, C. The Fecal Metabolome as a Functional Readout of the Gut Microbiome. *Nat. Genet. 2018 506* **2018**, *50* (6), 790–795. https://doi.org/10.1038/s41588-018-0135-7.

92. Hugenholtz, F.; de Vos, W. M. Mouse Models for Human Intestinal Microbiota Research: A Critical Evaluation. *Cell. Mol. Life Sci.* **2018**, *75* (1), 149–160. https://doi.org/10.1007/S00018-017-2693-8/FIGURES/3.

93. Knight, R.; Vrbanac, A.; Taylor, B. C.; Aksenov, A.; Callewaert, C.; Debelius, J.; Gonzalez, A.; Kosciolek, T.; McCall, L. I.; McDonald, D.; Melnik, A. V.; Morton, J. T.; Navas, J.; Quinn, R. A.; Sanders, J. G.; Swafford, A. D.; Thompson, L. R.; Tripathi, A.; Xu, Z. Z.; Zaneveld, J. R.; Zhu, Q.; Caporaso, J. G.; Dorrestein, P. C. Best Practices for Analysing Microbiomes. *Nat. Rev. Microbiol. 2018 167* **2018**, *16* (7), 410–422. https://doi.org/10.1038/s41579-018-0029-9.

94. Liu, Y. X.; Qin, Y.; Chen, T.; Lu, M.; Qian, X.; Guo, X.; Bai, Y. A Practical Guide to Amplicon and Metagenomic Analysis of Microbiome Data. *Protein Cell* **2021**, *12* (5), 315–330. https://doi.org/10.1007/S13238-020-00724-8/TABLES/3.

95. Bauermeister, A.; Mannochio-Russo, H.; Costa-Lotufo, L. V.; Jarmusch, A. K.; Dorrestein, P. C. Mass Spectrometry-Based Metabolomics in Microbiome Investigations. *Nat. Rev. Microbiol. 2021 203* **2021**, *20* (3), 143–160. https://doi.org/10.1038/s41579-021-00621-9.

R

96. Lindon, J. C.; Holmes, E.; Bollard, M. E.; Stanley, E. G.; Nicholson, J. K. Metabonomics Technologies and Their Applications in Physiological Monitoring, Drug Safety Assessment and Disease Diagnosis. *Biomarkers* **2004**, *9* (1), 1–31. https://doi.org/10.1080/13547500410001668379.

97. Vernocchi, P.; Del Chierico, F.; Putignani, L. Gut Microbiota Profiling: Metabolomics Based Approach to Unravel Compounds Affecting Human Health. *Front. Microbiol.* **2016**, *7* (JUL), 1144. https://doi.org/10.3389/FMICB.2016.01144/BIBTEX.

98. Parish, S. T.; Aschner, M.; Casey, W.; Corvaro, M.; Embry, M. R.; Fitzpatrick, S.; Kidd, D.; Kleinstreuer, N. C.; Lima, B. S.; Settivari, R. S.; Wolf, D. C.; Yamazaki, D.; Boobis, A. An Evaluation Framework for New Approach Methodologies (NAMs) for Human Health Safety Assessment. *Regul. Toxicol. Pharmacol.* **2020**, *112*, 104592. https://doi.org/10.1016/J.YRTPH.2020.104592.

99. Louisse, J.; Beekmann, K.; Rietjens, I. M. C. M. Use of Physiologically Based Kinetic Modeling-Based Reverse Dosimetry to Predict in Vivo Toxicity from in Vitro Data. *Chem. Res. Toxicol.* **2016**, *30* (1), 114–125. https://doi.org/10.1021/ACS.CHEMRESTOX.6B00302.

100. Mendez-Catala, D. M.; Wang, Q.; Rietjens, I. M. C. M. PBK Model-Based Prediction of Intestinal Microbial and Host Metabolism of Zearalenone and Consequences for Its Estrogenicity. *Mol. Nutr. Food Res.* **2021**, *65* (23), 2100443. https://doi.org/10.1002/MNFR.202100443.

101. Wang, Q.; Spenkelink, B.; Boonpawa, R.; Rietjens, I. M. C. M. Use of Physiologically Based Pharmacokinetic Modeling to Predict Human Gut Microbial Conversion of Daidzein to S-Equol. *J. Agric. Food Chem.* **2022**, *70* (1), 343–352. https://doi.org/10.1021/ACS.JAFC.1C03950/SUPPL_FILE/JF1C03950_SI_001.ZIP.

102. Piperi, C. Dietary Advanced Glycation End-Products: Molecular Mechanisms and Preventive Tools. *Current Nutrition Reports*. Current Science Inc. March 1, 2017, pp 1–8. https://doi.org/10.1007/s13668-017-0188-8.

103. Uribarri, J.; Woodruff, S.; Goodman, S.; Cai, W.; Chen, X.; Pyzik, R.; Yong, A.; Striker, G. E.; Vlassara, H. Advanced Glycation End Products in Foods and a Practical Guide to Their Reduction in the Diet. *J. Am. Diet. Assoc.* **2010**, *110* (6), 911-16.e12. https://doi.org/10.1016/j.jada.2010.03.018.

104. Maillard, L. C. Action Des Acides Amines Sur Les Sucres; Formation Des Melanoidines Par Voie Methodique. *Comptes R. Acad. Sci.* **1912**, *154*, 66–68.

105. Nguyen, H. T.; van der Fels-Klerx, H. J.; van Boekel, M. A. J. S. N ∈ -(Carboxymethyl)Lysine: A Review on Analytical Methods, Formation, and Occurrence in Processed Food, and Health Impact. *Food Rev. Int.* **2014**, *30* (1), 36–52. https://doi.org/10.1080/87559129.2013.853774.

106. Yaylayan, V. A.; Huyghues-Despointes, A.; Feather, M. S. Chemistry of Amadori Rearrangement Products: Analysis, Synthesis, Kinetics, Reactions, and Spectroscopic Properties. *Crit. Rev. Food Sci. Nutr.* **1994**, *34* (4), 321–369.

107. Buetler, T. M.; Leclerc, E.; Baumeyer, A.; Latado, H.; Newell, J.; Adolfsson, O.; Parisod, V.; Richoz, J.; Maurer, S.; Foata, F.; Piguet, D.; Junod, S.; Heizmann, C. W.; Delatour, T. Nε-Carboxymethyllysine-Modified Proteins Are Unable to Bind to RAGE and Activate an Inflammatory Response. *Mol. Nutr. Food Res.* **2008**, *52* (3), 370–378. https://doi.org/10.1002/mnfr.200700101.

108. Liang, Z.; Chen, X.; Li, L.; Li, B.; Yang, Z. The Fate of Dietary Advanced Glycation End Products in the Body: From Oral Intake to Excretion. *Critical Reviews in Food Science and Nutrition*. Taylor and Francis Inc. 2019. https://doi.org/10.1080/10408398.2019.1693958.

109. Perrone, A.; Giovino, A.; Benny, J.; Martinelli, F. Advanced Glycation End Products (AGEs): Biochemistry, Signaling, Analytical Methods, and Epigenetic Effects. *Oxidative Medicine and Cellular Longevity*. 2020. https://doi.org/10.1155/2020/3818196.

110. Delgado-Andrade, C. Carboxymethyl-Lysine: Thirty Years of Investigation in the Field of AGE Formation. *Food Funct.* **2016**, *7* (1), 46–57. https://doi.org/10.1039/C5FO00918A.

111. Zeng, J.; Davies, M. J. Evidence for the Formation of Adducts and S-(Carboxymethyl)Cysteine on Reaction of r-Dicarbonyl Compounds with Thiol Groups on Amino Acids, Peptides, and Proteins. *Chem. Res. Toxicol.* **2005**, *18*. https://doi.org/10.1021/tx050074u.

112. Ahmed, M. U.; Brinkmann Frye, E.; Degenhardt, T. P.; Thorpe, S. R.; Baynes, J. W. Nε-(Carboxyethyl) Lysine, a Product of the Chemical Modification of Proteins by Methylglyoxal, Increases with Age in Human Lens Proteins. *Biochem. J.* **1997**, *324* (2), 565–570. https://doi.org/10.1042/bj3240565.

113. Klöpfer, A.; Spanneberg, R.; Glomb, M. A. Formation of Arginine Modifications in a Model System of N α- Tert -Butoxycarbonyl (Boc)-Arginine with Methylglyoxal. *J. Agric. Food Chem.* **2011**, *59* (1), 394–401. https://doi.org/10.1021/jf103116c.

114. Miyata, S. Accumulation of Pyrraline-Modified Albumin in Phagocytes Due to Reduced Degradation by Lysosomal Enzymes. *J. Biol. Chem.* **1997**, *272* (7), 4037–4042. https://doi.org/10.1074/jbc.272.7.4037.

115. Monnier, V. M.; Nagaraj, R. H.; Portero-Otin, M.; Glomb, M.; Elgawish, A. H.; Sell, D. R.; Friedlander, M. A. Structure of Advanced Maillard Reaction Products and Their Pathological Role. In *Nephrology Dialysis Transplantation*; Oxford University Press, 1996; Vol. 11, pp 20–26. https://doi.org/10.1093/ndt/11.supp5.20.

116. Tsukushi, S.; Katsuzaki, T.; Aoyama, I.; Takayama, F.; Miyazaki, T.; Shimokata, K.; Niwa, T. Increased Erythrocyte 3-DG and AGEs in Diabetic Hemodialysis Patients: Role of the Polyol Pathway. *Kidney Int.* **1999**, *55* (5), 1970–1976. https://doi.org/10.1046/j.1523-1755.1999.00418.x.

117. Niwa, H.; Takeda, A.; Wakai, M.; Miyata, T.; Yasuda, Y.; Mitsuma, T.; Kurokawa, K.; Sobue, G. Accelerated Formation of N(ε)-(Carboxymethyl) Lysine, an Advanced Glycation End Product, by Glyoxal and 3-Deoxyglucosone in Cultured Rat Sensory Neurons. *Biochem. Biophys. Res. Commun.* **1998**, *248* (1), 93–97. https://doi.org/10.1006/bbrc.1998.8899.

118. Niwa, T.; Katsuzaki, T.; Ishizaki, Y.; Hayase, F.; Miyazaki, T.; Uematsu, T.; Tatemichi, N.; Takei, Y. Imidazolone, a Novel Advanced Glycation End Product, Is Present at High Levels in Kidneys of Rats with Streptozotocin-Induced Diabetes. *FEBS Lett.* **1997**, *407* (3), 297–302. https://doi.org/10.1016/S0014-5793(97)00362-1.

119. Ott, C.; Jacobs, K.; Haucke, E.; Navarrete Santos, A.; Grune, T.; Simm, A. Role of Advanced Glycation End Products in Cellular Signaling. *Redox Biology*. Elsevier B.V. 2014, pp 411–429. https://doi.org/10.1016/j.redox.2013.12.016.

120. Liu, J.; Desai, K.; Wang, R.; Wu, L. Up-Regulation of Aldolase A and Methylglyoxal Production in Adipocytes. *Br. J. Pharmacol.* **2013**, *168* (7), 1639–1646. https://doi.org/10.1111/bph.12046.

121. Ramasamy, R.; Yan, S. F.; Schmidt, A. M. Methylglyoxal Comes of AGE. *Cell*. 2006, pp 258–260. https://doi.org/10.1016/j.cell.2006.01.002.

122. Feskens, E.; Brennan, L.; Dussort, P.; Flourakis, M.; Lindner, L. M. E.; Mela, D.; Rabbani, N.; Rathmann, W.; Respondek, F.; Stehouwer, C.; Theis, S.; Thornalley, P.; Vinoy, S. Potential Markers of Dietary Glycemic Exposures for Sustained Dietary Interventions in Populations without Diabetes. *Advances in Nutrition*. Oxford University Press September 15, 2020, pp 1221–1236. https://doi.org/10.1093/advances/nmaa058.

123. Bieme, K. M.; Alexander Fried, D.; Lederer, M. O. Identification and Quantification of Major Maillard Cross-Links in Human Serum Albumin and Lens Protein: Evidence for Glucosepane as the Dominant Compound. *J. Biol. Chem.* **2002**, *277* (28), 24907–24915. https://doi.org/10.1074/jbc.M202681200.

R

124. Sell, D. R.; Biemel, K. M.; Reihl, O.; Lederer, M. O.; Strauch, C. M.; Monnier, V. M. Glucosepane Is a Major Protein Cross-Link of the Senescent Human Extracellular Matrix. *J. Biol. Chem.* **2005**, *280* (13), 12310–12315. https://doi.org/10.1074/jbc.M500733200.

125. Uribarri, J.; Cai, W.; Sandu, O.; Peppa, M.; Goldberg, T.; Vlassara, H. Diet-Derived Advanced Glycation End Products Are Major Contributors to the Body's AGE Pool and Induce Inflammation in Healthy Subjects. *Ann. N. Y. Acad. Sci.* **2005**, *1043* (1), 461–466. https://doi.org/10.1196/annals.1333.052.

126. Vlassara, H.; Cai, W.; Crandall, J.; Goldberg, T.; Oberstein, R.; Dardaine, V.; Peppa, M.; Rayfield, E. J. Inflammatory Mediators Are Induced by Dietary Glycotoxins, a Major Risk Factor for Diabetic Angiopathy. *Proc. Natl. Acad. Sci. U. S. A.* **2002**, *99* (24), 15596–15601. https://doi.org/10.1073/pnas.242407999.

127. Uribarri, J.; Peppa, M.; Cai, W.; Goldberg, T.; Lu, M.; He, C.; Vlassara, H. Restriction of Dietary Glycotoxins Reduces Excessive Advanced Glycation End Products in Renal Failure Patients. *J. Am. Soc. Nephrol.* **2003**, *14* (3), 728–731. https://doi.org/10.1097/01.ASN.0000051593.41395.B9.

128. Uribarri, J.; Peppa, M.; Cai, W.; Goldberg, T.; Lu, M.; Baliga, S.; Vassalotti, J. A.; Vlassara, H. Dietary Glycotoxins Correlate with Circulating Advanced Glycation End Product Levels in Renal Failure Patients. *Am. J. Kidney Dis.* **2003**, *42* (3), 532–538. https://doi.org/10.1016/S0272-6386(03)00779-0.

129. Erbersdobler, H. F.; Faist, V. Metabolic Transit of Amadori Products. *Nahrung/Food* **2001**, *45* (3), 177–181. https://doi.org/10.1002/1521-3803(20010601)45:3<177::AID-FOOD177>3.0.CO;2-A.

130. Lee, K.; Erbersdobler, H. F. Balance Experiments on Human Volunteers with ε-Fructoselysine (FL) and Lysinoalanine (LAL). *Mail. React. Chem. Food Heal.* **2005**, 358–363. https://doi.org/10.1533/9781845698393.4.358.

131. Hellwig, M.; Matthes, R.; Peto, A.; Löbner, J.; Henle, T. N-ε-Fructosyllysine and N-ε-Carboxymethyllysine, but Not Lysinoalanine, Are Available for Absorption after Simulated Gastrointestinal Digestion. *Amino Acids* **2014**, *46* (2), 289–299. https://doi.org/10.1007/s00726-013-1501-5.

132. Xu, H.; Wang, Z.; Wang, Y.; Hu, S.; Liu, N. Biodistribution and Elimination Study of Fluorine-18 Labeled Nε-Carboxymethyl-Lysine Following Intragastric and Intravenous Administration. *PLoS One* **2013**, *8* (3), e57897. https://doi.org/10.1371/journal.pone.0057897.

133. Li, M.; Zeng, M.; He, Z.; Zheng, Z.; Qin, F.; Tao, G.; Zhang, S.; Chen, J. Effects of Long-Term Exposure to Free Nε-(Carboxymethyl)Lysine on Rats Fed a High-Fat Diet. *J. Agric. Food Chem.* **2015**, *63* (51), 10995–11001. https://doi.org/10.1021/acs.jafc.5b05750.

134. Alamir, I.; Niquet-Leridon, C.; Jacolot, P.; Rodriguez, C.; Orosco, M.; Anton, P. M.; Tessier, F. J. Digestibility of Extruded Proteins and Metabolic Transit of N E-Carboxymethyllysine in Rats. *Amino Acids* **2012**, *44*, 1441–1449. https://doi.org/10.1007/s00726-012-1427-3.

135. Delgado-Andrade, C.; Tessier, F. É. J.; Niquet-Leridon, C.; Seiquer, I.; Navarro, M. P. Study of the Urinary and Faecal Excretion of Ne-Carboxymethyllysine in Young Human Volunteers. *Amino Acids* **2012**, *43* (2), 595–602. https://doi.org/10.1007/s00726-011-1107-8.

136. Degen, J.; Vogel, M.; Richter, D.; Hellwig, M.; Henle, T. Metabolic Transit of Dietary Methylglyoxal. In *Journal of Agricultural and Food Chemistry*; American Chemical Society, 2013; Vol. 61, pp 10253–10260. https://doi.org/10.1021/jf304946p.

137. Degen, J.; Beyer, H.; Heymann, B.; Hellwig, M.; Henle, T. Dietary Influence on Urinary Excretion of 3-Deoxyglucosone and Its Metabolite 3-Deoxyfructose. *J. Agric. Food Chem.* **2014**, *62* (11), 2449–2456. https://doi.org/10.1021/jf405546q.

138. Brighina, S.; Poveda Turrado, C.; Restuccia, C.; Walton, G.; Fallico, B.; Oruna-Concha, M. J.; Arena, E. Detrimental Effect on the Gut Microbiota of 1,2-Dicarbonyl Compounds after in Vitro Gastro-Intestinal and Fermentative Digestion. *Food Chem.* **2021**, *341*, 128237. https://doi.org/10.1016/j.foodchem.2020.128237.

139. Van Der Lugt, T.; Venema, K.; Van Leeuwen, S.; Vrolijk, M. F.; Opperhuizen, A.; Bast, A. Gastrointestinal Digestion of Dietary Advanced Glycation Endproducts Using an: In Vitro Model of the Gastrointestinal Tract (TIM-1). *Food Funct.* **2020**, *11* (7), 6297–6307. https://doi.org/10.1039/d0fo00450b.

140. Hellwig, M.; Geissler, S.; Peto, A.; Knütter, I.; Brandsch, M.; Henle, T. Transport of Free and Peptide-Bound Pyrraline at Intestinal and Renal Epithelial Cells. *J. Agric. Food Chem.* **2009**, *57* (14), 6474–6480. https://doi.org/10.1021/jf901224p.

141. Stefanie, G.; Michael, H.; Madlen, Z.; Fritz, M.; Thomas, H.; Matthias, B. Transport of the Advanced Glycation End Products Alanylpyrraline and Pyrralylalanine by the Human Proton-Coupled Peptide Transporter HPEPT1. *J. Agric. Food Chem.* **2010**, *58* (4), 2543–2547. https://doi.org/10.1021/jf903791u.

142. Zhao, D.; Sheng, B.; Wu, Y.; Li, H.; Xu, D.; Nian, Y.; Mao, S.; Li, C.; Xu, X.; Zhou, G. Comparison of Free and Bound Advanced Glycation End Products in Food: A Review on the Possible Influence on Human Health. *Journal of Agricultural and Food Chemistry*. American Chemical Society December 26, 2019, pp 14007–14018. https://doi.org/10.1021/acs.jafc.9b05891.

143. Finot, P. A.; Magnenat, E. Metabolic Transit of Early and Advanced Maillard Products. *Prog. Food Nutr. Sci.* **1981**, *5*, 193–207.

144. Sano, H.; Higashi, T.; Matsumoto, K.; Melkko, J.; Jinnouchi, Y.; Ikeda, K.; Ebina, Y.; Makino, H.; Smedsrød, B.; Horiuchi, S. Insulin Enhances Macrophage Scavenger Receptor-Mediated Endocytic Uptake of Advanced Glycation End Products. *J. Biol. Chem.* **1998**, *273* (15), 8630–8637. https://doi.org/10.1074/jbc.273.15.8630.

145. Svistounov, D.; Smedsrød, B. Hepatic Clearance of Advanced Glycation End Products (AGEs)—Myth or Truth? *J. Hepatol.* **2004**, *41* (6), 1038–1040. https://doi.org/10.1016/J.JHEP.2004.10.004.

146. Hansen, B.; Svistounov, D.; Olsen, R.; Nagai, R.; Horiuchi, S.; Smedsrød, B. Advanced Glycation End Products Impair the Scavenger Function of Rat Hepatic Sinusoidal Endothelial Cells. *Diabetologia* **2002**, *45*, 1379–1388. https://doi.org/10.1007/s00125-002-0912-8.

147. Dobi, A.; Rosanaly, S.; Devin, A.; Baret, P.; Meilhac, O.; Harry, G. J.; d'Hellencourt, C. L.; Rondeau, P. Advanced Glycation End-Products Disrupt Brain Microvascular Endothelial Cell Barrier: The Role of Mitochondria and Oxidative Stress. *Microvasc. Res.* **2021**, *133*, 104098. https://doi.org/10.1016/J.MVR.2020.104098.

148. Li, M.; Zeng, M.; He, Z.; Zheng, Z.; Qin, F.; Tao, G.; Zhang, S.; Chen, J. Increased Accumulation of Protein-Bound N ε-(Carboxymethyl)Lysine in Tissues of Healthy Rats after Chronic Oral N ε-(Carboxymethyl)Lysine. *J. Agric. Food Chem.* **2015**, *63*, 1658–1663. https://doi.org/10.1021/jf505063t.

149. de Courten, B.; de Courten, M. P.; Soldatos, G.; Dougherty, S. L.; Straznicky, N.; Schlaich, M.; Sourris, K. C.; Chand, V.; Scheijen, J. L.; Kingwell, B. A.; Cooper, M. E.; Schalkwijk, C. G.; Walker, K. Z.; Forbes, J. M. Diet Low in Advanced Glycation End Products Increases Insulin Sensitivity in Healthy Overweight Individuals: A Double-Blind, Randomized, Crossover Trial. *Am. J. Clin. Nutr.* **2016**, *103* (6), 1426–1433. https://doi.org/10.3945/ajcn.115.125427.

R

150. Semba, R. D.; Ang, A.; Talegawkar, S.; Crasto, C.; Dalal, M.; Jardack, P.; Traber, M. G.; Ferrucci, L.; Arab, L. Dietary Intake Associated with Serum versus Urinary Carboxymethyl-Lysine, a Major Advanced Glycation End Product, in Adults: The Energetics Study. *Eur. J. Clin. Nutr.* **2012**, *66* (1), 3–9. https://doi.org/10.1038/ejcn.2011.139.

151. van Dongen, K. C. W.; Linkens, A. M. A.; Wetzels, S. M. W.; Wouters, K.; Vanmierlo, T.; van de Waarenburg, M. P. H.; L.J.M. Scheijen, J.; de Vos, W. M.; Belzer, C.; Schalkwijk, C. G. Dietary Advanced Glycation Endproducts (AGEs) Increase Their Concentration in Plasma and Tissues, Result in Inflammation and Modulate Gut Microbial Composition in Mice; Evidence for Reversibility. *Food Res. Int.* **2021**, *147*, 110547. https://doi.org/10.1016/J.FOODRES.2021.110547.

152. Uribarri, J.; Cai, W.; Ramdas, M.; Goodman, S.; Pyzik, R.; Xue, C.; Li, Z.; Striker, G. E.; Vlassara, H. Restriction of Advanced Glycation End Products Improves Insulin Resistance in Human Type 2 Diabetes: Potential Role of AGER1 and SIRT1. *Diabetes Care* **2011**, *34* (7), 1610–1616. https://doi.org/10.2337/dc11-0091.

153. Peppa, M.; He, C.; Hattori, M.; McEvoy, R.; Zheng, F.; Vlassara, H. Fetal or Neonatal Low-Glycotoxin Environment Prevents Autoimmune Diabetes in NOD Mice. *Diabetes* **2003**, *52* (6), 1441–1448. https://doi.org/10.2337/diabetes.52.6.1441.

154. Hofmann, S. M.; Dong, H. J.; Li, Z.; Cai, W.; Altomonte, J.; Thung, S. N.; Zeng, F.; Fisher, E. A.; Vlassara, H. Improved Insulin Sensitivity Is Associated with Restricted Intake of Dietary Glycoxidation Products in the Db/Db Mouse. *Diabetes* **2002**, *51* (7), 2082–2089. https://doi.org/10.2337/diabetes.51.7.2082.

155. Lin, R. Y.; Reis, E. D.; Dore, A. T.; Lu, M.; Ghodsi, N.; Fallon, J. T.; Fisher, E. A.; Vlassara, H. Lowering of Dietary Advanced Glycation Endproducts (AGE) Reduces Neointimal Formation after Arterial Injury in Genetically Hypercholesterolemic Mice. *Atherosclerosis* **2002**, *163* (2), 303–311. https://doi.org/10.1016/S0021-9150(02)00008-4.

156. Zheng, F.; He, C.; Cai, W.; Hattori, M.; Steffes, M.; Vlassara, H. Prevention of Diabetic Nephropathy in Mice by a Diet Low in Glycoxidation Products. *Diabetes. Metab. Res. Rev.* **2002**, *18* (3), 224–237. https://doi.org/10.1002/dmrr.283.

157. Lin, R. Y.; Choudhury, R. P.; Cai, W.; Lu, M.; Fallon, J. T.; Fisher, E. A.; Vlassara, H. Dietary Glycotoxins Promote Diabetic Atherosclerosis in Apolipoprotein E-Deficient Mice. *Atherosclerosis* **2003**, *168* (2), 213–220. https://doi.org/10.1016/S0021-9150(03)00050-9.

158. Tuohy, K. M.; Hinton, D. J. S.; Davies, S. J.; Crabbe, M. J. C.; Gibson, G. R.; Ames, J. M. Metabolism of Maillard Reaction Products by the Human Gut Microbiota – Implications for Health. *Mol. Nutr. Food Res.* **2006**, *50* (9), 847–857. https://doi.org/10.1002/mnfr.200500126.

159. Wiame, E.; Delpierre, G.; Collard, F.; Van Schaftingen, E. Identification of a Pathway for the Utilization of the Amadori Product Fructoselysine in Escherichia Coli. *J. Biol. Chem.* **2002**, *277* (45), 42523–42529. https://doi.org/10.1074/jbc.M200863200.

160. Veiga da-Cunha, M.; Jacquemin, P.; Delpierre, G.; Godfraind, C.; Théate, I.; Vertommen, D.; Clotman, F.; Lemaigre, F.; Devuyst, O.; van Schaftingen, E. Increased Protein Glycation in Fructosamine 3-Kinase-Deficient Mice. *Biochem. J.* **2006**, *399* (Pt 2), 257. https://doi.org/10.1042/BJ20060684.

161. van Dongen, K. C. W.; van der Zande, M.; Bruyneel, B.; Vervoort, J. J. M.; Rietjens, I. M. C. M.; Belzer, C.; Beekmann, K. An in Vitro Model for Microbial Fructoselysine Degradation Shows Substantial Interindividual Differences in Metabolic Capacities of Human Fecal Slurries. *Toxicol. Vitr.* **2021**, *72*, 105078. https://doi.org/10.1016/j.tiv.2021.105078.

162. Raj, D. S. C.; Choudhury, D.; Welbourne, T. C.; Levi, M. Advanced Glycation End Products: A Nephrologist's Perspective. *Am. J. Kidney Dis.* **2000**, *35* (3), 365–380. https://doi.org/10.1016/S0272-6386(00)70189-2.

163. Singh, R.; Barden, A.; Mori, T.; Beilin, L. Advanced Glycation End-Products: A Review. *Diabetologia* **2001**, *44* (2), 129–146. https://doi.org/10.1007/s001250051591.

164. Rabbani, N.; Thornalley, P. J. Methylglyoxal, Glyoxalase 1 and the Dicarbonyl Proteome. *Amino Acids* **2012**, *42*, 1133–1142. https://doi.org/10.1007/s00726-010-0783-0.

165. Peculis, R.; Konrade, I.; Skapare, E.; Fridmanis, D.; Nikitina-Zake, L.; Lejnieks, A.; Pirags, V.; Dambrova, M.; Klovins, J. Identification of Glyoxalase 1 Polymorphisms Associated with Enzyme Activity. *Gene* **2013**, *515* (1), 140–143. https://doi.org/10.1016/j.gene.2012.11.009.

166. Xue, M.; Rabbani, N.; Momiji, H.; Imbasi, P.; Anwar, M. M.; Kitteringham, N.; Park, B. K.; Souma, T.; Moriguchi, T.; Yamamoto, M.; Thornalley, P. J. Transcriptional Control of Glyoxalase 1 by Nrf2 Provides a Stress-Responsive Defence against Dicarbonyl Glycation. *Biochem. J.* **2012**, *443* (1), 213–222. https://doi.org/10.1042/BJ20111648.

167. Vlassara, H.; Bucala, R. Recent Progress in Advanced Glycation and Diabetic Vascular Disease: Role of Advanced Glycation End Product Receptors. *Diabetes* **1996**, *45*, 65–66. https://doi.org/10.2337/diab.45.3.s65.

168. Asadipooya, K.; Uy, E. M. Advanced Glycation End Products (AGEs), Receptor for AGEs, Diabetes, and Bone: Review of the Literature. *J. Endocr. Soc.* **2019**, *3* (10), 1799–1818. https://doi.org/10.1210/js.2019-00160.

169. Grimm, S.; Ernst, L.; Grötzinger, N.; Höhn, A.; Breusing, N.; Reinheckel, T.; Grune, T. Cathepsin D Is One of the Major Enzymes Involved in Intracellular Degradation of AGE-Modified Proteins. *Free Radic. Res.* **2010**, *44* (9), 1013–1026. https://doi.org/10.3109/10715762.2010.495127.

170. Nagai, R.; Fujiwara, Y.; Mera, K.; Otagiri, M. Investigation of Pathways of Advanced Glycation End-Products Accumulation in Macrophages. *Mol. Nutr. Food Res.* **2007**, *51* (4), 462–467. https://doi.org/10.1002/MNFR.200600255.

171. Semba, R. D.; Nicklett, E. J.; Ferrucci, L. Does Accumulation of Advanced Glycation End Products Contribute to the Aging Phenotype? *Journals Gerontol. - Ser. A Biol. Sci. Med. Sci.* **2010**, *65 A* (9), 963–975. https://doi.org/10.1093/gerona/glq074.

172. Vlassara, H. The AGE-Receptor in the Pathogenesis of Diabetic Complications. *Diabetes. Metab. Res. Rev.* **2001**, *17* (6), 436–443. https://doi.org/10.1002/dmrr.233.

173. Steenbeke, M.; Bruyne, S. De; Buyzere, M. De; Lapauw, B.; Speeckaert, R.; Petrovic, M.; Delanghe, J. R.; Speeckaert, M. M. The Role of Soluble Receptor for Advanced Glycation End-Products (SRAGE) in the General Population and Patients with Diabetes Mellitus with a Focus on Renal Function and Overall Outcome. *Crit. Rev. Clin. Lab. Sci.* **2021**, *58* (2), 113–130. https://doi.org/10.1080/10408363.2020.1791045.

174. Miyata, T.; Ueda, Y.; Horie, K.; Nangaku, M.; Tanaka, S.; de Strihou, C. van Y.; Kurokawa, K. Renal Catabolism of Advanced Glycation End Products: The Fate of Pentosidine. *Kidney Int.* **1998**, *53* (2), 416–422. https://doi.org/10.1046/j.1523-1755.1998.00756.x.

175. Mori, B.; Kojima, K.; Saito, S. Fructoselysine in Urine of Rats Fed 14C-Lysine-Labeled Casein Browned by Amino-Carbonyl Reaction. *Agric. Biol. Chem.* **1980**, *44* (6), 1327–1331.

176. Bergmann, R.; Helling, R.; Scheunemann, M.; Mading, P.; Wittrisch, H.; Johannsen, B.; Henle, T. Radio Fluorination and Positron Emission Tomography (PET) as a New Approach to Study the in Vivo Distribution and Elimination of the Advanced Glycation Endproducts Nϵ-carboxymethyllysine (CML) and Nϵ-carboxyethyllysine (CEL). *Food/Nahrung* **2001**, *45*, 182–188.

R

177. Liardon, R.; De Weck-Gaudard, D.; Philippossian, G.; Finot, P.-A. Identification of N-Carboxymethyllysine: A New Maillard Reaction Product, in Rat Urine. **1987**, *35*, 427–431.

178. Saito, A.; Takeda, T.; Sato, K.; Hama, H.; Tanuma, A.; Kaseda, R.; Suzuki, Y.; Gejyo, F. Significance of Proximal Tubular Metabolism of Advanced Glycation End Products in Kidney Diseases. In *Annals of the New York Academy of Sciences*; New York Academy of Sciences, 2005; Vol. 1043, pp 637–643. https://doi.org/10.1196/annals.1333.072.

179. Horie, K.; Miyata, T.; Maeda, K.; Miyata, S.; Sugiyama, S.; Sakai, H.; Van Ypersele De Strihou, C.; Monnier, V. M.; Witztum, J. L.; Kurokawa, K. Immunohistochemical Colocalization of Glycoxidation Products and Lipid Peroxidation Products in Diabetic Renal Glomerular Lesions. Implication for Glycoxidative Stress in the Pathogenesis of Diabetic Nephropathy. *J. Clin. Invest.* **1997**, *100* (12), 2995–3004. https://doi.org/10.1172/JCI119853.

180. Asano, M.; Fujita, Y.; Ueda, Y.; Suzuki, D.; Miyata, T.; Sakai, H.; Saito, A. Renal Proximal Tubular Metabolism of Protein-Linked Pentosidine, an Advanced Glycation End Product. *Nephron* **2002**, *91* (4), 688–694. https://doi.org/10.1159/000065032.

181. Ramasamy, R.; Vannucci, S. J.; Yan, S. S. Du; Herold, K.; Yan, S. F.; Schmidt, A. M. Advanced Glycation End Products and RAGE: A Common Thread in Aging, Diabetes, Neurodegeneration, and Inflammation. *Glycobiology* **2005**, *15* (7), 16R-28R. https://doi.org/10.1093/glycob/cwi053.

182. Rabbani, N.; Xue, M.; Thornalley, P. J. Dicarbonyls and Glyoxalase in Disease Mechanisms and Clinical Therapeutics. *Glycoconj. J.* **2016**, *33* (4), 513–525. https://doi.org/10.1007/s10719-016-9705-z.

183. Beisswenger, P. J.; Howell, S. K.; Touchette, A. D.; Lal, S.; Szwergold, B. S. Metformin Reduces Systemic Methylglyoxal Levels in Type 2 Diabetes. *Diabetes* **1999**, *48* (1), 198–202. https://doi.org/10.2337/diabetes.48.1.198.

184. Lu, J.; Randell, E.; Han, Y. C.; Adeli, K.; Krahn, J.; Meng, Q. H. Increased Plasma Methylglyoxal Level, Inflammation, and Vascular Endothelial Dysfunction in Diabetic Nephropathy. *Clin. Biochem.* **2011**, *44* (4), 307–311. https://doi.org/10.1016/j.clinbiochem.2010.11.004.

185. Scheijen, J. L. J. M.; Schalkwijk, C. G. Quantification of Glyoxal, Methylglyoxal and 3-Deoxyglucosone in Blood and Plasma by Ultra Performance Liquid Chromatography Tandem Mass Spectrometry: Evaluation of Blood Specimen. *Clin. Chem. Lab. Med.* **2014**, *52* (1), 85–91. https://doi.org/10.1515/cclm-2012-0878.

186. Akhter, F.; Chen, D.; Akhter, A.; Yan, S. F.; Yan, S. S. Du. Age-Dependent Accumulation of Dicarbonyls and Advanced Glycation Endproducts (AGEs) Associates with Mitochondrial Stress. *Free Radic. Biol. Med.* **2021**, *164*, 429–438. https://doi.org/10.1016/j.freeradbiomed.2020.12.021.

187. Baynes, J. W.; Thorpe, S. R. Role of Oxidative Stress in Diabetic Complications: A New Perspective on an Old Paradigm. *Diabetes*. American Diabetes Association January 1, 1999, pp 1–9. https://doi.org/10.2337/diabetes.48.1.1.

188. Singh Jaggi, A.; Parkash Singh, V.; Bali, A.; Singh, N. Advanced Glycation End Products and Diabetic Complications. *Korean J Physiol Pharmacol* **2014**, *18*, 1–14. https://doi.org/10.4196/kjpp.2014.18.1.1.

189. Sharma, C.; Kaur, A.; Thind, S. S.; Singh, B.; Raina, S. Advanced Glycation End-Products (AGEs): An Emerging Concern for Processed Food Industries. *Journal of Food Science and Technology*. Springer India December 1, 2015, pp 7561–7576. https://doi.org/10.1007/s13197-015-1851-y.

190. Zieman, S. J.; Kass, D. A. Advanced Glycation Endproduct Crosslinking in the Cardiovascular System: Potential Therapeutic Target for Cardiovascular Disease. *Drugs*. Springer September 17, 2004, pp 459–470. https://doi.org/10.2165/00003495-200464050-00001.

191. Bussel, B. C. T. Van; Poll, M. C. G. Van de; Schalkwijk, C. G.; Bergmans, D. C. J. J. Increased Dicarbonyl Stress as a Novel Mechanism of Multi-Organ Failure in Critical Illness. *Int. J. Mol. Sci. 2017, Vol. 18, Page 346* **2017**, *18* (2), 346. https://doi.org/10.3390/IJMS18020346.

192. Lopes-Virella, M. F.; Baker, N. L.; Hunt, K. J.; Cleary, P. A.; Klein, R.; Virella, G. Baseline Markers of Inflammation Are Associated with Progression to Macroalbuminuria in Type 1 Diabetic Subjects. *Diabetes Care* **2013**, *36* (8), 2317–2323. https://doi.org/10.2337/dc12-2521.

193. Lin, J.-A.; Wu, C.-H.; Lu, C.-C.; Hsia, S.-M.; Yen, G.-C. Glycative Stress from Advanced Glycation End Products (AGEs) and Dicarbonyls: An Emerging Biological Factor in Cancer Onset and Progression. *Mol. Nutr. Food Res.* **2016**, *60* (8), 1850–1864. https://doi.org/10.1002/mnfr.201500759.

194. Roberts, M. J.; Wondrak, G. T.; Laurean, D. C.; Jacobson, M. K.; Jacobson, E. L. DNA Damage by Carbonyl Stress in Human Skin Cells. *Mutat. Res. Mol. Mech. Mutagen.* **2003**, *522* (1–2), 45–56. https://doi.org/10.1016/S0027-5107(02)00232-4.

195. Rabbani, N.; Thornalley, P. J. Dicarbonyl Stress in Cell and Tissue Dysfunction Contributing to Ageing and Disease. *Biochem. Biophys. Res. Commun.* **2015**, *458* (2), 221–226. https://doi.org/10.1016/J.BBRC.2015.01.140.

196. Maasen, K.; Scheijen, J. L. J. M.; Opperhuizen, A.; Stehouwer, C. D. A.; Van Greevenbroek, M. M.; Schalkwijk, C. G. Quantification of Dicarbonyl Compounds in Commonly Consumed Foods and Drinks; Presentation of a Food Composition Database for Dicarbonyls. *Food Chem.* **2021**, *339* (September 2020), 128063. https://doi.org/10.1016/j.foodchem.2020.128063.

197. Brett, J.; Marie Schmidt, A.; Du Yan, S.; Shan Zou, Y.; Weidman, E.; Pinsky, D.; Nowygrod, R.; Neeper, M.; Przysiecki, C.; Shaw, A.; Migheli, A.; Stern, D. Survey of the Distribution of a Newly Characterized Receptor for Advanced Glycation End Products in Tissues. *Am. J. ofPathology* **1993**, *143* (6).

198. Hulsmans, M.; Holvoet, P. The Vicious Circle between Oxidative Stress and Inflammation in Atherosclerosis. *J. Cell. Mol. Med.* **2010**, *14* (1–2), 70–78. https://doi.org/10.1111/J.1582-4934.2009.00978.X.

199. Gebhardt, C.; Riehl, A.; Durchdewald, M.; Németh, J.; Fürstenberger, G.; Müller-Decker, K.; Enk, A.; Arnold, B.; Bierhaus, A.; Nawroth, P. P.; Hess, J.; Angel, P. RAGE Signaling Sustains Inflammation and Promotes Tumor Development. *J. Exp. Med.* **2008**, *205* (2), 275–285. https://doi.org/10.1084/jem.20070679.

200. Penfold, S. A.; Coughlan, M. T.; Patel, S. K.; Srivastava, P. M.; Sourris, K. C.; Steer, D.; Webster, D. E.; Thomas, M. C.; MacIsaac, R. J.; Jerums, G.; Burrell, L. M.; Cooper, M. E.; Forbes, J. M. Circulating High-Molecular-Weight RAGE Ligands Activate Pathways Implicated in the Development of Diabetic Nephropathy. *Kidney Int.* **2010**, *78* (3), 287–295. https://doi.org/10.1038/ki.2010.134.

201. Sowndhar Rajan, B.; Manivasagam, S.; Dhanusu, S.; Chandrasekar, N.; Krishna, K.; Kalaiarasu, L. P.; Babu, A. A.; Vellaichamy, E. Diet with High Content of Advanced Glycation End Products Induces Systemic Inflammation and Weight Gain in Experimental Mice: Protective Role of Curcumin and Gallic Acid. *Food Chem. Toxicol.* **2018**, *114*, 237–245. https://doi.org/10.1016/j.fct.2018.02.016.

202. Grossin, N.; Auger, F.; Niquet-Leridon, C.; Durieux, N.; Montaigne, D.; Schmidt, A. M.; Susen, S.; Jacolot, P.; Beuscart, J. B.; Tessier, F. J.; Boulanger, E. Dietary CML-Enriched Protein Induces Functional Arterial Aging in a RAGE-Dependent Manner in Mice. *Mol. Nutr. Food Res.* **2015**, *59* (5), 927–938. https://doi.org/10.1002/mnfr.201400643.

203. Holik, A. K.; Stöger, V.; Hölz, K.; Somoza, M. M.; Somoza, V. Impact of Free Nε-Carboxymethyllysine, Its Precursor Glyoxal and AGE-Modified BSA on Serotonin Release from Human Parietal Cells in Culture. *Food Funct.* **2018**, *9* (7), 3906–3915. https://doi.org/10.1039/c8fo01045e.

R

204. Zill, H.; Bek, S.; Hofmann, T.; Huber, J.; Frank, O.; Lindenmeier, M.; Weigle, B.; Erbersdobler, H. F.; Scheidler, S.; Busch, A. E.; Faist, V. RAGE-Mediated MAPK Activation by Food-Derived AGE and Non-AGE Products. *Biochem. Biophys. Res. Commun.* **2003**, *300* (2), 311–315. https://doi.org/10.1016/S0006-291X(02)02856-5.

205. Uribarri, J.; del Castillo, M. D.; de la Maza, M. P.; Filip, R.; Gugliucci, A.; Luevano-Contreras, C.; Macías-Cervantes, M. H.; Markowicz Bastos, D. H.; Medrano, A.; Menini, T.; Portero-Otin, M.; Rojas, A.; Sampaio, G. R.; Wrobel, K.; Wrobel, K.; Garay-Sevilla, M. E. Dietary Advanced Glycation End Products and Their Role in Health and Disease. *Adv. Nutr.* **2015**, *6* (4), 461–473. https://doi.org/10.3945/an.115.008433.

206. Chen, P.; Zhao, J.; Gregersen, H. Up-Regulated Expression of Advanced Glycation End-Products and Their Receptor in the Small Intestine and Colon of Diabetic Rats. *Dig. Dis. Sci.* **2012**, *57* (1), 48–57. https://doi.org/10.1007/s10620-011-1951-0.

207. Carding, S.; Verbeke, K.; Vipond, D. T.; Corfe, B. M.; Owen, L. J. Dysbiosis of the Gut Microbiota in Disease. *Microb. Ecol. Heal. Dis.* **2015**, *26* (0). https://doi.org/10.3402/mehd.v26.26191.

208. Delgado-Andrade, C.; Pastoriza de la Cueva, S.; Peinado, M. J.; Rufián-Henares, J. Á.; Navarro, M. P.; Rubio, L. A. Modifications in Bacterial Groups and Short Chain Fatty Acid Production in the Gut of Healthy Adult Rats after Long-Term Consumption of Dietary Maillard Reaction Products. *Food Res. Int.* **2017**, *100*, 134–142. https://doi.org/10.1016/j.foodres.2017.06.067.

209. Mastrocola, R.; Collotta, D.; Gaudioso, G.; Le Berre, M.; Cento, A. S.; Ferreira Alves, G.; Chiazza, F.; Verta, R.; Bertocchi, I.; Manig, F.; Hellwig, M.; Fava, F.; Cifani, C.; Aragno, M.; Henle, T.; Joshi, L.; Tuohy, K.; Collino, M. Effects of Exogenous Dietary Advanced Glycation End Products on the Cross-Talk Mechanisms Linking Microbiota to Metabolic Inflammation. *Nutrients* **2020**, *12* (9), 2497. https://doi.org/10.3390/nu12092497.

210. Snelson, M.; Tan, S. M.; Clarke, R. E.; De Pasquale, C.; Thallas-Bonke, V.; Nguyen, T. V.; Penfold, S. A.; Harcourt, B. E.; Sourris, K. C.; Lindblom, R. S.; Ziemann, M.; Steer, D.; El-Osta, A.; Davies, M. J.; Donnellan, L.; Deo, P.; Kellow, N. J.; Cooper, M. E.; Woodruff, T. M.; Mackay, C. R.; Forbes, J. M.; Coughlan, M. T. Processed Foods Drive Intestinal Barrier Permeability and Microvascular Diseases. *Sci. Adv.* **2021**, *7* (14), 1–15. https://doi.org/10.1126/sciadv.abe4841.

211. Han, K.; Jin, W.; Mao, Z.; Dong, S.; Zhang, Q.; Yang, Y.; Chen, B.; Wu, H.; Zeng, M. Microbiome and Butyrate Production Are Altered in the Gut of Rats Fed a Glycated Fish Protein Diet. *J. Funct. Foods* **2018**, *47*, 423–433. https://doi.org/10.1016/j.jff.2018.06.007.

212. Qu, W.; Yuan, X.; Zhao, J.; Zhang, Y.; Hu, J.; Wang, J.; Li, J. Dietary Advanced Glycation End Products Modify Gut Microbial Composition and Partially Increase Colon Permeability in Rats. *Mol. Nutr. Food Res.* **2017**, *61* (10). https://doi.org/10.1002/mnfr.201700118.

213. Marungruang, N.; Fåk, F.; Tareke, E. Heat-Treated High-Fat Diet Modifies Gut Microbiota and Metabolic Markers in Apoe-/- Mice. *Nutr. Metab.* **2016**, *13* (1), 1–11. https://doi.org/10.1186/s12986-016-0083-0.

214. Qu, W.; Nie, C.; Zhao, J.; Ou, X.; Zhang, Y.; Yang, S.; Bai, X.; Wang, Y.; Wang, J.; Li, J. Microbiome–Metabolomics Analysis of the Impacts of Long-Term Dietary Advanced-Glycation-End-Product Consumption on C57BL/6 Mouse Fecal Microbiota and Metabolites. *J. Agric. Food Chem.* **2018**, *66* (33), 8864–8875. https://doi.org/10.1021/acs.jafc.8b01466.

215. Yang, S.; Wang, G.; Ma, Z. feei; Qin, L.; Zhai, Y.; Yu, Z.; Xue, M.; Zhang, Y.; Wan, Z. DietaryAdvancedGlycationEnd Products–InducedCognitive Impairment in Aged ICR Mice: Protective Role of Quercetin. *Mol. Nutr. Food Res.* **2020**, *64* (3), 1901019. https://doi.org/10.1002/mnfr.201901019.

216. Round, J. L.; Mazmanian, S. K. The Gut Microbiota Shapes Intestinal Immune Responses during Health and Disease. *Nat. Rev. Immunol.* **2009**, *9* (5), 313–323. https://doi.org/10.1038/nri2515.

217. Kellow, N. J.; Coughlan, M. T. Effect of Diet-Derived Advanced Glycation End Products on Inflammation. *Nutr. Rev.* **2015**, *73* (11), 737–759. https://doi.org/10.1093/nutrit/nuv030.

218. Gasaly, N.; de Vos, P.; Hermoso, M. A. Impact of Bacterial Metabolites on Gut Barrier Function and Host Immunity: A Focus on Bacterial Metabolism and Its Relevance for Intestinal Inflammation. *Front. Immunol.* **2021**, *0*, 1807. https://doi.org/10.3389/FIMMU.2021.658354.

219. Power, S. E.; O'Toole, P. W.; Stanton, C.; Ross, R. P.; Fitzgerald, G. F. Intestinal Microbiota, Diet and Health. *Br. J. Nutr.* **2014**, *111* (03), 387–402. https://doi.org/10.1017/S0007114513002560.

220. Chen, Y.; Zhou, J.; Wang, L. Role and Mechanism of Gut Microbiota in Human Disease. *Front. Cell. Infect. Microbiol.* **2021**, *11*. https://doi.org/10.3389/FCIMB.2021.625913.

221. Erbersdobler, H. F.; Somoza, V. Forty Years of Furosine – Forty Years of Using Maillard Reaction Products as Indicators of the Nutritional Quality of Foods. *Mol. Nutr. Food Res.* **2007**, *51* (4), 423–430. https://doi.org/10.1002/mnfr.200600154.

222. Mehta, B. M.; Deeth, H. C. Blocked Lysine in Dairy Products: Formation, Occurrence, Analysis, and Nutritional Implications. *Compr. Rev. Food Sci. Food Saf.* **2016**, *15* (1), 206–218. https://doi.org/10.1111/1541-4337.12178.

223. Hellwig, M.; Bunzel, D.; Huch, M.; Franz, C. M. A. P.; Kulling, S. E.; Henle, T. Stability of Individual Maillard Reaction Products in the Presence of the Human Colonic Microbiota. *J. Agric. Food Chem.* **2015**, *63* (30), 6723–6730. https://doi.org/10.1021/acs.jafc.5b01391.

224. Ahmed, M. U.; Thorpe, S. R.; Baynes, J. W. Identification of N Epsilon-Carboxymethyllysine as a Degradation Product of Fructoselysine in Glycated Protein. *J. Biol. Chem.* **1986**, *261* (11), 19.

225. Van Nguyen, C. Toxicity of the AGEs Generated from the Maillard Reaction: On the Relationship of Food-AGEs and Biological-AGEs. *Mol. Nutr. Food Res.* **2006**, *50* (12), 1140–1149. https://doi.org/10.1002/mnfr.200600144.

226. Delgado-Andrade, C.; Fogliano, V. Dietary Advanced Glycosylation End-Products (DAGEs) and Melanoidins Formed through the Maillard Reaction: Physiological Consequences of Their Intake. *Annu. Rev. Food Sci. Technol.* **2018**, *9*, 271–291. https://doi.org/10.1146/annurev-food-030117.

227. Ciccocioppo, R.; Vanoli, A.; Klersy, C.; Imbesi, V.; Boccaccio, V.; Manca, R.; Betti, E.; Cangemi, G. C.; Strada, E.; Besio, R.; Rossi, A.; Falcone, C.; Ardizzone, S.; Fociani, P.; Danelli, P.; Corazza, G. R. Role of the Advanced Glycation End Products Receptor in Crohn's Disease Inflammation. *World J. Gastroenterol.* **2013**, *19* (45), 8269–8281. https://doi.org/10.3748/wjg.v19.i45.8269.

228. Liu, X.; Zheng, L.; Zhang, R.; Liu, G.; Xiao, S.; Qiao, X.; Wu, Y.; Gong, Z. Toxicological Evaluation of Advanced Glycation End Product Nε-(Carboxymethyl)Lysine: Acute and Subacute Oral Toxicity Studies. *Regul. Toxicol. Pharmacol.* **2016**, *77*, 65–74. https://doi.org/10.1016/J.YRTPH.2016.02.013.

229. Xue, J.; Rai, V.; Singer, D.; Chabierski, S.; Xie, J.; Reverdatto, S.; Burz, D. S.; Schmidt, A. M.; Hoffmann, R.; Shekhtman, A. Advanced Glycation End Product Recognition by the Receptor for AGEs. *Structure* **2011**, *19* (5), 722–732. https://doi.org/10.1016/j.str.2011.02.013.

230. Zhao, D.; Sheng, B.; Wu, Y.; Li, H.; Xu, D.; Nian, Y.; Mao, S.; Li, C.; Xu, X.; Zhou, G. Comparison of Free and Bound Advanced Glycation End Products in Food: A Review on the Possible Influence on Human Health. *J. Agric. Food Chem.* **2019**, *67* (51), 14007–14018. https://doi.org/10.1021/acs.jafc.9b05891.

231. den Besten, G.; van Eunen, K.; Groen, A. K.; Venema, K.; Reijngoud, D.-J.; Bakker, B. M. The Role of Short-Chain Fatty Acids in the Interplay between Diet, Gut Microbiota, and Host Energy Metabolism. *J. Lipid Res.* **2013**, *54* (9), 2325–2340. https://doi.org/10.1194/jlr.R036012.

R

232. Hamer, H. M.; Jonkers, D.; Venema, K.; Vanhoutvin, S.; Troost, F. J.; Brummer, R.-J. The Role of Butyrate on Colonic Function. *Aliment. Pharmacol. Ther.* **2007**, *27* (2), 104–119. https://doi.org/10.1111/j.1365-2036.2007.03562.x.

233. Nicholson, J. K.; Holmes, E.; Kinross, J.; Burcelin, R.; Gibson, G.; Jia, W.; Pettersson, S. Host-Gut Microbiota Metabolic Interactions. *Science* **2012**, *336* (6086), 1262–1267. https://doi.org/10.1126/science.1223813.

234. Han, J.; Lin, K.; Sequeira, C.; Borchers, C. H. An Isotope-Labeled Chemical Derivatization Method for the Quantitation of Short-Chain Fatty Acids in Human Feces by Liquid Chromatography–Tandem Mass Spectrometry. *Anal. Chim. Acta* **2015**, *854*, 86–94. https://doi.org/10.1016/J.ACA.2014.11.015.

235. Poncheewin, W.; Hermes, G. D. A.; van Dam, J. C. J.; Koehorst, J. J.; Smidt, H.; Schaap, P. J. NG-Tax 2.0: A Semantic Framework for High-Throughput Amplicon Analysis. *Front. Genet.* **2020**, *10*. https://doi.org/10.3389/fgene.2019.01366.

236. Quast, C.; Pruesse, E.; Yilmaz, P.; Gerken, J.; Schweer, T.; Yarza, P.; Peplies, J.; Glöckner, F. O. The SILVA Ribosomal RNA Gene Database Project: Improved Data Processing and Web-Based Tools. *Nucleic Acids Res.* **2013**, *41*, D590–D596. https://doi.org/10.1093/nar/gks1219.

237. Mcmurdie, P. J.; Holmes, S. Phyloseq: An R Package for Reproducible Interactive Analysis and Graphics of Microbiome Census Data. *PLoS One* **2013**, *8* (4), e61217. https://doi.org/10.1371/journal.pone.0061217.

238. Lahti, L.; Shetty, S. A.; et al. Tools for microbiome analysis in R. http://microbiome.github.com/microbiome (accessed Jun 15, 2020).

239. Oksanen, J.; Guillaume, B.; Friendly, M.; Kindt, R.; Legendre, P.; McGlinn, D.; Minchin, P. R.; O'Hara, R. B.; Simpson, G. L.; Solymos, P.; Stevens, M. H. H.; Szoecs, E.; Wagner, H. vegan: Community Ecology Package. R package version 2.5-6 https://cran.r-project.org/package=vegan (accessed Jun 15, 2020).

240. Segata, N.; Izard, J.; Waldron, L.; Gevers, D.; Miropolsky, L.; Garrett, W. S.; Huttenhower, C. Metagenomic Biomarker Discovery and Explanation. *Genome Biol.* **2011**, *12* (6), R60. https://doi.org/10.1186/gb-2011-12-6-r60.

241. Wang, R.-F.; Cao, W.-W.; Cerniglia, C. E. PCR Detection and Quantitation of Predominant Anaerobic Bacteria in Human and Animal Fecal Samples. *Appl. Environ. Microbiol.* **1996**, *62* (4), 1242–1247.

242. Ishaq, H. M.; Mohammad, I. S.; Guo, H.; Shahzad, M.; Hou, Y. J.; Ma, C.; Naseem, Z.; Wu, X.; Shi, P.; Xu, J. Molecular Estimation of Alteration in Intestinal Microbial Composition in Hashimoto's Thyroiditis Patients. *Biomed. Pharmacother.* **2017**, *95*, 865–874. https://doi.org/10.1016/j.biopha.2017.08.101.

243. Mohajeri, M. H.; Brummer, R. J. M.; Rastall, R. A.; Weersma, R. K.; Harmsen, H. J. M.; Faas, M.; Eggersdorfer, M. The Role of the Microbiome for Human Health: From Basic Science to Clinical Applications. *Eur. J. Nutr.* **2018**, *57* (1), 1–14. https://doi.org/10.1007/s00394-018-1703-4.

244. Ze, X.; Duncan, S. H.; Louis, P.; Flint, H. J. Ruminococcus Bromii Is a Keystone Species for the Degradation of Resistant Starch in the Human Colon. *ISME J.* **2012**, *6* (8), 1535–1543. https://doi.org/10.1038/ismej.2012.4.

245. Waters, J. L.; Ley, R. E. The Human Gut Bacteria Christensenellaceae Are Widespread, Heritable, and Associated with Health. *BMC Biology*. BioMed Central Ltd. October 28, 2019, pp 1–11. https://doi.org/10.1186/s12915-019-0699-4.

246. Morotomi, M.; Nagai, F.; Sakon, H.; Tanaka, R. Dialister Succinatiphilus Sp. Nov. and Barnesiella Intestinihominis Sp. Nov., Isolated from Human Faeces. *Int. J. Syst. Evol. Microbiol.* **2008**, *58* (12), 2716–2720. https://doi.org/10.1099/IJS.0.2008/000810-0.

247. Song, Y.; Könönen, E.; Rautio, M.; Liu, C.; Bryk, A.; Eerola, E.; Finegold, S. M. Alistipes Onderdonkii Sp. Nov. and Alistipes Shahii Sp. Nov., of Human Origin. *Int. J. Syst. Evol. Microbiol.* **2006**, *56* (8), 1985–1990. https://doi.org/10.1099/ijs.0.64318-0.

248. Vacca, M.; Celano, G.; Calabrese, F. M.; Portincasa, P.; Gobbetti, M.; De Angelis, M. The Controversial Role of Human Gut Lachnospiraceae. *Microorganisms* **2020**, *8* (4), 573. https://doi.org/10.3390/microorganisms8040573.

249. Seth, E. C.; Taga, M. E. Nutrient Cross-Feeding in the Microbial World. *Front. Microbiol.* **2014**, *5*, 350. https://doi.org/10.3389/fmicb.2014.00350.

250. Falony, G.; Vlachou, A.; Verbrugghe, K.; De Vuyst, L. Cross-Feeding between Bifidobacterium Longum BB536 and Acetate-Converting, Butyrate-Producing Colon Bacteria during Growth on Oligofructose. *Appl. Environ. Microbiol.* **2006**, *72* (12), 7835–7841. https://doi.org/10.1128/AEM.01296-06.

251. Delgado-Andrade, C.; Pastoriza de la Cueva, S.; Peinado, M. J.; Rufián-Henares, J. Á.; Navarro, M. P.; Rubio, L. A. Modifications in Bacterial Groups and Short Chain Fatty Acid Production in the Gut of Healthy Adult Rats after Long-Term Consumption of Dietary Maillard Reaction Products. *Food Res. Int.* **2017**, *100*, 134–142. https://doi.org/10.1016/J.FOODRES.2017.06.067.

252. De Weirdt, R.; Possemiers, S.; Vermeulen, G.; Moerdijk-Poortvliet, T. C. W.; Boschker, H. T. S.; Verstraete, W.; Van de Wiele, T. Human Faecal Microbiota Display Variable Patterns of Glycerol Metabolism. *FEMS Microbiol. Ecol.* **2010**, *74* (3), 601–611. https://doi.org/10.1111/j.1574-6941.2010.00974.x.

253. Scheijen, J.; Hanssen, N. M. J.; van Greevenbroek, M. M.; Van der Kallen, C. J.; Feskens, E. J. M.; Stehouwer, C. D. A.; Schalkwijk, C. G. Dietary Intake of Advanced Glycation Endproducts Is Associated with Higher Levels of Advanced Glycation Endproducts in Plasma and Urine: The CODAM Study. *Clin Nutr* **2018**, *37* (3), 919–925. https://doi.org/10.1016/j.clnu.2017.03.019.

254. Uribarri, J.; Cai, W.; Peppa, M.; Goodman, S.; Ferrucci, L.; Striker, G.; Vlassara, H. Circulating Glycotoxins and Dietary Advanced Glycation Endproducts: Two Links to Inflammatory Response, Oxidative Stress, and Aging. *J Gerontol A Biol Sci Med Sci* **2007**, *62* (4), 427–433.

255. Qu, W.; Nie, C.; Zhao, J.; Ou, X.; Zhang, Y.; Yang, S.; Bai, X.; Wang, Y.; Wang, J.; Li, J. Microbiome-Metabolomics Analysis of the Impacts of Long-Term Dietary Advanced-Glycation-End-Product Consumption on C57BL/6 Mouse Fecal Microbiota and Metabolites. *J. Agric. Food Chem.* **2018**, *66* (33), 8864–8875. https://doi.org/10.1021/acs.jafc.8b01466.

256. Hellwig, M.; Bunze1, D.; Huch, M.; Franz, C. M. A. P.; Kulling, S. E.; Hen1e1, T. Metabolization of Maillard Reaction Products by the Human Colonic Microbiota. **2016**.

257. Garud, N. R.; Good, B. H.; Hallatschek, O.; Pollard, K. S. Evolutionary Dynamics of Bacteria in the Gut Microbiome within and across Hosts. *PLoS Biol.* **2019**, *17* (1), e3000102. https://doi.org/10.1371/JOURNAL.PBIO.3000102.

258. Wilms, E.; An, R.; Smolinska, A.; Stevens, Y.; Weseler, A. R.; Elizalde, M.; Drittij, M. J.; Ioannou, A.; van Schooten, F. J.; Smidt, H.; Masclee, A. A. M.; Zoetendal, E. G.; Jonkers, D. M. A. E. Galacto-Oligosaccharides Supplementation in Prefrail Older and Healthy Adults Increased Faecal Bifidobacteria, but Did Not Impact Immune Function and Oxidative Stress. *Clin. Nutr.* **2021**, *40* (5), 3019–3031. https://doi.org/10.1016/j.clnu.2020.12.034.

R

259. Větrovský, T.; Baldrian, P. The Variability of the 16S RRNA Gene in Bacterial Genomes and Its Consequences for Bacterial Community Analyses. *PLoS One* **2013**, *8* (2). https://doi.org/10.1371/JOURNAL.PONE.0057923.

260. Paradis, E.; Claude, J.; Strimmer, K. APE: Analyses of Phylogenetics and Evolution in R Language. *Bioinformatics* **2004**, *20* (2), 289–290. https://doi.org/10.1093/BIOINFORMATICS/BTG412.

261. Jian, C.; Luukkonen, P.; Yki-Järvinen, H.; Salonen, A.; Korpela, K. Quantitative PCR Provides a Simple and Accessible Method for Quantitative Microbiota Profiling. *PLoS One* **2020**, *15* (1), e0227285. https://doi.org/10.1371/JOURNAL.PONE.0227285.

262. Clive G. WIlson. Gastrointestinal Transit and Drug Absorption. In *Oral Drug Absorption Prediction and Assessment*; Dressman, J. B., Lennernas, H., Eds.; 2000; pp 1–17.

263. Rose, C.; Parker, A.; Jefferson, B.; Cartmell, E. The Characterization of Feces and Urine: A Review of the Literature to Inform Advanced Treatment Technology. *Crit. Rev. Environ. Sci. Technol.* **2015**, *45* (17), 1827–1879. https://doi.org/10.1080/10643389.2014.1000761.

264. Falony, G.; Joossens, M.; Vieira-Silva, S.; Wang, J.; Darzi, Y.; Faust, K.; Kurilshikov, A.; Bonder, M. J.; Valles-Colomer, M.; Vandeputte, D.; Tito, R. Y.; Chaffron, S.; Rymenans, L.; Verspecht, C.; Sutter, L. De; Lima-Mendez, G.; D'hoe, K.; Jonckheere, K.; Homola, D.; Garcia, R.; Tigchelaar, E. F.; Eeckhaudt, L.; Fu, J.; Henckaerts, L.; Zhernakova, A.; Wijmenga, C.; Raes, J. Population-Level Analysis of Gut Microbiome Variation. *Science (80-.).* **2016**, *352* (6285), 560–564. https://doi.org/10.1126/SCIENCE.AAD3503/SUPPL_FILE/TABLE_S9.XLSX.

265. Schlomann, B. H.; Parthasarathy, R. Timescales of Gut Microbiome Dynamics. *Curr. Opin. Microbiol.* **2019**, *50*, 56–63. https://doi.org/10.1016/J.MIB.2019.09.011.

266. Mehta, R. S.; Abu-Ali, G. S.; Drew, D. A.; Lloyd-Price, J.; Subramanian, A.; Lochhead, P.; Joshi, A. D.; Ivey, K. L.; Khalili, H.; Brown, G. T.; DuLong, C.; Song, M.; Nguyen, L. H.; Mallick, H.; Rimm, E. B.; Izard, J.; Huttenhower, C.; Chan, A. T. Stability of the Human Faecal Microbiome in a Cohort of Adult Men. *Nat. Microbiol.* **2018**, *3* (3), 347–355. https://doi.org/10.1038/s41564-017-0096-0.

267. Bui, T. P. N.; Troise, A. D.; Fogliano, V.; De Vos, W. M. Anaerobic Degradation of N-ε-Carboxymethyllysine, a Major Glycation End-Product, by Human Intestinal Bacteria. *J. Agric. Food Chem.* **2019**, *67*, 6594–6602. https://doi.org/10.1021/acs.jafc.9b02208.

268. Bui, T. P. N.; Troise, A. D.; Nijsse, B.; Roviello, G. N.; Fogliano, V.; de Vos, W. M. Intestinimonas-like Bacteria Are Important Butyrate Producers That Utilize Nε-Fructosyllysine and Lysine in Formula-Fed Infants and Adults. *J. Funct. Foods* **2020**, *70*, 103974. https://doi.org/10.1016/j.jff.2020.103974.

269. Sillner, N.; Walker, A.; Hemmler, D.; Bazanella, M.; Heinzmann, S. S.; Haller, D.; Schmitt-Kopplin, P. Milk-Derived Amadori Products in Feces of Formula-Fed Infants. *J. Agric. Food Chem.* **2019**, *67* (28), 8061–8069. https://doi.org/10.1021/acs.jafc.9b01889.

270. Chen, L.; Wang, D.; Garmaeva, S.; Kurilshikov, A.; Vich Vila, A.; Gacesa, R.; Sinha, T.; Segal, E.; Weersma, R. K.; Wijmenga, C.; Zhernakova, A.; Fu, J. The Long-Term Genetic Stability and Individual Specificity of the Human Gut Microbiome. *Cell* **2021**, *184* (9), 2302-2315.e12. https://doi.org/10.1016/J.CELL.2021.03.024.

271. Brown, R. P.; Delp, M. D.; Lindstedt, S. L.; Rhomberg, L. R.; Beliles, R. P. Physiological Parameter Values for Physiologically Based Pharmacokinetic Models: *Toxicol. Ind. Health* **1997**, *13* (4), 407–484. https://doi.org/10.1177/074823379701300401.

272. Hodge, J. E. Chemistry of Browning Reactions in Model Systems. *J. Agric. Food Chem.* **1953**, *1* (15), 928–943.

273. Penndorf, I.; Biedermann, D.; Maurer, S. V.; Henle, T. Studies on N-Terminal Glycation of Peptides in Hypoallergenic Infant Formulas: Quantification of α-N-(2-Furoylmethyl) Amino Acids. *J. Agric. Food Chem.* **2007**, *55* (3), 723–727. https://doi.org/10.1021/JF061821B.

274. Akıllıoğlu, H. G.; Lund, M. N. Quantification of Advanced Glycation End Products and Amino Acid Cross-Links in Foods by High-Resolution Mass Spectrometry: Applicability of Acid Hydrolysis. *Food Chem.* **2022**, *366*, 130601. https://doi.org/10.1016/J.FOODCHEM.2021.130601.

275. Fenaille, F.; Parisod, V.; Visani, P.; Populaire, S.; Tabet, J. C.; Guy, P. A. Modifications of Milk Constituents during Processing: A Preliminary Benchmarking Study. *Int. Dairy J.* **2006**, *16* (7), 728–739. https://doi.org/10.1016/J.IDAIRYJ.2005.08.003.

276. Wopereis, H.; Oozeer, R.; Knipping, K.; Belzer, C.; Knol, J. The First Thousand Days - Intestinal Microbiology of Early Life: Establishing a Symbiosis. *Pediatr. Allergy Immunol.* **2014**, *25* (5), 428–438. https://doi.org/10.1111/pai.12232.

277. Casaburi, G.; Duar, R. M.; Brown, H.; Mitchell, R. D.; Kazi, S.; Chew, S.; Cagney, O.; Flannery, R. L.; Sylvester, K. G.; Frese, S. A.; Henrick, B. M.; Freeman, S. L. Metagenomic Insights of the Infant Microbiome Community Structure and Function across Multiple Sites in the United States. *Sci. Reports 2021 111* **2021**, *11* (1), 1–12. https://doi.org/10.1038/s41598-020-80583-9.

278. Wiame, E.; Delpierre, G.; Ois Collard, F.; Schaftingen, E. Van. Identification of a Pathway for the Utilization of the Amadori Product Fructoselysine in Escherichia Coli*. **2002**. https://doi.org/10.1074/jbc.M200863200.

279. Graf von Armansperg, B.; Koller, F.; Gericke, N.; Hellwig, M.; Jagtap, P. K. A.; Heermann, R.; Hennig, J.; Henle, T.; Lassak, J. Transcriptional Regulation of the N ε -fructoselysine Metabolism in Escherichia Coli by Global and Substrate-specific Cues. *Mol. Microbiol.* **2020**, mmi.14608. https://doi.org/10.1111/mmi.14608.

280. Su, M. Y.; Broadhurst, M.; Liu, C. P.; Gathercole, J.; Cheng, W. L.; Qi, X. Y.; Clerens, S.; Dyer, J. M.; Day, L.; Haigh, B. Comparative Analysis of Human Milk and Infant Formula Derived Peptides Following in Vitro Digestion. *Food Chem.* **2017**, *221*, 1895–1903. https://doi.org/10.1016/J.FOODCHEM.2016.10.041.

281. Nayfach, S.; Shi, Z. J.; Seshadri, R.; Pollard, K. S.; Kyrpides, N. C. New Insights from Uncultivated Genomes of the Global Human Gut Microbiome. *Nature* **2019**, *568* (7753), 505–510. https://doi.org/10.1038/s41586-019-1058-x.

282. Hyatt, D.; Chen, G. L.; LoCascio, P. F.; Land, M. L.; Larimer, F. W.; Hauser, L. J. Prodigal: Prokaryotic Gene Recognition and Translation Initiation Site Identification. *BMC Bioinformatics* **2010**, *11*, 119. https://doi.org/10.1186/1471-2105-11-119.

283. Altschul, S. F.; Gish, W.; Miller, W.; Myers, E. W.; Lipman, D. J. Basic Local Alignment Search Tool. *J. Mol. Biol.* **1990**, *215* (3), 403–410. https://doi.org/10.1016/S0022-2836(05)80360-2.

284. Parks, D. H.; Chuvochina, M.; Rinke, C.; Mussig, A. J.; Chaumeil, P.-A.; Hugenholtz, P. GTDB: An Ongoing Census of Bacterial and Archaeal Diversity through a Phylogenetically Consistent, Rank Normalized and Complete Genome-Based Taxonomy. *Nucleic Acids Res.* **2021**. https://doi.org/10.1093/NAR/GKAB776.

285. Le, S. Q.; Gascuel, O. An Improved General Amino Acid Replacement Matrix. *Mol. Biol. Evol.* **2008**, *25* (7), 1307–1320. https://doi.org/10.1093/MOLBEV/MSN067.

286. Letunic, I.; Bork, P. Interactive Tree Of Life (ITOL) v5: An Online Tool for Phylogenetic Tree Display and Annotation. *Nucleic Acids Res.* **2021**, *49* (W1), W293–W296. https://doi.org/10.1093/NAR/GKAB301.

R

287. Apprill, A.; McNally, S.; Parsons, R.; Weber, L. Minor Revision to V4 Region SSU RRNA 806R Gene Primer Greatly Increases Detection of SAR11 Bacterioplankton. *Aquat. Microb. Ecol.* **2015**, *75* (129), 129–137.

288. Parada, A. E.; Needham, D. M.; Fuhrman, J. A. Every Base Matters: Assessing Small Subunit RRNA Primers for Marine Microbiomes with Mock Communities, Time Series and Global Field Samples. *Environ. Microbiol.* **2016**, *18* (5), 1403–1414. https://doi.org/10.1111/1462-2920.13023/SUPPINFO.

289. Lemoh J.N.; Brooke O.G. Frequency and Weight of Normal Stools in Infancy. *Br. Med. J.* **1978**, *1*, 1282–1283.

290. Gustin, J.; Gibb, R.; Kenneally, D.; Kutay, B.; Waimin Siu, S.; Roe, D. Characterizing Exclusively Breastfed Infant Stool via a Novel Infant Stool Scale. *J. Parenter. Enter. Nutr.* **2018**, *42*, S5–S11. https://doi.org/10.1002/jpen.1468.

291. Uribarri, J.; Woodruff, S.; Goodman, S.; Cai, W.; Chen, X.; Pyzik, R.; Yong, A.; Striker, G. E.; Vlassara, H. Advanced Glycation End Products in Foods and a Practical Guide to Their Reduction in the Diet. *J Am Diet Assoc* **2010**, *110* (6), 911-16 e12. https://doi.org/10.1016/j.jada.2010.03.018.

292. Uribarri, J.; Cai, W.; Peppa, M.; Goodman, S.; Ferrucci, L.; Striker, G.; Vlassara, H. Circulating Glycotoxins and Dietary Advanced Glycation Endproducts: Two Links to Inflammatory Response, Oxidative Stress, and Aging. *Journals Gerontol. Ser. A* **2007**, *62* (4), 427–433. https://doi.org/10.1093/GERONA/62.4.427.

293. Tessier, F. J.; Niquet-Leridon, C.; Jacolot, P.; Jouquand, C.; Genin, M.; Schmidt, A. M.; Grossin, N.; Boulanger, E. Quantitative Assessment of Organ Distribution of Dietary Protein-Bound 13 C-Labeled Nε -Carboxymethyllysine after a Chronic Oral Exposure in Mice. *Mol Nutr Food Res* **2016**, *60* (11), 2446–2456. https://doi.org/10.1002/mnfr.201600140.

294. Nowotny, K.; Schroter, D.; Schreiner, M.; Grune, T. Dietary Advanced Glycation End Products and Their Relevance for Human Health. *Ageing Res Rev* **2018**, *47*, 55–66. https://doi.org/10.1016/j.arr.2018.06.005.

295. Tilg, H.; Moschen, A. R. Microbiota and Diabetes: An Evolving Relationship. *Gut* **2014**, *63* (9), 1513–1521. https://doi.org/10.1136/gutjnl-2014-306928.

296. Seiquer, I.; Rubio, L. A.; Peinado, M. J.; Delgado-Andrade, C.; Navarro, M. P. Maillard Reaction Products Modulate Gut Microbiota Composition in Adolescents. *Mol Nutr Food Res* **2014**, *58* (7), 1552–1560. https://doi.org/10.1002/mnfr.201300847.

297. Qu, W.; Yuan, X.; Zhao, J.; Zhang, Y.; Hu, J.; Wang, J.; Li, J. Dietary Advanced Glycation End Products Modify Gut Microbial Composition and Partially Increase Colon Permeability in Rats. *Mol. Nutr. Food Res.* **2017**, *61* (10), 1700118. https://doi.org/10.1002/mnfr.201700118.

298. Mastrocola, R.; Collotta, D.; Gaudioso, G.; Le Berre, M.; Cento, A. S.; Ferreira Alves, G.; Chiazza, F.; Verta, R.; Bertocchi, I.; Manig, F.; Hellwig, M.; Fava, F.; Cifani, C.; Aragno, M.; Henle, T.; Joshi, L.; Tuohy, K.; Collino, M. Effects of Exogenous Dietary Advanced Glycation End Products on the Cross-Talk Mechanisms Linking Microbiota to Metabolic Inflammation. *Nutrients* **2020**, *12* (9), 2497. https://doi.org/10.3390/nu12092497.

299. Yang, S.; Wang, G.; Ma, Z. feei; Qin, L.; Zhai, Y.; Yu, Z.; Xue, M.; Zhang, Y.; Wan, Z. Dietary Advanced Glycation End Products–Induced Cognitive Impairment in Aged ICR Mice: Protective Role of Quercetin. *Mol. Nutr. Food Res.* **2020**, *64* (3), 1901019. https://doi.org/10.1002/mnfr.201901019.

300. Bettiga, A.; Fiorio, F.; Di Marco, F.; Trevisani, F.; Romani, A.; Porrini, E.; Salonia, A.; Montorsi, F.; Vago, R. The Modern Western Diet Rich in Advanced Glycation End-Products (AGEs): An Overview of Its Impact on Obesity and Early Progression of Renal Pathology. *Nutrients* **2019**, *11* (8), 1748. https://doi.org/10.3390/nu11081748.

301. Fernando, D. H.; Forbes, J. M.; Angus, P. W.; Herath, C. B. Development and Progression of Non-Alcoholic Fatty Liver Disease: The Role of Advanced Glycation End Products. *International Journal of Molecular Sciences*. MDPI AG October 2, 2019. https://doi.org/10.3390/ijms20205037.

302. Hanssen, N. M. J.; Wouters, K.; Huijberts, M. S.; Gijbels, M. J.; Sluimer, J. C.; Scheijen, J. L. J. M.; Heeneman, S.; Biessen, E. A. L.; Daemen, M. J. A. P.; Brownlee, M.; De Kleijn, D. P.; Stehouwer, C. D. A.; Pasterkamp, G.; Schalkwijk, C. G. Higher Levels of Advanced Glycation Endproducts in Human Carotid Atherosclerotic Plaques Are Associated with a Rupture-Prone Phenotype. *Eur. Heart J.* **2014**, *35* (17), 1137–1146. https://doi.org/10.1093/EURHEARTJ/EHT402.

303. Maasen, K.; Scheijen, J. L. J. M.; Opperhuizen, A.; Stehouwer, C. D. A.; Van Greevenbroek, M. M.; Schalkwijk, C. G. Quantification of Dicarbonyl Compounds in Commonly Consumed Foods and Drinks; Presentation of a Food Composition Database for Dicarbonyls. *Food Chem.* **2021**, *339*, 128063. https://doi.org/10.1016/j.foodchem.2020.128063.

304. Beal, S. L. Ways to Fit a PK Model with Some Data below the Quantification Limit. *J. Pharmacokinet. Pharmacodyn.* **2001**, *28* (5), 481–504. https://doi.org/10.1023/A:1012299115260.

305. Fernández-Calleja, J. M. S.; Konstanti, P.; Swarts, H. J. M.; Bouwman, L. M. S.; Garcia-Campayo, V.; Billecke, N.; Oosting, A.; Smidt, H.; Keijer, J.; van Schothorst, E. M. Non-Invasive Continuous Real-Time in Vivo Analysis of Microbial Hydrogen Production Shows Adaptation to Fermentable Carbohydrates in Mice. *Sci. Rep.* **2018**, *8* (1), 1–16. https://doi.org/10.1038/s41598-018-33619-0.

306. Yudkin, J. S.; Stehouwer, C. D. A.; Emeis, J. J.; Coppack, S. W. C-Reactive Protein in Healthy Subjects: Associations with Obesity, Insulin Resistance, and Endothelial Dysfunction: A Potential Role for Cytokines Originating from Adipose Tissue? *Arterioscler. Thromb. Vasc. Biol.* **1999**, *19* (4), 972–978. https://doi.org/10.1161/01.ATV.19.4.972.

307. de Courten, B.; de Courten, M. P.; Soldatos, G.; Dougherty, S. L.; Straznicky, N.; Schlaich, M.; Sourris, K. C.; Chand, V.; Scheijen, J. L.; Kingwell, B. A.; Cooper, M. E.; Schalkwijk, C. G.; Walker, K. Z.; Forbes, J. M. Diet Low in Advanced Glycation End Products Increases Insulin Sensitivity in Healthy Overweight Individuals: A Double-Blind, Randomized, Crossover Trial. *Am. J. Clin. Nutr.* **2016**, *103* (6), 1426–1433. https://doi.org/10.3945/ajcn.115.125427.

308. Penfold, S. A.; Coughlan, M. T.; Patel, S. K.; Srivastava, P. M.; Sourris, K. C.; Steer, D.; Webster, D. E.; Thomas, M. C.; MacIsaac, R. J.; Jerums, G.; Burrell, L. M.; Cooper, M. E.; Forbes, J. M. Circulating High-Molecular-Weight RAGE Ligands Activate Pathways Implicated in the Development of Diabetic Nephropathy. *Kidney Int.* **2010**, *78* (3), 287–295. https://doi.org/10.1038/ki.2010.134.

309. Xie, J.; Reverdatto, S.; Frolov, A.; Hoffmann, R.; Burz, D. S.; Shekhtman, A. Structural Basis for Pattern Recognition by the Receptor for Advanced Glycation End Products (RAGE). *J. Biol. Chem.* **2008**, *283* (40), 27255–27269. https://doi.org/10.1074/jbc.M801622200.

310. Roncero-Ramos, I.; Delgado-Andrade, C.; Haro, A.; Ruiz-Roca, B.; Morales, F. J.; Navarro, M. P. Effects of Dietary Bread Crust Maillard Reaction Products on Calcium and Bone Metabolism in Rats. *Amino Acids* **2013**, *44* (6), 1409–1418. https://doi.org/10.1007/s00726-011-1160-3.

311. Elmhiri, G.; Mahmood, D. F.; Niquet-Leridon, C.; Jacolot, P.; Firmin, S.; Guigand, L.; Tessier, F. J.; Larcher, T.; Abdennebi-Najar, L. Formula-Derived Advanced Glycation End Products Are Involved in the Development of Long-Term Inflammation and Oxidative Stress in Kidney of IUGR Piglets. *Mol Nutr Food Res* **2015**, *59* (5), 939–947. https://doi.org/10.1002/mnfr.201400722.

R

312. Cai, W.; Ramdas, M.; Zhu, L.; Chen, X.; Striker, G. E.; Vlassara, H. Oral Advanced Glycation Endproducts (AGEs) Promote Insulin Resistance and Diabetes by Depleting the Antioxidant Defenses AGE Receptor-1 and Sirtuin 1. *Proc Natl Acad Sci U S A* **2012**, *109* (39), 15888–15893. https://doi.org/10.1073/pnas.1205847109.

313. Sowndhar Rajan, B.; Manivasagam, S.; Dhanusu, S.; Chandrasekar, N.; Krishna, K.; Kalaiarasu, L. P.; Babu, A. A.; Vellaichamy, E. Diet with High Content of Advanced Glycation End Products Induces Systemic Inflammation and Weight Gain in Experimental Mice: Protective Role of Curcumin and Gallic Acid. *Food Chem Toxicol* **2018**, *114*, 237–245. https://doi.org/10.1016/j.fct.2018.02.016.

314. Hong, E. G.; Hwi, J. K.; Cho, Y. R.; Kim, H. J.; Ma, Z.; Yu, T. Y.; Friedline, R. H.; Kurt-Jones, E.; Finberg, R.; Fischer, M. A.; Granger, E. L.; Norbury, C. C.; Hauschka, S. D.; Philbrick, W. M.; Lee, C. G.; Elias, J. A.; Kim, J. K. Interleukin-10 Prevents Diet-Induced Insulin Resistance by Attenuating Macrophage and Cytokine Response in Skeletal Muscle. *Diabetes* **2009**, *58* (11), 2525–2535. https://doi.org/10.2337/db08-1261.

315. Baye, E.; Kiriakova, V.; Uribarri, J.; Moran, L. J.; De Courten, B. Consumption of Diets with Low Advanced Glycation End Products Improves Cardiometabolic Parameters: Meta-Analysis of Randomised Controlled Trials. *Sci. Rep.* **2017**, *7* (1), 1–9. https://doi.org/10.1038/s41598-017-02268-0.

316. Förster, A.; Henle, T. Glycation in Food and Metabolic Transit of Dietary AGEs (Advanced Glycation End-Products): Studies on the Urinary Excretion of Pyrraline. *Biochem. Soc. Trans.* **2003**, *31* (6), 1383–1385.

317. Kerrigan, J. J.; Mansell, J. P.; Sandy, J. R. Matrix Turnover. *Journal of Orthodontics*. Maney Publishing 2000, pp 227–233. https://doi.org/10.1179/ortho.27.3.227.

318. Pinto, M. S.; Léonil, J.; Henry, G.; Cauty, C.; Carvalho, A. Ô. F.; Bouhallab, S. Heating and Glycation of β-Lactoglobulin and β-Casein: Aggregation and in Vitro Digestion. *Food Res. Int.* **2014**, *55*, 70–76. https://doi.org/10.1016/j.foodres.2013.10.030.

319. Cordova, R.; Knaze, V.; Viallon, V.; Rust, P.; Schalkwijk, C. G.; Weiderpass, E.; Wagner, K.; Mayen-Chacon, A.; Aglago, E. K. Dietary Intake of Advanced Glycation End Products (AGEs) and Changes in Body Weight in European Adults. *Eur. J. Nutr.* **2019**. https://doi.org/10.1007/s00394-019-02129-8.

320. Waqas, K.; Chen, J.; van der Eerden, B. C. J.; Ikram, M. A.; Uitterlinden, A. G.; Voortman, T.; Zillikens, M. C. Dietary Advanced Glycation End-Products (DAGEs) Intake and Bone Health: A Cross-Sectional Analysis in the Rotterdam Study. *Nutrients* **2020**, *12* (8), 2377. https://doi.org/10.3390/nu12082377.

321. Cox, L. M.; Sohn, J.; Tyrrell, K. L.; Citron, D. M.; Lawson, P. A.; Pate, N. B.; Iizumi, T.; Perez-Perez, G. I.; Goldstein, E. J. C.; Blaser, M. J. Description of Two Novel Members of the Family Erysipelotrichaceae: Ileibacterium Valens Gen. Nov., Sp. Nov. and Dubosiella Newyorkensis, Gen. Nov., Sp. Nov., from the Murine Intestine, and Emendation to the Description of Faecalibacterium Rodentium. *Int. J. Syst. Evol. Microbiol.* **2017**, *67* (5), 1247–1254. https://doi.org/10.1099/ijsem.0.001793.

322. Qu, W.; Nie, C.; Zhao, J.; Ou, X.; Zhang, Y.; Yang, S.; Bai, X.; Wang, Y.; Wang, J.; Li, J. Microbiome-Metabolomics Analysis of the Impacts of Long-Term Dietary Advanced-Glycation-End-Product Consumption on C57BL/6 Mouse Fecal Microbiota and Metabolites. *J. Agric. Food Chem.* **2018**, *66* (33), 8864–8875. https://doi.org/10.1021/acs.jafc.8b01466.

323. Bui, T. P. N.; Troise, A. D.; Fogliano, V.; De Vos, W. M. Anaerobic Degradation of N-ε-Carboxymethyllysine, a Major Glycation End-Product, by Human Intestinal Bacteria. *J. Agric. Food Chem.* **2019**, *67* (23), 6594–6602. https://doi.org/10.1021/acs.jafc.9b02208.

324. Hellwig, M.; Auerbach, C.; Mü, N.; Samuel, P.; Kammann, S.; Beer, F.; Gunzer, F.; Henle, T. Metabolization of the Advanced Glycation End Product N-ε-Carboxymethyllysine (CML) by Different Probiotic E. Coli Strains. **2019**. https://doi.org/10.1021/acs.jafc.8b06748.

325. Ravussin, Y.; Koren, O.; Spor, A.; Leduc, C.; Gutman, R.; Stombaugh, J.; Knight, R.; Ley, R. E.; Leibel, R. L. Responses of Gut Microbiota to Diet Composition and Weight Loss in Lean and Obese Mice. *Obesity* **2012**, *20* (4), 738–747. https://doi.org/10.1038/oby.2011.111.

326. Everard, A.; Belzer, C.; Geurts, L.; Ouwerkerk, J. P.; Druart, C.; Bindels, L. B.; Guiot, Y.; Derrien, M.; Muccioli, G. G.; Delzenne, N. M.; De Vos, W. M.; Cani, P. D. Cross-Talk between Akkermansia Muciniphila and Intestinal Epithelium Controls Diet-Induced Obesity. *Proc. Natl. Acad. Sci. U. S. A.* **2013**, *110* (22), 9066–9071. https://doi.org/10.1073/pnas.1219451110.

327. Hugenholtz, F.; de Vos, W. M. Mouse Models for Human Intestinal Microbiota Research: A Critical Evaluation. *Cellular and Molecular Life Sciences*. Birkhauser Verlag AG January 1, 2018, pp 149–160. https://doi.org/10.1007/s00018-017-2693-8.

328. Lloyd-Price, J.; Mahurkar, A.; Rahnavard, G.; Crabtree, J.; Orvis, J.; Hall, A. B.; Brady, A.; Creasy, H. H.; McCracken, C.; Giglio, M. G.; McDonald, D.; Franzosa, E. A.; Knight, R.; White, O.; Huttenhower, C. Strains, Functions and Dynamics in the Expanded Human Microbiome Project. *Nat. 2017 5507674* **2017**, *550* (7674), 61–66. https://doi.org/10.1038/nature23889.

329. Trégoat, V.; Brohée, M.; Cordeiro, F.; Van Hengel, A. J. Immunofluorescence Detection of Advanced Glycation End Products (AGEs) in Cookies and Its Correlation with Acrylamide Content and Antioxidant Activity. *Food Agric. Immunol.* **2009**, *20* (3), 253–268. https://doi.org/10.1080/09540100903168165.

330. Koszucka, A.; Nowak, A. Thermal Processing Food-Related Toxicants: A Review. *https://doi.org/10.1080/10408398.2018.1500440* **2018**, *59* (22), 3579–3596. https://doi.org/10.1080/10408398.2018.1500440.

331. Harcourt, B. E.; Sourris, K. C.; Coughlan, M. T.; Walker, K. Z.; Dougherty, S. L.; Andrikopoulos, S.; Morley, A. L.; Thallas-Bonke, V.; Chand, V.; Penfold, S. A.; De Courten, M. P. J.; Thomas, M. C.; Kingwell, B. A.; Bierhaus, A.; Cooper, M. E.; Courten, B. De; Forbes, J. M. Targeted Reduction of Advanced Glycation Improves Renal Function in Obesity. *Kidney Int.* **2011**, *80* (2), 190–198. https://doi.org/10.1038/KI.2011.57.

332. Deo, P.; Chern, C.; Peake, B.; Tan, S. Y. Non-Nutritive Sweeteners Are in Concomitant with the Formation of Endogenous and Exogenous Advanced Glycation End-Products. *https://doi.org/10.1080/09637486.2020.1712683* **2020**, *71* (6), 706–714. https://doi.org/10.1080/09637486.2020.1712683.

333. Maasen, K.; van Greevenbroek, M. M. J.; Scheijen, J. L. J. M.; van der Kallen, C. J. H.; Stehouwer, C. D. A.; Schalkwijk, C. G. High Dietary Glycemic Load Is Associated with Higher Concentrations of Urinary Advanced Glycation Endproducts: The Cohort on Diabetes and Atherosclerosis Maastricht (CODAM) Study. *Am. J. Clin. Nutr.* **2019**, *110* (2), 358–366. https://doi.org/10.1093/ajcn/nqz119.

334. Mendez-Catala, D. M.; Spenkelink, A.; Rietjens, I. M. C. M.; Beekmann, K. An in Vitromodel to Quantify Interspecies Differences in Kinetics for Intestinal Microbial Bioactivation and Detoxification of Zearalenone. *Toxicol. Reports* **2020**, *7*, 938–946. https://doi.org/10.1016/J.TOXREP.2020.07.010.

R

335. Jin, J.; Spenkelink, A.; Beekmann, K.; Baccaro, M.; Xing, F.; Rietjens, I. M. C. M. Species Differences in in Vitro and Estimated in Vivo Kinetics for Intestinal Microbiota Mediated Metabolism of Acetyl-Deoxynivalenols. *Mol. Nutr. Food Res.* **2021**, *65* (9), 2001085. https://doi.org/10.1002/MNFR.202001085.

336. Sekirov, I.; Russell, S. L.; Caetano M Antunes, L.; Finlay, B. B. Gut Microbiota in Health and Disease. *Physiol. Rev.* **2010**, *90* (3), 859–904. https://doi.org/10.1152/PHYSREV.00045.2009/ASSET/IMAGES/LARGE/Z9J0031025430009.JPEG.

337. Donaldson, G. P.; Lee, S. M.; Mazmanian, S. K. Gut Biogeography of the Bacterial Microbiota. *Nat. Rev. Microbiol. 2015 141* **2015**, *14* (1), 20–32. https://doi.org/10.1038/nrmicro3552.

338. Tang, Q.; Jin, G.; Wang, G.; Liu, T.; Liu, X.; Wang, B.; Cao, H. Current Sampling Methods for Gut Microbiota: A Call for More Precise Devices. *Front. Cell. Infect. Microbiol.* **2020**, *10*, 151. https://doi.org/10.3389/FCIMB.2020.00151/BIBTEX.

339. Rios-Morales, M.; van Trijp, M. P. H.; Rösch, C.; An, R.; Boer, T.; Gerding, A.; de Ruiter, N.; Koehorst, M.; Heiner-Fokkema, M. R.; Schols, H. A.; Reijngoud, D. J.; Hooiveld, G. J. E. J.; Bakker, B. M. A Toolbox for the Comprehensive Analysis of Small Volume Human Intestinal Samples That Can Be Used with Gastrointestinal Sampling Capsules. *Sci. Reports 2021 111* **2021**, *11* (1), 1–14. https://doi.org/10.1038/s41598-021-86980-y.

340. Soars, M. G.; Burchell, B.; Riley, R. J. In Vitro Analysis of Human Drug Glucuronidation and Prediction of in Vivo Metabolic Clearance. *J. Pharmacol. Exp. Ther.* **2002**, *301* (1), 382–390. https://doi.org/10.1124/JPET.301.1.382.

341. Pelkonen, O.; Turpeinen, M. In Vitro–in Vivo Extrapolation of Hepatic Clearance: Biological Tools, Scaling Factors, Model Assumptions and Correct Concentrations. *http://dx.doi.org/10.1080/00498250701620726* **2008**, *37* (10–11), 1066–1089. https://doi.org/10.1080/00498250701620726.

342. Punt, A.; Peijnenburg, A. A. C. M.; Hoogenboom, R. L. A. P.; Bouwmeester, H. Non-Animal Approaches for Toxicokinetics in Risk Evaluations of Food Chemicals. *ALTEX* **2017**, *34* (4).

343. Nissen, L.; Casciano, F.; Gianotti, A. Intestinal Fermentation in Vitro Models to Study Food-Induced Gut Microbiota Shift: An Updated Review. *FEMS Microbiol. Lett.* **2020**, *367* (12), 97. https://doi.org/10.1093/FEMSLE/FNAA097.

344. Venema, K.; Van Den Abbeele, P. Experimental Models of the Gut Microbiome. *Best Pract. Res. Clin. Gastroenterol.* **2013**, *27* (1), 115–126. https://doi.org/10.1016/J.BPG.2013.03.002.

345. Moon, J. S.; Li, L.; Bang, J.; Han, N. S. Application of In Vitro Gut Fermentation Models to Food Components: A Review. *Food Sci. Biotechnol* **2016**, *25* (S), 1–7. https://doi.org/10.1007/s10068-016-0091-x.

346. Macfarlane, G. T.; Macfarlane, S.; Gibson, G. R. Validation of a Three-Stage Compound Continuous Culture System for Investigating the Effect of Retention Time on the Ecology and Metabolism of Bacteria in the Human Colon. *Microb. Ecol. 1998 352* **1998**, *35* (2), 180–187. https://doi.org/10.1007/S002489900072.

347. Van Den Abbeele, P.; Grootaert, C.; Marzorati, M.; Possemiers, S.; Verstraete, W.; Gérard, P.; Rabot, S.; Bruneau, A.; Aidy, S. El; Derrien, M.; Zoetendal, E.; Kleerebezem, M.; Smidt, H.; Van De Wiele, T. Microbial Community Development in a Dynamic Gut Model Is Reproducible, Colon Region Specific, and Selective for Bacteroidetes and Clostridium Cluster IX #. *Appl. Environ. Microbiol.* **2010**, *76* (15), 5237–5246. https://doi.org/10.1128/AEM.00759-10.

348. Guzman-Rodriguez, M.; McDonald, J. A. K.; Hyde, R.; Allen-Vercoe, E.; Claud, E. C.; Sheth, P. M.; Petrof, E. O. Using Bioreactors to Study the Effects of Drugs on the Human Microbiota. *Methods* **2018**, *149*, 31–41. https://doi.org/10.1016/J.YMETH.2018.08.003.

349. Kavlock, R. J.; Bahadori, T.; Barton-Maclaren, T. S.; Gwinn, M. R.; Rasenberg, M.; Thomas, R. S. Accelerating the Pace of Chemical Risk Assessment. *Chem. Res. Toxicol.* **2018**, *31* (5), 287–290. https://doi.org/10.1021/ACS.CHEMRESTOX.7B00339.

350. Clarke, G.; Sandhu, K. V.; Griffin, B. T.; Dinan, T. G.; Cryan, J. F.; Hyland, N. P. Gut Reactions: Breaking Down Xenobiotic–Microbiome Interactions. *Pharmacol. Rev.* **2019**, *71* (2), 198–224. https://doi.org/10.1124/pr.118.015768.

351. Manor, O.; Dai, C. L.; Kornilov, S. A.; Smith, B.; Price, N. D.; Lovejoy, J. C.; Gibbons, S. M.; Magis, A. T. Health and Disease Markers Correlate with Gut Microbiome Composition across Thousands of People. *Nat. Commun. 2020 111* **2020**, *11* (1), 1–12. https://doi.org/10.1038/s41467-020-18871-1.

352. de Vos, W. M.; De Vos, E. A. J. Role of the Intestinal Microbiome in Health and Disease: From Correlation to Causation. *Nutr. Rev.* **2012**, *70* (suppl_1), S45–S56. https://doi.org/10.1111/J.1753-4887.2012.00505.X.

353. Leist, M.; Ghallab, A.; Graepel, R.; Marchan, R.; Hassan, R.; Bennekou, S. H.; Limonciel, A.; Vinken, M.; Schildknecht, S.; Waldmann, T.; Danen, E.; van Ravenzwaay, B.; Kamp, H.; Gardner, I.; Godoy, P.; Bois, F. Y.; Braeuning, A.; Reif, R.; Oesch, F.; Drasdo, D.; Höhme, S.; Schwarz, M.; Hartung, T.; Braunbeck, T.; Beltman, J.; Vrieling, H.; Sanz, F.; Forsby, A.; Gadaleta, D.; Fisher, C.; Kelm, J.; Fluri, D.; Ecker, G.; Zdrazil, B.; Terron, A.; Jennings, P.; van der Burg, B.; Dooley, S.; Meijer, A. H.; Willighagen, E.; Martens, M.; Evelo, C.; Mombelli, E.; Taboureau, O.; Mantovani, A.; Hardy, B.; Koch, B.; Escher, S.; van Thriel, C.; Cadenas, C.; Kroese, D.; van de Water, B.; Hengstler, J. G. Adverse Outcome Pathways: Opportunities, Limitations and Open Questions. *Arch. Toxicol. 2017 9111* **2017**, *91* (11), 3477–3505. https://doi.org/10.1007/S00204-017-2045-3.

354. Vinken, M.; Knapen, D.; Vergauwen, L.; Hengstler, J. G.; Angrish, M.; Whelan, M. Adverse Outcome Pathways: A Concise Introduction for Toxicologists. *Arch. Toxicol.* **2017**, *91* (11), 3697–3707. https://doi.org/10.1007/S00204-017-2020-Z/FIGURES/5.

355. Marcobal, A.; Kashyap, P. C.; Nelson, T. A.; Aronov, P. A.; Donia, M. S.; Spormann, A.; Fischbach, M. A.; Sonnenburg, J. L. A Metabolomic View of How the Human Gut Microbiota Impacts the Host Metabolome Using Humanized and Gnotobiotic Mice. *ISME J. 2013 710* **2013**, *7* (10), 1933–1943. https://doi.org/10.1038/ismej.2013.89.

356. Turner, P. V. The Role of the Gut Microbiota on Animal Model Reproducibility. *Anim. Model. Exp. Med.* **2018**, *1* (2), 109. https://doi.org/10.1002/AME2.12022.

357. Schoultz, I.; Keita, Å. V. The Intestinal Barrier and Current Techniques for the Assessment of Gut Permeability. *Cells 2020, Vol. 9, Page 1909* **2020**, *9* (8), 1909. https://doi.org/10.3390/CELLS9081909.

358. Foerster, A.; Henle, T. Glycation in Food and Metabolic Transit of Dietary AGEs (Advanced Glycation End-Products): Studies on the Urinary Excretion of Pyrraline. In *Biochemical Society Transactions*; Portland Press Ltd, 2003; Vol. 31, pp 1383–1385. https://doi.org/10.1042/bst0311383.

359. Makita, Z.; Bucala, R.; Rayfield, E. J.; Fuh, H.; Manogue, K. R.; Cerami, A.; Viassara, H.; Friedman, E. A.; Kaufman, A. M.; Korbet, S. M.; Barth, R. H.; Winston, J. A. Reactive Glycosylation Endproducts in Diabetic Uraemia and Treatment of Renal Failure. *Lancet (London, England)* **1994**, *343* (8912), 1519–1522. https://doi.org/10.1016/S0140-6736(94)92935-1.

360. Perkins, B. A.; Rabbani, N.; Weston, A.; Adaikalakoteswari, A.; Lee, J. A.; Lovblom, L. E.; Cardinez, N.; Thornalley, P. J. High Fractional Excretion of Glycation Adducts Is Associated with Subsequent Early Decline in Renal Function in Type 1 Diabetes. *Sci. Reports 2020 101* **2020**, *10* (1), 1–11. https://doi.org/10.1038/s41598-020-69350-y.

R

361. Fosmark, D. S.; Torjesen, P. A.; Kilhovd, B. K.; Berg, T. J.; Sandvik, L.; Hanssen, K. F.; Agardh, C. D.; Agardh, E. Increased Serum Levels of the Specific Advanced Glycation End Product Methylglyoxal-Derived Hydroimidazolone Are Associated with Retinopathy in Patients with Type 2 Diabetes Mellitus. *Metabolism* **2006**, *55* (2), 232–236. https://doi.org/10.1016/J.METABOL.2005.08.017.

362. Somoza, V.; Wenzel, E.; Weiß, C.; Clawin-Rädecker, I.; Grübel, N.; Erbersdobler, H. F. Dose-Dependent Utilisation of Casein-Linked Lysinoalanine, N(Epsilon)-Fructoselysine and N(Epsilon)-Carboxymethyllysine in Rats. *Mol. Nutr. Food Res.* **2006**, *50* (9), 833–841. https://doi.org/10.1002/mnfr.200600021.

363. Zhou, X.; Ulaszewska, M. M.; De Gobba, C.; Rinnan, Å.; Poulsen, M. W.; Chen, J.; Mattivi, F.; Hedegaard, R. V.; Skibsted, L. H.; Dragsted, L. O. New Advanced Glycation End Products Observed in Rat Urine by Untargeted Metabolomics after Feeding with Heat-Treated Skimmed Milk Powder. *Mol. Nutr. Food Res.* **2021**, *65* (7), 2001049. https://doi.org/10.1002/MNFR.202001049.

364. Frolova, N.; Soboleva, A.; Nguyen, V. D.; Kim, A.; Ihling, C.; Eisenschmidt-Bönn, D.; Mamontova, T.; Herfurth, U. M.; Wessjohann, L. A.; Sinz, A.; Birkemeyer, C.; Frolov, A. Probing Glycation Potential of Dietary Sugars in Human Blood by an Integrated in Vitro Approach. *Food Chem.* **2021**, *347*. https://doi.org/10.1016/J.FOODCHEM.2020.128951.

365. Chrysanthou, M.; Estruch, I. M.; Rietjens, I. M. C. M.; Wichers, H. J.; Hoppenbrouwers, T. In Vitro Methodologies to Study the Role of Advanced Glycation End Products (AGEs) in Neurodegeneration. *Nutr. 2022, Vol. 14, Page 363* **2022**, *14* (2), 363. https://doi.org/10.3390/NU14020363.

366. Schalkwijk, C. G.; Stehouwer, C. D. A. Methylglyoxal, a Highly Reactive Dicarbonyl Compound, in Diabetes, Its Vascular Complications, and Other Age-Related Diseases. *Physiol. Rev.* **2020**, *100* (1), 407–461. https://doi.org/10.1152/physrev.00001.2019.

367. Hellwig, M.; Gensberger-Reigl, S.; Henle, T.; Pischetsrieder, M. Food-Derived 1,2-Dicarbonyl Compounds and Their Role in Diseases. **2017**. https://doi.org/10.1016/j.semcancer.2017.11.014.

368. Frischmann, M.; Bidmon, C.; Angerer, J.; Pischetsrieder, M. Identification of DNA Adducts of Methylglyoxal. *Chem. Res. Toxicol.* **2005**, *18* (10), 1586–1592. https://doi.org/10.1021/TX0501278.

369. Kasai, H.; Iwamoto-Tanaka, N.; Fukada, S. DNA Modifications by the Mutagen Glyoxal: Adduction to G and C, Deamination of C and GC and GA Cross-Linking. *Carcinogenesis* **1998**, *19* (8), 1459–1465.

370. Hayase, F.; Kaneko, K. Formation of N-(1-Oxo-2,4,5,6-Hydroxyhexyl)-2'-Deoxyguanosine by the Reaction of 2'-Deoxyguanosine with 3-Deoxyglucosone. *Biosci. Biotechnol. Biochem.* **1998**, *62* (8), 1630–1632. https://doi.org/10.1271/bbb.62.1630.

371. Zheng, L.; Dongen, K. C. W. van; Bakker, W.; Estruch, I. M.; Rietjens, I. M. C. M. The Influence of Intracellular Glutathione Levels on the Induction of Nrf2-Mediated Gene Expression by α-Dicarbonyl Precursors of Advanced Glycation End Products. *Nutr. 2022, Vol. 14, Page 1364* **2022**, *14* (7), 1364. https://doi.org/10.3390/NU14071364.

372. Liu, C.; Vervoort, J.; van den Elzen, J.; Beekmann, K.; Baccaro, M.; de Haan, L.; C M Rietjens, I. M.; Liu, C.; van den Elzen, J.; Beekmann, K.; Baccaro, M.; de Haan, L.; C M Rietjens, I. M. Interindividual Differences in Human In Vitro Intestinal Microbial Conversion of Green Tea (-)-Epigallocatechin-3-O-Gallate and Consequences for Activation of Nrf2 Mediated Gene Expression. *Mol. Nutr. Food Res.* **2021**, *65* (2), 2000934. https://doi.org/10.1002/MNFR.202000934.

373. Nishimoto, S.; Koike, S.; Inoue, N.; Suzuki, T.; Ogasawara, Y. Activation of Nrf2 Attenuates Carbonyl Stress Induced by Methylglyoxal in Human Neuroblastoma Cells: Increase in GSH Levels Is a Critical Event for the Detoxification Mechanism. *Biochem. Biophys. Res. Commun.* **2017**, *483* (2), 874–879. https://doi.org/10.1016/j.bbrc.2017.01.024.

374. He, Y.; Zhou, C.; Huang, M.; Tang, C.; Liu, X.; Yue, Y.; Diao, Q.; Zheng, Z.; Liu, D. Glyoxalase System: A Systematic Review of Its Biological Activity, Related-Diseases, Screening Methods and Small Molecule Regulators. *Biomedicine and Pharmacotherapy*. Elsevier Masson SAS November 1, 2020, p 110663. https://doi.org/10.1016/j.biopha.2020.110663.

375. Niwa, T. 3-Deoxyglucosone: Metabolism, Analysis, Biological Activity, and Clinical Implication. *J. Chromatogr. B Biomed. Sci. Appl.* **1999**, *731* (1), 23–36. https://doi.org/10.1016/S0378-4347(99)00113-9.

376. Rabbani, N.; Thornalley, P. J. Dicarbonyl Stress in Cell and Tissue Dysfunction Contributing to Ageing and Disease. *Biochem. Biophys. Res. Commun.* **2015**, *458* (2), 221–226. https://doi.org/10.1016/J.BBRC.2015.01.140.

377. Zhang, H.; Zhang, H.; Troise, A. D.; Fogliano, V. Melanoidins from Coffee, Cocoa, and Bread Are Able to Scavenge α-Dicarbonyl Compounds under Simulated Physiological Conditions. *J. Agric. Food Chem.* **2019**, *67* (39), 10921–10929. https://doi.org/10.1021/ACS.JAFC.9B03744/SUPPL_FILE/JF9B03744_SI_001.PDF.

378. Glomb, M. A.; Tschirnich, R. Detection of α-Dicarbonyl Compounds in Maillard Reaction Systems and in Vivo. *J. Agric. Food Chem.* **2001**, *49* (11), 5543–5550. https://doi.org/10.1021/JF010148H.
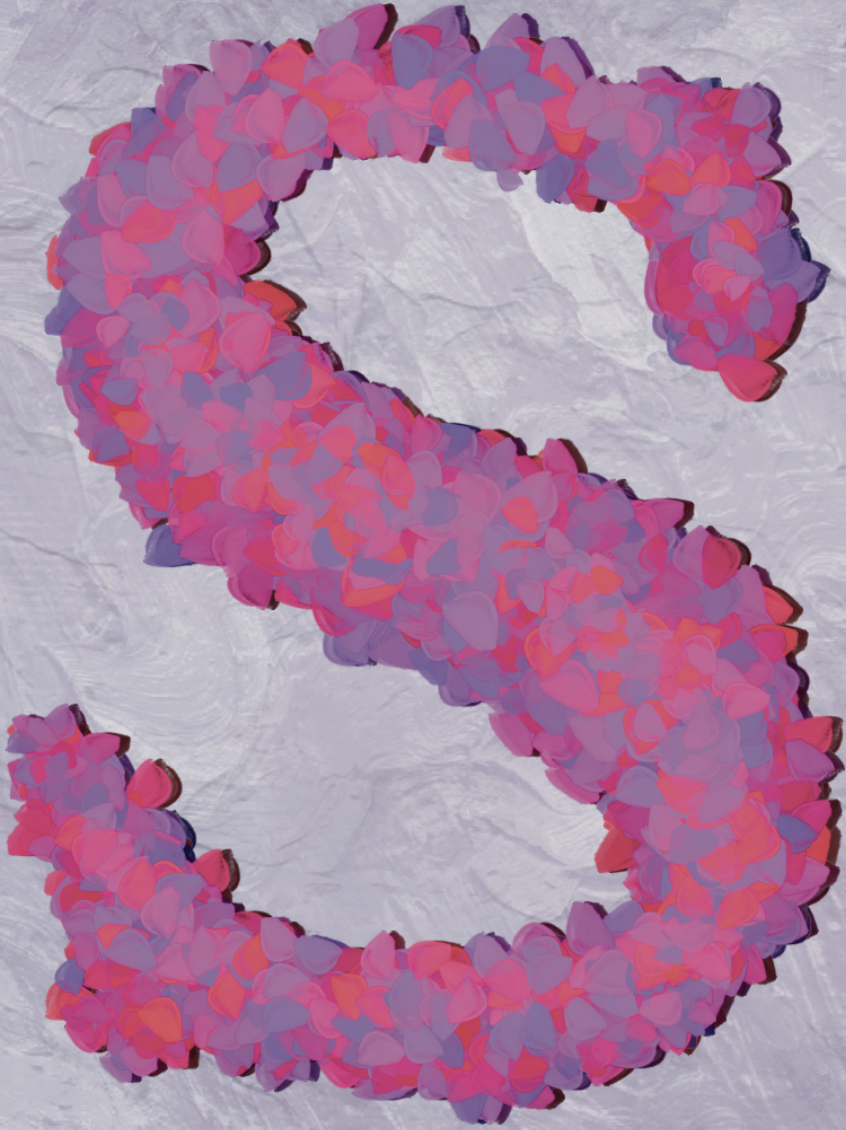
R

Summary

Samenvatting

Summary

Glycation products comprise a heterogenous group of compounds which can be formed upon thermal processing of food products and include advanced glycation end products (AGEs), such as carboxymethyllysine, and their precursors such as the Amadori product fructoselysine and α-dicarbonyl compounds like methylglyoxal, glyoxal and 3-deoxyglucosone. Besides being present in exogenous dietary sources, glycation products can also be produced endogenously inside the human body. AGEs have been associated with the development of multiple adverse health effects, such as diabetes and cardiovascular diseases, but whether exposure to exogenous dietary AGEs and their precursors contributes to these effects remains debated. In **Chapter 2** an overview was presented of the toxicokinetics and toxicodynamics of exogenous and endogenous AGEs and their precursors which are of relevance to consider when evaluating whether exposure to exogenous dietary glycation products can contribute to the adverse health effects associated with AGEs. It was concluded that better characterization of the tested AGEs and precursors, and to distinguish between their low molecular mass (LMM) and high molecular mass (HMM) forms, as well as quantification of the exposure from endogenous formation relative to that resulting from dietary intake are all of importance to provide a definite conclusion on whether dietary exposure to glycation products can contribute to the adverse health effects associated to AGEs. In addition, it was concluded that part of the AGEs and their precursors remain unabsorbed upon dietary exposure and can reach the colon. Consequently at least part of the AGEs and their precursors can interact with the gut microbiota in a bi-directional manner. This can affect the toxicokinetics of the AGEs and their precursors but on the other hand can also result in exerted toxicodynamic effects by altering the gut microbiota composition and possibly function. The aim of this project was to characterize these interactions of the gut microbiota with selected dietary glycation products and vice versa, and to characterize inter- and intraindividual differences in gut microbial reactions using the Amadori product fructoselysine and the AGE carboxymethyllysine as model compounds.

In **Chapter 3** 16 individual human fecal samples were collected and anaerobically incubated with fructoselysine. Upon optimization of this applied *in vitro* model, interindividual differences in the Michaelis-Menten kinetic parameters of fructoselysine degradation were quantified. This resulted in the identification of microbial non-metabolizers and microbial metabolizers of fructoselysine, with the latter group showing interindividual differences with V_{max}, K_m and kcat-values varying up to 14.6-fold, 9.5-fold and 4.4-fold, respectively. In addition, significantly increased production of the short chain fatty acid butyrate was quantified following fructoselysine exposure. Multiple bacterial genera were positively correlated with fructoselysine degradation and butyrate production, showing that the potential to convert fructoselysine may originate from multiple bacterial genera.

Besides reported and observed interindividual differences in the gut microbiota composition and its metabolic functions, intraindividual differences in these parameters can exist as well. The gut microbiota is a dynamic ecosystem and thus intraindividual temporal differences are of possible relevance for its functioning. In **Chapter 4** both inter- and intraindividual differences in gut microbial degradation of the AGE carboxymethyllysine and its precursor

fructoselysine were quantified. Three fecal samples were collected from 13 individual human volunteers over a time frame with an interval of ≥3 weeks between fecal sample donations. Pronounced inter- and intraindividual variation was observed in both carboxymethyllysine and fructoselysine degradation. However, the average capacity to degrade fructoselysine was 27.7-fold higher compared to that for carboxymethyllysine, and the two degradation rates were not correlated (R^2=0.08), showing the need to evaluate toxicokinetics for individual AGEs and precursors instead of evaluating them on a group level. In addition, again multiple bacterial genera were correlated with the individuals' carboxymethyllysine and fructoselysine degradation activities, corroborating that showing that the potential to convert fructoselysine and carboxymethyllysine may originate from multiple bacterial genera.

Considering the dynamic aspects of the gut microbiota, it was evaluated whether different dietary exposures could affect fructoselysine degradation activities, thereby potentially contributing to the intra- and interindividual differences. Fructoselysine is present in high levels in infant formula while being absent in breast milk. Functional differences in microbial fructoselysine degradation were compared between breast-fed (BF) and formula-fed (FF) infants in **Chapter 5**, in view of their different exclusive diets and consequent different dietary fructoselysine exposures. A publicly available metagenome dataset analysis with metagenome assembled genomes (MAGs) from infant fecal samples showed that genes involved in microbial fructoselysine degradation were present in multiple taxa in both BF and FF infant fecal samples but were higher prevalent in fecal samples from FF infants compared to the BF infants. Further collection of individual fecal samples from exclusively BF and FF infants showed that both groups were able to degrade fructoselysine anaerobically but fecal samples from the FF infants resulted in a significantly higher degradation activity compared to the BF infants. This indicated that the infant gut microbiota adapts towards dietary fructoselysine exposure.

This dynamic adaptive aspect of the gut microbiota was also observed in **Chapter 6** in which mice were exposed to a heated diet high in AGEs which resulted in an altered gut microbiota composition compared to mice exposed to the control diet. Exposure to the heated diet high in AGEs followed by the control diet (i.e. the switch group) showed that the altered gut microbiota composition was reversible and adapted to the dietary exposure. This reversibility was also observed for the accumulation of the tested AGEs in plasma, kidney and liver (as analyzed in their protein-bound and free form), a result that also pointed to at least partial bioavailability of the dietary AGEs and/or their precursors that appeared to be enriched in the heated chow diet.

Overall, it can be concluded that the bi-directional relation of the gut microbiota with exogenous AGEs and their precursors is of relevance when evaluating their toxicokinetic and toxicodynamic characteristics. To accurately evaluate the hazards and risks of dietary exposure to AGEs and precursors, better characterization and quantification of the applied test substances and biological outcomes, and also of the exposure from endogenous formation relative to that resulting from dietary intake, are essential.

Samenvatting

Glycatieproducten zijn een heterogene groep verbindingen die gevormd kunnen worden door verhitting en opslag van voedselproducten. Onder deze glycatieproducten vallen de gevorderde glycatieproducten (de zogenoemde "advanced glycation end products", afgekort AGEs) zoals carboxymethyllysine, en hun voorlopers zoals het Amadori-product fructoselysine en α-dicarbonyls zoals methylglyoxal, glyoxal en 3-deoxyglucosone. Deze stoffen zijn aanwezig in exogene bronnen, zoals voeding, maar kunnen ook endogeen gevormd worden, in het menselijk lichaam. AGEs zijn in verband gebracht met verschillende nadelige gezondheidseffecten, zoals diabetes en hart- en vaatziekten. Of blootstelling aan exogene glycatieproducten, bijvoorbeeld via voeding, bijdraagt aan deze nadelige effecten staat nog ter discussie. In **Hoofdstuk 2** is een overzicht gegeven van de toxicokinetiek en toxicodynamiek van exogene en endogene AGEs en hun voorlopers. De toxicokinetiek en toxicodynamiek zijn beiden van belang wanneer er wordt geëvalueerd of exogene glycatieproducten uit voeding bij kunnen dragen aan nadelige gezondheidseffecten die in verband worden gebracht met AGEs. Op basis van het gegeven overzicht is geconcludeerd dat verschillende verbeterpunten noodzakelijk zijn voordat een definitieve conclusie getrokken kan worden of blootstelling aan glycatieproducten via de voeding bij kan dragen aan de nadelige gezondheidseffecten die in verband worden gebracht met AGEs. Dit omvat onder andere dat de geteste AGEs en hun voorlopers beter gekarakteriseerd moeten worden, en wordt er aangeraden om de stoffen op basis van molecuulgewicht te onderscheiden. Verder is het van belang om een onderscheid te maken in de relatieve bijdrage van endogene en exogene blootstelling en om dat te kwantificeren. Ook wordt er geconcludeerd dat een deel van de AGEs en hun voorlopers die via voeding in het menselijk lichaam komen, niet direct opgenomen worden en dus de colon kunnen bereiken. De AGEs en hun voorlopers kunnen vervolgens in twee richtingen (bi-directioneel) in interactie komen met de darmbacteriën: enerzijds kan dit de toxicokinetiek van de glycatieproducten beïnvloeden, en anderzijds kan dit ook leiden tot een toxicodynamisch effect doordat de darmbacterie-compositie en mogelijk functie kunnen veranderen. Het doel van dit project was om deze bi-directionele interacties tussen de darmbacteriën en glycatieproducten uit voeding te bestuderen, en om inter- en intra-individuele verschillen te karakteriseren in de reacties tussen darmbacteriën waarbij het Amadori product fructoselysine en de AGE carboxymethyllysine als modelstoffen worden gebruikt.

In **Hoofdstuk 3** zijn interindividuele verschillen in de Michaelis-Menten kinetische parameters gekwantificeerd van de microbiële afbraak van fructoselysine. Hiervoor zijn fecale samples van 16 vrijwilligers verzameld en met fructoselysine geïncubeerd onder anaerobe omstandigheden. Hieruit bleek dat niet alle fecale samples van de individuen fructoselysine konden afbreken. In de fecale samples van de individuen die wel fructoselysine konden afbreken verschilden de V_{max}, K_m en kcat-parameters tot 14.6, 9.5 en 4.4 keer, respectievelijk. Ook werd er significant meer butyraat, een kortketenig vetzuur, gekwantificeerd na blootstelling aan fructoselysine. Meerdere bacteriële genera waren positief gecorreleerd met zowel fructoselysine afbraak als butyraat productie. Dit liet zien dat meerdere bacteriën waarschijnlijk in staat zijn om fructoselysine om te zetten.

De samenstelling van de darmbacteriën en bijbehorende metabolische functionaliteiten kunnen verschillen tussen mensen (inter-individueel), maar ook binnen een mens (intra-individueel). Dit komt doordat de microbiota in de darm een dynamisch ecosysteem is, en dus kan veranderen over tijd. In **Hoofdstuk 4** zijn zowel inter- als intra-individuele verschillen gekwantificeerd in de microbiële afbraak van carboxymethyllysine en fructoselysine, door meerdere fecale samples van 13 individuen te incuberen die verzameld zijn over een langere tijdsperiode (≥3 weken tussen de verschillende collectie momenten). Zowel de inter- als intra-individuele verschillen voor zowel de microbiële afbraak van carboxymethyllysine als van fructoselysine waren opvallend, en gemiddeld genomen was de capaciteit om fructoselysine af te breken 27.7 keer groter vergeleken met carboxymethyllysine. De degradatiesnelheden van beide stoffen waren niet aan elkaar gecorreleerd (R^2=0.08), wat de noodzaak laat zien om de toxicokinetiek van glycatieproducten individueel te beoordelen in plaats van op groepsniveau. Ook waren meerdere bacteriële genera positief gecorreleerd aan de afbraak van carboxymethyllysine en fructoselysine, wat kon bekrachtigen dat meerdere bacteriën betrokken zijn bij deze metabolische reacties.

In **Hoofdstuk 5** werd verder onderzocht in hoeverre voeding effect heeft op de gekwantificeerde individuele verschillen. In kunstvoeding voor baby's zijn grote hoeveelheden fructoselysine gevonden, terwijl in moedermelk fructoselysine niet of nauwelijks aanwezig is. Om dit verschil in blootstelling aan fructoselysine verder te onderzoeken en te relateren aan de (potentiële) microbiële afbraak van fructoselysine zijn fecale samples van borst-gevoede (BV) en kunst-gevoede (KV) baby's vergeleken. Ten eerste werd een openbare metagenoom dataset analyse uitgevoerd met metagenoom geassembleerde genomen (metagenome assembled genomes; MAGs) van fecale samples van baby's. Dit liet zien dat genen die betrokken zijn bij fructoselysine afbraak zich kunnen bevinden in verschillende bacteriële taxa in fecale samples van zowel BV als KV baby's, maar dat deze in een hogere prevalentie aanwezig zijn in de fecale samples van KV baby's. Fecale samples van exclusief BV en KV baby's werden vervolgens verzameld en anaerobe incubaties lieten zien dat beide groepen fructoselysine konden afbreken, maar dat de microbiële fructoselysine afbraak door fecale samples van KV baby's significant hoger was. Dit duidde erop dat de darmbacteriën van baby's zich aanpassen aan fructoselysine blootstelling via voeding.

Deze dynamische karakteristieken van de darmbacteriën zijn ook in **Hoofdstuk 6** waargenomen, waarin muizen zijn blootgesteld aan een verhit dieet met daardoor verhoogde AGE waarden. Dit leidde tot een verandering in de samenstelling van de darmbacteriën in vergelijking tot de controle groep. De muizen in de schakel groep kregen na het verhitte dieet verhoogd in AGEs het controle dieet, waaruit bleek dat de verandering in de samenstelling van de darmbacteriën omkeerbaar was en dat de darmbacteriën zich aanpassen aan het dieet. Naast deze gevonden omkeerbaarheid in de samenstelling van de darmbacteriën bleek dit ook zo te zijn voor de ophoping van geanalyseerde AGEs in plasma, nieren en de lever (in zowel de eiwitgebonden als de vrije vorm). Dit duidt er op dat ten minste een gedeelte van de AGEs en/of de voorlopers vanuit het verhitte dieet opgenomen kunnen worden.

Over het algemeen kan worden geconcludeerd dat de bi-directionele interactie tussen de darmbacteriën en exogene glycatieproducten relevant is bij het bepalen en evalueren van

de toxicokinetiek en toxicodynamiek. Om mogelijke gevaren en risico's van blootstelling aan AGEs en voorlopers via de voeding nauwkeurig te evalueren is het nodig om de toegepaste blootstellingen en biologische uitkomsten beter te karakteriseren en kwantificeren. Daarnaast is het ook van belang om exogene blootstelling via voeding relatief aan endogene formatie te evalueren.

S

Acknowledgements

Yes, I did it! My PhD journey is now really finished and I am very happy and proud that I managed to finalize this big challenge. Past years have been great, intense, and everything in-between and were accompanied with struggle, laughter, frustration, growth, and happy and sad tears. Now that my 'book' is out there I would like to thank many people who contributed to my PhD in all kind of ways.

First of all, I want to thank my supervision team: Prof. dr. Ivonne Rietjens, dr. Clara Belzer and dr. Karsten Beekmann. Your guidance and support have been very helpful. You all contributed in your own way and taught me different things for which I am grateful.

Ivonne, thank you for all your important scientific input, knowledge, guidance and feedback. You always made time for me when needed. Overall I learned a lot from you and I am also grateful for the nice conversations we had. Thank you for this opportunity!

Clara, thank you for introducing me to new topics, persons, collaborations, knowledge and involving me in your group. Your addition to the supervision team gave a whole new dimension to the thesis which also broadened my knowledge and horizon for sure. I am very glad I got to know you and work with you!

Karsten, last but definitely not least. We already worked together during my master thesis and I am very happy that you gave me the opportunity to join this PhD project. You taught me a lot, trusted me and supported me from the very beginning towards the end. I am glad you were still able to be highly involved after changing your career to WFSR, and I am happy that we can stay colleagues. Thank you for everything!

I also would like to thank the members of the thesis committee for their valuable time and effort to evaluate my thesis.

An important part of this research could not have been done without the contribution of many volunteers. Thank you for your contribution! It is highly appreciated.

Furthermore, I would like to thank all co-authors who contributed to this thesis, in particular the following persons. Dr. Meike van der Zande, thank you for being involved as a supervisor in the initial phase of my PhD research. Athanasia Ioannou (Nancy), thank you for your great contribution to the infant chapter, I am thankful for our collaboration! Prof. dr. Casper Schalkwijk, Armand Linkens and Prof. dr. Willem de Vos – thank you all for the fruitful collaboration and the opportunity.

I also would like to thank Prof. dr. Jacques Vervoort. Unfortunately he is no longer with us, but I am glad that I got to know him, work with him and that he involved me in other projects.

To all at TOX, thank you for being so kind and helpful! When looking back to the past years I really enjoyed working at TOX thanks to all the nice people around. Carla, Gerda, Lidy and Letty, thank you for all your (administrative) support the past years. Nico, Hans B., Nynke, thank you for all the talks. To the current and former 'core' of TOX: Laura, Sebas,

A

Marco, Engelien, Madelief, Thijs, Noël en Carline, het is fijn om altijd bij jullie in Oeken te kunnen aanwaaien (of aanfietsen) voor een ontspannen middagje in het groen waar ik altijd weer van alles nieuws leer over brood, bloemen en trekkers. Bedankt voor alles, jullie interesse, support en natuurlijk de regelmatige BBQs!

Aan mijn lieve familie, bedankt! Aan de familie van Dongen en familie Hopman, maar vooral natuurlijk aan de beste ouders, zus, broertje en zwager-to-be. Afgelopen half jaar was echt een rollercoaster maar ik ben zo blij met jullie allemaal! Papa en mama ik kan jullie niet genoeg bedanken. Jullie staan echt altijd voor mij klaar. Voor advies en aanmoediging, gewoon even bijkletsen, gezelligheid in Bakkum of St. Maixant, of als er geklust moet worden. Ook tijdens mijn PhD heb ik regelmatig met jullie kunnen sparren over van alles en nog wat. Dank jullie wel voor alles! Heleen, dank je wel voor het 'er doorheen prikken' op z'n tijd, de bemoedigende woorden en de gezelligheid bij jullie thuis in Amsterdam. Ik voel me altijd erg welkom als ik weer eens bij jullie kom aanwaaien voor één of heel veel nachtjes, bedankt Bram & Heleen, ook voor jullie hulp en leuke gesprekken! Jan, jij verbaast ons allemaal telkens weer met je nieuwe plannen en inspirerende avonturen. Het is fijn om altijd met jou te kunnen bijkletsen over van alles en nog wat: werk, reizen, hobby's, mijn PhD... Hopelijk heb je een goede live-verbinding vanuit Zuid-Amerika en we gaan het later nog eens goed vieren samen!

Het laatste stuk is natuurlijk voor Valentijn. Jij bent echt mijn thuisbasis. Het is zo fijn en relaxed met jou! Bedankt voor je eindeloze steun, schoudermassages, goede vragen, het relativeren, meedenken en de gezelligheid. Ik ben trots op ons toch best goed gelukte verbouw-avontuur en onze VS-trip was voor mij de perfecte afsluiter van mijn PhD. Ik kijk uit naar alle avonturen samen die nog volgen!
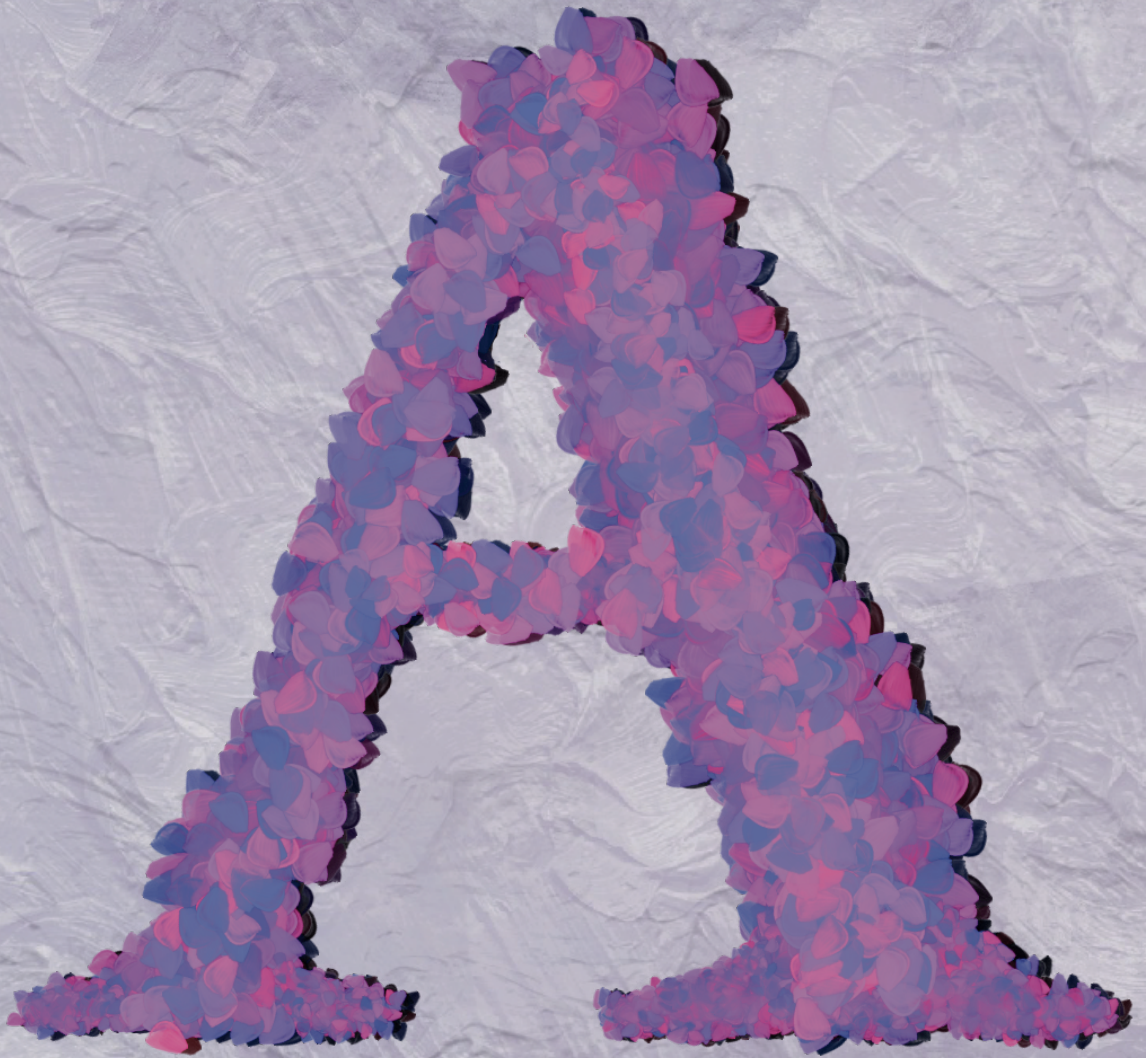
About the author

Curriculum Vitae

Katja Catharina Wilhelmina van Dongen was born on September 3rd, 1994 in Castricum, the Netherlands. In 2011, she obtained her secondary school diploma from Jac. P. Thijsse College, Castricum, and continued her education at Wageningen University & Research (WUR). There she studied Nutrition and Health and obtained her bachelor's degree in 2014 and continued the master program Food Safety. During her master thesis, she started the work of *in vitro* microbial metabolism at the department of Toxicology (WUR) under direct supervision of dr. Karsten Beekmann. For her internship, she joined the Alternative to Animal testing laboratory of BASF SE in Ludwigshafen (Germany) and under the direct supervision of dr. Caroline Gomes she optimized an *in vitro* placental transfer model. After obtaining her master's degree *cum laude* in 2017 she started her PhD research under supervision of Prof. dr. Ivonne Rietjens, dr. Karsten Beekmann and dr. Clara Belzer at the division of Toxicology (WUR). The research was performed in collaboration with the laboratory of Microbiology (WUR) and Wageningen Food Safety Research, and resulted in this dissertation. During her PhD, she focused on dietary glycation products and their interactions with the (human) gut microbiota. In addition, she followed postgraduate courses in toxicology required for the registration as European Toxicologist and she supervised multiple master thesis students. Also, she co-organized the annual meeting of the Dutch Society of Toxicology (NVT) in 2019. Currently, she works as a researcher in the Agrochains team of Wageningen Food Safety Research, working on food safety aspects of different transitions in the food supply chain.

A

List of publications

This thesis

van Dongen, K. C. W., van der Zande, M., Bruyneel, B., Vervoort, J. J. M., Rietjens, I. M. C. M., Belzer, C., & Beekmann, K. (2021). An in vitro model for microbial fructoselysine degradation shows substantial interindividual differences in metabolic capacities of human fecal slurries. Toxicology in Vitro, 72, 105078. https://doi.org/10.1016/j.tiv.2021.105078

van Dongen, K. C. W., Linkens, A. M. A., Wetzels, S. M. W., Wouters, K., Vanmierlo, T., van de Waarenburg, M. P. H., L.J.M. Scheijen, J., de Vos, W. M., Belzer, C., & Schalkwijk, C. G. (2021). Dietary advanced glycation endproducts (AGEs) increase their concentration in plasma and tissues, result in inflammation and modulate gut microbial composition in mice; evidence for reversibility. Food Research International, 147, 110547. https://doi.org/10.1016/J.FOODRES.2021.110547

van Dongen, K. C. W., Kappetein, L., Miro Estruch, I., Belzer, C., Beekmann, K., & Rietjens, I. M. C. M. (2022). Differences in kinetics and dynamics of endogenous versus exogenous advanced glycation end products (AGEs) and their precursors. Food and Chemical Toxicology, 164, 112987. https://doi.org/10.1016/J.FCT.2022.112987

van Dongen, K.C.W., Belzer, C., Bakker, W., Rietjens, I.M.C.M., & Beekmann, K. (Submitted). Inter- and intraindividual differences in the capacity of the human intestinal microbiome in fecal slurries to metabolize fructoselysine and carboxymethyllysine.

van Dongen, K.C.W., Ioannou, A., Wesseling, S., Beekmann, K., & Belzer, C. (Submitted). Differences in gut microbial fructoselysine degradation activity between breast-fed and formula-fed infants.

Other publications

Dimopoulou, M., Verhoef, A., Gomes, C. A., **van Dongen, C. W.**, Rietjens, I. M. C. M., Piersma, A. H., & van Ravenzwaay, B. (2018). A comparison of the embryonic stem cell test and whole embryo culture assay combined with the BeWo placental passage model for predicting the embryotoxicity of azoles. Toxicology Letters, 286, 10–21. https://doi.org/10.1016/J.TOXLET.2018.01.009

Zheng, L., **van Dongen, K. C. W.**, Bakker, W., Estruch, I. M., & Rietjens, I. M. C. M. (2022). The influence of intracellular glutathione levels on the induction of Nrf2-mediated gene expression by α-dicarbonyl precursors of advanced glycation end products. Nutrients, 14, 1364. https://doi.org/10.3390/NU14071364

Overview of completed training activities

Discipline specific activities		
Courses		
Immunotoxicology	PET, Utrecht	2018
Pathobiology	PET, Utrecht	2018
Cell toxicology	PET, Leiden	2019
Molecular toxicology	PET, Amsterdam	2019
Laboratory of animal science	PET, Utrecht	2019
Intestinal microbiome in human and animals	VLAG, Wageningen	2019
Organ toxicology	PET, Nijmegen	2020
Meetings		
45th Annual meeting of the Japanese Society of Toxicology (oral presentation)	jSOT, Osaka, Japan	2018
Symposium 'Food, microbiome and immunity'	VLAG, Wageningen	2018
Annual Gut Day	MIB-WUR, Wageningen	2018
45th Annual meeting of the Dutch Society of Toxicology (poster presentation)	NVT, Ede	2019
56th Congress of the European societies of Toxicology (poster presentation)	EUROTOX, online	2021
61st Annual meeting Society of Toxicology (poster presentation)	SOT, San Diego, USA	2022

General courses		
VLAG PhD week	VLAG, Baarlo	2018
The essentials of scientific writing and presenting	WGS, Wageningen	2018
Introduction to R	VLAG, Wageningen	2019
Philosophy of ethics of food science and technology	VLAG, Wageningen	2020
Scientific publishing	WGS, Wageningen	2020
Critical thinking and argumentation	WGS, online	2020
Scientific artwork, data visualization and infographics with Adobe Illustrator	WGS, online	2020

Other activities		
Preparation of research proposal	TOX-WUR	2017
Scientific presentations	TOX-WUR	2017-2021
Environmental toxicology	WUR, Wageningen	2018
PhD study tour to Japan	TOX-WUR, Japan	2018

Approved by Graduate School VLAG.